UNIVERSITY OF CALIFORNIA SAN DIEGO

Development of Antibody-RNA Conjugates for Targets Beyond the Liver

A dissertation submitted in partial satisfaction of the requirements
for the degree Doctor of Philosophy

in

Biomedical Sciences

by

Carlos Arturo Medina

Committee in charge:

Professor Steven F. Dowdy, Chair
Professor Ezra Cohen
Professor Jeffrey D. Esko
Professor Stephen B. Howell
Professor Peter J. Novick
Professor Gene W. Yeo

2021

The dissertation of Carlos Arturo Medina is approved, and it is acceptable in quality and form for publication on microfilm and electronically.

University of California San Diego

2021

TABLE OF CONTENTS

LIST OF FIGURES

ACKNOWLEDGEMENTS

First and foremost, I would like to thank my thesis advisor, Steven F. Dowdy, for the opportunity to work in his lab over the past years and for providing me with invaluable training and mentorship. I would also like to thank my committee members for agreeing to take the time to serve on my committee and provide guidance and feedback for my project.

I would like to extend a special thank you to Ian Huggins for the incredible and patient mentorship that he provided to me during the several years that we overlapped in the Dowdy Lab. His creativity, enthusiasm, and optimism are inspiring, and I learned very much from him. I thank him for his support, tutelage, and all the engaging and spirited conversations that we had over the years.

I would like to thank Satish Jadhav for his superb abilities in the chemistry lab and his regular production of essential reagents. I also thank him for his suggestions, advice, and scientific insights. I would also like to thank Xianshu Cui for her support over the years and for masterfully managing and keeping the Dowdy Lab afloat.

I would like to thank former lab members for their essential help and guidance when I was first starting out, including Alex Hamil, Aaron Springer, Arjen van den Berg, and Apollo Kacsinta. I would also like to thank Ryan Setten, a more recent lab member, for his creative insights and advice.

Finally, I would like to thank my family, especially my mother and father, for their ceaseless and steadfast support over my years in graduate school, and really, over the course of my entire life. My parents have always taught me the value of hard work and education and from an early age instilled in me a strong work ethic and keen sense of responsibility. They have always encouraged me to take up new challenges and have supported me in everything I have ever chosen to do. My parents have largely shaped who I am today, and for that I owe them an immense debt of gratitude.

During my graduate training, I was supported in part by the Cancer Biology, Informatics, and Omics (CBIO) Training Grant from the National Cancer Institute (NCI T32 CA067754-22).

Chapter Three has been published in part in *Molecules*, coauthored by this dissertation's author. The citation for the published work is: Huggins, I.J., Medina, C.A., Springer, A.D., van den Berg, A., Jadhav, S., Cui, X., Dowdy, S.F., 2019. Site Selective Antibody-Oligonucleotide Conjugation via Microbial Transglutaminase. Molecules 24, 3287.

Chapter Four contains unpublished material that was coauthored in part by Alex Hamil and Xianshu Cui. This dissertation's author was the primary researcher and author of this material. Oligonucleotides were synthesized by Alex Hamil and the linker peptides were synthesized by Xianshu Cui. Steven Dowdy provided guidance throughout the work presented in this chapter.

Chapter Five contains unpublished material that was coauthored in part by Ian Huggins, Satish Jadhav, and Yu Yan Kwan. This dissertation's author was the primary researcher and author of this material. Ian Huggins established the conjugation reaction conditions for the earlier generations of uEEDs and conjugation chemistries. Synthesis of uEEDs and oligonucleotides and the HPLC analysis of the uEED monomeric unit was performed by Satish Jadhav. Later batches of anti-CD33 monoclonal antibodies were produced by Yu Yan Kwan. Steven Dowdy provided guidance throughout the work presented in this chapter.

VITA

EDUCATION:

2016 – 2021 Doctor of Philosophy, Biomedical Sciences
Department of Cellular and Molecular Medicine
University of California San Diego
Graduate Advisor: Professor Steven F. Dowdy, Ph.D.

2012 – 2016 Bachelor of Science
Major: Bioengineering Minor: Biology
Research Excellence Award (Bioengineering); Dean's Merit Scholarship
Santa Clara University

RESEARCH EXPERIENCE:

2016 – 2021 Ph.D. Graduate Student with Professor Steven F. Dowdy
Dept. of Cellular & Molecular Medicine, UCSD School of Medicine
Thesis Project: Development of Antibody-RNA Conjugates for Targets Beyond the Liver

2015 – 2016 Research Intern, Bone & Signaling Lab
NASA Ames Research Center, Mountain View, CA
Thesis written & published at Santa Clara University
Project: Mitigation of Radiation-Induced Bone Loss by Dried Plum

2015 Research Intern, Department of Biochemistry
DuPont Industrial Biosciences, Palo Alto, CA
Project: New Applications for Novel Proteases

2014 – 2015 Research Assistant, with Profs. Prashanth Asuri & Christelle Sabatier
Departments of Bioengineering and Biology
Santa Clara University, Santa Clara, CA
Project: Analyzing Matrix Stiffness for Cancer Cell Response to Toxins

2013 Biospecimen Management Intern
Roche Molecular Systems, Pleasanton, CA
Inventory Management, Research Workshops, Cell Culture

RESEARCH SUPPORT:

2017 – 2019 Trainee, NCI Cancer Biology Training Grant (T32 CA067754-22)

TEACHING EXPERIENCE:

2019 – 2021 Teaching Assistant for the Salk Mobile Science Lab
Salk Institute of Biological Studies
San Diego County, CA

SCIENTIFIC PRESENTATIONS:

Feb. 2019	Oral Presentation: “Role of MLL-AF9 Fusion Oncogene in Establishment, Maintenance, and Recurrence of Acute Myeloid Leukemia” UC San Diego CBIO Training Grant Annual Presentation, La Jolla, CA.
Oct. 2018	Poster Presentation: “Role of MLL-AF9 Fusion Oncogene in Establishment, Maintenance, and Recurrence of Acute Myeloid Leukemia” Oligonucleotide Therapeutics Society Annual Conference, Seattle, WA.
Oct. 2017	Oral Presentation: “Role of MLL-AF9 Fusion Oncogene in Establishment, Maintenance, and Recurrence of Acute Myeloid Leukemia” UC San Diego CBIO Training Grant Annual Presentation, La Jolla, CA.
May 2016	Oral Presentation: “Mitigation of Radiation-Induced Bone Loss by Dried Plum” Santa Clara University Senior Design Conference, Santa Clara, CA.
Sep. 2015	Oral Presentation: “New Applications for Novel Proteases” End of Internship Company-Wide Research Talk at DuPont Industrial Biosciences, Palo Alto, CA.
Aug. 2015	Poster Presentation: “New Applications for Novel Proteases” DuPont Industrial Biosciences Summer Intern Poster Session, Palo Alto, CA.
Aug. 2013	Poster Presentation: “Summer Internship in Biospecimen Management” Roche Summer Interns Poster Session, Pleasanton, CA.

PUBLICATIONS:

Huggins, I.J., **Medina, C.A.**, Springer, A.D., van den Berg, A., Jadhav, S., Cui, X., Dowdy, S.F., 2019. Site Selective Antibody-Oligonucleotide Conjugation via Microbial Transglutaminase. Molecules 24, 3287. https://doi.org/10.3390/molecules24183287

Medina, C., Steczina, S., 2016. Mitigation of Radiation-Induced Bone Loss by Dried Plum. Santa Clara University Bioengineering Senior Thesis, 49. https://scholarcommons.scu.edu/bioe_senior/49/

Zustiak, S.P., Dadhwal, S., **Medina, C.**, Steczina, S., Chehreghanianzabi, Y., Ashraf, A., Asuri, P., 2016. Three-dimensional matrix stiffness and adhesive ligands affect cancer cell response to toxins: Cancer Cell Responses to Toxins in a 3D Matrix. Biotechnol. Bioeng. 113, 443–452. https://doi.org/10.1002/bit.25709

ABSTRACT OF THE DISSERTATION

Development of Antibody-RNA Conjugates for Targets Beyond the Liver

by

Carlos Arturo Medina

Doctor of Philosophy in Biomedical Sciences

University of California San Diego, 2021

Professor Steven F. Dowdy, Chair

While cancer treatment modalities have improved in recent decades, each subsequent improvement in therapy has brought mixed results and has fallen short of achieving a lasting cure. From chemotherapy and radiotherapy to small molecule inhibitors and monoclonal antibodies to antibody-drug conjugates, each has brought a unique approach and improvement to preceding modalities. Yet, the limitations of these approaches are evident. The discovery of RNA interference (RNAi) and its potential to treat genetic diseases like cancer opened a new therapeutic avenue. Yet, for many years, RNAi faced multiple setbacks and limitations at both the biological and chemical levels.

Among the challenges faced in the RNAi field are the inherently large size (>14,000 Da) and highly charged (>40 phosphates) nature of siRNA molecules, which prevents them from passively diffusing across the cell membrane the way that small molecular inhibitors do. Other obstacles include nucleases, innate immunity, and potential off-target silencing effects from siRNAs. Many of the same problems that affect siRNAs also affect antisense oligonucleotides. Delivery with an antibody would significantly improve the prospects of an oligonucleotide reaching its target. But building an antibody with a clearly defined drug-antibody ratio comes with difficulties. Other challenges include delivery and identification of suitable target receptors that are expressed in sufficiently high numbers and can rapidly internalize via endocytosis. The most limiting barrier preventing adequate delivery of siRNA is the difficulty of achieving endosomal escape, which prevents oligonucleotides from reaching the cytoplasm and nucleus of cells.

Over the past decade, our laboratory has worked extensively to address these challenges. Oligonucleotide stability and protection from the immune system were achieved in large part through chemical modifications during the oligo synthesis process. Furthermore, a site-specific conjugation approach was developed to create clearly defined antibody-RNA conjugates (ARCs). Currently, a work-in-progress on the chemistry side is the development of universal endosomal escape domains (uEEDs). The work described herein encompasses the development and building of a complex ARC macromolecular therapeutic that, under the right conditions, could hold great potential for the specific knockdown of previously undruggable oncogenes, such as Kras and Myc, and other aberrant genetic targets in viral infections and chronic diseases.

CHAPTER ONE

CANCER THERAPY AND THE POTENTIAL OF OLIGONUCLEOTIDE THERAPEUTICS

CANCER THERAPY AND THE POTENTIAL OF OLIGONUCLEOTIDE THERAPEUTICS

ABSTRACT

RNA-based therapeutics hold significant potential for treating and possibly also curing cancer. Older therapeutic approaches have sometimes demonstrated limited efficacy at best, whereas immunotherapy has shown promise in certain cases, and oligonucleotides have overcome many of the shortcomings of its predecessors. Chemotherapy on its own leads to high recurrence rates of cancer, and combination with targeted therapies, such as small molecule inhibitors or monoclonal antibodies, confers mild improvements. However, relapse remains prevalent when the tumor mutates sufficiently enough to render the targeted therapy ineffective. Antibody-drug conjugates (ADCs) have shown better results in certain cases by specifically delivering a cytotoxic payload to target cancer cells but can still indiscriminately kill healthy cells that express the same target receptors.

Starting in 1984 with the introduction of phosphorothioate backbones in antisense oligonucleotides and the discovery of RNA interference (RNAi) in worms in 1998, the past few decades have seen significant advancements in the development of oligonucleotide-based therapies. While various other types of oligonucleotides have been developed and numerous chemical modifications have now been analyzed to address the various biological barriers present in animals and humans, in many cases, problems of delivery and endosomal escape remain by far the largest problems to address. Current successful applications of oligonucleotide therapeutics in the clinics are limited to diseases in a few delivery-permissive, essentially non-dividing tissues, including the liver or central nervous system. Unfortunately, no oligonucleotides have yet been successfully used to treat cancer in humans. Oligonucleotide therapeutics hold great potential for the treatment of cancer and are inherently advantageous over the more standard treatment modalities in their customizability and target specificity. The biggest remaining challenge to solve is the delivery of oligonucleotides into the cell cytoplasm.

CANCER THERAPIES

The standard treatment for cancer began with chemotherapy but its limitations soon led to the development of numerous, targeted options that have been in use over the past several decades. Unfortunately, even these targeted modalities often fall short of becoming lasting cures.

Chemotherapy

For much of the first half of the twentieth century, cancer was considered a mysterious black box in a world where medicine was rapidly advancing. Whereas antibiotics brought about significant progress in the treatment of many infections, cancer continued to outpace other diseases (DeVita et al, 2008). During this time purine analogs were developed, and leukemia cases became among the most responsive of cancers studied by physicians (Hitchings and Elion, 1954; Elion et al., 1954; Kersey, 1997). When Sidney Farber tested numerous antifolates and other chemicals in pediatric leukemia patients, the initial results were so promising that Farber noted that the “bone marrow [of his patient] looked so normal that one could dream of a cure” (Mukherjee, 2010). While the remission cases brought great excitement in the field of medicine, the drawbacks of chemotherapy soon became evident, and chemotherapeutic agents fell short of becoming the lasting cure that Farber had dreamed about. Chemotherapy alone only extended survival by several months or half a year. The 1960s and 1970s saw some cases of complete and lasting remission after aggressive chemotherapy used against leukemias, but relapse was often inevitable, especially in other cancer types (DeVita et al., 2008). Chemotherapy is a broad-spectrum cytotoxic drug that targets both healthy and cancer cells alike but fails to eliminate the resistant cancer clones. Toxicity is significant and side effects can become intolerable. For this reason, chemotherapy is now used as an adjuvant therapy, in conjunction with surgery, radiotherapy, and/or other targeted therapies such as the ones described in the following sections.

Small-Molecule Inhibitors

Due to the significant limitations of chemotherapy to bring about lasting results in cancer patients, small molecule inhibitors (SMIs) have become a prominent part of standard cancer treatments. SMIs often target key protein kinases, enzymes that catalyze protein phosphorylation, involved in the development and progression of certain cancers to block specific molecular pathways, and stem the spread of the cancer (Wilson et al., 2018). SMIs' small size makes them apt drug options for entry into cells and efficient binding to and inhibition of specific protein kinases (Chhabra, 2021). FDA approval of tyrosine kinase inhibitor imatinib in 2001 for the treatment of chronic myeloid leukemia and acute lymphoblastic leukemia led to a rapid expansion of SMI development in the pharmaceutical industry in the two decades that followed (Zhong et al., 2021). Among the numerous SMIs that have been FDA approved are certinib (Novartis) against ALS/ROS in metastatic non-small cell lung cancer, ponatinib (ARIAD Pharmaceuticals) against FLT3 in chronic myeloid leukemia, axitinib (Pfizer) against VEGFR-1/2/3 in renal cell carcinoma, and vandetanib (AstraZeneca) against EGFR/VEGFR/RET/BRK metastatic medullary thyroid cancer (Khera and Rajput, 2017). Unfortunately, benefits seen from treatment with SMIs are short-lived.

Cancer cells inevitably acquire mutations to confer resistance to the SMI, thus rendering the SMI ineffective and leading to a resurgence of the cancer. Moreover, only a small portion of kinases can be targeted and there remains a large space of "undruggable" targets in any given cancer (Zhang et al., 2009). PARP inhibitors have been more successful in BRCA-mutant cancers due to the effectiveness of blocking the double stranded break and single stranded break repair pathways that subsequently induces cell death (King et al., 2003; Lord and Ashworth, 2017). The efficacy of PARP inhibitors has led the FDA to extend their indications to multiple cancers, including BRCA-mutant ovarian cancer, epithelial ovarian cancer, fallopian tube cancer, and BRCA-mutated HER2-negative locally advanced or metastatic breast cancer (Zhong et al., 2021). Unfortunately, many other SMIs can only bring about a more temporary

and less pronounced effect and their inherent limitations will in many cases mean that the cancer becomes drug resistant and relapse an inevitability.

Monoclonal Antibodies

Monoclonal antibody (mAb) therapies for cancer are designed to either block a key receptor in the cancer cell to interfere with its signaling network, activate the innate immune system, flag a cancer cell to mark it for destruction by the immune system, or deliver a toxic payload to the cancer cell (see next section).

There are five distinct antibody isotypes: IgA, IgD, IgE, IgG, and IgM, of which, IgG is the most common isotype used in cancer therapies. Since the 1980s, mAbs with high specificity to their target receptor have been produced from hybridoma cells and the ability to humanize these antibodies has significantly increased their therapeutic value (Oldham et al., 2008). mAbs that are designed to interfere with cancer signaling can target either soluble molecules like cytokines to prevent them from binding their receptors or bind overexpressed membrane bound receptors on the cancer cell to inhibit its proper function. For example, the epidermal growth factor receptor (EGFR) is often overexpressed in several types of cancer and is involved in overall growth, differentiation, migration, and cell survival pathways in these cancer cells. Panitumumab is a human anti-EGFR mAb approved for the treatment of metastatic colorectal cancer that binds to EGFR to prevent its ligand (EGF) from binding and inhibit receptor dimerization. Conversely, mAbs such as bevacizumab, an anti-VEGFA antibody, reduces tumor growth by inhibiting angiogenesis, sequestering VEGF ligand VEGFA, and preventing it from binding to its receptor (Shuptrine et al., 2013).

mAbs can also tap into the innate immune system through complement dependent cytotoxicity (CDC) where two or more antibodies binding to a cell activates a proteolytic pathway that leads to the formation of the membrane attack complex (MAC) (Janeway et al., 2005; Walport, 2001). The antibody-bound cell is viewed as foreign, and the immune system then

attempts to eliminate it through cell lysis or phagocytosis (Dunkelberger and Song, 2009). For example, anti-CD20 ofatumumab binds to a distinct epitope of CD20 to induce CDC and effectively lyse B-cell lymphoma cell lines, that has shown benefits for patients with refractory lymphocytic leukemia (Teeling et al., 2004; Coiffier et al., 2008). Fc regions of antibodies can also activate antibody dependent cell-mediated cytotoxicity (ADCC) after interactions with Fc gamma receptors on effector immune cells (mainly natural killer cells, but also macrophages) (Ochoa et al., 2017). Effector cells, through their Fc gamma receptors, detect a target cell coated by antibodies and carry out its lysis through the use of granzymes and perforin. *In vivo* studies of trastuzumab and rituximab revealed that their clinical efficacy was dependent on the activation of Fc gamma receptors (Clynes et al., 2000).

The biggest setback of mAb therapy for cancer is the tendency for the cancer to acquire resistance to the antibodies by various mechanisms starting about 6 months after treatment (Uchida et al., 2004; Zahavi and Weiner, 2020; Torka et al., 2019). A change in the antigen density expression, a mutation in the receptor itself, or a shift in the cancer cell's cellular pathways are the most common causes of resistance to mAbs (Torka et al., 2019). In the case of rituximab, an IgG1 mAb directed against CD20, the efficacy diminishes in response to downregulation of CD20 expression, as seen in patients with B-Cell Non-Hodgkin Lymphoma (Torka et al., 2019; Manshouri et al., 2003; Keating et al., 2002). The common issue of resistance necessitates the administration of mAbs in conjunction with chemotherapy, but even this often only provides a limited duration of clinical benefit.

Antibody-Drug Conjugates (ADCs)

mAbs can also be used to deliver a toxic payload to the cancer cell. Antibody-drug conjugates (ADCs) consist of a mAb, linker and a highly active cytotoxic drug (Khongorzul et al., 2020). The advantage of ADCs over other options is their high specificity, as conferred by the mAb, in delivering cytotoxic compounds, such as calicheamicin, doxorubicin, auristatins, and

maytansine (Lu et al., 2016). The requirements for a successful ADC include a high binding affinity to the target receptor, ability to induce endocytosis in the target cancer cells, a highly selective endosomal cleavable linker that will allow for release of the cytotoxic drug, and the efficacy of the cytotoxic drug.

The choice of linker is especially important to ensure that the ADC remains stable in plasma during the time it takes for the ADC to localize its target cancer cell and to allow for the release of the cytotoxic drugs after internalization into the cell (Khongorzul et al., 2020). Non-cleavable linkers tend to be more stable in plasma than their cleavable counterparts, but cannot release their cytotoxic payload until the antibody is degraded in the lysosome. One such example is ado-trastuzumab emtansine (T-DM1; DM1 is a microtubule disrupting drug) which is delivered into cells that overexpress HER2 and reduces the cytotoxic exposure in normal cells (de Paula Costa Monteiro et al., 2015, Verma et al., 2012). Another thioether non-cleavable linker is N-succinimidyl-4-(N-maleimidomethyl)cyclohexane-1-carboxylate (SMCC), which was used to link an anti-CD242 monoclonal antibody and DM1 and tested against colon adenocarcinoma cells for their ability to kill CanAg-positive cells (Kovtun et al., 2006). Unfortunately, it was found that this ADC also killed neighboring cells that do not express the CanAg tumor antigen (Kovtun et al., 2006).

ADCs can also contain cleavable linkers that function in a variety of ways. Reducible linkers contain a disulfide link that take advantage of the increased intracellular glutathione concentration of cancer cells for cleavage (Balendiran et al; 2004; Wu et al., 2004; Khongorzul et al., 2020). Acid-cleavable linkers are designed to exploit the increasing acidity of the endosome-lysosome pathway. For example, gemtuzumab ozogamicin is an ADC used for patients with acute myeloid leukemia that consists of an anti-CD33 mAb and calicheamicin linked together by an acid-cleavable hydrazone linker that relies on a pH-dependent mechanism for drug release in the low pH environment of the lysosome (van der Velden et al., 2001; Hamann et al., 2002). Another example of a cleavable linker is the valine-citrulline-*p*-

aminocarbamate (VC-PABC) linker that relies on cleavage by lysosomal protease cathepsin B for cytotoxic drug release (Dorywalska et al., 2016). The β-glucuronide linker is another protease-sensitive linker that is hydrolyzed by the β-glucuronidase enzyme, prevalently found in lysosomes, to allow for release of the cytotoxic drug (Jaracz et al., 2005; de Graaf et al., 2002). The choice of linker is, therefore, a highly influential factor in the ultimate efficacy of an ADC.

In multiple tumor types, ADCs have proven to be a more effective targeted therapy over chemotherapeutic agents or mAbs on their own (Nasiri et al., 2018; McKertish and Kayser, 2021). Today, there are nine approved ADCs, including gemtuzumab ozogamicin (Mylotarg) for new or relapsed acute myeloid leukemia, trastuzumab emtansine (Kadcyla) for breast cancer, and polatuzumab vedotin (Polivy) for relapsed diffuse large B-cell lymphoma (Mckertish and Kayser, 2021). However, ADCs still face some limitations. First among them is off-target toxicity which can result either from the release of the cytotoxic drug into the blood stream or uptake into a healthy cell that presents the same receptor as the cancer cell, which in turn can result in hepatotoxicity, thrombocytopenia, neutropenia and possibly anemia (Ponziani et al., 2020; Hamblett et al., 2004). Moreover, a higher drug load (drug-antibody ratios of 8 compared to 2) can lead to faster clearance rates, thereby reducing the overall efficacy of the ADC treatment (Hamblett et al., 2004). ADCs also have the tendency to aggregate at any point during their development and storage which will interfere its ability to bind its target antigen (García-Alonso et al., 2018). The bystander effect, which is the passive diffusion and/or transport of cytotoxic payloads out from the cancer cells into the bloodstream or into neighboring cells, is also seen after ADC treatment (Malik et al., 2017). Drug resistance has also been seen with ADCs when cancer cells reduce their antigen levels, activate drug efflux pumps, and/or when they develop defects in either the trafficking pathways or lysosomal functions (Sifniotis et al., 2019).

Thus, there remains a need for a therapy that is more specific to its target cell while being more tolerable to the neighboring cells and tissues. It is in this context that

oligonucleotides would be better suited to take the place of the cytotoxic drugs in the ADC molecule.

Immunotherapy

Immune checkpoint inhibitors utilize anti-CTLA-4 or anti-PD-1 mAbs (such as nivolumab and pembrolizumab, respectively) to promote the overactivation of the immune system, which has shown clinical benefit in patients with melanoma, lung cancer, and renal cancer (Haanen and Robert, 2015; Spain et al., 2016). However, while being a significant medical breakthrough in the treatment of cancer, immune checkpoint inhibitor mAbs have also been observed to come with significant toxicities, termed immune-related adverse events, and the risk of over activating the immune system (Spain et al., 2016; Weber et al., 2012; Ibrahim et al., 2011). Even though many patients experience a significant tumor regression when treated by immune checkpoint inhibitors, these inhibitors do not lead to a beneficial response in most patients and cancer types, and those patients that do experience a response also subsequently experience tumor relapse later on (Bagchi et al., 2021). The efficacy of immune checkpoint inhibitors depends largely on the type of cancer, such as >80% in refractory Hodgkin's lymphoma patients to almost no response in mismatch repair-proficient colorectal cancer, and an average response rate of 20-40% for many other cancer types (Nayak et al., 2017; Le et al., 2015; Ribas and Wolchok, 2018). The efficacy of immune checkpoint inhibitors is dependent on the mutational burden of a tumor, wherein a tumor with low mutational burden will respond weakly or not very well, as in the case of prostate, pancreatic, and even certain subtypes of colorectal cancer (Le et al., 2015; Maleki Vareki, 2018; Bagchi et al., 2021).

Another type of immunotherapy involves the engineering of autologous T cells to express a fusion of the T cell receptor intracellular domain and the antigen binding domain of a B-cell receptor to reprogram T cells to attack cells that have the designated tumor-specific antigen (Kennedy and Salama, 2020). The most promising results for CAR-T cell therapy have

been observed against hematological malignancies, such as B-cell lymphoblastic leukemia and refractory or diffuse large B-cell lymphoma, (Maude et al., 2018; Schuster et al., 2019; Locke et al., 2019). Unfortunately, patients will often experience cytokine release syndrome adverse events of variable severity and may also encounter a progression of immune effector cell-associated neurotoxicity syndrome that includes tremors, dysgraphia, apraxia, and expressive aphasia, and upon higher levels of neurotoxicity also seizures (Frey and Porter, 2019; Lee et al., 2019; Santomasso et al., 2018). Cancer immunotherapies have shown much promise in certain types of cancers in certain patients, but unfortunately, they are not effective in many other patients and can produce significant toxicities (Kennedy and Salama, 2020).

OLIGONUCLEOTIDE THERAPEUTICS

Oligonucleotide-based therapeutic approaches hold a unique advantage over many of the previously discussed therapeutic options. Oligonucleotides can theoretically and effectively target any and all oncogenes and currently “undruggable” genes (Dowdy, 2017). Oligonucleotides can be synthesized with high sequence specificity in a scalable manner and are streamlined to be easily customizable based on the desired target sequence. Whereas the cytotoxic drugs delivered by an ADC will kill healthy and cancer cells alike if they share the same receptors, an oligonucleotide can be designed to target only the mutated form of an oncogene that will spare healthy cells expressing the wild type version of the same gene due to the high level of complementarity required between the oligonucleotide and its target (Lam et al., 2015).

Although there are a variety of oligonucleotide therapeutics, the focus of the present dissertation will be on antisense oligonucleotides (ASOs) and short interfering RNAs (siRNAs). While in principle, these oligonucleotides hold much promise for the treatment of cancer and other diseases, they face significant challenges that prevent them from producing a satisfactory target knockdown in cancer cells *in vivo*. The past several decades have seen extensive efforts

in addressing the most prominent barriers (Stec et al., 1998; Fire et al., 1998; Khvorova and Watts, 2017).

Antisense Oligonucleotides

ASOs are single stranded oligonucleotides of 16 to 28 nucleotides in length that primarily effect their knockdown function against their target mRNA molecules inside the nucleus of the cell (Scoles et al., 2019). The first ASO was synthesized in 1978 in the laboratory of Paul Zamecnik (Stephenson and Zamecnik, 1978; Zamecnik and Stephenson, 1978). This ASO was designed to target the sequence of the Rous sarcoma virus 35S RNA and 70S RNA that led to the successful inhibition of virus production (Stephenson and Zamecnik, 1978; Zamecnik and Stephenson, 1978). There are three possible mechanisms of action that an ASO can function: 1) steric blocking of target RNA to prevent translation, 2) steric blocking of pre-mRNA to induce splice switching, and 3) RNase H mediated degradation.

Steric blocking ASOs bind to the target RNA through Watson-Crick base pairing and form a steric blockade to prevent the ribosome from interacting with the mRNA of interest, thereby suppressing its translation into a protein (Kole et al., 2012). For example, steric blocking ASOs were screened against beta-site amyloid precursor protein cleaving enzyme 1 (BACE1), that is partly responsible for cleaving the precursor amyloid protein into amyloid beta in Alzheimer's patients (Chakravarthy and Veedu, 2019). A specific ASO sequence, named AO2, was observed to successfully downregulate BACE1 mRNA levels (Chakravarthy and Veedu, 2019). A different study demonstrated the ability of a steric blocking ASO, radavirsen, to block the translation of influenza A proteins and interfere with influenza virus replication and conferred protection from viral infection in a preclinical ferret influenza model (Beigel et al., 2017; Smith and Zain, 2019). These modified ASOs were well tolerated and effective at protecting ferrets from influenza infections compared to the placebo group (Beigel et al., 2017).

Splice switching ASOs base-pair with pre-mRNAs to modulate their splicing patterns. By blocking the protein-RNA binding or snRNA-RNA pairing, splice switching ASOs can interfere with the splicing components by either effectuating exon skipping or exon inclusion (Havens et al., 2016). Both small nuclear RNAs (snRNAs) and proteins function in concert to direct the spliceosome to the correct sites of the pre-mRNA for splicing and this can result in a variety of combinations of final mRNA that arise from a single gene (Lee and Rio, 2015). When splice switching ASOs bind to the target sequence, they sterically block that location and thereby prevent splicing factors from accessing the pre-mRNA at that location which leads to a modification in the splicing and the final resulting mRNA (Havens et al., 2016). Among the most recent and well-known examples of a successful splice switching ASO is nusinersen (Spinraza) for the treatment of spinal muscular atrophy (SMA) (Finkel et al., 2017; Mercuri et al., 2018). Similar splice switching ASOs are being used or are in development for Duchenne's Muscular Dystrophy and Huntington's Disease (Smith and Zain, 2019).

The third type of ASO is called a gapmer ASO that is characterized by a ~16-20 nt long oligonucleotide of 10 internal "Gap" DNA bases flanked on both sides by 3-5 RNA bases (Shen et al., 2018; Aguti et al., 2020). Gapmer ASOs rely on the activity of RNase H, an endogenous endonuclease enzyme that catalyzes the cleavage of RNA within an RNA/DNA duplex. Gapmer ASOs promote RNA degradation by binding to the target mRNA in the nucleus and then recruiting RNase H to cleave the mRNA portion of the RNA/DNA duplex (Roberts et al., 2020; Gagliardi and Ashizawa, 2021). RNase H requires a stretch of about 6-10 complementary bases in the RNA-DNA duplex for its catalytic activity to be possible. Gapmer ASOs, as all other ASOs, also have further chemical modifications to enhance their potency and stability and to promote their activity, as will be discussed later. While ASOs have been traditionally assumed to be active primarily in the nucleus, a more recent study has suggested that the RNase H enzyme localizes in both the nucleus and cytoplasm and can be active in both locations, though its activity in the cytoplasm is generally not well understood (Liang et al., 2017).

After the RNAse H enzyme cleaves the RNA portion of an mRNA transcript in the DNA-RNA duplex, the ASO is then released and can continue unhindered to find the next mRNA target to bind to for repeated cycles of RNase H recruitment and mRNA degradation (**Figure 1.1**). In this manner, Gapmer ASOs knockdown their target mRNA and reduce protein expression.

RNA Interference

Micro RNAs (miRNAs) and siRNAs are the effector molecules of RNAi, a gene silencing pathway that occurs via cleavage of mRNAs. The RNAi mechanism was first discovered in an exogenous double-stranded RNA molecule from *Caenorhabditis elegans* that could effectively knock down gene expression (Fire et al., 1998). RNAi swiftly brought great hope for its potential to treat human disease after it was established that 21-nt synthetic siRNAs could knockdown the expression of targeted genes *in vitro* in mammalian cells (Elbashir et al., 2001). RNAi relies on a ribonucleoprotein complex called the RNA-induced silencing complex (RISC) that minimally contains a member of the Argonaute (Ago) family and the antisense or guide strand from the siRNA or miRNA (Ender and Meister, 2010; Pratt and Rae, 2009). The RISC complex silences target gene expression in a highly sequence specific manner, dependent on the guide strand RNA (~20-30 nt) that is bound to the Ago protein (Wilson and Doudna, 2013). Both miRNAs and siRNAs have similar mechanisms of action that underscore key aspects of gene silencing that heavily impact the therapeutic prospects of RNAi-based approaches.

miRNAs are endogenously expressed, noncoding dsRNA molecules from 19 to 27 nucleotides (nt) in length that modulate many cellular pathways involved in development, growth and proliferation, tissue differentiation, and regulate the nervous system, immunity, and the response to viral infections (Bartel, 2004; MacFarlane and Murphy, 2010). For this reason, it is known that many diseases, including cardiovascular and gastrointestinal diseases and cancer,

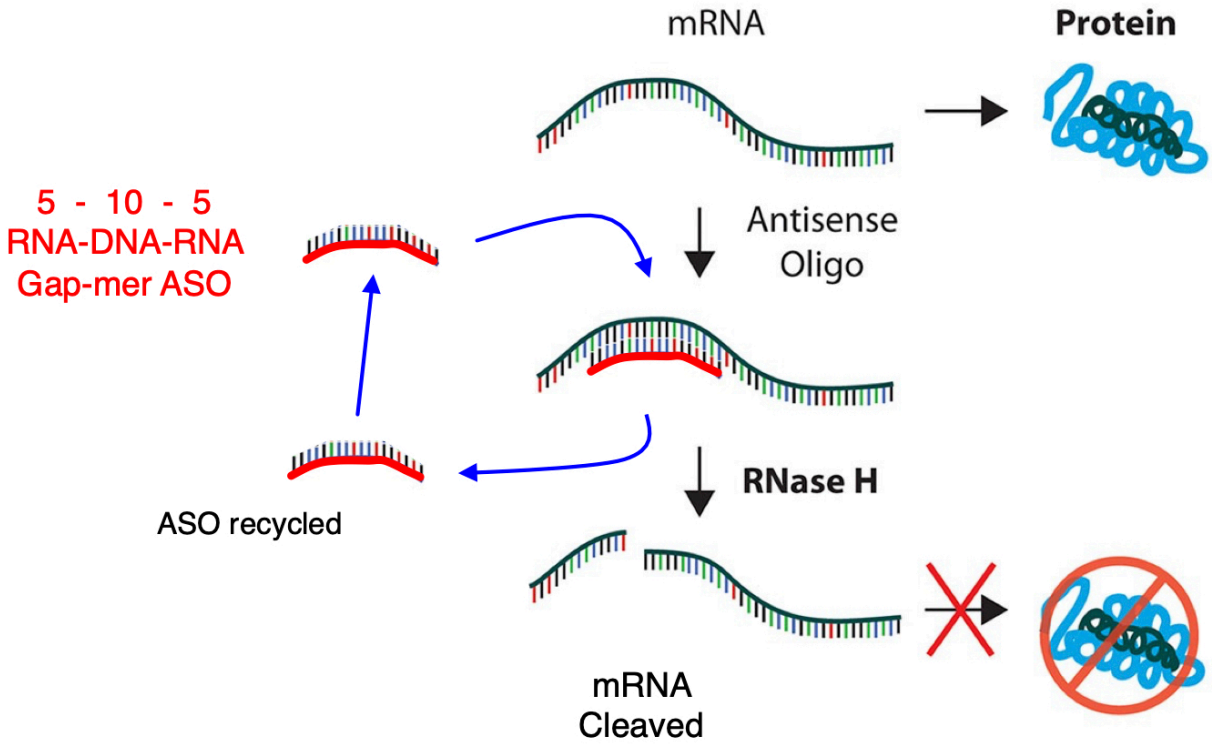

Figure 1.1. Gapmer ASO Mechanism of Action
Gapmer ASOs consist of RNA bases flanking a central 10-nt long DNA region (5-10-5 pattern; note that there are also commonly 3-10-3 gapmer ASOs used). Once inside the nucleus, a gapmer ASO will bind its mRNA target which will lead to the recruitment of the RNase H enzyme. RNase H recognizes and cleaves the RNA portion of the DNA-RNA duplex, thereby degrading the targeted mRNA transcript. The ASO is released and will search for its next mRNA target to bind.

are associated with a dysregulation of miRNAs (Huang et al., 2011). miRNAs bind to target mRNAs through Watson-Crick base pairing that results in either mRNA cleavage or inhibition of translation. Because miRNAs do not bind with full complementarity to their targets, a single miRNA can regulate dozens or even hundreds of distinct mRNA transcripts (Lu et al., 2008; refs). While the seed region of the miRNA, that runs from nucleotides 2 through 8 makes the first critical contact with the target mRNA, some binding to target mRNAs has been shown to occur with only three nucleotides (2-5) of the seed region (Herzog and Ameres, 2015).

The first step of the miRNA production pathway is the transcription of primary micro RNAs (pri-miRNAs) from long noncoding RNAs by RNA polymerase II in the nucleus followed by capping, splicing and polyadenylation (Lin and Gregory, 2015). This pri-miRNA contains at least one double-stranded hairpin loop domain that is recognized and cleaved by the microprocessor complex that consists of the Drosha enzyme, an RNase III enzyme, and RNA binding domain-containing partner DiGeorge syndrome critical region gene 8 (DGCR8) (Kim and Kim, 2007; Han et al., 2006). After the microprocessor complex cuts the hairpin, the resulting 60-70 nt precursor miRNA (pre-miRNA) is exported to the cytoplasm with the help of Exportin 5, a Ran-GTP-dependent cytoplasmic cargo transporter (Lund et al., 2004; Azlan et al., 2016). In the cytoplasm, a complex made of RNase enzyme Dicer and dsRNA-binding protein TAR RNA-binding protein (TRBP) further cleaves the pre-miRNA into the final mature miRNA with 5’ phosphates, 3’ dinucleotide overhangs, and a final length between 19-27 nt (Chendrimada et al., 2005; MacRae et al., 2007). TRBP loads the mature miRNA onto any of the four Argonaute family members (Ago 1-4). However, only Ago2 contains an active endonuclease catalytic site with the ability to specifically cleave target mRNAs (Meister, 2013).

Once loaded with a miRNA, the resulting complex is referred as the RISC-loading complex (RLC) (MacRae et al., 2008). Only the guide (antisense) strand of the double-stranded miRNA is loaded into the RISC complex, while the passenger (sense) strand is discarded. For miRNAs, this strand selection depends, in part, on the weaker thermodynamic stability of the 5’

end of a strand and/or preferentially loads the strand with a 5'U as the first base (Preall et al., 2006; Azlan et al., 2016). The RISC complex, loaded with the guide strand, is now active and will roam the cytoplasm for target mRNAs. Upon encountering its target mRNA, it will bind via complementary base pairing of the seed region to prevent its translation. However, only an siRNA with complete complementarity to the target mRNA sequence, and not a miRNA with incomplete complementarity, can activate the Ago2 slicing activity, though binding can still occur with both types of RNA (Lam et al., 2015).

Unlike miRNAs, siRNA processing and activity occurs entirely within the cytoplasm of the cell. When a double stranded RNA (dsRNA) is introduced, whether from a virus or synthetically produced, Dicer will process it into a 21-23 nt-long siRNA molecule (Bernstein et al., 2001). At this point, it will be loaded into the RISC complex to perform its RNAi activity. siRNAs are typically characterized by a 19 to 23 nt RNA duplex with a 2 nt 3' overhang, 5'-phosphate groups, and 3' hydroxyl groups (Murchison et al., 2005). Synthetic siRNAs made in this form do not require Dicer processing. Instead, the siRNA will be recognized by TRBP and rapidly loaded into Ago2 directly (Murchison et al., 2005). In the case of longer double stranded RNA molecules (25-27 nt), a 3' 2-nt overhang is recognized and bound by the Dicer PAZ domain to form a Dicer-substrate siRNA (dsiRNA) that has been shown to have an equally effective ability to knockdown mRNA expression (Sakurai et al., 2011; Snead et al., 2013). Like miRNAs, siRNAs also consist of two strands: the passenger (sense) strand and the guide (antisense) strand. Both miRNAs and siRNAs can be loaded into all four members of the Ago family to form the pre-RISC complex, but only Ago2 will have the mRNA slicing function (Meister et al., 2004; Yoda et al., 2010). In all cases, the sequence specificity of the RISC complex is dependent on the seed region of the guide strand (nucleotides 2-8) binding to target mRNAs (Ha and Kim, 2014; Schirle and MacRae, 2012). Unlike miRNAs, siRNAs bind to target mRNAs with perfect or near perfect base complementarity that leads to the efficient Ago2 slicer activity to cleave target mRNAs with a very high sequence selectivity (Lam et al., 2015). Conversely,

there is considerable tolerance of mismatches between a miRNA guide strand and target mRNAs (Carthew and Sontheimer, 2009) that in turn leads to regulation of expression of over a third of all human genes (Kim et al., 2009). siRNAs have been studied more extensively for their potential as a therapeutic in many human diseases. Like ASOs, siRNAs have the potential to target undruggable oncogenes and other aberrant genes that are not accessible by SMIs or mAbs alone. For this reason, siRNAs hold a great therapeutic promise over other treatment modalities. A simplified model of the siRNA RNAi mechanism of action is shown in **Figure 1.2**.

BARRIERS AGAINST THERAPEUTIC RNA ENTRY INTO CELLS

The emergence of the lipid bilayer during the prebiotic era was the central development in the history of life that allowed for the formation of primitive cells. This amphipathic lipid bilayer allowed self-aggregation in the aqueous environment of past eras that led to the compartmentalization of molecules within small vesicles, within which were likely self-replicating RNA molecules capable of performing various primitive functions (Alberts et al., 2002). Inside the lipid bilayer vesicle, chemical and metabolic reactions were allowed to develop and over many millions of years, multiple cellular components arose and evolved in function and complexity. Eventually ribozymes and later ribosomes came along that allowed for more complex protein synthesis (Neveu et al., 2013). Lipid bilayers have protected all the internal components of a cell and at some point, the cell acquired the ability to assemble, grow, and divide (Blain and Szostak, 2014). Over many millennia, cells developed more complex mechanisms to maintain their internal conditions and processes. This was necessary because foreign nucleic acids, especially exogenous invading RNAs, are exceptionally dangerous to the stability and health of any cell and organism. So, it is no surprise that with more time, cellular defenses against RNAs increased in various ways.

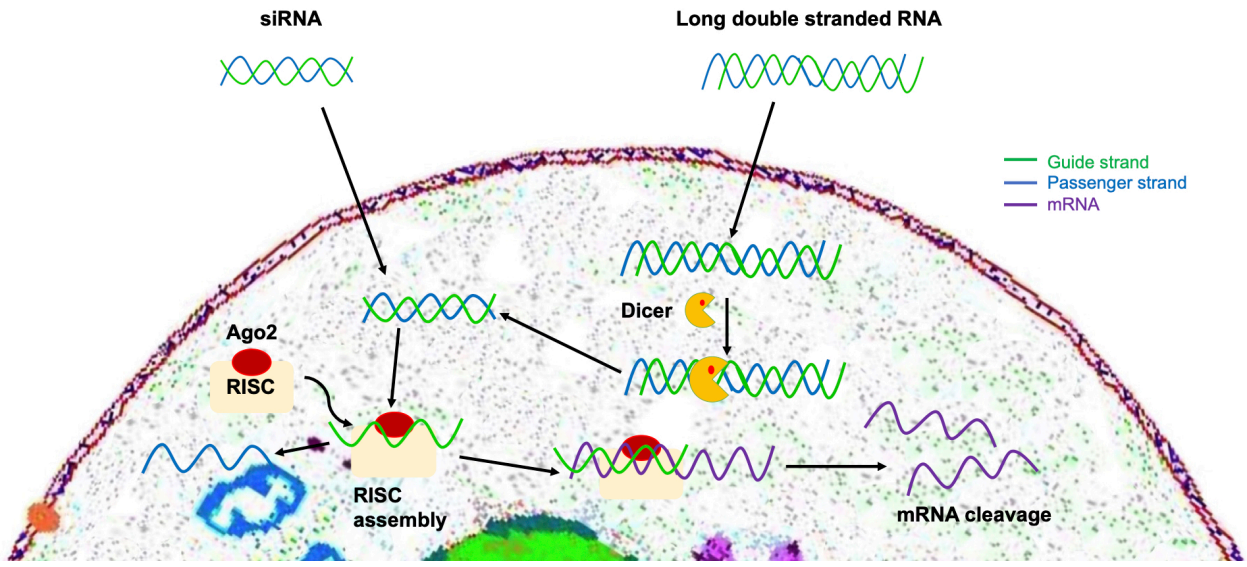

Figure 1.2. RNA Interference (RNAi) Mechanism of Action.
When a synthetic siRNA molecule is introduced into the cytoplasm of a cell, it is loaded into the RISC complex which contains Argonaute 2 (Ago2). The passenger strand is discarded from the pre-RISC complex and the resulting RISC complex binds with high specificity to its target mRNA sequence in the cytoplasm. The target mRNA is then cleaved and the active RISC complex can continue cleaving more of the same mRNA transcript to ultimately silence the target gene. Similarly, viral long double-stranded RNA is first cut by the Dicer enzyme to become siRNA after which the same process for mRNA targeting will occur.

The lipid bilayer that surrounds every cell is so robust that only small neutral molecules (<1,000 Daltons, Da) can passively diffuse across it (Blain et al., 2014; Abe and Fujiyoshi, 2016). But, highly charged, macromolecular RNAs are unable to enter by passive diffusion. In addition, there is also a prevalent ribonuclease activity present in serum. Moreover, other evolutionary defenses enacted by cells to protect cells against foreign RNAs include the innate immune system's endosomal toll-like receptors (TLRs) 3, 7, and 8, and double-stranded RNA receptors retinoic acid inducible gene I (RIG-I) and melanoma differentiation associated protein 5 (MDA-5) (Dowdy, 2017). A further challenge is that naked or unmodified RNA molecules are eliminated by scavenger receptors on liver hepatocytes and filtered out of the blood by the kidneys (Juliano et al., 2012; Iversen et al., 2013). These barriers necessitate a strategy for successful oligonucleotide delivery.

Oligonucleotide Size and Charge

Due to their small size of 1000 Da or less, small-molecule drugs can passively diffuse across the cell's lipid bilayer membrane, whereas larger molecules like double-stranded siRNA (~14,000 Da) are unable to cross passively. A small molecule (<1,000 Da) that has the right combination of small size, polarity, and hydrophobicity can cross the lipid bilayer (Lipinski et al., 2001; Lipinski, 2004). In this case, no membrane or carrier proteins are required nor any energy expenditure by the cell; rather, the molecule simply partitions into the lipid bilayer, diffuses across it, and is released into the cytoplasm (Cooper, 2000). Based on the permeability coefficient calculations, polarity and size, there are highly variable rates of diffusion across the membrane (Yang and Hinner, 2015). Regardless of the rate of passive diffusion, the biggest advantage of therapeutic small molecules is their ability to enter a cell without assistance. In contrast, siRNAs are far too big to accomplish this task. A naked siRNA is also highly charged, with a typical double-stranded siRNA containing 40 negatively charged phosphates in its

backbone (Dowdy, 2017). Molecules that are highly negatively charged have very poor cellular permeability rendering them useless without a delivery vehicle (Stewart et al., 2018).

Ribonuclease Degradation of RNA

Crossing the lipid bilayer is not the only challenge of a naked siRNA molecule. Ribonucleases (RNases) catalyze the degradation of RNA molecules and are abundantly found in serum where they rapidly degrade RNA. RNases are also overexpressed in certain cancers, leading to the exacerbation of the disease state (Loverix and Steyaert, 2003). For potential therapeutic siRNAs, the consequence is their elimination before they come into close contact with the target cancer cell. RNases are the first barrier that an siRNA encounters in the human body, and 99% of native, 2'-OH single-stranded RNA is degraded within seconds in blood (Tsui et al., 2002). While double-stranded RNA, such as siRNA, is more stable in general, it is also rapidly degraded in a matter of minutes when exposed to human blood (Gao et al., 2009). RNases greatly inhibit an siRNA's circulation time and prevent siRNA s from accumulating in the desired tissue at a sufficiently high concentration to be of therapeutic benefit. The susceptibility of siRNAs to RNases in serum has been observed and confirmed by multiple approaches, including MALDI-TOF spectrometry (Turner et al., 2007). siRNA-based therapies can be encapsulated within lipid nanoparticles (LNPs) of various types to protect them from degradation by RNases while in circulation (Ashley et al., 2012). This results in a very poor diffusion coefficient that primarily only targets liver hepatocytes and macrophages (Dowdy, 2017). Alternatively, chemical modifications to the RNA backbone, specially at the 2' position, can be installed during oligonucleotide synthesis to enhance siRNA stability.

Reticuloendothelial System

The reticuloendothelial system refers to a collection of phagocytic cells throughout the connective tissues in the body that clear toxins, immune complexes, bacteria, and other foreign and potentially dangerous antigens from circulation (Canalese et al., 1982; Springer and Dowdy, 2018; Tang et al., 2019). Reticular connective tissues are found in the kidney, spleen, lymph nodes, and bone marrow and the overall reticuloendothelial system also includes alveolar macrophages and Kupffer cells in the liver (Canalese et al., 1982; Kasravi et al., 1995). This poses a problem for siRNAs because they will be either rapidly degraded while in circulation by RNAse, excreted by the kidneys or pulled out of blood by liver scavenger receptors before the siRNA ever gets the chance to hit its target (Dowdy, 2017).

The kidney's glomerular endothelial cells have large open fenestrae and a charged surface layer that helps maintain a charge-selective barrier to form the glomerular filtration barrier (Daehn and Duffield, 2021). The glomerular filtration molecular weight cutoff is ~60 kDa, dependent on size and charge, but also influenced by molecular radius and conformation of the compound in question. Compounds over 30 kDa are excreted at slower, variable rates, while those lower than 30 kDa are eliminated far more quickly and efficiently (Meibohm and Zhou, 2012). Because of this, it was observed that conjugating a polyethylene glycol (PEG) molecule to an siRNA improved its blood circulation time by about 4-fold over the naked siRNA control which confirmed that increasing the size of the siRNA-conjugate also improves its bioavailability *in vivo* (Iversen et al., 2013).

Scavenger receptors on the liver's hepatocytes and Kupffer cells are actively involved in removing foreign substances and toxins from circulation. Scavenger receptors have been observed to uptake dsRNA very efficiently, such as in the case of *Drosophila* S2 cells that efficiently internalized dsRNA (Ulvila et al., 2006) and in tick cells expressing scavenger receptor CD36 that internalized exogenous dsRNA to mediate an RNAi response (Aung et al., 2011). These scavenger receptors play a role in the viral entry of hepatitis C, macrophage

activation and lipid uptake and liver disease as well (Armengol et al., 2013). Elimination of RNA molecules by the kidney and scavenger receptors is very problematic for the pharmacological potential of any RNA-based therapeutic. Thus, without protection, having an siRNA in circulation becomes an unfeasible therapeutic strategy.

Innate Immunity

The innate immune system interferes with the proper function and delivery of exogenous RNA molecules. Double stranded RNA is a hallmark of viral infection that is recognized as dangerous and triggers an innate immune response (Whitehead et al., 2011). The innate immune system's recognition of a double stranded RNA molecule will lead to an inflammatory response that includes high levels of cytokines and interferons (Robbins et al., 2009). There are innate immune receptors both inside and outside of cells.

Toll-Like Receptors (TLRs) are pathogen-associated molecular patterns (PAMPs) that recognize single and double stranded nucleic acids, primarily by their phospho-ribose backbone (Heil et al., 2004; Mogensen, 2009; Whitehead et al., 2011). TLR3, TLR7, and TLR8 are the main antagonists of synthetic, double stranded siRNAs (Heil et al., 2004; Karikó et al., 2004). TLR3 recognizes viral dsRNA and is expressed in the endosome of peripheral blood mononuclear cells (PBMCs) and other cells such as dendritic cells as well as some epithelial cells including airway, corneal, cervical, biliary, and intestinal, as well as in astrocytes and glial cells, and some of these express it on the cell surface too (Akira et al., 2006, Maitra et al., 2017). The recognition of dsRNAs by TLR3 leads to the activation of the NF-kB and IRF3 transcription factors which ultimately increases the expression of type I interferons and other pro-inflammatory cytokines like TNF-α (Maitra et al., 2017). Conversely, TLR7 and TLR8 detect both short dsRNAs (19-21 bp) and single stranded RNA (ssRNA) (Karikó et al., 2004; Schön and Schön, 2008). TLR7 and TLR8 are expressed at high levels in dendritic cells and

monocytes, respectively, and function through different molecular adaptors to achieve the same outcome as TLR3, namely, an increased inflammatory response through cytokines (Gantier and Williams, 2007).

RIG-1 and RIG-1-like receptors (RLRs) are cytosolic sensors of viral infection that are widely expressed in most cell types and can be activated by viral RNA to initiate a type I-interferon immune response (Liu et al., 2018; Li et al., 2014). Furthermore, characteristics of exogenous RNAs that trigger a RIG-I response include the presence of a 5' triphosphate, RNAs with uncapped 5' diphosphate groups, and a 5' terminal nucleotide that is unmethylated at the 2'-O position (Rehwinkel and Gack, 2020).

MDA-5 is another RLR that, like RIG-1, is both ubiquitously expressed and able to recognize exogenous double stranded RNAs (Yoneyama et al., 2005). RLRs contain an RNA helicase core that enables recognition of dsRNA, binding, and recruits an adaptor of MAVS (Chow et al., 2018). This leads to the activation of a complex signaling cascade that ultimately results in a heightened inflammatory response aimed at eliminating the invading dsRNA (Chow et al., 2018).

Innate immunity poses a significant challenge for the successful delivery and function of nucleic acid-based therapeutics, especially siRNAs. Fortunately, extensive research and experimentation has led to the identification of several chemical modifications that can be synthetically introduced into oligonucleotides to minimize recognition by innate immune response receptors and thereby avoid an adverse innate immune response.

Chemical Modifications of siRNAs and ASOs

The success in knocking down target gene expression by siRNAs *in vitro* increased hope in the potential of RNAi for the field of medicine. However, the success of RNAi was significantly dampened when siRNAs were brought *in vivo*, largely due to the reasons discussed in the preceding section: too large and charged, RNase susceptibility, fast elimination by the

kidneys and liver, and activation of the innate immune system. However, after extensive experimentation, development of synthetic chemistry for oligonucleotides has led to the customizable incorporation of chemical modifications to overcome many, but not yet all, of the barriers to RNA delivery.

Modifications of an siRNA strand are limited by certain requirements that are necessary for the function of RNAi machinery inside cells. TRBP, the RISC loading enzyme, binds exclusively to dsRNA (not dsDNA nor DNA-RNA hybrids) with the aid of two of its double-stranded RNA binding domains (dsRBDs) to position the dsRNA into the proper conformation (Vukovic et al., 2014). TRBP's dsRBDs fit into three grooves of A-form dsRNA that are highly dependent on RNA's 2'-OH groups and phosphate groups that line the backbone (Vukovic et al., 2014). Importantly, TRBP does not come in contact with any of the nucleobases in the dsRNA and thereby allows for the sequence-independent loading of thousands of endogenous miRNAs and ectopically introduced siRNAs (Schirle et al., 2016; Rettig and Behlke, 2012). Argonaute 2 (Ago2) within the RISC complex is responsible for site selective slicing activity. Ago2 function depends on several contacts with the guide strand: the 5'-terminal phosphate, 3'-OH binding to the Ago2 PAZ domain, and several sections of the phosphodiester backbone (Schirle et al., 2016; Schirle and MacRae 2012; Rettig and Behlke, 2012). Ago2 preferentially functions with siRNAs 19-27 nt long, while guide strands shorter than 19 nt led to a significant reduction of RNAi-mediated knockdown (Hagopian et al., 2017).

Extensive research from the design of ASOs has been adapted to siRNAs as well, though siRNAs have more stringent modification requirements to ensure proper hybridization and compatibility with the RNAi machinery in the cell. There are several classes of modifications that can generally be made to oligonucleotides: modifications of the backbone, modifications of the ribose sugar, and modifications of the nucleobase itself.

Backbone modifications most often center on the substitution of phosphates with phosphorothioate groups. Phosphorothioate groups are similar to phosphodiester linkages

except for the replacement of one of the oxygens with a sulfur atom, that creates a chiral center and numerous resulting stereoisomers, depending on ASO length (**Figure 1.3a**) (Eckstein, 2014; Dowdy, 2017). This can potentially impact enzymatic interactions, though there is conflicting evidence on this matter with some studies suggesting the importance of an ASO's stereoisomerism (Stec et al., 1998), while others found an optimal activity with ASOs containing a random mixture of phosphorothioate stereoisomers (Wan et al., 2014). Phosphorothioate groups in the backbone confer significant stability against nucleases, increased bioavailability due its ability to bind plasma proteins like albumin, and consequently remain in circulation for a longer duration, and a reduction in immune stimulation due to the absence of the characteristic unmethylated CpG dinucleotides that are prevalent in regular phosphodiester ASOs, all while maintaining functional compatibility with the RNase H cleavage mechanism (Eckstein, 2014). Furthermore, a full PS backbone gives ASOs a significantly improved ability for cell uptake, crossing the endosomal lipid bilayer without a transfection or delivery agent, by an unknown mechanism called gymnosis (Stein et al., 2010). So great are the benefits, that phosphorothioate groups are routinely incorporated into ASOs today.

Phosphorothioate groups are also included into the design of siRNAs, but to a lesser extent due to the constraints of the endogenous RNAi machinery. Ago2 tolerates one to two phosphorothioates at the ends of both siRNA strands, a modification that is possible because TRBP binds the siRNA strand around the center of the molecule. This modification improves the stability, potency, and duration of RNAi response (Dowdy, 2017). Phosphorothioate modifications on siRNA strands have been incorporated into RNAi-therapeutics being clinically tested, such as Alnylam's/Novartis' inclisiran (Fitzgerald et al., 2017), which has been approved in Europe and is pending FDA approval in the United States.

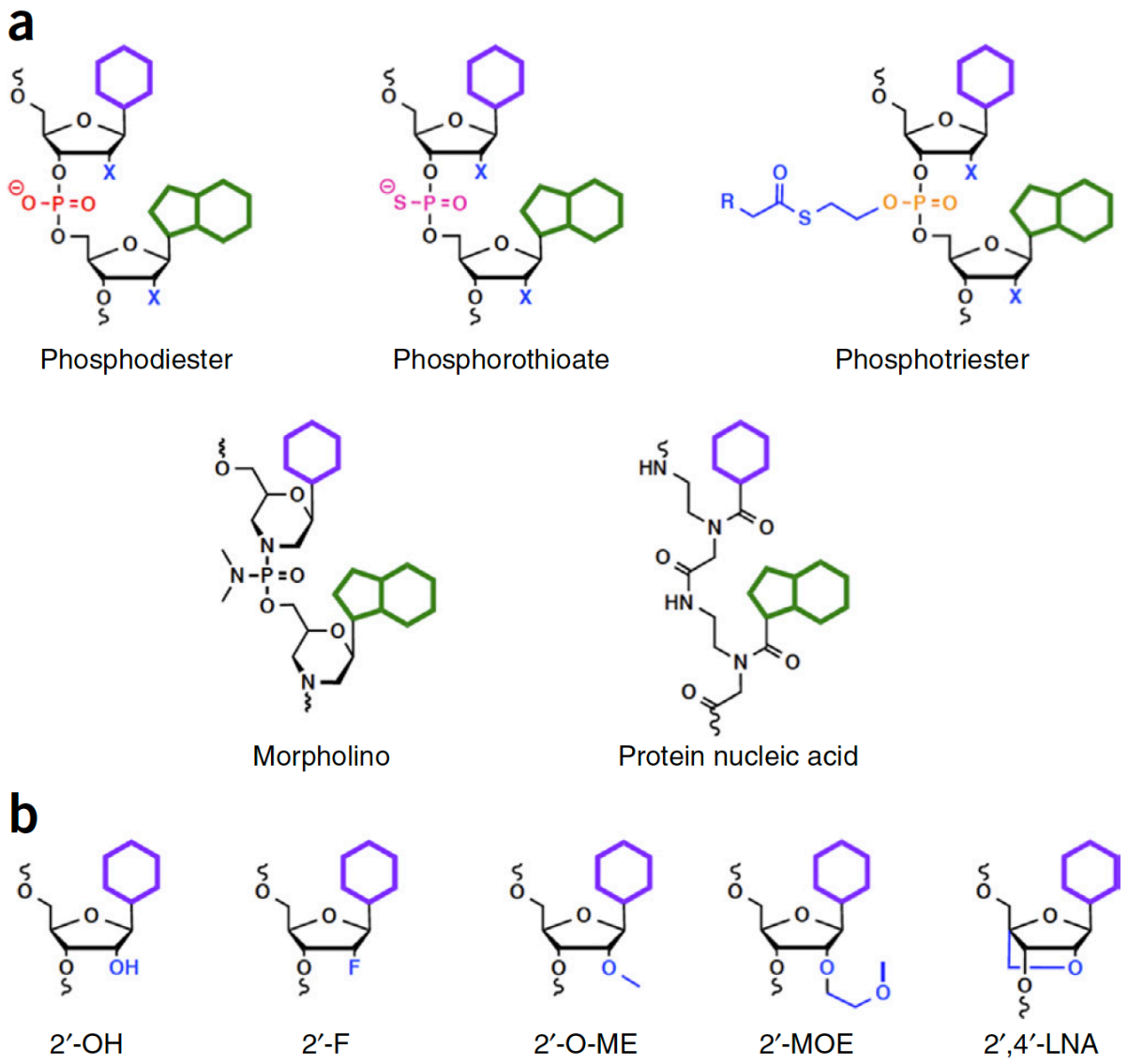

Figure 1.3. Common Modifications used in ASOs and siRNAs
(a) The phosphodiester linkage is ordinarily found in RNA and DNA molecules and is negatively charged. Modifications to the oligonucleotide backbone include the phosphorothioate group, marked by the replacement of a negatively charged oxygen with a sulfur, a neutral-charge phosphotriester group, neutral-charge morpholino (PMO), and peptide nucleic acid (PNA).
(b) 2'-OH is ordinarily found in unmodified RNA molecules. Modifications to the sugar occur at the 2'-position and include: 2'-fluoro (F), 2'-hydroxymethyl (O-Me), 2'-methoxyethyl (MOE), and other bicyclics with an O-methylene bridge (locked nucleic acids, LNA).

Taken from Dowdy, 2017.

A unique alternative approach to overcome the problem of the highly negatively charged backbone of an siRNA molecule was addressed by the development of neutral phosphotriester groups (**Figure 1.3a**). The irreversible phosphotriester groups were originally explored in single stranded DNA ASOs for charge neutralization experiments; however, due to the constraints imposed by the RISC machinery, this modification was not investigated in the context of RNAi (Krishna and Caruthers, 2012; Dellinger et al., 2003). More recently, short interfering ribonucleic neutrals (siRNNs) with bioreversible phosphotriester groups were developed in the Dowdy lab with the unique capability to induce RNAi responses (Meade et al., 2014; Hamil et al., 2017). siRNNs contain any of several bioreversible phosphotriester groups in its backbone that neutralize the negative charge and are resistant to RNases. Upon reaching the cytoplasm, the phosphotriesters are cleaved off by cytoplasmic restricted thioestereases to convert the siRNN into an active and native phosphodiester backbone siRNA. These siRNNs also contain 2'-modifications and were shown to be biologically active and able to successfully mediate an RNAi response *in vitro* to knock down GFP expression and *in vivo* when conjugated to a liver-targeting domain (Meade et al., 2014).

Phosphorodiamidate morpholino oligomers (PMOs), or morpholinos, use an alternate antisense oligonucleotide backbone chemistry to fix the backbone in place (Summerton and Weller, 1997; Summerton, 2007). In a morpholino, the morpholine ring replaces the ribose sugar and the phosphodiester linkages of the backbone are replaced with phosphorodiamidate linkages (**Figure 1.3a**). The morpholino structure affords the oligonucleotide a significantly higher stability against nucleases. Despite the chemical modifications that comprise a morpholino, it still maintains the ability for Watson-Crick base pairing to effectively block translation of target mRNA (Summerton and Weller, 1997).

Peptide nucleic acids (PNAs) are another type of oligonucleotide analogue where the traditional sugar-phosphate backbone has been removed and replaced with a pseudopeptide amide backbone comprised of N-(2-aminoethyl)glycine units (**Figure 1.3a**). Like PMOs, PNAs

bind RNA and DNA molecules with high specificity via Watson-Crick base pairing and greater stability than RNA. PNAs are also resistant to nuclease and protease degradation, though their solubility remains problematic (Menchise et al., 2003). PNAs also maintain intramolecular distances and configuration between each unit that matches natural DNA or RNA molecules to promote specific hybridization and thereby have greater stability than RNAs due to their uncharged nature (Rathee et al., 2012). Due to their structural characteristics, neither PMOs nor PNAs are capable of recruiting RNase H for target mRNA degradation, instead both function as steric blockers or splice switching oligonucleotides (Dowdy, 2017).

Sugar modifications are among the best studied modifications in oligonucleotides. Replacing the characteristic 2'-OH group on the ribose sugar with a 2'-Fluoro (2'-F) or a 2'-O-methyl (2'-OMe) is critical to reduce degradation by RNases, reduce innate immune recognition and response, and improve the RNA binding affinity (Dowdy, 2017). For ASOs, a 2'-methoxyethyl (2'-MOE) modification further increases an RNA against nuclease degradation and confers an increase in binding affinity (Khvorova and Watts, 2017). Refer to **Figure 1.3b.** These 2'-modifications recapitulate the biophysical properties of the unmodified RNA 3' pucker (Khvorova and Watts, 2017). The 2'-F modification, for example, is well-tolerated by the RNAi machinery because it shares similar electronegativity to the native 2'-OH group (Blidner et al., 2007). These 2'-modifications allow the siRNA itself to maintain a proper A-form RNA structure that conforms with TRBP and Ago2 binding requirements (Wang et al., 2009; Ipsaro and Joshua-Tor, 2015).

For siRNAs, varying combinations of 2'-OMe and 2'-F with no 2'-OHs, combined with terminal phosphorothioate groups in the backbone lead to greater efficiency in the assembly of the RISC complex and RNAi activity and duration of response (Allerson et al., 2005; Dowdy, 2017, Khvorova and Watts, 2017). Experimentation with 2'modifications (mainly 2'-F and 2'OMe) of the whole siRNA in alternating patterns ultimately led to enhanced stability chemistry (ESC) design for better RNAi responses (Foster et al., 2018). The ESC design includes full 2'-

modification of the entire double stranded molecule and dual terminal 5'-phosphorothioate groups on each strand for extra protection against nucleases (Foster et al., 2018). After further development, the Advanced ESC design reduced the overall 2'-F content in the siRNA molecule, though 2'-F is still required at specified locations on the guide strand for proper loading into the RISC complex (Schlegel et al., 2017). However, full 2'-OMe modification instead leads to a reduction or elimination of RNAi entirely, likely due to excessive steric interference of the bulkier 2'-OMe groups, lack of electronegativity and no H-bonds from a 2'-OMe group (Chiu and Rana, 2003; Khvorova and Watts, 2017).

Locked nucleic acids (LNAs) are bicyclic modifications of the ribose sugar whereby the 2'-OH and the 4'-C are joined by a methylene bridge to lock the ribose sugar into the 3' pucker position that improves A-form dsRNA helical structure and efficiency of RNAi-mediated gene silencing. Used in moderation, LNA modifications can maintain a high efficiency in target gene silencing while reducing off-target effects and enhancing nuclease stability; however, when used in excess, LNAs on siRNAs lead to a decrease in RNAi potency (Bramsen and Kjems, 2012). LNA modifications are therefore excluded from the central region of the siRNA, especially surrounding the Ago2 cleavage site (Dallas et al., 2012).

Nucleobase modifications of ASOs and siRNAs include 5-methyl cytosine, 5-propynyl cytidine, 5-methyluridine, 2-thiol thymine, and 2,6-diaminopurine with the aim of enhancing the binding affinity to the target mRNA and a stable conformation of the double helix (Lakhin et al., 2013). However, nucleobase modifications of this nature are most common in aptamers for proper folding to achieve the three-dimensional structure they require to target various molecules or protein complexes (Smith and Zain, 2018). Conversely, modified nucleobases in both passenger and guide strands of the siRNA can lead to significant reductions of the RNAi-mediated gene silencing, which makes siRNA nucleobase modification considerably more challenging (Herdewijn 2000; Shukla et al., 2010; Hassler et al., 2018).

For siRNAs, a 5'-phosphate group on the guide strand is critically required for loading into Ago (Frank et al., 2010; Chen et al., 2008). However, a 5'-phosphate group is very metabolically unstable (Khvorova and Watts, 2017). To circumvent this problem, a 5'-vinyl phosphonate (5'-VP) modification is recognized by Ago and extremely stable to RNAse cleavage (Prakash et al., 2015). Importantly, the 5'-VP modification maintains the required conformation for proper RISC binding and phosphatase resistance to improve the overall siRNA potency and affinity for Ago2. Moreover, the 5'-VP improves distribution and accumulation of siRNAs in target tissues, thereby improving retention of the oligonucleotide and duration of effect (Khvorova and Watts, 2017; Parmar et al., 2016).

Many of the barriers against oligonucleotide therapeutic development have been overcome largely by the modifications described in this section that improve metabolic stability, resistance to RNases, and improve overall pharmacokinetics. Despite these improvements, however, there is one more significant challenge that prevents oligonucleotides from realizing their full therapeutic potential: escape from the endosome.

ENDOCYTOSIS AND THE ENDOSOMAL ESCAPE PROBLEM

After an oligonucleotide is internalized into the endosome with the help of a targeting ligand, it must still find a way to reach the cytoplasm where it can carry out its gene silencing function. The lipid bilayer has evolved to prevent foreign nucleic acids and other macromolecules into the cell. As such, it is very difficult for an siRNA molecule to traverse this barrier without assistance. Regardless the delivery method for siRNAs, some form of endocytosis is always involved in the process of cell uptake.

The types of endocytosis include clathrin-mediated, caveolin-dependent, phagocytosis, and macropinocytosis and the specific type used depends on the mode of oligo delivery (Doherty and McMahon, 2009). For example, cell penetrating peptides (CPPs)/protein transduction domains (PTDs) and lipid nanoparticles (LNPs) can enter cells by

macropinocytosis (Kaplan et al., 2005; Gilleron et al., 2013; Wadia et al., 2004). Phosphorothioate-modified ASOs can enter cells through non-specific adsorptive/fluid endocytosis after binding to serum proteins while uncharged oligonucleotides (such as morpholinos or PNAs) are likely also taken up by fluid phase endocytosis (Juliano and Carver, 2015). Antibody-drug conjugates (ADCs) depend on clathrin-mediated endocytosis, that is the primary mechanism for cell surface receptor internalization (Mayor and Pagano, 2007). Regardless of the form of endocytosis employed by a given delivery modality, the endosomal escape problem remains the same: while the oligonucleotide-containing compound is technically inside the cell, it remains trapped inside the endosome and out of the cytoplasm where it must be for its gene silencing function (Dowdy, 2017). Escaping the endosome is the rate-limiting step that all siRNAs face when delivered into cells and is the major challenge for siRNA therapeutics (Dominska and Dykxhoorn, 2010; Dowdy, 2017; Juliano, 2016). Even when lipid nanoparticles deliver siRNA into mammalian cells *in vitro*, it has been observed that only 1-2% of lipid nanoparticles escape into the cytoplasm while the rest remained trapped in the endosome (Gilleron et al., 2013).

After endocytosis, regardless of the specific mechanism, endocytotic vesicles fuse together to become the early endosome where there are mildly acidic conditions (pH 5.9-6.8). At this point, the endocytosed material can either be recycled back to the plasma membrane, redirected to the Golgi complex for repackaging, or be retained within the endosomal network. As early endosomal vesicles mature, they transition into late endosomes or multivesicular bodies, where the pH continues to decrease (pH ~5.5). Later, further maturation leads to the formation of intraluminal vesicles that deliver the endocytosed materials into the even more acidic lysosomes (~pH 4.5) (Ritchie et al., 2013; Hu et al., 2015). Achieving endosomal escape to allow an oligonucleotide to reach the cytoplasm and engage the RNAi machinery arguably remains the biggest hurdle to overcome for developing extrahepatic oligonucleotide therapeutics.

Cell-Penetrating Peptides (CPPs)

Cell penetrating peptides (CPPs), also known as protein/peptide transduction domains (PTDs), are potentially promising additions to macromolecules that could improve the delivery efficiency of oligonucleotides. CPPs are positively charged peptides between 5 and 30 amino acids in length that can help carry proteins, peptides, or nucleic acids across cell membranes to improve the delivery efficiency (Derakhshankhah and Jafari, 2018). PTDs/CPPs were first discovered in the 1980s where the HIV-1 Trans-Activator of Transcription (TAT) protein could cross the cell membrane and mediate the transcription of the HIV-1 promoter and that a specific arginine-heavy truncated peptide (TAT-PTD) was the main effector of this successful transduction into cell nuclei (Frankel and Pabo, 1988; Green and Loewenstein, 1988;). It was thereafter shown that TAT-PTD could aid in the delivery of larger enzymes without inhibiting enzymatic function as well as other macromolecules *in vivo*, such as ß-galactosidase (Schwarze et al., 1999). In the years that followed, there have been over 100 engineered or synthetic peptides developed with many types of cargo successfully delivered including proteins, peptides, DNA, RNA, and other chemical compounds (Palm-Apergi et al., 2012; Duchardt et al., 2007; Lindgren and Langel, 2011). Clinical trials over past decades have demonstrated the safety and efficacy of CPPs *in vivo* and there is extensive development in therapeutics incorporating these CPPs (Lönn and Dowdy, 2015).

The mechanism of CPP-mediated uptake depends on the CPP and cell type, but primarily occurs by endocytosis. For example, TAT-PTD enters cells by lipid raft-mediated endocytosis, a form of fluid phase endocytosis, after binding to the cell surface occurs between the cationic peptide and likely the negatively charged surface proteoglycans (Wadia et al., 2004; Kaplan et al., 2005). Lipid rafts refer to membrane microdomains that have a high density of cholesterol and sphingolipids that can interact with the CPPs. Macropinocytosis is the main internalization mechanism for cationic, arginine-rich CPPs (Wadia et al., 2004). In HeLa cells, it was observed that other cationic peptides derived from human calcitonin are also internalized

by lipid raft-mediated endocytosis (Foerg et al., 2005). After endocytosis occurs, CPPs disrupt the endosomal membrane to facilitate escape of its cargo into the cell cytoplasm, also taking advantage of the permeability of some endosomes and possibly implicating a role for retrograde transport through the trans-Golgi network (Fischer et al., 2004; Kawamura et al., 2006). The value of CPPs lies in their ability to both induce endocytosis and then help mediate endosomal escape.

A notable example took advantage of TAT's inherent ability to stimulate endocytosis by testing various synthetic endosomal escape domains (EEDs) to determine the best combination of amino acids to improve delivery to the cytoplasm. In this example, EEDs were conjugated to the TAT-PTD with a fixed linker length of six PEG units and it was determined that the best endosomal-escape-enhancing EEDs were those that contained either two aromatic indole rings or one indole ring and two flanking phenylalanine groups. Specifically, the best candidates were found to be EEDs consisting of Gly-Phe-Trp-Phe-Gly or Gly-Trp-Trp-Gly, improving escape by five- to eight-fold (Lönn et al., 2016). These results underscored the importance of having a concentrated hydrophobic patch of reasonable length, as an excessive length will instead lead to significant cytotoxicity. The hydrophobic interaction between peptides and membranes is critical for successful membrane destabilization and subsequent transduction into a cell.

Larger molecules such antibodies have a limited targeting efficacy and poorer clinical utility due to their inability to cross into the cell cytoplasm. However, it was seen that endosomolytic peptides derived from the cationic membrane-lytic spider venom peptide M-lycotoxin and modified with the addition of one or two glutamic acid amino acids into the hydrophobic region were found to facilitate the micropinocytosis of an antibody when added *in trans* to HeLa cells (Akishiba et al., 2017). In this example, the glutamic acid's negative charge prevented lysis at the membrane by preventing a strong peptide-membrane interaction but maintained the ability to adsorb to the cell surface where perturbation of the cell membrane was

possible. The main drawback to this approach is the nonspecific and nontargeted uptake mechanism into cells that would be problematic in systemic clinical applications.

While CPPs have been shown to facilitate endocytosis and endosomal escape in specific cases, they remain broadly incompatible with oligonucleotide therapeutics for several reasons. Negatively charged oligonucleotides and cationic CPPs do not mix well and instead aggregate into nanoparticles (Nakase et al., 2013; Meade et al., 2014). CPPs are reliant on their positive charge for transduction across cell membrane, but negatively charged oligonucleotides will quickly neutralize a CPP when both components are conjugated together, resulting in failed delivery and aggregation (Moschos et al., 2007). A potential solution to this problem can be seen in the incorporation of a dsRNA binding domain (DRBD) that binds and masks an siRNA's negative charges to allow proper function of the TAT peptide and thus successful siRNA delivery *in vitro* (Eguchi et al., 2009) and *in vivo* to generate a tumor-specific synthetic lethal response in intracerebral glioblastoma mouse models (Michiue et al., 2009). Unfortunately, successful siRNA delivery requires a high enough siRNA concentration that makes aggregation and precipitation problems prevalent, thereby significantly limiting a CPP's clinical value.

Other Approaches for Endosomal Escape

There are several small molecule endosomolytic agents that are known to either disrupt or lyse endosomes. Unfortunately, each of these options are highly toxic, making them impractical for use in conjunction with oligonucleotides.

It was observed in the 1980s that chloroquine, a weakly basic molecule, can diffuse across the cell membrane and becomes protonated within the increasingly acidic endosomes (Maxfield, 1982). Consequently, chloroquine becomes trapped in the endosome leading to a net dramatic increase of its concentration and the insertion of its hydrophobic bicyclic motif into the endosomal membrane (Maxfield, 1982). Upon reaching a critical threshold in concentration, chloroquine lyses the endosome, and all of the endosomal contents are released within the cell.

The drawback of chloroquine is that it requires a high concentration (micromolar range) for its efficacy and at this concentration, it will indiscriminately lyse all endosomes and produce an unacceptably high cytotoxicity (Dowdy, 2017; Hajimolaali et al., 2021).

An alternate approach involves the melittin peptide, a 26-amino-acid, alpha helical, pore-forming peptide that is derived from the European honeybee and is capable of lysing membranes (Hou et al., 2015). Membrane disruption depends on multiple variables, such as pH, salt concentration, and membrane composition. The membrane disruption mechanism is not well understood, but is thought to involve electrostatic interactions with the anionic lipid membrane, followed by melittin peptides reaching a critical concentration, and then a pore-forming rearrangement of melittin (Lee et al., 2008; Hou et al., 2015). Arrowhead Pharmaceuticals adapted melittin by adding pH-sensitive protecting groups and incorporating it within a GalNAc conjugate to protect the melittin until it is delivered into an endosome where it can become deprotected and capable of endosomal membrane lysis. Melittin is highly toxic, however, and the FDA put a hold on their clinical trials that relied on melittin after the initial results (Arrowhead, 2016) (all three were eventually dropped).

DELIVERING OLIGONUCLEOTIDES

Gymnosis

ASOs that have a phosphorothioate-modified backbone possess the unique ability to enter a cell by endocytosis and then escape into the cytoplasm without the assistance of any delivery vehicle or transfection reagent by an unknown mechanism termed gymnosis (Stein et al., 2010). Gymnosis was initially observed with phosphorothioate gapmer LNA ASOs when tested *in vitro* on several adherent cell lines and a suspension Burkitt's lymphoma cell line, resulting in successful gene silencing (Stein et al., 2010; Castanotto et al., 2015). Similar results were observed in non-LNA containing phosphorothioate ASOs when tested on prostate cancer

(LNCaP) cells (Souleimanian et al., 2012) and on HeLa cells (Takahashi et al., 2017). Because ASOs cannot cross the blood brain barrier, they must be injected intrathecally into the cerebrospinal fluid from where they will be widely distributed within the brain parenchyma and taken up by various cell types (Smith et al., 2006). ASOs have a unique advantage over siRNAs because they can enter a cell without the assistance of a delivery agent that in turn has led to the development of many ASO-based drugs targeting the liver and the central nervous system (CNS). However, the efficacy of ASOs can be further enhanced by conjugating them to delivery vehicles that will direct the ASOs to the correct target cell rather than allow for the nonspecific broad distribution.

Nanoparticle Delivery

In the absence of an innate ability to cross the lipid bilayer through gymnosis, siRNAs are pharmacokinetically unfavorable due to their inability to enter cells. To circumvent this problem, lipid nanoparticle (LNP) and synthetic nanoparticle (NP) systems are commonly used wherein siRNAs are encapsulated within a formulation of synthetic ionizable lipids that are neutral at physiological pH but positively charged at low pH, such as in the late endosome, to reduce toxicity (Hajj and Whitehead, 2017; Kauffman et al., 2016). Due to the risk of an innate immune response or negatively charged serum proteins binding and saturating the nanoparticle surface in the bloodstream, it is useful to coat the surface with hydrophilic molecules such as polyethylene glycol (PEG) to provide an aqueous shield (Whitehead et al., 2009). LNPs and NPs mask an siRNA's negative charge and provides it with further protection from RNases. Furthermore, their size improves their circulation time *in vivo* and significantly reduces its rate of glomerular filtration because naked oligonucleotides usually accumulate and are filtered by out by the kidneys (Schroeder et al., 2010; Rappaport et al., 1995; van de Water et al., 2006). When systemically administered, nanoparticles accumulate in the reticuloendothelial system, primarily in the liver, but to a certain extent also in the spleen, kidneys, and lungs, which also explains

why most instances of successful siRNA delivery have been observed within these organs (Akinc et al., 2008; Zimmermann et al., 2006). In mice, it was observed that the nanoparticles can also accumulate in tumors due to a phenomenon termed the enhanced permeability and retention (EPR) effect where macromolecules accumulate in tumors due to the rapidly expanding and permeable tumor vasculature (Kim et al., 2008; Takei et al., 2004).

Nanoparticle development unfortunately relies on very specific amounts of different components, all at variable ratios and each with their own toxicity profile (Schroeder et al., 2010). Moreover, LNPs shed their components in solution and blood. Biodegradable polymers that can degrade into smaller, nontoxic molecules can be incorporated into nanoparticles to reduce the overall cytotoxic profile (Vandenbroucke et al., 2008). Beyond their inherent cytotoxicity, nanoparticles have other significant limitations. An LNP is very large in size, about 100 nm in diameter is ~100 megaDa, which is 5,000-fold larger than the siRNAs being delivered. Their large size results in a poor pharmacokinetic profile and so they most often end up in the liver (Dowdy, 2017). Even though LNPs are too large to be filtered out of blood by the kidneys, they are cleared by the liver (Akinc et al., 2009). While PEGylation has greatly improved the efficacy of nanoparticles, it has still been observed that PEGylated nanoparticles lose their ability for long-term circulation in the bloodstream and may even impair the proper endosomal escape of the siRNAs upon delivery into cells (Gomes-Da-Silva et al., 2012). Furthermore, PEGylated nanoparticles can elicit immune responses and the prompt generation of anti-PEG IgM antibodies and complement system activation, resulting in unfavorable side effects and/or rapid clearance by the liver's Kupffer cells (Ishida et al., 2006). Delivery of nanoparticles to solid tumors heavily relies on the EPR effect and may be problematic if tumors are not sufficiently vascularized in a rapid manner as observed in murine preclincial models, but rarely in de novo derived human tumors. Nanoparticle delivery systems, unless locally administered, generally have considerably limited efficacy against targets outside the reticuloendothelial system.

ASGPR & the GalNAc Targeting Domain

The asialoglycoprotein receptor (ASGPR) is abundantly expressed on hepatocytes, where between 500,000 and 1 million per cell, and is a receptor that is rapidly recycled back to the surface (~15 minutes) after being internalized when bound to its ligand, *tris*-N-acetylgalactosamine (GalNAc) (Juliano, 2016; Khvorova and Watts, 2017). Due to the high abundance of ASGPR, GalNAc conjugated molecules localize to liver hepatocytes. Extensive development has led to the generation of a GalNAc trimer for an optimized uptake efficiency in hepatocytes (Nair et al., 2014). The binding of GalNAc to the trimeric ASGPR receptor triggers a rapid local aggregation of GalNAc-bound receptors, resulting in extensive aggregation in clathrin-coated pits followed by endocytosis into the hepatocyte (Steer and Ashwell, 1980; Schwartz et al., 1982; Stockert et al., 1980). Following endocytosis, increased acidity within the maturing endosome results in dissociation of the GalNAc molecule from ASGPR and subsequent lysosomal degradation (Gregoriadis et al., 1970), afterwards recycling the ASGPR back to the cell surface where it can once more bind to a new GalNAc ligand (**Figure 1.4**) (Bridges et al., 1982; Geuze et al., 1983). These characteristics makes GalNAc molecules incredibly promising targeting ligands that can be easily conjugated to siRNAs for optimal delivery against liver targets. The position and valency of GalNAc is important, and over several decades was optimized for its linker length and sugar arrangement. Early in this development, tris-galactoside was used to deliver lipids and ASOs *in vivo* in rats where uptake by hepatocytes was greatly enhanced and the oligonucleotides accumulated in liver cells – a success that was attributed to the presence of ASGPR (Biessen et al., 1999). In the years that followed, tris-GalNAc was developed and optimized.

The identification of an efficacious delivery ligand in GalNAc and a highly metabolically stabilized siRNA molecule with the chemical modifications previously described led to the creation of GalNAc-siRNA conjugates, dramatically smaller and simpler than LNP-based siRNA delivery systems (Springer and Dowdy, 2018). GalNAc-siRNA conjugates are now commonly

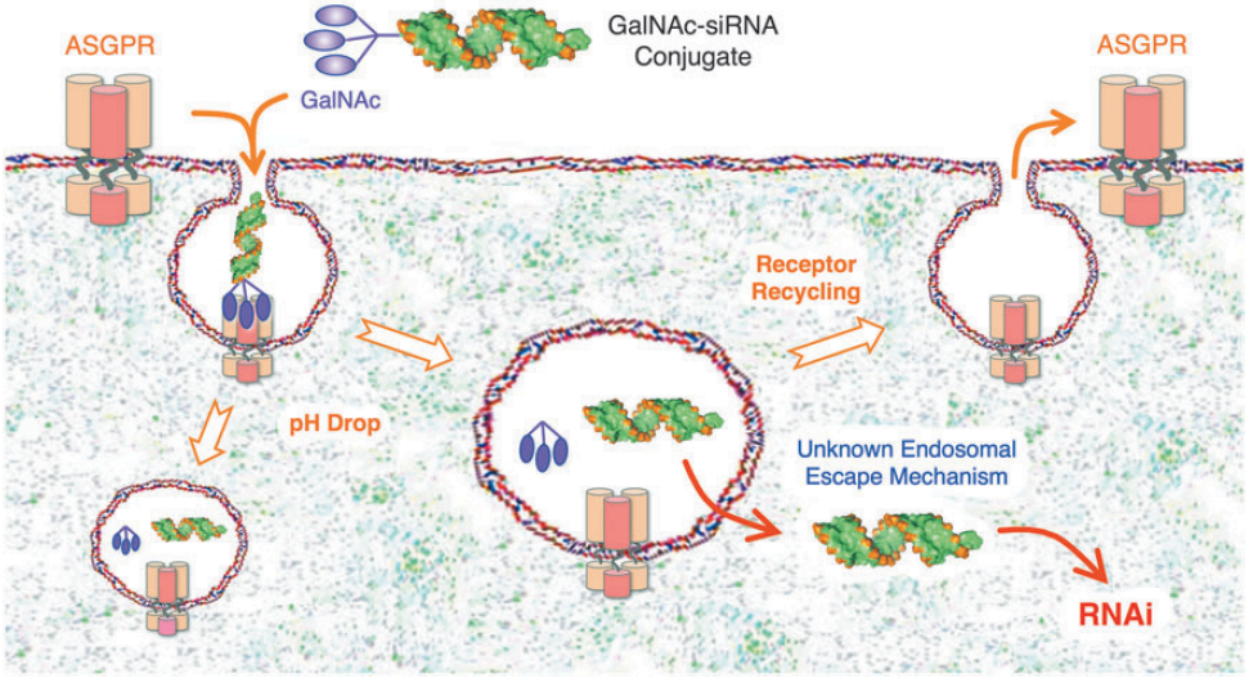

Figure 1.4. GalNAc-mediated Delivery of siRNA – Uptake and Recycling.
Asialoglycoprotein receptors are abundantly found on hepatocytes. When an siRNA is conjugated to a trivalent GalNAc molecule, the conjugate can efficiently bind to ASGPR from where it will be rapidly internalized into the hepatocyte. As the endosome matures, the decrease in pH will release the GalNAc from the ASGPR. The ASGPR will be recycled to the cell surface and will be able to bind to another GalNAc. Meanwhile, the GalNAc will dissociate from the siRNA and is degraded. The siRNA will largely remain trapped within the endosome, but a small portion (<1%) will be able to escape into the cytoplasm by an unknown mechanism where it will be able to interact with the RNAi machinery to carry out its gene silencing function in association with Argonaute2.

Taken from Springer and Dowdy, 2018.

made and are the best delivery ligands for RNAi in the liver. Even though ASOs do not require a delivery vehicle to access a cell's cytoplasm, conjugation of ASOs to GalNAc resulted in a 10-fold increase in delivery to mouse hepatocytes compared to free, unconjugated ASOs alone, thereby reducing the dose required to achieve the same level of gene silencing (Prakash et al., 2014). The success of GalNAc conjugates can be attributed to the unique advantage of a high ASGPR abundance in hepatocytes with a fast receptor turnover which allows fast and efficient uptake of GalNAc conjugates. There are currently three FDA/EU approved GalNAc siRNA conjugates.

Despite the great promise of GalNAc, it is important to note that the vast majority of siRNAs delivered to hepatocytes remain trapped inside of endosomes. Only a small amount of siRNA (~0.3%) is able to escape into the cytoplasm by an unknown mechanism, but the remaining >99% of siRNA is rendered clinically useless (Brown et al., 2020; Springer and Dowdy, 2018). Either way, improvements to the rate of endosomal escape would predictably lower the dose requirements for any GalNAc (or other) conjugate as well as for all other targeting methods to deliver siRNAs.

Other Targeting Domains

Antibodies are among the best studied delivery vehicles for other macromolecules, as they can bind to target receptors with high specificity and in many cases trigger receptor-mediated endocytosis (Tarcic and Yarden, 2013). Since the 1990s, mAbs have been extensively developed. As previously discussed, there are already several mAb-based cancer therapies that either seek to outcompete the cancer cell's natural ligands or to harness the immune system against a tumor. Antibody-drug conjugates (ADCs) are also commonly used to deliver cytotoxic compounds to cancer cells. Antibody fragments and bispecific antibodies have been approved for various diseases such as blood cancers and other autoimmune diseases (Carter et al., 2018).

Antibody-siRNA conjugates in general are limited largely by the endosomal escape problem. In general, the combination of an antibody, oligonucleotide, linker, and possibly an additional CPP or EED increases the difficulty of the conjugation reactions and purification process at each step along the way and conjugate aggregation or precipitation is not uncommon. Moreover, antibody-oligonucleotide conjugates have only produced lackluster results at best. For example, Genentech developed the THIOMAB-siRNA platform where the siRNA was site-selectively conjugated onto two engineered cysteines on the heavy chains of an anti-TENB2 antibody with a reducible or non-reducible linker to generate an antibody-siRNA conjugate (ARC) (Cuellar et al., 2014). Unfortunately, even though it was shown that siRNA functions normally when conjugated to an antibody and that ARCs can successfully internalize into target cells, the THIOMAB ARCs showed poor activity and required unreasonably high concentrations for adequate gene silencing. Without a way to escape the endosome, ARCs are unlikely to become successful oligonucleotide therapeutics. Further investigation is needed to modify ARCs to achieve this end.

Other unique delivery approaches have been used. One example used fluorescent peptides of varying charge and hydrophobicity that were conjugated onto a proapoptotic peptide, that self-assembled into stable nanoparticles that were subsequently endocytosed into HeLa cells (Rong et al., 2020). However, this approach is not cell specific, is expected to fail when tested *in vivo* and is not sequence-specific either as with oligonucleotide-based therapies. Another group developed palmitic acid-ASO conjugates and other fatty acid-ASO conjugates to promote albumin binding and enhance delivery from blood circulation into muscle, using albumin as the ligand due to its capacity to interact with numerous receptors (Prakash et al., 2019). Another unique approach involves an EGFR-binding fibronectin type III domain, called a centyrin. Centyrins are targeting domains that are far smaller in size (~10 kDa) than antibodies and can bind to various receptors, can be engineered to include cysteine conjugation handles, and are expressed well by *E. coli* (Goldberg et al., 2016). The main problem of centyrins is their

lack of solubility that inevitably leads to aggregation and precipitation. Yet a different approach involves the conjugation of a siRNA to cholesterol, improving siRNA delivery *in vivo* by binding to circulating low density lipoprotein (LDL) and subsequent uptake via hepatocytes' LDL receptors (Osborn and Khvorova, 2018).

Unlike GalNAc conjugates, however, antibodies and other targeting domains lack many advantages that have enabled the success of GalNAc-siRNA conjugates. ASGPR is found on the order of 500,000-1,000,000 per hepatocyte, whereas most other cell surface receptors are usually found on the order of 10^4-10^5 per cell (Dowdy, 2017). Moreover, other cell receptors have a considerably slower rate of endocytosis, so non-GalNAc targeting domains introduce far fewer oligonucleotides into the target endosome than its GalNAc counterpart in a given amount of time (**Figure 1.5**). These observations highlight the importance of developing better endosomal escape strategies.

OLIGONUCLEOTIDE THERAPEUTICS IN THE CLINIC

There are 15 oligonucleotide therapeutics that have been FDA approved. All of these in some form or other contain oligonucleotides with the chemical modifications that were described above and rely on either LNP or GalNAc for delivery or no delivery system in the case of ASOs.

Short Interfering RNAs (siRNAs)

Hereditary transthyretin (TTR)-mediated amyloidosis (hATTR) is an autosomal dominant disorder that forces hepatocytes to create an abnormal form of the TTR protein. The resulting amyloid deposition occurs in the peripheral nervous system and impacts the heart, gastrointestinal tract, and kidneys (Hoy, 2018). Patisiran (*Onpattro*, Alnylam Pharmaceuticals) consists of a 19 + 2-mer 2'-OMe modified siRNA encapsulated within an LNP formulation that targets the *TTR* gene in patients with hereditary transthyretin amyloidosis (Roberts et al., 2020).

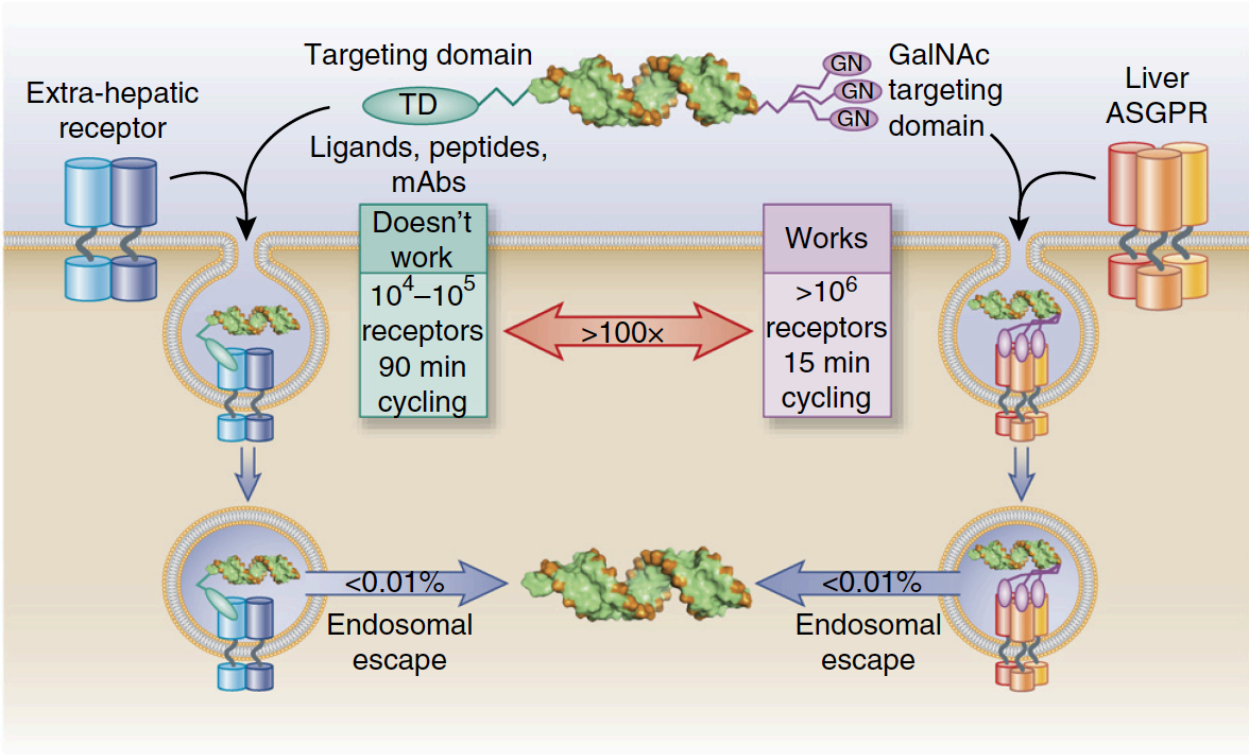

Figure 1.5. GalNAc versus Other Targeting Domains
ASGPR is abundantly expressed on hepatocytes and internalize rapidly upon binding its GalNAc ligand (~15 minutes). In contrast, other cell receptors are found in far lower densities and have a considerably longer endocytosis cycling time. As a result, non-GalNAc targeting domains are not able to deliver sufficient levels of oligonucleotides to the endosome, leading to insufficient oligo escape into the cytoplasm and therefore a failure to silence the target gene. Both GalNAc and other targeting domains such as antibodies can successfully deliver oligonucleotides into endosomes, but neither can mediate endosomal escape.

Taken from Dowdy, 2017.

Patisiran reduced abnormal TTR serum levels by 80% within two weeks after a single administration with a 0.3 mg/kg dosing every three weeks and the response was confirmed to be a result of the RNAi process (Alnylam, 2018; Coelho et al., 2013; Suhr et al., 2015). Patisiran was approved in August of 2018 and was the first siRNA drug to receive FDA approval.

Acute hepatic porphyria is a rare genetic disorder with abnormalities of the hepatic ALA synthase 1 (ALAS1) leads to the accumulation of neurotoxic heme intermediates. Consequently, this causes damage to the nervous system and can lead to other chronic disease events, such as hypertension, neuropathy, kidney disease, and liver disease (Sardh et al., 2018). Givosiran (*Givlaari*, Alnylam Pharmaceuticals) is a GalNAc-siRNA conjugate with ESC siRNA that targets the *ALAS1* gene in patients with acute hepatic porphyria (Roberts et al., 2020). During phase 3 clinical trials, givosiran demonstrated a 74% reduction in porphyria attacks over six months and a significant reduction of urine ALA and porphobilinogen levels (neurotoxic heme intermediates) by 86% and 91%, respectively (Balwani et al., 2020). Givosiran received FDA approval in November 2019.

There are numerous more examples of siRNAs in different phases of clinical trials. Inclisiran (Alnylam/Novartis) is an EU approved (under review at the FDA) GalNAc-siRNA conjugate that targets proprotein convertase subtilisin-kexin type 9 (PCSK9) in patients with hypercholesterolaemia and atherosclerotic cardiovascular disease to prevent binding to low-density lipoprotein (LDL) receptors (Kosmas et al., 2018). Fitusiran (Alnylam/Genzyme) is another GalNAc-siRNA conjugate that targets anti-thrombin 3 (AT3) in the context of Hemophilia A and B with promising Phase I/II results and ongoing Phase III trials; cemdisiran (Alnylam), another GalNAc-siRNA conjugate, suppresses liver production of complement 5 (C5) protein in the context of atypical haemolytic uraemic syndrome; lumasiran (Alnylam), a GalNAc-siRNA conjugate with recent FDA approval, targets the hydroxyacid oxidase 1 gene to reduce glycolate oxidase in patients with primary hyperoxaluria type 1; ARO-HBV (Arrowhead), a GalNAc-siRNA conjugate that targets the hepatitis B surface antigen (HBsAg) with promising Phase I/II results;

and ARO-AAT (Arrowhead/Takeda) that is used for patients with the rare genetic liver disease alpha-1 antitrypsin deficiency (Setten et al., 2019). A basic search on clinicaltrials.gov reveals around seventy active or completed trials, or trials in open enrollment, that utilize siRNAs in some capacity.

Antisense Oligonucleotides (ASOs)

Mipomersen (*Kynamro*, Ionis/Genzyme) is a 20-nt phosphorothioate 5-10-5 (RNA-DNA-RNA) gapmer ASO with 2'-MOE modifications that targets apolipoprotein B (apoB) to reduce plasma LDL-C and apoB levels in patients with hypercholesteremia and dyslipidemia and cardiovascular disease (Smith and Zain, 2019). Increased levels of LDL-cholesterol and apoB are major risk factors for atherosclerotic cardiovascular disease (CVD) and patients with familial hypercholesterolemia who inherit high LDL-cholesterol due to mutated LDL receptors develop higher risks for LDL accumulation and CVD far earlier in life (Goldstein and Brown, 2009). Mipomersen mainly distributes to the liver after subcutaneous administration and successful Phase III trials demonstrated significant reductions in apoB, LDL-C, and triglycerides with reasonable safety and tolerability profiles (Bell et al., 2011). A 200 mg dose of mipomersen reduced apoB and LDL-C levels by 50% and 35%, respectively and had a response duration of over thirty days (Hair et al., 2013). Mipomersen received FDA approval in January 2013.

Inotersen (*Tegsedi*, Ionis/Akcea) is another 2'-MOE phosphorothioate gapmer ASO that targets an aberrant form the *TTR* gene that produces abnormal transthyretin plasma protein and leads to detrimental transthyretin amyloidosis. Transthyretin amyloidosis often leads to many serious polyneuropathies and cardiomyopathies. Moreover, this general condition can involve over 100 amino acid substitutions, derived from numerous single nucleotide polymorphisms (SNPs), each of which produces variability in the disease phenotype (Sikora et al., 2015). Phase III clinical trials demonstrated that a weekly subcutaneous injection of inotersen led to significant reductions in circulating transthyretin, slower disease progression, and better quality of life

based on a standardized Neuropathy Impairment scoring system (Benson et al., 2018). Inotersen received FDA approval in October 2018.

Spinal muscular atrophy (SMA) describes a wide spectrum of autosomal recessively inherited degenerative neuromuscular disorders for which, in the more severe cases, rapid degradation of spinal cord and brainstem motor neurons leads to respiratory failure, loss of other motor function, and ultimately death (Neil and Bisaccia, 2019). SMA arises from mutations in the survival motor neuron (*SMN1*) gene, which affects the *SMN1* gene but not the closely related *SMN2* gene, both of which produce SMN proteins. However, even though *SMN2* remains functional, it produces an unstable form of the SMN protein in small amounts and it does not compensate for the degenerative effects of the mutation in *SMN1* (Hua et al., 2007). It was observed that modifying and upregulating *SMN2* by modifying its splicing to include exon 7, an exon critical for correct SMN protein production, with a splice switching ASO led to increase in SMN protein production and ameliorated SMA symptoms in mice (Passini et al., 2011). Nusinersen (Ionis) is a splice switching ASO that alters SMN2 pre-mRNA to include the exon 7 and restore normal expression for the full-length SMN protein (Wurster and Ludolph, 2018). Phase III trials reported significantly improved motor function and increased SM2 levels in children who received 12 mg of nusinersen intrathecally on days 1, 29, 85, and 274 (Mercuri et al., 2018). Nusinersen received FDA approval in December 2016.

As of this writing, a total of eight ASO drugs have received FDA approval, three of which are gapmer ASOs that rely on RNaseH activity and five of which are splice switching ASOs. Other than the ones already discussed, these include: Formivirsen (Ionis), a first generation phosphodiester ASO approved in 1998 for cytomegalovirus retinitis but withdrawn in the US in 2006 due to the introduction of a cocktail of antivirals that obviated the need for this ASO; Eteplirsen (Sarepta Therapeutics), a splice switching PMO ASO approved in 2016 for patients with Duchenne muscular dystrophy (DMD); Golodirsen (Sarepta), another splice switching PMO ASO approved in 2019 for DMD patients; Viltolarsen (Nippon Shinyaku/National Center of

Neurology and Psychiatry), another splice switching PMO ASO approved in 2020 for DMD patients; and Casimersen (Sarepta), another splice switching PMO ASO that targets a different DMD-relevant exon from its predecessors and received accelerated approval in 2021 (Gagliardi and Ashizawa, 2021). And there are many more ASO therapeutics currently in clinical trials.

CONCLUSIONS

The past several decades have seen major advancements in the field of oligonucleotide therapeutics. While the initial versions of oligonucleotide therapeutics were ineffective due to many biological barriers, modifications to the oligonucleotide backbone and ribose sugar have overcome many of these challenges. Metabolic stability has been enhanced by an array of 2'-modifications and gene silencing efficacy is phenomenal. There has been extensive development of the delivery systems, especially with GalNAc and LNPs, to improve delivery and there has been extensive research into many different types of CPPs. Unfortunately, the endosomal escape problem still remains unsolved and currently prevents oligonucleotide-based therapeutics from reaching their true potential.

Oligonucleotides hold a major advantage over other treatment modalities in that they epitomize the potential of personalized medicine because they are relatively inexpensive to produce, especially when being dosed once quarterly or every six months, highly specific, and easily customizable based on the desired target sequence. For example, milasen is a 22-base splice switching ASO that was developed exclusively to treat a single patient, a six-year-old girl with the fatal, albeit rare, neurodegenerative Batten disease. Treatment with milasen led to a significant improvement in the quality of life and reduction in seizures and other symptoms within the first year of treatment (Kim et al., 2019). A drug developed exclusively for a single patient would have been unheard of not so long ago.

Most oligonucleotide therapeutics have focused on liver, CNS, and recently muscle targets because they are accessible for LNPs, GalNAc and other conjugates. Unfortunately,

very little, if any, progress has been made with other extrahepatic targets like cancer. Endosomal escape remains a major problem that gets in the way of this. Oligonucleotide therapeutics are uniquely poised to target specific oncogenes in cancer, especially because oligonucleotides are highly scalable and can quickly keep pace with the changing mutational landscape of a tumor. Oligonucleotide therapeutics have achieved great successes and have come far since the initial discoveries of ASO and siRNA mechanisms, but much remains to be done in order for oligonucleotides to access many other disease targets, especially cancer.

In this dissertation I will describe my progress in building antibody-RNA conjugates (ARCs) and optimizing them in every step of the development process. Though unfortunately these ARCs did not produce the desired gene knockdown, they represent a foundation to develop further modifications for improvement. I will also describe a new type of molecule being developed in our lab intended to promote endosomal escape.

REFERENCES

Abe, K., Fujiyoshi, Y., 2016. Cryo-electron microscopy for structure analyses of membrane proteins in the lipid bilayer. Current Opinion in Structural Biology 39, 71–78. https://doi.org/10.1016/j.sbi.2016.06.001

Aguti, S., Marrosu, E., Muntoni, F., Zhou, H, 2020. Gapmer Antisense Oligonucleotides to Selectively Suppress the Mutant Allele in *COL6A* Genes in Dominant Ullrich Congenital Muscular Dystrophy. In: Yokota, T., Maruyama, R., (eds) Gapmers. Methods in Molecular Biology 2176, 221-230.

Akinc, A., Zumbuehl, A., Goldberg, M., Leshchiner, E.S., Busini, V., Hossain, N., Bacallado, S.A., Nguyen, D.N., Fuller, J., Alvarez, R., Borodovsky, A., Borland, T., Constien, R., de Fougerolles, A., Dorkin, J.R., Narayanannair Jayaprakash, K., Jayaraman, M., John, M., Koteliansky, V., Manoharan, M., Nechev, L., Qin, J., Racie, T., Raitcheva, D., Rajeev, K.G., Sah, D.W.Y., Soutschek, J., Toudjarska, I., Vornlocher, H.-P., Zimmermann, T.S., Langer, R., Anderson, D.G., 2008. A combinatorial library of lipid-like materials for delivery of RNAi therapeutics. Nat Biotechnol 26, 561–569. https://doi.org/10.1038/nbt1402

Akira, S., Uematsu, S., Takeuchi, O., 2006. Pathogen Recognition and Innate Immunity. Cell 124, 783–801. https://doi.org/10.1016/j.cell.2006.02.015

Akishiba, M., Takeuchi, T., Kawaguchi, Y., Sakamoto, K., Yu, H.-H., Nakase, I., Takatani-Nakase, T., Madani, F., Gräslund, A., Futaki, S., 2017. Cytosolic antibody delivery by lipid-sensitive endosomolytic peptide. Nature Chem 9, 751–761. https://doi.org/10.1038/nchem.2779

Alberts, B., Johnson, A., Lewis, J, 2002. The RNA World and the Origins of Life, in: Molecular Biology of the Cell. Garland Science, New York.

Allerson, C.R., Sioufi, N., Jarres, R., Prakash, T.P., Naik, N., Berdeja, A., Wanders, L., Griffey, R.H., Swayze, E.E., Bhat, B., 2005. Fully 2‘-Modified Oligonucleotide Duplexes with Improved in Vitro Potency and Stability Compared to Unmodified Small Interfering RNA. J. Med. Chem. 48, 901–904. https://doi.org/10.1021/jm049167j

Alnylam Pharmaceuticals, 2018. Onpattro (Patisiran) lipid complex injection, for intravenous use: US prescribing information. https://www.accessdata.fda.gov/drugsatfda_docs/label/2018/210922s000lbl.pdf

Armengol, C., Bartoli, R., Sanjurjo, L., Serra, I., Amezaga, N., Sala, M., Sarrias, M.-R., 2013. Role of scavenger receptors in the pathophysiology of chronic liver diseases. Crit Rev Immunol. https://doi.org/10.1615/CritRevImmunol.2013006794

Arrowhead Pharmaceuticals, 2016. Arrowhead Pharmaceuticals Focuses Resources on Subcutaneous and Extra-hepatic RNAi therapeutics. https://ir.arrowheadpharma.com/news-releases/news-release-details/arrowhead-pharmaceuticals-focuses-resources-subcutaneous-and

Ashley, C.E., Carnes, E.C., Epler, K.E., Padilla, D.P., Phillips, G.K., Castillo, R.E., Wilkinson, D.C., Wilkinson, B.S., Burgard, C.A., Kalinich, R.M., Townson, J.L., Chackerian, B.,

Willman, C.L., Peabody, D.S., Wharton, W., Brinker, C.J., 2012. Delivery of Small Interfering RNA by Peptide-Targeted Mesoporous Silica Nanoparticle-Supported Lipid Bilayers. ACS Nano 6, 2174–2188. https://doi.org/10.1021/nn204102q

Aung, K.M., Boldbaatar, D., Umemiya-Shirafuji, R., Liao, M., Xuenan, X., Suzuki, H., Linggatong Galay, R., Tanaka, T., Fujisaki, K., 2011. Scavenger Receptor Mediates Systemic RNA Interference in Ticks. PLoS ONE 6, e28407. https://doi.org/10.1371/journal.pone.0028407

Azlan, A., Dzaki, N., Azzam, G., 2016. Argonaute: The executor of small RNA function. Journal of Genetics and Genomics 43, 481–494. https://doi.org/10.1016/j.jgg.2016.06.002

Bagchi, S., Yuan, R., Engleman, E.G., 2021. Immune Checkpoint Inhibitors for the Treatment of Cancer: Clinical Impact and Mechanisms of Response and Resistance. Annu. Rev. Pathol. Mech. Dis. 16, 223–249. https://doi.org/10.1146/annurev-pathol-042020-042741

Balendiran, G.K., Dabur, R., Fraser, D., 2004. The role of glutathione in cancer. Cell Biochem Funct. 22, 343-352. https:/doi.org/10.1002/cbf.1149

Balwani, M., Sardh, E., Ventura, P., Peiró, P.A., Rees, D.C., Stölzel, U., Bissell, D.M., Bonkovsky, H.L., Windyga, J., Anderson, K.E., Parker, C., Silver, S.M., Keel, S.B., Wang, J.-D., Stein, P.E., Harper, P., Vassiliou, D., Wang, B., Phillips, J., Ivanova, A., Langendonk, J.G., Kauppinen, R., Minder, E., Horie, Y., Penz, C., Chen, J., Liu, S., Ko, J.J., Sweetser, M.T., Garg, P., Vaishnaw, A., Kim, J.B., Simon, A.R., Gouya, L., 2020. Phase 3 Trial of RNAi Therapeutic Givosiran for Acute Intermittent Porphyria. N Engl J Med 382, 2289–2301. https://doi.org/10.1056/NEJMoa1913147

Bartel, D.P., 2004. MicroRNAs: Genomics, Biogenesis, Mechanism, and Function. Cell Review 116, 281-297. https://doi.org/10.1016/S0092-8674(04)00045-5

Beigel, J.H., Voell, J., Muñoz, P., Kumar, P., Brooks, K.M., Zhang, J., Iversen, P., Heald, A., Wong, M., Davey, R.T., 2018. Safety, tolerability, and pharmacokinetics of radavirsen (AVI-7100), an antisense oligonucleotide targeting influenza a M1/M2 translation: Radavirsen phase I study. Br J Clin Pharmacol 84, 25–34. https://doi.org/10.1111/bcp.13405

Bell, D.A., Hooper, A.J., Burnett, J.R., 2011. Mipomersen, an antisense apolipoprotein B synthesis inhibitor. Expert Opinion on Investigational Drugs 20, 265–272. https://doi.org/10.1517/13543784.2011.547471

Benson, M.D., Waddington-Cruz, M., Berk, J.L., Polydefkis, M., Dyck, P.J., Wang, A.K., Planté-Bordeneuve, V., Barroso, F.A., Merlini, G., Obici, L., Scheinberg, M., Brannagan, T.H., Litchy, W.J., Whelan, C., Drachman, B.M., Adams, D., Heitner, S.B., Conceição, I., Schmidt, H.H., Vita, G., Campistol, J.M., Gamez, J., Gorevic, P.D., Gane, E., Shah, A.M., Solomon, S.D., Monia, B.P., Hughes, S.G., Kwoh, T.J., McEvoy, B.W., Jung, S.W., Baker, B.F., Ackermann, E.J., Gertz, M.A., Coelho, T., 2018. Inotersen Treatment for Patients with Hereditary Transthyretin Amyloidosis. N Engl J Med 379, 22–31. https://doi.org/10.1056/NEJMoa1716793

Bernstein, E., Caudy, A.A., Hammond, S.M., Hannon, G.J., 2001. Role for a bidentate ribonuclease in the initiation step of RNA interference. Nature 409, 363–366. https://doi.org/10.1038/35053110

Blain, J.C., Szostak, J.W., 2014. Progress Toward Synthetic Cells. Annu. Rev. Biochem. 83, 615–640. https://doi.org/10.1146/annurev-biochem-080411-124036

Blidner, R.A., Hammer, R.P., Lopez, M.J., Robinson, S.O., Monroe, W.T., 2007. Fully 2'-Deoxy-2'-Fluoro Substituted Nucleic Acids Induce RNA Interference in Mammalian Cell Culture. Chem Biol Drug Design 70, 113–122. https://doi.org/10.1111/j.1747-0285.2007.00542.x

Bramsen, J.B., Kjems, J., 2012. Development of Therapeutic-Grade Small Interfering RNAs by Chemical Engineering. Front. Gene. 3. https://doi.org/10.3389/fgene.2012.00154

Bridges, K., Harford, J., Ashwell, G., Klausner, R.D., 1982. Fate of receptor and ligand during endocytosis of asialoglycoproteins by isolated hepatocytes. Proceedings of the National Academy of Sciences 79, 350–354. https://doi.org/10.1073/pnas.79.2.350

Brown, C.R., Gupta, S., Qin, J., Racie, T., He, G., Lentini, S., Malone, R., Yu, M., Matsuda, S., Shulga-Morskaya, S., Nair, A.V., Theile, C.S., Schmidt, K., Shahraz, A., Goel, V., Parmar, R.G., Zlatev, I., Schlegel, M.K., Nair, J.K., Jayaraman, M., Manoharan, M., Brown, D., Maier, M.A., Jadhav, V., 2020. Investigating the pharmacodynamic durability of GalNAc–siRNA conjugates. Nucleic Acids Research 48, 11827–11844. https://doi.org/10.1093/nar/gkaa670

Canalese, J., Gove, C.D., Gimson, A.E., Wilkinson, S.P., Wardle, E.N., Williams, R. 1982. Reticuloendothelial system and hepatocyte function in fulminant hepatic failure. Gut 23, 265-269. doi: 10.1136/gut.23.4.265

Carter, P.J., Lazar, G.A., 2018. Next generation antibody drugs: pursuit of the "high-hanging fruit." Nat Rev Drug Discov 17, 197–223. https://doi.org/10.1038/nrd.2017.227

Carthew, R.W., Sontheimer, E.J., 2009. Origins and Mechanisms of miRNAs and siRNAs. Cell 136, 642–655. https://doi.org/10.1016/j.cell.2009.01.035

Castanotto, D., Lin, M., Kowolik, C., Wang, L., Ren, X.-Q., Soifer, H.S., Koch, T., Hansen, B.R., Oerum, H., Armstrong, B., Wang, Z., Bauer, P., Rossi, J., Stein, C.A., 2015. A cytoplasmic pathway for gapmer antisense oligonucleotide-mediated gene silencing in mammalian cells. Nucleic Acids Res 43, 9350–9361. https://doi.org/10.1093/nar/gkv964

Chakravarthy, Veedu, 2019. BACE1 Inhibition Using 2'-OMePS Steric Blocking Antisense Oligonucleotides. Genes 10, 705. https://doi.org/10.3390/genes10090705

Chen, P.Y., Weinmann, L., Gaidatzis, D., Pei, Y., Zavolan, M., Tuschl, T., Meister, G., 2007. Strand-specific 5'-O-methylation of siRNA duplexes controls guide strand selection and targeting specificity. RNA 14, 263–274. https://doi.org/10.1261/rna.789808

Chendrimada, T.P., Gregory, R.I., Kumaraswamy, E., Norman, J., Cooch, N., Nishikura, K., Shiekhattar, R., 2005. TRBP recruits the Dicer complex to Ago2 for microRNA processing and gene silencing. Nature 436, 740–744. https://doi.org/10.1038/nature03868

Chhabra, M., 2021. Biological therapeutic modalities, in: Translational Biotechnology. Elsevier, pp. 137–164. https://doi.org/10.1016/B978-0-12-821972-0.00015-0

Chiu, Y.-L., 2003. siRNA function in RNAi: A chemical modification analysis. RNA 9, 1034–1048. https://doi.org/10.1261/rna.5103703

Chow, K.T., Gale, M., Loo, Y.-M., 2018. RIG-I and Other RNA Sensors in Antiviral Immunity. Annu. Rev. Immunol. 36, 667–694. https://doi.org/10.1146/annurev-immunol-042617-053309

Clynes, R.A., Towers, T.L., Presta, L.G., Ravetch, J.V., 2000. Inhibitory Fc receptors modulate in vivo cytoxicity against tumor targets. Nat Med 6, 443–446. https://doi.org/10.1038/74704

Coelho, T., Adams, D., Silva, A., Lozeron, P., Hawkins, P.N., Mant, T., Perez, J., Chiesa, J., Warrington, S., Tranter, E., Munisamy, M., Falzone, R., Harrop, J., Cehelsky, J., Bettencourt, B.R., Geissler, M., Butler, J.S., Sehgal, A., Meyers, R.E., Chen, Q., Borland, T., Hutabarat, R.M., Clausen, V.A., Alvarez, R., Fitzgerald, K., Gamba-Vitalo, C., Nochur, S.V., Vaishnaw, A.K., Sah, D.W.Y., Gollob, J.A., Suhr, O.B., 2013. Safety and Efficacy of RNAi Therapy for Transthyretin Amyloidosis. N Engl J Med 369, 819–829. https://doi.org/10.1056/NEJMoa1208760

Coiffier, B., Lepretre, S., Pedersen, L.M., Gadeberg, O., Fredriksen, H., van Oers, M.H.J., Wooldridge, J., Kloczko, J., Holowiecki, J., Hellmann, A., Walewski, J., Flensburg, M., Petersen, J., Robak, T., 2008. Safety and efficacy of ofatumumab, a fully human monoclonal anti-CD20 antibody, in patients with relapsed or refractory B-cell chronic lymphocytic leukemia: a phase 1-2 study. Blood 111, 1094–1100. https://doi.org/10.1182/blood-2007-09-111781

Cooper, G., 2000. The Cell: A Molecular Approach, 2nd Ed. ed. Sinauer Associates, Sunderland, MA. https://www.ncbi.nlm.nih.gov/books/NBK9847/

Cuellar, T.L., Barnes, D., Nelson, C., Tanguay, J., Yu, S.-F., Wen, X., Scales, S.J., Gesch, J., Davis, D., van Brabant Smith, A., Leake, D., Vandlen, R., Siebel, C.W., 2015. Systematic evaluation of antibody-mediated siRNA delivery using an industrial platform of THIOMAB–siRNA conjugates. Nucleic Acids Research 43, 1189–1203. https://doi.org/10.1093/nar/gku1362

Daehn, I.S., Duffield, J.S., 2021. The glomerular filtration barrier: a structural target for novel kidney therapies. Nat Rev Drug Discov 20, 770–788. https://doi.org/10.1038/s41573-021-00242-0

Dallas, A., Ilves, H., Ge, Q., Kumar, P., Shorenstein, J., Kazakov, S.A., Cuellar, T.L., McManus, M.T., Behlke, M.A., Johnston, B.H., 2012. Right- and left-loop short shRNAs have distinct and unusual mechanisms of gene silencing. Nucleic Acids Research 40, 9255–9271. https://doi.org/10.1093/nar/gks662

de Graaf, M., Boven, E., Scheeren, H.W., Haisma, H.J., Pinedo, H.M., 2002. Beta-Glucuronidase-Mediated Drug Release. Curr Pharm Des 8, 1391-1403. https://doi.org/10.2174/131612023394485

de Paula Costa Monteiro, I., Madureira, P., de Vasconscelos, A., Humberto Pozza, D., Andrade de Mello, R., 2015. Targeting HER family in HER2-positive metastatic breast cancer: potential biomarkers and novel targeted therapies. Pharmacogenomics 16, 257–271. https://doi.org/10.2217/pgs.14.133

Derakhshankhah, H., Jafari, S., 2018. Cell penetrating peptides: A concise review with emphasis on biomedical applications. Biomedicine & Pharmacotherapy 108, 1090–1096. https://doi.org/10.1016/j.biopha.2018.09.097

DeVita, V.T., Chu, E., 2008. A History of Cancer Chemotherapy. Cancer Res 68, 8643–8653. https://doi.org/10.1158/0008-5472.CAN-07-6611

Doherty, G.J., McMahon, H.T., 2009. Mechanisms of Endocytosis. Annu. Rev. Biochem. 78, 857–902. https://doi.org/10.1146/annurev.biochem.78.081307.110540

Dominska, M., Dykxhoorn, D.M., 2010. Breaking down the barriers: siRNA delivery and endosome escape. Journal of Cell Science 123, 1183–1189. https://doi.org/10.1242/jcs.066399

Dorywalska, M., Dushin, R., Moine, L., Farias, S.E., Zhou, D., Navaratnam, T., Lui, V., Hasa-Moreno, A., Casas, M.G., Tran, T.-T., Delaria, K., Liu, S.-H., Foletti, D., O'Donnell, C.J., Pons, J., Shelton, D.L., Rajpal, A., Strop, P., 2016. Molecular Basis of Valine-Citrulline-PABC Linker Instability in Site-Specific ADCs and Its Mitigation by Linker Design. Mol Cancer Ther 15, 958–970. https://doi.org/10.1158/1535-7163.MCT-15-1004

Dowdy, S.F., 2017. Overcoming cellular barriers for RNA therapeutics. Nat Biotechnol 35, 222–229. https://doi.org/10.1038/nbt.3802

Duchardt, F., Fotin-Mleczek, M., Schwarz, H., Fischer, R., Brock, R., 2007. A Comprehensive Model for the Cellular Uptake of Cationic Cell-penetrating Peptides. Traffic 8, 848–866. https://doi.org/10.1111/j.1600-0854.2007.00572.x

Dunkelberger, J.R., Song, W.-C., 2010. Complement and its role in innate and adaptive immune responses. Cell Res 20, 34–50. https://doi.org/10.1038/cr.2009.139

Eckstein, F., 2014. Phosphorothioates, Essential Components of Therapeutic Oligonucleotides. Nucleic Acid Therapeutics 24, 374–387. https://doi.org/10.1089/nat.2014.0506

Elion, G.B., Singer, S., Hitchings, G.H., 1954. Antagonists of nucleic acid derivatives. VIII. Synergism in combination of biochemically related antimetabolites. J Biol Chem 208, 477-488.

Eguchi, A., Meade, B.R., Chang, Y.-C., Fredrickson, C.T., Willert, K., Puri, N., Dowdy, S.F., 2009. Efficient siRNA delivery into primary cells by a peptide transduction domain–dsRNA binding domain fusion protein. Nat Biotechnol 27, 567–571. https://doi.org/10.1038/nbt.1541

Elbashir, S.M., Harborth, J., Lendeckel, W., Yalcin, A., Weber, K., Tuschl, T., 2001. Duplexes of 21-nucleotide RNAs mediate RNA interference in cultured mammalian cells. Nature 411, 494–498. https://doi.org/10.1038/35078107

Ender, C., Meister, G., 2010. Argonaute proteins at a glance. Journal of Cell Science 123, 1819–1823. https://doi.org/10.1242/jcs.055210

Finkel, R.S., Mercuri, E., Darras, B.T., Connolly, A.M., Kuntz, N.L., Kirschner, J., Chiriboga, C.A., Saito, K., Servais, L., Tizzano, E., Topaloglu, H., Tulinius, M., Montes, J., Glanzman, A.M., Bishop, K., Zhong, Z.J., Gheuens, S., Bennett, C.F., Schneider, E., Farwell, W., De Vivo, D.C., 2017. Nusinersen versus Sham Control in Infantile-Onset Spinal Muscular Atrophy. N Engl J Med 377, 1723–1732. https://doi.org/10.1056/NEJMoa1702752

Fire, A., Xu, S., Montgomery, M.K., Kostas, S.A., Driver, S.E., Mello, C.C., 1998. Potent and specific genetic interference by double-stranded RNA in Caenorhabditis elegans. Nature 391, 806-811.

Fischer, R., Köhler, K., Fotin-Mleczek, M., Brock, R., 2004. A Stepwise Dissection of the Intracellular Fate of Cationic Cell-penetrating Peptides. Journal of Biological Chemistry 279, 12625–12635. https://doi.org/10.1074/jbc.M311461200

Fitzgerald, K., White, S., Borodovsky, A., Bettencourt, B.R., Strahs, A., Clausen, V., Wijngaard, P., Horton, J.D., Taubel, J., Brooks, A., Fernando, C., Kauffman, R.S., Kallend, D., Vaishnaw, A., Simon, A., 2017. A Highly Durable RNAi Therapeutic Inhibitor of PCSK9. N Engl J Med 376, 41–51. https://doi.org/10.1056/NEJMoa1609243

Foerg, C., Ziegler, U., Fernandez-Carneado, J., Giralt, E., Rennert, R., Beck-Sickinger, A.G., Merkle, H.P., 2005. Decoding the Entry of Two Novel Cell-Penetrating Peptides in HeLa Cells: Lipid Raft-Mediated Endocytosis and Endosomal Escape †. Biochemistry 44, 72–81. https://doi.org/10.1021/bi048330+

Foster, D.J., Brown, C.R., Shaikh, S., Trapp, C., Schlegel, M.K., Qian, K., Sehgal, A., Rajeev, K.G., Jadhav, V., Manoharan, M., Kuchimanchi, S., Maier, M.A., Milstein, S., 2018. Advanced siRNA Designs Further Improve In Vivo Performance of GalNAc-siRNA Conjugates. Molecular Therapy 26, 708–717. https://doi.org/10.1016/j.ymthe.2017.12.021

Frank, F., Sonenberg, N., Nagar, B., 2010. Structural basis for 5′-nucleotide base-specific recognition of guide RNA by human AGO2. Nature 465, 818–822. https://doi.org/10.1038/nature09039

Frankel, A.D., Pabo, C.O, 1988. Cellular uptake of the tat protein from human immunodeficiency virus. Cell 55, 1189-1193.

Frey, N., Porter, D., 2019. Cytokine Release Syndrome with Chimeric Antigen Receptor T Cell Therapy. Biology of Blood and Marrow Transplantation 25, e123–e127. https://doi.org/10.1016/j.bbmt.2018.12.756

Gagliardi, M., Ashizawa, A.T., 2021. The Challenges and Strategies of Antisense Oligonucleotide Drug Delivery. Biomedicines 9, 433. https://doi.org/10.3390/biomedicines9040433

Gantier, M.P., Williams, B.R.G., 2007. The response of mammalian cells to double-stranded RNA. Cytokine & Growth Factor Reviews 18, 363–371. https://doi.org/10.1016/j.cytogfr.2007.06.016

Gao, S., Dagnaes-Hansen, F., Nielsen, E.J.B., Wengel, J., Besenbacher, F., Howard, K.A., Kjems, J., 2009. The Effect of Chemical Modification and Nanoparticle Formulation on Stability and Biodistribution of siRNA in Mice. Molecular Therapy 17, 1225–1233. https://doi.org/10.1038/mt.2009.91

García-Alonso, S., Ocaña, A., Pandiella, A., 2018. Resistance to Antibody–Drug Conjugates. Cancer Res 78, 2159–2165. https://doi.org/10.1158/0008-5472.CAN-17-3671

Geuze, H.J., Willem, J., Strous, G., 1983. Intracellular Site of Asialoglycoprotein Receptor-Ligand Uncoupling: Double-Label Immunoelectron Microscopy during Receptor-Mediated Endocytosis. Cell 11, 277-287.

Gilleron, J., Querbes, W., Zeigerer, A., Borodovsky, A., Marsico, G., Schubert, U., Manygoats, K., Seifert, S., Andree, C., Stöter, M., Epstein-Barash, H., Zhang, L., Koteliansky, V., Fitzgerald, K., Fava, E., Bickle, M., Kalaidzidis, Y., Akinc, A., Maier, M., Zerial, M., 2013. Image-based analysis of lipid nanoparticle–mediated siRNA delivery, intracellular trafficking and endosomal escape. Nat Biotechnol 31, 638–646. https://doi.org/10.1038/nbt.2612

Goldberg, S.D., Cardoso, R.M.F., Lin, T., Spinka-Doms, T., Klein, D., Jacobs, S.A., Dudkin, V., Gilliland, G., O'Neil, K.T., 2016. Engineering a targeted delivery platform using Centyrins. Protein Engineering, Design and Selection proeng;gzw054v1. https://doi.org/10.1093/protein/gzw054

Goldstein, J.L., Brown, M.S., 2009. The LDL Receptor. ATVB 29, 431–438. https://doi.org/10.1161/ATVBAHA.108.179564

Gomes-da-Silva, L.C., Fonseca, N.A., Moura, V., Pedroso de Lima, M.C., Simões, S., Moreira, J.N., 2012. Lipid-Based Nanoparticles for siRNA Delivery in Cancer Therapy: Paradigms and Challenges. Acc. Chem. Res. 45, 1163–1171. https://doi.org/10.1021/ar300048p

Green, M., Loewenstein, P.M., 1988. Autonomous Functional Domains of Chemically Synthesized Human Immunodeficiency Virus Tat Trans-Activator Protein 55, 1179-1188.

Gregoriadis, G., Morell, A.G., Sternlieb, I., Scheinberg, I.H., 1970. Catabolism of Desialylated Ceruloplasmin in the Liver. Journal of Biological Chemistry 245, 5833–5837. https://doi.org/10.1016/S0021-9258(18)62728-0

Ha, M., Kim, V.N., 2014. Regulation of microRNA biogenesis. Nat Rev Mol Cell Biol 15, 509–524. https://doi.org/10.1038/nrm3838

Haanen, J.B.A.G., Robert, C., 2015. Immune Checkpoint Inhibitors, in: Michielin, O., Coukos, G. (Eds.), Progress in Tumor Research. S. Karger AG, pp. 55–66. https://doi.org/10.1159/000437178

Hagopian, J.C., Hamil, A.S., van den Berg, A., Meade, B.R., Eguchi, A., Palm-Apergi, C., Dowdy, S.F., 2017. Induction of RNAi Responses by Short Left-Handed Hairpin RNAi Triggers. Nucleic Acid Therapeutics 27, 260–271. https://doi.org/10.1089/nat.2017.0686

Hair, P., Cameron, F., McKeage, K., 2013. Mipomersen Sodium: First Global Approval. Drugs 73, 487–493. https://doi.org/10.1007/s40265-013-0042-2

Hajimolaali, M., Mohammadian, H., Torabi, A., Shirini, A., Khalife Shal, M., Barazandeh Nezhad, H., Iranpour, S., Baradaran Eftekhari, R., Dorkoosh, F., 2021. Application of chloroquine as an endosomal escape enhancing agent: new frontiers for an old drug. Expert Opinion on Drug Delivery 18, 877–889. https://doi.org/10.1080/17425247.2021.1873272

Hajj, K.A., Whitehead, K.A., 2017. Tools for translation: non-viral materials for therapeutic mRNA delivery. Nat Rev Mater 2, 17056. https://doi.org/10.1038/natrevmats.2017.56

Hamann, P.R., Hinman, L.M., Beyer, C.F., Lindh, D., Upeslacis, J., Flowers, D.A., Bernstein, I., 2002. An Anti-CD33 Antibody−Calicheamicin Conjugate for Treatment of Acute Myeloid Leukemia. Choice of Linker. Bioconjugate Chem. 13, 40–46. https://doi.org/10.1021/bc0100206

Hamblett, K.J., Senter, P.D., Chace, D.F., Sun, M.M.C., Lenox, J., Cerveny, C.G., Kissler, K.M., Bernhardt, S.X., Kopcha, A.K., Zabinski, R.F., Meyer, D.L., Francisco, J.A., 2004. Effects of Drug Loading on the Antitumor Activity of a Monoclonal Antibody Drug Conjugate. Clin Cancer Res 10, 7063–7070. https://doi.org/10.1158/1078-0432.CCR-04-0789

Han, J., Lee, Y., Yeom, K.-H., Nam, J.-W., Heo, I., Rhee, J.-K., Sohn, S.Y., Cho, Y., Zhang, B.-T., Kim, V.N., 2006. Molecular Basis for the Recognition of Primary microRNAs by the Drosha-DGCR8 Complex. Cell 125, 887–901. https://doi.org/10.1016/j.cell.2006.03.043

Hassler, M.R., Turanov, A.A., Alterman, J.F., Haraszti, R.A., Coles, A.H., Osborn, M.F., Echeverria, D., Nikan, M., Salomon, W.E., Roux, L., Godinho, B.M.D.C., Davis, S.M., Morrissey, D.V., Zamore, P.D., Karumanchi, S.A., Moore, M.J., Aronin, N., Khvorova, A., 2018. Comparison of partially and fully chemically-modified siRNA in conjugate-mediated delivery in vivo. Nucleic Acids Research 46, 2185–2196. https://doi.org/10.1093/nar/gky037

Havens, M.A., Hastings, M.L., 2016. Splice-switching antisense oligonucleotides as therapeutic drugs. Nucleic Acids Res 44, 6549–6563. https://doi.org/10.1093/nar/gkw533

Heil, F., 2004. Species-Specific Recognition of Single-Stranded RNA via Toll-like Receptor 7 and 8. Science 303, 1526–1529. https://doi.org/10.1126/science.1093620

Herdewijn, P., 2000. Heterocyclic Modifications of Oligonucleotides and Antisense Technology. Antisense and Nucleic Acid Drug Development 10, 297–310. https://doi.org/10.1089/108729000421475

Herzog, V.A., Ameres, S.L., 2015. Approaching the Golden Fleece a Molecule at a Time: Biophysical Insights into Argonaute-Instructed Nucleic Acid Interactions. Molecular Cell 59, 4–7. https://doi.org/10.1016/j.molcel.2015.06.021

Hitchings, G.H., Elion, G.B., 1954. The Chemistry and Biochemistry of Purine Analogs. Annals of NY Academy of Sciences 60, 195-199. https://doi..org/10.1111/j.1749-6632.1954.tb40008.x

Hou, K.K., Pan, H., Schlesinger, P.H., Wickline, S.A., 2015. A role for peptides in overcoming endosomal entrapment in siRNA delivery — A focus on melittin. Biotechnology Advances 33, 931–940. https://doi.org/10.1016/j.biotechadv.2015.05.005

Hoy, S.M., 2018. Patisiran: First Global Approval. Drugs 78, 1625–1631. https://doi.org/10.1007/s40265-018-0983-6

Hu, Y.-B., Dammer, E.B., Ren, R.-J., Wang, G., 2015. The endosomal-lysosomal system: from acidification and cargo sorting to neurodegeneration. Transl Neurodegener 4, 18. https://doi.org/10.1186/s40035-015-0041-1

Hua, Y., Vickers, T.A., Baker, B.F., Bennett, C.F., Krainer, A.R., 2007. Enhancement of SMN2 Exon 7 Inclusion by Antisense Oligonucleotides Targeting the Exon. PLoS Biol 5, e73. https://doi.org/10.1371/journal.pbio.0050073

Huang, Y., Shen, X.J., Zou, Q., Wang, S.P., Tang, S.M., Zhang, G.Z., 2011. Biological functions of microRNAs: a review. J Physiol Biochem 67, 129–139. https://doi.org/10.1007/s13105-010-0050-6

Ibrahim, R.A., Berman, D.M., DePril, V., Humphrey, R.W., Chen, T., Messina, M., Chin, K.M., Liu, H.Y., Bielefield, M., Hoos, A., 2011. Ipilimumab safety profile: Summary of findings from completed trials in advanced melanoma. J Clin Oncology, 29, 8583-8583. https://doi.org/10.1200/jco.2011.29.15_suppl.8583

Ishida, T., Ichihara, M., Wang, X., Yamamoto, K., Kimura, J., Majima, E., Kiwada, H., 2006. Injection of PEGylated liposomes in rats elicits PEG-specific IgM, which is responsible for rapid elimination of a second dose of PEGylated liposomes. Journal of Controlled Release 112, 15–25. https://doi.org/10.1016/j.jconrel.2006.01.005

Ipsaro, J.J., Joshua-Tor, L., 2015. From guide to target: molecular insights into eukaryotic RNA-interference machinery. Nat Struct Mol Biol 22, 20–28. https://doi.org/10.1038/nsmb.2931

Iversen, F., Yang, C., Dagnæs-Hansen, F., Schaffert, D.H., Kjems, J., Gao, S., 2013. Optimized siRNA-PEG Conjugates for Extended Blood Circulation and Reduced Urine Excretion in Mice. Theranostics 3, 201–209. https://doi.org/10.7150/thno.5743

Janeway, C.A., Travers, P., Walport, M., Schlomchik, M., 2005. Immuno-biology: The Immune System in Health and Disease. 6th Edition, New York: Garland Publishing.

Jaracz, S., Chen, J., Kuznetsova, L.V., Ojima, I., 2005. Recent advances in tumor-targeting anticancer drug conjugates. Bioorganic & Medicinal Chemistry 13, 5043–5054. https://doi.org/10.1016/j.bmc.2005.04.084

Judge, A., Sood, V., Shaw, J., Fang, D., McClintock, K., MacLach, I, 2005. Sequence-dependent stimulation of the mammalian innate immune response by synthetic siRNA. Nat Biotechnol 23, 457–462. https://doi.org/10.1038/nbt1081

Juliano, R.L., Ming, X., Nakagawa, O., 2012. Cellular Uptake and Intracellular Trafficking of Antisense and siRNA Oligonucleotides. Bioconjugate Chem. 23, 147–157. https://doi.org/10.1021/bc200377d

Juliano, R.L., Carver, K., 2015. Cellular uptake and intracellular trafficking of oligonucleotides. Advanced Drug Delivery Reviews 87, 35–45. https://doi.org/10.1016/j.addr.2015.04.005

Juliano, R.L., 2016. The delivery of therapeutic oligonucleotides. Nucleic Acids Res 44, 6518–6548. https://doi.org/10.1093/nar/gkw236

Kaplan, I.M., Wadia, J.S., Dowdy, S.F., 2005. Cationic TAT peptide transduction domain enters cells by macropinocytosis. Journal of Controlled Release 102, 247–253. https://doi.org/10.1016/j.jconrel.2004.10.018

Karikó, K., Bhuyan, P., Capodici, J., Weissman, D., 2004. Small Interfering RNAs Mediate Sequence-Independent Gene Suppression and Induce Immune Activation by Signaling through Toll-Like Receptor 3. J Immunol 172, 6545–6549. https://doi.org/10.4049/jimmunol.172.11.6545

Kasravi, F.B., Wang, X., Guo, W., Andersson, R., Norgren, L., Jeppsson, B., Bengmark, S. 1995. Reticuloendothelial system function in acute livery injury induced by D-galactosamine. J Hepatology 23, 727-733.

Kauffman, K.J., Webber, M.J., Anderson, D.G., 2016. Materials for non-viral intracellular delivery of messenger RNA therapeutics. Journal of Controlled Release 240, 227–234. https://doi.org/10.1016/j.jconrel.2015.12.032

Kawamura, K.S., Sung, M., Bolewska-Pedyczak, E., Gariépy, J., 2006. Probing the Impact of Valency on the Routing of Arginine-Rich Peptides into Eukaryotic Cells. Biochemistry 45, 1116–1127. https://doi.org/10.1021/bi051338e

Keating, M.J., O'Brien, S., Albitar, M., 2002. Emerging information on the use of rituximab in chronic lymphocytic leukemia. Seminars in Oncology 29, 70-74. https://doi.org/10.1053/sonc.2002.30142

Kennedy, L.B., Salama, A.K.S., 2020. A review of cancer immunotherapy toxicity. CA A Cancer J Clin 70, 86–104. https://doi.org/10.3322/caac.21596

Kersey, J.H., 1997. Fifty Years of Studies of the Biology and Therapy of Childhood Leukemia. Blood 90, 4243-4251. https://doi.org/10.1182/blood.V90.11.4243

Khera, N., Rajput, S., 2017. Therapeutic Potential of Small Molecule Inhibitors: THERAPEUTIC POTENTIAL OF SMI. J. Cell. Biochem. 118, 959–961. https://doi.org/10.1002/jcb.25782

Khongorzul, P., Ling, C.J., Khan, F.U., Ihsan, A.U., Zhang, J., 2020. Antibody–Drug Conjugates: A Comprehensive Review. Mol Cancer Res 18, 3–19. https://doi.org/10.1158/1541-7786.MCR-19-0582

Khvorova, A., Watts, J.K., 2017. The chemical evolution of oligonucleotide therapies of clinical utility. Nat Biotechnol 35, 238–248. https://doi.org/10.1038/nbt.3765

Kim, Y.-K., Kim, V.N., 2007. Processing of intronic microRNAs. EMBO J 26, 775–783. https://doi.org/10.1038/sj.emboj.7601512

Kim, V.N., Han, J., Siomi, M.C., 2009. Biogenesis of small RNAs in animals. Nat Rev Mol Cell Biol 10, 126–139. https://doi.org/10.1038/nrm2632

Kim, S.H., Jeong, J.H., Lee, S.H., Kim, S.W., Park, T.G., 2008. Local and systemic delivery of VEGF siRNA using polyelectrolyte complex micelles for effective treatment of cancer. Journal of Controlled Release 129, 107–116. https://doi.org/10.1016/j.jconrel.2008.03.008

Kim, J., Hu, C., Moufawad El Achkar, C., Black, L.E., Douville, J., Larson, A., Pendergast, M.K., Goldkind, S.F., Lee, E.A., Kuniholm, A., Soucy, A., Vaze, J., Belur, N.R., Fredriksen, K., Stojkovska, I., Tsytsykova, A., Armant, M., DiDonato, R.L., Choi, J., Cornelissen, L., Pereira, L.M., Augustine, E.F., Genetti, C.A., Dies, K., Barton, B., Williams, L., Goodlett, B.D., Riley, B.L., Pasternak, A., Berry, E.R., Pflock, K.A., Chu, S., Reed, C., Tyndall, K., Agrawal, P.B., Beggs, A.H., Grant, P.E., Urion, D.K., Snyder, R.O., Waisbren, S.E., Poduri, A., Park, P.J., Patterson, A., Biffi, A., Mazzulli, J.R., Bodamer, O., Berde, C.B., Yu, T.W., 2019. Patient-Customized Oligonucleotide Therapy for a Rare Genetic Disease. N Engl J Med 381, 1644–1652. https://doi.org/10.1056/NEJMoa1813279

King, M.-C., Marks, J.H., Mandell, J.B., 2003. Breast and Ovarian Cancer Risks Due to Inherited Mutations in *BRCA1* and *BRCA2*. Science 302, 643–646. https://doi.org/10.1126/science.1088759

Kole, R., Krainer, A.R., Altman, S., 2012. RNA therapeutics: beyond RNA interference and antisense oligonucleotides. Nat Rev Drug Discov 11, 125–140. https://doi.org/10.1038/nrd3625

Kosmas, C., Muñoz Estrella, A., Sourlas, A., Silverio, D., Hilario, E., Montan, P., Guzman, E., 2018. Inclisiran: A New Promising Agent in the Management of Hypercholesterolemia. Diseases 6, 63. https://doi.org/10.3390/diseases6030063

Kovtun, Y.V., Audette, C.A., Ye, Y., Xie, H., Ruberti, M.F., Phinney, S.J., Leece, B.A., Chittenden, T., Blättler, W.A., Goldmacher, V.S., 2006. Antibody-Drug Conjugates Designed to Eradicate Tumors with Homogeneous and Heterogeneous Expression of the Target Antigen. Cancer Res 66, 3214–3221. https://doi.org/10.1158/0008-5472.CAN-05-3973

Lakhin, A.V., Tarantul, V.Z., Gening, L.V., 2013. Aptamers: Problems, Solutions and Prospects. Acta Naturae 5, 34–43. https://doi.org/10.32607/20758251-2013-5-4-34-43

Lam, J.K.W., Chow, M.Y.T., Zhang, Y., Leung, S.W.S., 2015. siRNA Versus miRNA as Therapeutics for Gene Silencing. Molecular Therapy - Nucleic Acids 4, e252. https://doi.org/10.1038/mtna.2015.23

Le, D.T., Uram, J.N., Wang, H., Bartlett, B.R., Kemberling, H., Eyring, A.D., Skora, A.D., Luber, B.S., Azad, N.S., Laheru, D., Biedrzycki, B., Donehower, R.C., Zaheer, A., Fisher, G.A., Crocenzi, T.S., Lee, J.J., Duffy, S.M., Goldberg, R.M., de la Chapelle, A., Koshiji, M., Bhaijee, F., Huebner, T., Hruban, R.H., Wood, L.D., Cuka, N., Pardoll, D.M., Papadopoulos, N., Kinzler, K.W., Zhou, S., Cornish, T.C., Taube, J.M., Anders, R.A., Eshleman, J.R., Vogelstein, B., Diaz, L.A., 2015. PD-1 Blockade in Tumors with Mismatch-Repair Deficiency. N Engl J Med 372, 2509–2520. https://doi.org/10.1056/NEJMoa1500596

Lee, M.-T., Hung, W.-C., Chen, F.-Y., Huang, H.W., 2008. Mechanism and kinetics of pore formation in membranes by water-soluble amphipathic peptides. PNAS 105, 5087-5092.

Lee, Y., Rio, D.C., 2015. Mechanisms and Regulation of Alternative Pre-mRNA Splicing. Annu. Rev. Biochem. 84, 291–323. https://doi.org/10.1146/annurev-biochem-060614-034316

Lee, D.W., Santomasso, B.D., Locke, F.L., Ghobadi, A., Turtle, C.J., Brudno, J.N., Maus, M.V., Park, J.H., Mead, E., Pavletic, S., Go, W.Y., Eldjerou, L., Gardner, R.A., Frey, N., Curran, K.J., Peggs, K., Pasquini, M., DiPersio, J.F., van den Brink, M.R.M., Komanduri, K.V., Grupp, S.A., Neelapu, S.S., 2019. ASTCT Consensus Grading for Cytokine Release Syndrome and Neurologic Toxicity Associated with Immune Effector Cells. Biology of Blood and Marrow Transplantation 25, 625–638. https://doi.org/10.1016/j.bbmt.2018.12.758

Li, W., Chen, H., Sutton, T., Obadan, A., Perez, D.R., 2014. Interactions between the Influenza A Virus RNA Polymerase Components and Retinoic Acid-Inducible Gene I. Journal of Virology 88, 10432–10447. https://doi.org/10.1128/JVI.01383-14

Liang, X.-H., Sun, H., Nichols, J.G., Crooke, S.T., 2017. RNase H1-Dependent Antisense Oligonucleotides Are Robustly Active in Directing RNA Cleavage in Both the Cytoplasm and the Nucleus. Molecular Therapy 25, 2075–2092. https://doi.org/10.1016/j.ymthe.2017.06.002

Lindgren, M., Langel, Ü, 2011. Classes and Prediction of Cell-Penetrating Peptides. Cell Penetrating Peptides. Methods in Molecular Biology (Methods and Protocols). Humana Press, 683.

Lipinski, C.A., Lombardo, F., Dominy, B.W., Feeney, P.J., 2001. Experimental and computational approaches to estimate solubility and permeability in drug discovery and development settings. Advanced Drug Delivery Reviews 46, 3-26.

Lipinski, C.A., 2004. Lead- and drug-like compounds: the rule-of-five revolution. Drug Discovery Today: Technologies 1, 337–341. https://doi.org/10.1016/j.ddtec.2004.11.007

Liu, G., Lu, Y., Thulasi Raman, S.N., Xu, F., Wu, Q., Li, Z., Brownlie, R., Liu, Q., Zhou, Y., 2018. Nuclear-resident RIG-I senses viral replication inducing antiviral immunity. Nat Commun 9, 3199. https://doi.org/10.1038/s41467-018-05745-w

Locke, F.L., Ghobadi, A., Jacobson, C.A., Miklos, D.B., Lekakis, L.J., Oluwole, O.O., Lin, Y., Braunschweig, I., Hill, B.T., Timmerman, J.M., Deol, A., Reagan, P.M., Stiff, P., Flinn, I.W., Farooq, U., Goy, A., McSweeney, P.A., Munoz, J., Siddiqi, T., Chavez, J.C., Herrera, A.F., Bartlett, N.L., Wiezorek, J.S., Navale, L., Xue, A., Jiang, Y., Bot, A., Rossi, J.M., Kim, J.J., Go, W.Y., Neelapu, S.S., 2019. Long-term safety and activity of axicabtagene ciloleucel in refractory large B-cell lymphoma (ZUMA-1): a single-arm, multicentre, phase 1–2 trial. The Lancet Oncology 20, 31–42. https://doi.org/10.1016/S1470-2045(18)30864-7

Lönn, P., Dowdy, S.F., 2015. Cationic PTD/CPP-mediated macromolecular delivery: charging into the cell. Expert Opinion on Drug Delivery 12, 1627–1636. https://doi.org/10.1517/17425247.2015.1046431

Lönn, P., Kacsinta, A.D., Cui, X.-S., Hamil, A.S., Kaulich, M., Gogoi, K., Dowdy, S.F., 2016. Enhancing Endosomal Escape for Intracellular Delivery of Macromolecular Biologic Therapeutics. Sci Rep 6, 32301. https://doi.org/10.1038/srep32301

Lord, C.J., Ashworth, A., 2017. PARP inhibitors: Synthetic lethality in the clinic. Science 355, 1152–1158. https://doi.org/10.1126/science.aam7344

Loverix, S., Steyaert, J., 2003. Ribonucleases: from prototypes to therapeutic targets? Curr Med Chem 10, 779-85. doi: 10.2174/0929867033457845.

Lu, J., Jiang, F., Lu, A., Zhang, G., 2016. Linkers Having a Crucial Role in Antibody–Drug Conjugates. IJMS 17, 561. https://doi.org/10.3390/ijms17040561

Lu, M., Zhang, Q., Deng, M., Miao, J., Guo, Y., Gao, W., Cui, Q., 2008. An Analysis of Human MicroRNA and Disease Associations. PLoS ONE 3, e3420. https://doi.org/10.1371/journal.pone.0003420

Lund, E., 2004. Nuclear Export of MicroRNA Precursors. Science 303, 95–98. https://doi.org/10.1126/science.1090599

MacFarlane, L.-A., R. Murphy, P., 2010. MicroRNA: Biogenesis, Function and Role in Cancer. CG 11, 537–561. https://doi.org/10.2174/138920210793175895

MacRae, I.J., Kaihong Z., Doudna, J.A., 2007. “Structural Determinants of RNA Recognition and Cleavage by Dicer.” Nature Structural & Molecular Biology 14, 934-940. https://doi.org/10.1038/nsmb1293

MacRae, I.J., Ma, E., Zhou, M., Robinson, C.V., Doudna, J.A., 2008. In vitro reconstitution of the human RISC-loading complex. Proceedings of the National Academy of Sciences 105, 512–517. https://doi.org/10.1073/pnas.0710869105

Maitra, R., Augustine, T., Dayan, Y., Chandy, C., Coffey, M., Goel, S., 2017. Toll-like receptor 3 as an immunotherapeutic target for *KRAS* mutated colorectal cancer. Oncotarget 8, 35138–35153. https://doi.org/10.18632/oncotarget.16812

Maleki Vareki, S., 2018. High and low mutational burden tumors versus immunologically hot and cold tumors and response to immune checkpoint inhibitors. j. immunotherapy cancer 6, 157, s40425-018-0479–7. https://doi.org/10.1186/s40425-018-0479-7

Malik, P., Phipps, C., Edginton, A., Blay, J., 2017. Pharmacokinetic Considerations for Antibody-Drug Conjugates against Cancer. Pharm Res 34, 2579–2595. https://doi.org/10.1007/s11095-017-2259-3

Maude, S.L., Laetsch, T.W., Buechner, J., Rives, S., Boyer, M., Bittencourt, H., Bader, P., Verneris, M.R., Stefanski, H.E., Myers, G.D., Qayed, M., De Moerloose, B., Hiramatsu, H., Schlis, K., Davis, K.L., Martin, P.L., Nemecek, E.R., Yanik, G.A., Peters, C., Baruchel, A., Boissel, N., Mechinaud, F., Balduzzi, A., Krueger, J., June, C.H., Levine, B.L., Wood, P., Taran, T., Leung, M., Mueller, K.T., Zhang, Y., Sen, K., Lebwohl, D., Pulsipher, M.A., Grupp, S.A., 2018. Tisagenlecleucel in Children and Young Adults with B-Cell Lymphoblastic Leukemia. N Engl J Med 378, 439–448. https://doi.org/10.1056/NEJMoa1709866

Maxfield, F.R., 1982. Weak bases and ionophores rapidly and reversibly raise the pH of endocytic vesicles in cultured mouse fibroblasts. Journal of Cell Biology 95, 676–681. https://doi.org/10.1083/jcb.95.2.676

Mayor, S., Pagano, R.E., 2007. Pathways of clathrin-independent endocytosis. Nat Rev Mol Cell Biol 8, 603–612. https://doi.org/10.1038/nrm2216

Mckertish, C.M., Kayser, V., 2021. Advances and Limitations of Antibody Drug Conjugates for Cancer. Biomedicines 9, 872. https://doi.org/10.3390/biomedicines9080872

Meade, B.R., Gogoi, K., Hamil, A.S., Palm-Apergi, C., Berg, A. van den, Hagopian, J.C., Springer, A.D., Eguchi, A., Kacsinta, A.D., Dowdy, C.F., Presente, A., Lönn, P., Kaulich, M., Yoshioka, N., Gros, E., Cui, X.-S., Dowdy, S.F., 2014. Efficient delivery of RNAi prodrugs containing reversible charge-neutralizing phosphotriester backbone modifications. Nat Biotechnol 32, 1256–1261. https://doi.org/10.1038/nbt.3078

Meibohm, B., Zhou, H., 2012. Characterizing the Impact of Renal Impairment on the Clinical Pharmacology of Biologics. The Journal of Clinical Pharmacology 52. https://doi.org/10.1177/0091270011413894

Meister, G., 2013. Argonaute proteins: functional insights and emerging roles. Nat Rev Genet 14, 447–459. https://doi.org/10.1038/nrg3462

Meister, G., Landthaler, M., Patkaniowska, A., Dorsett, Y., Teng, G., Tuschl, T., 2004. Human Argonaute2 Mediates RNA Cleavage Targeted by miRNAs and siRNAs. Molecular Cell 15, 185–197. https://doi.org/10.1016/j.molcel.2004.07.007

Menchise, V., De Simone, G., Tedeschi, T., Corradini, R., Sforza, S., Marchelli, R., Capasso, D., Saviano, M., Pedone, C., 2003. Insights into peptide nucleic acid (PNA) structural features: The crystal structure of a D-lysine-based chiral PNA-DNA duplex. Proceedings of the National Academy of Sciences 100, 12021–12026. https://doi.org/10.1073/pnas.2034746100

Mercuri, E., Darras, B.T., Chiriboga, C.A., Day, J.W., Campbell, C., Connolly, A.M., Iannaccone, S.T., Kirschner, J., Kuntz, N.L., Saito, K., Shieh, P.B., Tulinius, M., Mazzone, E.S., Montes, J., Bishop, K.M., Yang, Q., Foster, R., Gheuens, S., Bennett, C.F., Farwell, W.,

Schneider, E., De Vivo, D.C., Finkel, R.S., 2018. Nusinersen versus Sham Control in Later-Onset Spinal Muscular Atrophy. N Engl J Med 378, 625–635. https://doi.org/10.1056/NEJMoa1710504

Michiue, H., Eguchi, A., Scadeng, M., Dowdy, S.F., 2009. Induction of in vivo synthetic lethal RNAi responses to treat glioblastoma. Cancer Biology & Therapy 8, 2304–2311. https://doi.org/10.4161/cbt.8.23.10271

Mogensen, T.H., 2009. Pathogen Recognition and Inflammatory Signaling in Innate Immune Defenses. Clin Microbiol Rev 22, 240–273. https://doi.org/10.1128/CMR.00046-08

Moschos, S.A., Jones, S.W., Perry, M.M., Williams, A.E., Erjefalt, J.S., Turner, J.J., Barnes, P.J., Sproat, B.S., Gait, M.J., Lindsay, M.A., 2007. Lung Delivery Studies Using siRNA Conjugated to TAT(48−60) and Penetratin Reveal Peptide Induced Reduction in Gene Expression and Induction of Innate Immunity. Bioconjugate Chem. 18, 1450–1459. https://doi.org/10.1021/bc070077d

Mukherjee, S., 2010. The Emperor of All Maladies, 1st ed. Scribner.

Murchison, E.P., Partridge, J.F., Tam, O.H., Cheloufi, S., Hannon, G.J., 2005. Characterization of Dicer-deficient murine embryonic stem cells. Proceedings of the National Academy of Sciences 102, 12135–12140. https://doi.org/10.1073/pnas.0505479102

Nair, J.K., Willoughby, J.L.S., Chan, A., Charisse, K., Alam, Md.R., Wang, Q., Hoekstra, M., Kandasamy, P., Kel'in, A.V., Milstein, S., Taneja, N., O'Shea, J., Shaikh, S., Zhang, L., van der Sluis, R.J., Jung, M.E., Akinc, A., Hutabarat, R., Kuchimanchi, S., Fitzgerald, K., Zimmermann, T., van Berkel, T.J.C., Maier, M.A., Rajeev, K.G., Manoharan, M., 2014. Multivalent *N* -Acetylgalactosamine-Conjugated siRNA Localizes in Hepatocytes and Elicits Robust RNAi-Mediated Gene Silencing. J. Am. Chem. Soc. 136, 16958–16961. https://doi.org/10.1021/ja505986a

Nakase, I., Tanaka, G., Futaki, S., 2013. Cell-penetrating peptides (CPPs) as a vector for the delivery of siRNAs into cells. Mol. BioSyst. 9, 855. https://doi.org/10.1039/c2mb25467k

Nasiri, H., Valedkarimi, Z., Aghebati-Maleki, L., Majidi, J., 2018. Antibody-drug conjugates: Promising and efficient tools for targeted cancer therapy. J Cell Physiol 233, 644-6457. https://doi.org/10.1002/jcp.26435

Nayak, L., Iwamoto, F.M., LaCasce, A., Mukundan, S., Roemer, M.G.M., Chapuy, B., Armand, P., Rodig, S.J., Shipp, M.A., 2017. PD-1 blockade with nivolumab in relapsed/refractory primary central nervous system and testicular lymphoma. Blood 129, 3071–3073. https://doi.org/10.1182/blood-2017-01-764209

Neil, E.E., Bisaccia, E.K., 2019. Nusinersen: A Novel Antisense Oligonucleotide for the Treatment of Spinal Muscular Atrophy. The Journal of Pediatric Pharmacology and Therapeutics 24, 194–203. https://doi.org/10.5863/1551-6776-24.3.194

Neveu, M., Kim, H.-J., Benner, S.A., 2013. The "Strong" RNA World Hypothesis: Fifty Years Old. Astrobiology 13, 391–403. https://doi.org/10.1089/ast.2012.0868

Ochoa, M.C., Minute, L., Rodriguez, I., Garasa, S., Perez-Ruiz, E., Inogés, S., Melero, I., Berraondo, P., 2017. Antibody-dependent cell cytotoxicity: immunotherapy strategies enhancing effector NK cells. Immunol Cell Biol 95, 347–355. https://doi.org/10.1038/icb.2017.6

Oldham, R.K., Dillman, R.O., 2008. Monoclonal Antibodies in Cancer Therapy: 25 Years of Progress. JCO 26, 1774–1777. https://doi.org/10.1200/JCO.2007.15.7438

Osborn, M.F., Khvorova, A., 2018. Improving siRNA Delivery *In Vivo* Through Lipid Conjugation. Nucleic Acid Therapeutics 28, 128–136. https://doi.org/10.1089/nat.2018.0725

Palm-Apergi, C., Lönn, P., Dowdy, S.F., 2012. Do Cell-Penetrating Peptides Actually "Penetrate" Cellular Membranes? Molecular Therapy 20, 695–697. https://doi.org/10.1038/mt.2012.40

Parmar, R., Willoughby, J., Liu, J., Foster, D.J., Brighma, B., Theile, C.S., Charisse, K., Akinc, A., Guidry, E., Pei, Y., Strapps, W., Cancilla, M., Stanton, M.G., Rajeev, K.G., Sepp-Lorenzino, L., Manoharan, M., Meyers, R., Maier, M.A., Jadhav, V., 2016. 5'-(E)-Vinylphosphonate: A Stable Phosphate Mimic Can Improve the RNAi Activity of siRNA-GalNAc Conjugates. ChemBioChem 17, 985-989. https://doi.org/10.1002/cbic.201600130

Passini, M.A., Bu, J., Richards, A.M., Kinnecom, C., Sardi, S.P., Stanek, L.M., Hua, Y., Rigo, F., Matson, J., Hung, G., Kaye, E.M., Shihabuddin, L.S., Krainer, A.R., Bennett, C.F., Cheng, S.H., 2011. Antisense Oligonucleotides Delivered to the Mouse CNS Ameliorate Symptoms of Severe Spinal Muscular Atrophy. Sci. Transl. Med. 3. https://doi.org/10.1126/scitranslmed.3001777

Ponziani, S., Di Vittorio, G., Pitari, G., Cimini, A.M., Ardini, M., Gentile, R., Iacobelli, S., Sala, G., Capone, E., Flavell, D.J., Ippoliti, R., Giansanti, F., 2020. Antibody-Drug Conjugates: The New Frontier of Chemotherapy. IJMS 21, 5510. https://doi.org/10.3390/ijms21155510

Prakash, T.P., Graham, M.J., Yu, J., Carty, R., Low, A., Chappell, A., Schmidt, K., Zhao, C., Aghajan, M., Murray, H.F., Riney, S., Booten, S.L., Murray, S.F., Gaus, H., Crosby, J., Lima, W.F., Guo, S., Monia, B.P., Swayze, E.E., Seth, P.P., 2014. Targeted delivery of antisense oligonucleotides to hepatocytes using triantennary *N* -acetyl galactosamine improves potency 10-fold in mice. Nucleic Acids Research 42, 8796–8807. https://doi.org/10.1093/nar/gku531

Prakash, T.P., Lima, W.F., Murray, H.M., Li, W., Kinberger, G.A., Chappell, A.E., Gaus, H., Seth, P.P., Bhat, B., Crooke, S.T., Swayze, E.E., 2015. Identification of metabolically stable 5′-phosphate analogs that support single-stranded siRNA activity. Nucleic Acids Research 43, 2993–3011. https://doi.org/10.1093/nar/gkv162

Pratt, A.J., MacRae, I.J., 2009. The RNA-induced Silencing Complex: A Versatile Gene-silencing Machine. Journal of Biological Chemistry 284, 17897–17901. https://doi.org/10.1074/jbc.R900012200

Preall, J.B., He, Z., Gorra, J.M., Sontheimer, E.J., 2006. Short Interfering RNA Strand Selection Is Independent of dsRNA Processing Polarity during RNAi in Drosophila. Current Biology 16, 530–535. https://doi.org/10.1016/j.cub.2006.01.061

Rappaport, J., Hanss, B., Kopp, J.B., Copeland, T.D., Bruggeman, L.A., Coffman, T.M., Klotman, P.E., 1995. Transport of phosphorothioate oligonucleotides in kidney: Implications for molecular therapy. Kidney International 47, 1462–1469. https://doi.org/10.1038/ki.1995.205

Rathee, P., Rathee, D., Hooda, A., Kumar, V., Rathee, S., 2012. Peptide Nucleic Acids: An Overview. Pharm Jour 1, 25-42.

Rehwinkel, J., Gack, M.U., 2020. RIG-I-like receptors: their regulation and roles in RNA sensing. Nat Rev Immunol 20, 537–551. https://doi.org/10.1038/s41577-020-0288-3

Rettig, G.R., Behlke, M.A., 2012. Progress Toward In Vivo Use of siRNAs-II. Molecular Therapy 20, 483–512. https://doi.org/10.1038/mt.2011.263

Ribas, A., Wolchok, J.D., 2018. Cancer immunotherapy using checkpoint blockade. Science 359, 1350–1355. https://doi.org/10.1126/science.aar4060

Ritchie, M., Tchistiakova, L., Scott, N., 2013. Implications of receptor-mediated endocytosis and intracellular trafficking dynamics in the development of antibody drug conjugates. mAbs 5, 13–21. https://doi.org/10.4161/mabs.22854

Robbins, M., Judge, A., MacLachlan, I., 2009. siRNA and Innate Immunity. Oligonucleotides 19, 89–102. https://doi.org/10.1089/oli.2009.0180

Roberts, T.C., Langer, R., Wood, M.J.A., 2020. Advances in oligonucleotide drug delivery. Nat Rev Drug Discov 19, 673–694. https://doi.org/10.1038/s41573-020-0075-7

Rong, G., Wang, C., Chen, L., Yan, Y., Cheng, Y., 2020. Fluoroalkylation promotes cytosolic peptide delivery. Sci. Adv. 6, eaaz1774. https://doi.org/10.1126/sciadv.aaz1774

Sakurai, K., Amarzguioui, M., Kim, D.-H., Alluin, J., Heale, B., Song, M., Gatignol, A., Behlke, M.A., Rossi, J.J., 2011. A role for human Dicer in pre-RISC loading of siRNAs. Nucleic Acids Research 39, 1510–1525. https://doi.org/10.1093/nar/gkq846

Santomasso, B.D., Park, J.H., Salloum, D., Riviere, I., Flynn, J., Mead, E., Halton, E., Wang, X., Senechal, B., Purdon, T., Cross, J.R., Liu, H., Vachha, B., Chen, X., DeAngelis, L.M., Li, D., Bernal, Y., Gonen, M., Wendel, H.-G., Sadelain, M., Brentjens, R.J., 2018. Clinical and Biological Correlates of Neurotoxicity Associated with CAR T-cell Therapy in Patients with B-cell Acute Lymphoblastic Leukemia. Cancer Discov 8, 958–971. https://doi.org/10.1158/2159-8290.CD-17-1319

Sardh, E., Harper, P., Balwani, M., Stein, P., Rees, D., Bloomer, J., Bissell, D.M., Desnick, R., Parker, C., Phillips, J., Bonkovsky, H., Al-Tawil, N., Rock, S., Penz, C., Chan, A., He, Q., Querbes, W., Simon, A., Anderson, K., 2018. Phase 1/2, Randomized, Placebo Controlled and Open Label Extension Studies of Givosiran, an Investigational RNA Interference (RNAi) Therapeutic, in Patients with Acute Intermittent Porphyria.

Schirle, N.T., MacRae, I.J., 2012. The Crystal Structure of Human Argonaute2. Science 336, 1037–1040. https://doi.org/10.1126/science.1221551

Schirle, N.T., Kinberger, G.A., Murray, H.F., Lima, W.F., Prakash, T.P., MacRae, I.J., 2016. Structural Analysis of Human Argonaute-2 Bound to a Modified siRNA Guide. J. Am. Chem. Soc. 138, 8694–8697. https://doi.org/10.1021/jacs.6b04454

Schlegel, M.K., Foster, D.J., Kel'in, A.V., Zlatev, I., Bisbe, A., Jayaraman, M., Lackey, J.G., Rajeev, K.G., Charissé, K., Harp, J., Pallan, P.S., Maier, M.A., Egli, M., Manoharan, M., 2017. Chirality Dependent Potency Enhancement and Structural Impact of Glycol Nucleic Acid Modification on siRNA. J. Am. Chem. Soc. 139, 8537–8546. https://doi.org/10.1021/jacs.7b02694

Schön, M.P., Schön, M., 2008. TLR7 and TLR8 as targets in cancer therapy. Oncogene 27, 190–199. https://doi.org/10.1038/sj.onc.1210913

Schroeder, A., Levins, C.G., Cortez, C., Langer, R., Anderson, D.G., 2010. Lipid-based nanotherapeutics for siRNA delivery: Symposium: Lipid-based siRNA nanotherapeutics. Journal of Internal Medicine 267, 9–21. https://doi.org/10.1111/j.1365-2796.2009.02189.x

Schuster, S.J., Bishop, M.R., Tam, C.S., Waller, E.K., Borchmann, P., McGuirk, J.P., Jäger, U., Jaglowski, S., Andreadis, C., Westin, J.R., Fleury, I., Bachanova, V., Foley, S.R., Ho, P.J., Mielke, S., Magenau, J.M., Holte, H., Pantano, S., Pacaud, L.B., Awasthi, R., Chu, J., Anak, Ö., Salles, G., Maziarz, R.T., 2019. Tisagenlecleucel in Adult Relapsed or Refractory Diffuse Large B-Cell Lymphoma. N Engl J Med 380, 45–56. https://doi.org/10.1056/NEJMoa1804980

Schwartz, A.L., Fridovich, S.E., Lodish, H.F., 1982. Kinetics of internalization and recycling of the asialoglycoprotein receptor in a hepatoma cell line. Journal of Biological Chemistry 257, 4230–4237. https://doi.org/10.1016/S0021-9258(18)34710-0

Schwarze, S.R., Ho, A., Vocero-Akbani, A., Dowdy, S.F., 1999. In Vivo Protein Transduction: Delivery of a Biologically Active Protein into the Mouse. Science 285, 1569–1572. https://doi.org/10.1126/science.285.5433.1569

Setten, R.L., Rossi, J.J., Han, S., 2019. The current state and future directions of RNAi-based therapeutics. Nat Rev Drug Discov 18, 421–446. https://doi.org/10.1038/s41573-019-0017-4

Shen, X., Corey, D.R., 2018. Chemistry, mechanism and clinical status of antisense oligonucleotides and duplex RNAs. Nucleic Acids Research 46, 1584–1600. https://doi.org/10.1093/nar/gkx1239

Shukla, S., Sumaria, C.S., Pradeepkumar, P.I., 2010. Exploring Chemical Modifications for siRNA Therapeutics: A Structural and Functional Outlook. ChemMedChem 5, 328–349. https://doi.org/10.1002/cmdc.200900444

Shuptrine, C.W., Surana, R., Weiner, L.M., 2012. Monoclonal antibodies for the treatment of cancer. Seminars in Cancer Biology 22, 3–13. https://doi.org/10.1016/j.semcancer.2011.12.009

Sifniotis, V., Cruz, E., Eroglu, B., Kayser, V., 2019. Current Advancements in Addressing Key Challenges of Therapeutic Antibody Design, Manufacture, and Formulation. Antibodies 8, 36. https://doi.org/10.3390/antib8020036

Sikora, J.L., Logue, M.W., Chan, G.G., Spencer, B.H., Prokaeva, T.B., Baldwin, C.T., Seldin, D.C., Connors, L.H., 2015. Genetic variation of the transthyretin gene in wild-type transthyretin amyloidosis (ATTRwt). Hum Genet 134, 111–121. https://doi.org/10.1007/s00439-014-1499-0

Smith, C.I.E., Zain, R., 2019. Therapeutic Oligonucleotides: State of the Art. Annu. Rev. Pharmacol. Toxicol. 59, 605–630. https://doi.org/10.1146/annurev-pharmtox-010818-021050

Smith, R.A., 2006. Antisense oligonucleotide therapy for neurodegenerative disease. Journal of Clinical Investigation 116, 2290–2296. https://doi.org/10.1172/JCI25424

Snead, N.M., Wu, X., Li, A., Cui, Q., Sakurai, K., Burnett, J.C., Rossi, J.J., 2013. Molecular basis for improved gene silencing by Dicer substrate interfering RNA compared with other siRNA variants. Nucleic Acids Research 41, 6209–6221. https://doi.org/10.1093/nar/gkt200

Souleimanian, N., Deleavey, G., Soifer, H., Wang, S., Tiemann, K., Damha, M., Stein, C., 2012. Antisense 2′-Deoxy, 2′-Fluoroarabino Nucleic Acid (2′F-ANA) Oligonucleotides: In Vitro Gymnotic Silencers of Gene Expression. Molecular Therapy 9, 1-9. doi:10.1038/mtna.2012.35

Spain, L., Diem, S., Larkin, J., 2016. Management of toxicities of immune checkpoint inhibitors. Cancer Treatment Reviews 44, 51–60. https://doi.org/10.1016/j.ctrv.2016.02.001

Springer, A.D., Dowdy, S.F., 2018. GalNAc-siRNA Conjugates: Leading the Way for Delivery of RNAi Therapeutics. Nucleic Acid Therapeutics 28, 109–118. https://doi.org/10.1089/nat.2018.0736

Stec, W.J., Karwowski, B., Boczkowska, M., Guga, P., Koziołkiewicz, M., Sochacki, M., Wieczorek, M.W., Błaszczyk, J., 1998. Deoxyribonucleoside 3‘- *O* -(2-Thio- and 2-Oxo-“spiro”-4,4-pentamethylene-1,3,2-oxathiaphospholane)s: Monomers for Stereocontrolled Synthesis of Oligo(deoxyribonucleoside phosphorothioate)s and Chimeric PS/PO Oligonucleotides. J. Am. Chem. Soc. 120, 7156–7167. https://doi.org/10.1021/ja973801j

Steer, C.J., Ashwell, G., 1980. Studies on a mammalian hepatic binding protein specific for asialoglycoproteins. Evidence for receptor recycling in isolated rat hepatocytes. Journal of Biological Chemistry 255, 3008–3013. https://doi.org/10.1016/S0021-9258(19)85843-X

Stein, C.A., Hansen, J.B., Lai, J., Wu, S., Voskresenskiy, A., H∅g, A., Worm, J., Hedtjärn, M., Souleimanian, N., Miller, P., Soifer, H.S., Castanotto, D., Benimetskaya, L., Ørum, H., Koch, T., 2010. Efficient gene silencing by delivery of locked nucleic acid antisense oligonucleotides, unassisted by transfection reagents. Nucleic Acids Research 38, e3–e3. https://doi.org/10.1093/nar/gkp841

Stephenson, M.L., Zamecnik, P.C., 1978. Inhibition of Rous sarcoma viral RNA translation by a specific oligodeoxyribonucleotide. Proceedings of the National Academy of Sciences 75, 285–288. https://doi.org/10.1073/pnas.75.1.285

Stewart, M.P., Langer, R., Jensen, K.F., 2018. Intracellular Delivery by Membrane Disruption: Mechanisms, Strategies, and Concepts. Chem. Rev. 118, 7409–7531. https://doi.org/10.1021/acs.chemrev.7b00678

Stockert, R.J., Morell, A.G., Novikoff, P.M., Novikoff, A.B>, Quintana, N., Sternlieb, I., 1980. Endocytosis of Asialoglycoprotein-Enzyme Conjugates by Hepatocytes. Laboratory Investigation; a Journal of Technical Methods and Pathology 43, 556-563.

Suhr, O.B., Coelho, T., Buades, J., Pouget, J., Conceicao, I., Berk, J., Schmidt, H., Waddington-Cruz, M., Campistol, J.M., Bettencourt, B.R., Vaishnaw, A., Gollob, J., Adams, D., 2015. Efficacy and safety of patisiran for familial amyloidotic polyneuropathy: a phase II multi-dose study. Orphanet J Rare Dis 10, 109. https://doi.org/10.1186/s13023-015-0326-6

Summerton, J., Weller, D., 1997. Morpholino Antisense Oligomers: Design, Preparation, and Properties. Antisense Nuc. Acid Dev. 7, 187-195.

Summerton, J., 2007. Morpholino, siRNA, and S-DNA Compared: Impact of Structure and Mechanism of Action on Off-Target Effects and Sequence Specificity. CTMC 7, 651–660. https://doi.org/10.2174/156802607780487740

Takahashi, M., Contu, V.R., Kabuta, C., Hase, K., Fujiwara, Y., Wada, K., Kabuta, T., 2017. SIDT2 mediates gymnosis, the uptake of naked single-stranded oligonucleotides into living cells. RNA Biology 14, 1534–1543. https://doi.org/10.1080/15476286.2017.1302641

Takei, Y., Kadomatsu, K., Yuzawa, Y., Matsuo, S., Muramatsu, T., 2004. A Small Interfering RNA Targeting Vascular Endothelial Growth Factor as Cancer Therapeutics. Cancer Res 64, 3365–3370. https://doi.org/10.1158/0008-5472.CAN-03-2682

Tang, Y., Wang, X., Li, J., Nie, Y., Liao, G., Yu, Y., Li, C., 2019. Overcoming the Reticuloendothelial System Barrier to Drug Delivery with a “Don’t-Eat-Us” Strategy. ACS Nano 13, 13015–13026. https://doi.org/10.1021/acsnano.9b05679

Tarcic, G., Yarden, Y., 2013. Antibody-Mediated Receptor Endocytosis: Harnessing the Cellular Machinery to Combat Cancer, in: Yarden, Y., Tarcic, G. (Eds.), Vesicle Trafficking in Cancer. Springer New York, New York, NY, pp. 361–384. https://doi.org/10.1007/978-1-4614-6528-7_17

Teeling, J.L., 2004. Characterization of new human CD20 monoclonal antibodies with potent cytolytic activity against non-Hodgkin lymphomas. Blood 104, 1793–1800. https://doi.org/10.1182/blood-2004-01-0039

Torka, P., Barth, M., Ferdman, R., Hernandez-Ilizaliturri, F.J., 2019. Mechanisms of Resistance to Monoclonal Antibodies (mAbs) in Lymphoid Malignancies. Curr Hematol Malig Rep 14, 426–438. https://doi.org/10.1007/s11899-019-00542-8

Tsui, N.B.Y., Ng, E.K.O., and Lo, Y.M.D., 2002. Stability of endogenous and added RNA in blood specimens, serum, and plasma. Clin. Chem. *48*, 1647–1653.

Turner, J.J., Jones, S.W., Moschos, S.A., Lindsay, M.A., Gait, M.J., 2007. MALDI-TOF mass spectral analysis of siRNA degradation in serum confirms an RNAse A-like activity. Mol. BioSyst. 3, 43–50. https://doi.org/10.1039/B611612D

Uchida, J., Hamaguchi, Y., Oliver, J.A., Ravetch, J.V., Poe, J.C., Haas, K.M., Tedder, T.F., 2004. The Innate Mononuclear Phagocyte Network Depletes B Lymphocytes through Fc Receptor–dependent Mechanisms during Anti-CD20 Antibody Immunotherapy. Journal of Experimental Medicine 199, 1659–1669. https://doi.org/10.1084/jem.20040119

Ulvila, J., Parikka, M., Kleino, A., Sormunen, R., Ezekowitz, R.A., Kocks, C., Rämet, M., 2006. Double-stranded RNA Is Internalized by Scavenger Receptor-mediated Endocytosis in Drosophila S2 Cells. Journal of Biological Chemistry 281, 14370–14375. https://doi.org/10.1074/jbc.M513868200

van de Water, F.M., Boerman, O.C., Wouterse, A.C., Peters, J.G.P., Russel, F.G.M., Masereeuw, R., 2006. Intravenously Administered Short Interfering RNA Accumulates in the Kidney and Selectively Suppresses Gene Function in Renal Proximal Tubules. Drug Metab Dispos 34, 1393–1397. https://doi.org/10.1124/dmd.106.009555

van der Velden, V.H.J., te Marvelde, J.G., Hoogeveen, P.G., Bernstein, I.D., Houtsmuller, A.B., Berger, M.S., van Dongen, J.J.M., 2001. Targeting of the CD33-calicheamicin immunoconjugate Mylotarg (CMA-676) in acute myeloid leukemia: in vivo and in vitro saturation and internalization by leukemic and normal myeloid cells. Blood 97, 3197–3204. https://doi.org/10.1182/blood.V97.10.3197

Vandenbroucke, R.E., De Geest, B.G., Bonné, S., Vinken, M., Van Haecke, T., Heimberg, H., Wagner, E., Rogiers, V., De Smedt, S.C., Demeester, J., Sanders, N.N., 2008. Prolonged gene silencing in hepatoma cells and primary hepatocytes after small interfering RNA delivery with biodegradable poly(β-amino esters). J. Gene Med. 10, 783–794. https://doi.org/10.1002/jgm.1202

Verma, S., Miles, D., Gianni, L., Krop, I.E., Welslau, M., Baselga, J., Pegram, M., Oh, D.-Y., Diéras, V., Guardino, E., Fang, L., Lu, M.W., Olsen, S., Blackwell, K., 2012. Trastuzumab Emtansine for HER2-Positive Advanced Breast Cancer. N Engl J Med 367, 1783–1791. https://doi.org/10.1056/NEJMoa1209124

Vivès, E., Brodin, P., Lebleu, B., 1997. A Truncated HIV-1 Tat Protein Basic Domain Rapidly Translocates through the Plasma Membrane and Accumulates in the Cell Nucleus. Journal of Biological Chemistry 272, 16010–16017. https://doi.org/10.1074/jbc.272.25.16010

Vuković, L., Koh, H.R., Myong, S., Schulten, K., 2014. Substrate Recognition and Specificity of Double-Stranded RNA Binding Proteins. Biochemistry 53, 3457–3466. https://doi.org/10.1021/bi500352s

Wadia, J.S., Stan, R.V., Dowdy, S.F., 2004. Transducible TAT-HA fusogenic peptide enhances escape of TAT-fusion proteins after lipid raft micropinocytosis. Nat. Med 10, 310-315.

Walport, M.J., 2001. Complement First of Two Parts. N Engl Jour Med. 344, 1058-1066. https://doi.org/10.1056/NEJM200104053441406

Wan, W.B., Migawa, M.T., Vasquez, G., Murray, H.M., Nichols, J.G., Gaus, H., Berdeja, A., Lee, S., Hart, C.E., Lima, W.F., Swayze, E.E., Seth, P.P., 2014. Synthesis, biophysical properties and biological activity of second generation antisense oligonucleotides containing chiral phosphorothioate linkages. Nucleic Acids Research 42, 13456–13468. https://doi.org/10.1093/nar/gku1115

Wang, Y., Juranek, S., Li, H., Sheng, G., Wardle, G.S., Tuschl, T., Patel, D.J., 2009. Nucleation, propagation and cleavage of target RNAs in Ago silencing complexes. Nature 461, 754–761. https://doi.org/10.1038/nature08434

Weber, J.S., Kähler, K.C., Hauschild, A., 2012. Management of Immune-Related Adverse Events and Kinetics of Response With Ipilimumab. JCO 30, 2691–2697. https://doi.org/10.1200/JCO.2012.41.6750

Whitehead, K.A., Dahlman, J.E., Langer, R.S., Anderson, D.G., 2011. Silencing or Stimulation? siRNA Delivery and the Immune System. Annu. Rev. Chem. Biomol. Eng. 2, 77–96. https://doi.org/10.1146/annurev-chembioeng-061010-114133

Whitehead, K.A., Langer, R., Anderson, D.G., 2009. Knocking down barriers: advances in siRNA delivery. Nat Rev Drug Discov 8, 129–138. https://doi.org/10.1038/nrd2742

Wilson, R.C., Doudna, J.A., 2013. Molecular Mechanisms of RNA Interference. Annu. Rev. Biophys. 42, 217–239. https://doi.org/10.1146/annurev-biophys-083012-130404

Wilson, L.J., Linley, A., Hammond, D.E., Hood, F.E., Coulson, J.M., MacEwan, D.J., Ross, S.J., Slupsky, J.R., Smith, P.D., Eyers, P.A., Prior, I.A., 2018. New Perspectives, Opportunities, and Challenges in Exploring the Human Protein Kinome. Cancer Res 78, 15–29. https://doi.org/10.1158/0008-5472.CAN-17-2291

Wu, G., Fang, Y.-Z., Yang, S., Lupton, J.R., Turner, N.D., 2004. Glutathione Metabolism and Its Implications for Health. The Journal of Nutrition 134, 489–492. https://doi.org/10.1093/jn/134.3.489

Wurster, C.D., Ludolph, A.C., 2018. Nusinersen for spinal muscular atrophy. Ther Adv Neurol Disord 11, 1-3. https://doi.org/10.1177/1756285618754459

Yang, N.J., Hinner, M.J., 2015. Getting Across the Cell Membrane: An Overview for Small Molecules, Peptides, and Proteins, in: Gautier, A., Hinner, M.J. (Eds.), Site-Specific Protein Labeling, Methods in Molecular Biology. Springer New York, New York, NY, pp. 29–53. https://doi.org/10.1007/978-1-4939-2272-7_3

Yoda, M., Kawamata, T., Paroo, Z., Ye, X., Iwasaki, S., Liu, Q., Tomari, Y., 2010. ATP-dependent human RISC assembly pathways. Nat Struct Mol Biol 17, 17–23. https://doi.org/10.1038/nsmb.1733

Yoneyama, M., Kikuchi, M., Matsumoto, K., Imaizumi, T., Miyagishi, M., Taira, K., Foy, E., Loo, Y.-M., Gale, M., Akira, S., Yonehara, S., Kato, A., Fujita, T., 2005. Shared and Unique Functions of the DExD/H-Box Helicases RIG-I, MDA5, and LGP2 in Antiviral Innate Immunity. J Immunol 175, 2851–2858. https://doi.org/10.4049/jimmunol.175.5.2851

Zahavi, D., Weiner, L., 2020. Monoclonal Antibodies in Cancer Therapy. Antibodies 9, 34. https://doi.org/10.3390/antib9030034

Zamecnik, P.C., Stephenson, M.L., 1978. Inhibition of Rous sarcoma virus replication and cell transformation by a specific oligodeoxynucleotide. Proceedings of the National Academy of Sciences 75, 280–284. https://doi.org/10.1073/pnas.75.1.280

Zhang, J., Yang, P.L., Gray, N.S., 2009. Targeting cancer with small molecule kinase inhibitors. Nat Rev Cancer 9, 28–39. https://doi.org/10.1038/nrc2559

Zhong, L., Li, Y., Xiong, L., Wang, W., Wu, M., Yuan, T., Yang, W., Tian, C., Miao, Z., Wang, T., Yang, S., 2021. Small molecules in targeted cancer therapy: advances, challenges, and future perspectives. Sig Transduct Target Ther 6, 201. https://doi.org/10.1038/s41392-021-00572-w

Zimmermann, T.S., Lee, A.C.H., Akinc, A., Bramlage, B., Bumcrot, D., Fedoruk, M.N., Harborth, J., Heyes, J.A., Jeffs, L.B., John, M., Judge, A.D., Lam, K., McClintock, K., Nechev, L.V., Palmer, L.R., Racie, T., Röhl, I., Seiffert, S., Shanmugam, S., Sood, V., Soutschek, J., Toudjarska, I., Wheat, A.J., Yaworski, E., Zedalis, W., Koteliansky, V., Manoharan, M., Vornlocher, H.-P., MacLachlan, I., 2006. RNAi-mediated gene silencing in non-human primates. Nature 441, 111–114. https://doi.org/10.1038/nature04688

CHAPTER TWO

MATERIALS AND METHODS

MATERIALS AND METHODS

Phosphoramidite Synthesis

Specific methods for synthesizing the phosphoramidites used have been described previously (Meade et al., 2014). An example protocol for the synthesis of 5'-O-(4,4'-Dimethoxytrityl)-2'-F-uridine 3'-O-[(S-pivaloyl-2-thioethyl) N,N-diisopropylphosphoramidite] is as follows: N,N-Diisopropylethylamine (DIEA) (Sigma Aldrich) (0.907 mL, 5.47 mmol) was added dropwise over 10 min to a magnetically stirred cooled solution (-78 ˚C) of 5'-O-(4,4'-Dimethoxytrityl)-2'-F-uridine (2 g, 3.65 nmol, RI CHEMICAL). A solution of bis- (N,N-diisopropylamino)-chlorophosphine (1.23 g, 95% purity, 4.38 nmol, Sigma Aldrich) in dry CH_2CL_2 (5 mL) was then added dropwise over 10 min and the reaction mixture was allowed to warm to room temperature while stirring was maintained for 1 hr. S-(2-hydroxyethyl) thipivaloate (0.71 g, 4.3 nmol) was added portion wise followed by ethyl thiotetrazole (8.76 mL, 0.25 M solution in acetonitrile (ACN), 2.19 mmol) and the reaction was stirred for 2-12 hr. Then the reaction mixture was washed with brine (2 x 20 mL) and dried over anhydrous sodium sulfate. The solvent was evaporated *in vacuo* and the residue was subjected to flash silica gel column purification on a combi-flash instrument (Teledyne Isco) using hexane-ethyl acetate (0.5% triethylammonium acetate) as the solvent (0-70%). The fractions containing the products were pooled together and evaporated to dryness. The foamy residue was re-dissolved in benzene, frozen and lyophilized, affording a final product as a colorless powder (~2.2 g), 80% yield as diastereomeric mixture.

Oligonucleotide Synthesis

All oligonucleotide synthesis was carried out on a BioAutomation Mermade-6 oligonucleotide synthesizer (BioAutomation). Oligonucleotide synthesis reagents include: Activator = 0.25 M 5-Benzylthio-1H-tetrazole (BTT) in ACN (Glen Research, 30-3170); Cap Mix

B = 16% 1-Methylimidazole (v/v), 84% THF (Glen Research, 40-4220); Deblock = 3% Trichloroacetic acid (w/v) in DCM (VWR, EM-I0830-0950); Oxidizing Reagent = 0.02 M Iodine in 70% THF (v/v), 20% pyridine, 10% water (VWR, EM-BI0420-4000); Sulfurizing Reagent = 0.05 M 3-((N,N-dimethylaminomethylidene)amino)-3H-1,2,4-dithiazole-5-thione (Sulfurizing Reagent II) in 40% pyridine (v/v), 60% ACN (Glen Research, 40-4137-52); Anhydrous ACN (VWR, AX0151-1). Commercially available amidites used are: dT-CE (Glen Research, 10-1030), 2'-OMe-5'-O-DMTr-PAC-A-CE (Glen Research, 10-3601), 2'-Fluoro-5'-O-DMTr-PAC-C-CE (Carbosynth, PD-158882), 2'-OMe-5'-O-DMTr-iPr-PAC-G-CE (Glen Research, 10-3621), and 2'-Fluoro-5'-O-DMTr-U-CE (Carbosynth, PD09874). Phosphoramidites were coupled at concentrations and time following manufacturer recommendations. For modifications, 5'-DBCO-TEG phosphoramidite (Glen Research, 10-1941-90), 5'-IRDye 800 phosphoramidite (LI-COR Biosciences, 4000-33), 5'-Thiol modifier phosphoramidite (Glen Research, 10-1936), 5'-Aldehyde modifier phosphoramidite (Glen Research, 10-1933), and Cy3 phosphoramidite (Glen Research, 10-5913) were coupled following manufacturer's recommendation. All phosphotriester phosphoramidites were coupled at 100 mM with two coupling cycles at 6 minutes each. CPG supports used were dT-Q-CPG 500 (Glen Research, 21-2230) and Universal Q SynBase 500/110 (Link Technologies Ltd., 2300-C001) at 1 μmol scale. Manual detritylation was accomplished by flowing 1 mL of deblock solution through the CPG column into 3 ml of 100 mM p-toluenesulfonic acid in anhydrous ACN followed by 2 mL anhydrous ACN wash. Absorbance readings at 498 nm were measured to quantify full-length oligonucleotide yield by DMT concentration and ensure full-length coupling.

Primary Oligonucleotide Deprotection

For all wild type (2'-OH) oligonucleotide deprotection, CPG was incubated in 1 mL of AMA (Ammonium Hydroxide/40% Aqueous Methylamine (1:1)) (Sigma-Aldrich, 295531) for 1 hr at 65 ˚C. For all oligonucleotides with only irreversible phosphotriesters (AX, KX, DMB

phosphotriesters), CPG was incubated in 3:1 ammonium hydroxide:ethanol for 2 hr at 65 ˚C. After deprotection, oligonucleotide solutions were placed in a centrifugal evaporator for drying.

For 2'O-TBDMS deprotection, oligonucleotides were dissolved in 100 µl of anhydrous DMSO. To each oligonucleotide solution, 125 µL of 98% triethylamine trihydrofluoride (Sigma Aldrich, 344648) was added and reactions were left at room temperature for 4 hr. After 4 hr, oligonucleotides were precipitated by the addition of 35 µL of 3 M sodium acetate and 1 mL of 1-Butanol. Oligonucleotides were then incubated at -80 ˚C for 2 hr. After incubation, the oligonucleotides were centrifuged at 16,000 *g* for 5 min, supernatant was aspirated, oligonucleotide pellets were dissolved in 1 mL of water and desalted with NAP-10 columns (GE Healthcare, 83-468).

Oligonucleotide Purification

All oligonucleotides were purified by RP-HPLC on an Agilent 1200 Series Analytical HPLC with an Agilent SB-C18 column (9.4 x 150 mm) (Agilent, 883975-202). Linear gradients were run from 50 mM triethylammonium acetate (TEAA) pH 7.0 in water to 90% ACN/10% water at a flow rate of 2 mL/min. Length and steepness of gradient varied with number and type of groups present on oligonucleotides. For DMT-On purifications, DMT-oligonucleotide HPLC peaks were collected, analyzed for presence of full-length oligonucleotides by MALDI-TOF mass spectrometry, and selected fractions were pooled and frozen on dry ice and lyophilized twice to remove TEAA.

Mass Spectrometry

Oligonucleotides and other conjugates were analyzed by MALDI-TOF mass spectrometry using a Voyager-DE PRO MALDI-TOF mass spectrometer (Applied Biosystem). 10 pmol of RNA was spotted with 1 µL of matrix from a 20mg/mL solution of 2',4',6'-

Trihydroxyacetophenone (Sigma-Aldrich, 91928), 20 mM ammonium citrate dibasic (Sigma-Aldrich, 09831) in 50% ACN/50% water. Spectra were collected in negative mode with accelerating voltage = 20,000 V, grid = 90%, guide wire = 0.15%, 100-150 nsec delay time. 200-500 shots were collected for each sample. THAP matrix was used for all analyses of oligonucleotides and oligonucleotide-containing molecules.

Secondary Oligonucleotide Deprotection and Desalting

For all oligonucleotides aside from those containing an acetal-AldSATE phosphotriester, detritylation and removal of acetal protection from any present acetal-AX phosphotriesters was accomplished by treatment with 200 µL 80% acetic acid and heating at 65 ˚C for 1 hr. Following deprotection, oligonucleotides were frozen and lyophilized until dry.

Following lyophilization, deprotected oligonucleotides were dissolved in 20% ACN and desalted with NAP-10 columns (GE Healthcare Life Sciences 17-0854-02). Desalted oligonucleotides were dried in a centrifugal evaporator. Once dry, completed oligonucleotides were dissolved in 50% ACN, quantified, and stored at -20 ˚C.

Oligonucleotide Sequences

Chapter 3:

5’-DBCO-TEG-AGAAGAUGCUUCAGACAGAUT-3’ (sense/passenger)

5’-UCUGUCUGAAGCAUCUUCUUT-3’ (antisense/guide)

2’-OMe ribose modifications were incorporated into the purines (A,G), shown in blue, and 2’-F ribose modifications were incorporated into the pyrimidines (C,U), shown in orange. Deoxy-T bases remain on the 3’-ends of the oligos after being cleaved from the CPG support during the synthesis procedure.

Chapter 4:

5’-3XPO-Thio-UTCAGCGGATCTTGAAGTTCACCU-3’ (Thio GFP-6 ASO, 5-10-5 gapmer)

5’-3XPO-UTCAGCGGATCTTGAAGTTCACCU-3’ (GFP-6 ASO, 5-10-5 gapmer)

5’-3XPO-Thio-UTCAGACCCCGTGTTCGACCUCAU-3’ (Thio GFP-I ASO, 5-10-5 gapmer)

5’-3XPO-UTCAGACCCCGTGTTCGACCUCAU-3’ (GFP-I ASO, 5-10-5 gapmer)

ASOs contain a full PS backbone. 3X PO refers to phosphodiester groups on the end for instability. All ASOs are Ax-modified at their 5’terminal base, Ax refers to the benzaldehyde modification for HyNic conjugation onto the KP1H linker peptide. RNA ends of the gapmer are 2’-OMe modified and shown in blue. Thio refers to the thiol/disulfide group, intended for reduction after internalization.

Chapter 5:

5’-XCCACUACCUGAGCACCCAAUT-3’ (sense/passenger #1)

5’-AACCACUACCUGAGCACCCAA-3’ (sense/passenger #2)

5’-UUGGGUGCUCAGGUAGUGGUUU-3’ (antisense/guide)

5’-UUGGGUGCUCAGGUAGUGGUUU-3’ (antisense/guide)

All GFP siRNA strands have dual phosphorothioate backbone modifications at each end. Blue bases have the 2’-OMe modification. Orange bases have the 2’-F modification. Underlined base indicates a vinyl-phosphonate amidite. The first passenger strand contains a biotin amidite as the 5’- terminal base (denoted with an X) and a 3’-terminal benzaldehyde modification at the last U base. The second passenger strand contains a 5’-terminal BCN amidite.

Gel Electrophoresis

Single stranded RNA (ssRNA) oligonucleotides were analyzed by denaturing gel electrophoresis using 15% acrylamide/7 M Urea denaturing gels and stained with methylene blue for visualization. dsRNA oligonucleotides were hybridized by heating to 65 ˚C for 2 min and

allowed to cool to room temperature. dsRNA analysis was performed by non-denaturing gel electrophoresis using 15% acrylamide non-denaturing gels and ethidium bromide staining for visualization. Standard run for a urea gel is 200V for 1 hr.

For analysis of antibodies, antibody-peptide conjugates, and ARCs, conjugation efficiency was assessed on an SDS PAGE reducing gel (10%). Standard run involves 120V for 24 minutes followed by 180V for 36 min. UV protein staining (Blazin' Bright™ Luminescent UV Protein Gel Stain, Gold Biotechnology) was used to visualize all SDS PAGE gels and visualized on a standard BioRad gel dock. Fluorescein imaging occurred prior to UV protein staining using an Alexa488 filter on an epifluorescence/UV transilluminator.

Peptide Synthesis

All protected amino acids and coupling reagents were purchased from Nova Biochem or Bachem, BOC 6-hydrazino-nicotinic acid (Solulink, s-3003-500), and Fmoc-N-amido-dPEG$_6$ acid (Quanta Biodesign, 10063). Lysine peptides: K-PEG$_6$-SG-N$_3$ (KN$_3$, or KP1Z), K-PEG$_6$-HyNic (KP1H), KAYA-PEG$_6$-FITC-K-fluorescein (KF). Peptide synthesis was performed at 25 μM scale using Fmoc solid phase peptide synthesis on Symphony Quartet peptide synthesizer (Ranin) and rink-amide MBHA resin as solid support. All HyNic peptides were cleaved and deprotected using standard conditions (92.5% TFA, 2.5% acetone, 2.5% water, 2.5% TIS) for 2 hr. Crude peptides were precipitated with cold diethylether and purified by RP-HPLC on an Agilent 1200 Series Preparative HPLC Prep-C18 with a Prep-C18 30x250 mm column (Agilent, 410910-302). Peptide purity was confirmed by mass spectrometry using α-CHCA matrix (Sigma-Aldrich, 70990) and an Applied Biosystems Voyager-DE PRO MALDI-TOF mass spectrometer.

Oligonucleotide Conjugation

For all hydrazinonicotinic acid (HyNic) conjugations, Peptide-HyNic was reacted with oligonucleotides bearing either AX or AldSATE phosphotriester insertions at variable ratios between 2.5:1 and 5:1 (peptide:aldehyde conjugation site). Reactions were carried out above 0.5 mM oligonucleotide concentration in a 1% Aniline (Tokyo Chemical Industry, A0463) solution in 5% ACN/50% water at RT for 1 hr. Conjugates were purified by FPLC using an Enrich-SEC 650 10/300 column (Biorad, 780-1650) with a flow rate of 1.8 mL/min 1X PBS in water. Fractions were checked by gel electrophoresis and/or MALDI-TOF, pooled, frozen on dry ice, and lyophilized to yield the final product. When lyophilization was impractical, samples were pooled and instead re-concentrated with a Vivaspin6 (GE Healthcare) spin filter 30K MWCO, and re-quantified on a spectrophotometer. Antibody containing conjugates were kept in 1X PBS and later duplexed.

For conjugations between linker peptides and oligonucleotides on ARCs, copper-free click chemistry was utilized with single stranded oligonucleotides bearing DBCO or BCN modification that were incubated together at various ratios depending on the specific experiment. Copper free click reactions were reacted at room temperature and allowed to incubate overnight. Conjugation efficiency was checked by gel electrophoresis on either 15% urea denaturing or SDS PAGE reducing gels, depending on the conjugate. Oligo containing conjugations were checked by MALDI-TOF, pooled, frozen, and lyophilized as needed.

Antibody Production

Amino acid sequences for the variable regions of antibodies targeting CD33 and CD71 were collected and codon optimized for ExpiCHO expression system. Variable regions were cloned into a pcDNA3 backbone into both κ or λ light chains and IgG1 or IgG4 heavy chain subtypes. Gene blocks (gBlocks, from IDT), were used to clone the variable regions from the anti-CD33 mAb into expression plasmids. Microbial transglutaminase recognition sequences

(LLQGA) were cloned onto the C-terminus of HCs by PCR-mediated mutagenesis to provide a site-specific conjugation site. Antibody expression was driven from a cytomegalovirus (CMV) promoter and BGH polyA signals were used on the 3'-end of the heavy and light chain transcripts **(Figure 2.2)**. Heavy chain signal peptide: MEFGLSWVFLVALFRGVQC. Light chain signal peptide: MDMRVPAQLLGLLLLWLSGARC. Cloning was carried out using the InFusion HD Cloning System (Takara Bio USA, 639645). Antibodies were produced using the ExpiCHO Expression system (ThermoFisher) following manufacturer protocols. Heavy chain (HC) and light chain (LC) plasmids were transfected into the ExpiCHO cells in a 2:1 HC:LC ratio for most antibodies and up to 4:1 ratio for some antibodies. After transfection, ExpiCHO cells were incubated in 37 ˚C with 8% CO_2 on a shaking platform (140 RPM setting). The next day, cells were treated with enhancer reagent according to manufacturer's protocol and moved into 32 ˚C 5% CO_2 for 10-14 days of additional incubation. Antibodies were harvested at about day 12 post-transfection by collecting and centrifuging the cell supernatant, followed by transfer into new 50 mL conical tubes to avoid the pellet. Cell supernatant was passed through 0.45 μm and 0.22 μm PVDF syringe filters followed by processing through a Protein A chromatography column. Lastly, antibody samples were purified by size exclusion chromatography on FPLC (Enrich-SEC 650 10/300 column).

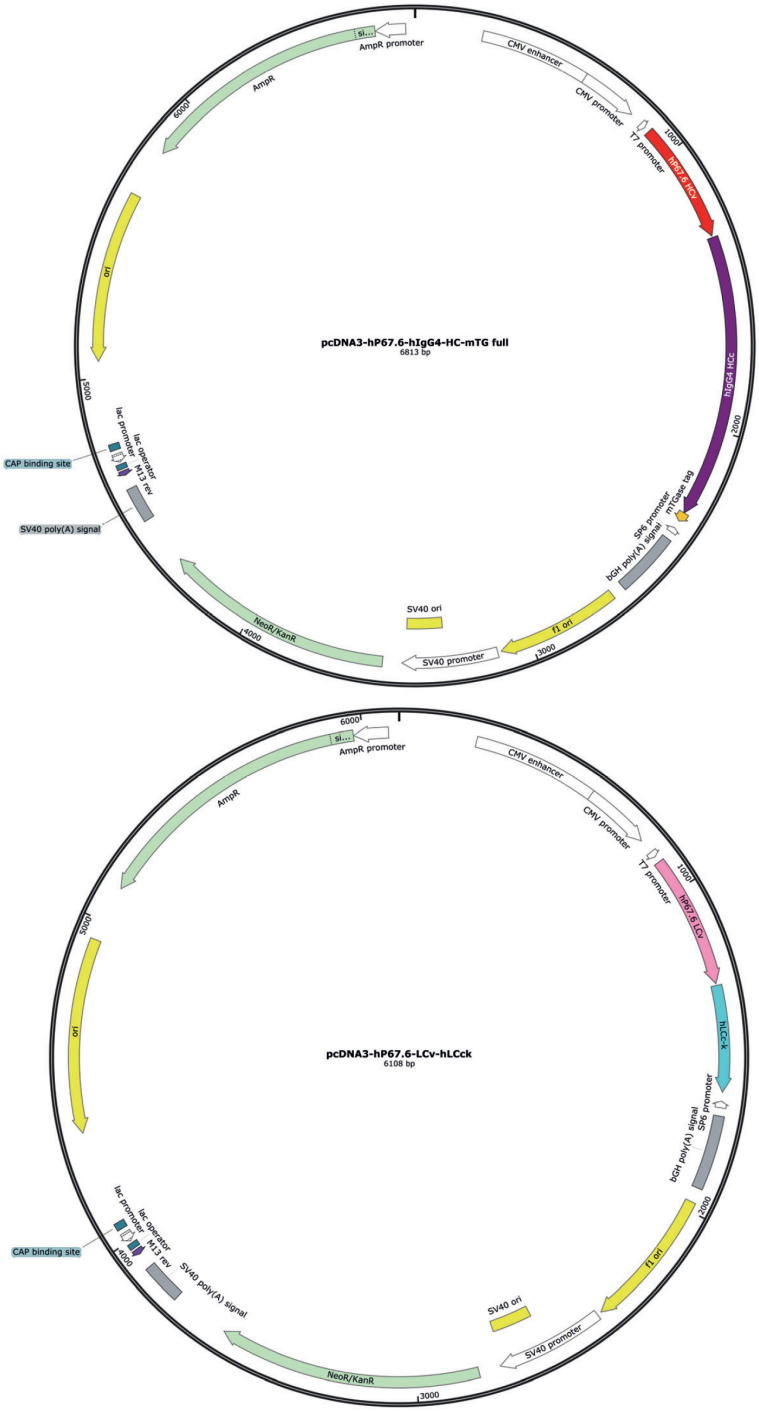

Figure 2.1. Antibody Expression Plasmid Maps
Representative plasmid maps for heavy chain (upper) and light chain (lower) production. Heavy chain variable regions (HCv) were cloned into both human heavy chain IgG1 and IgG4 heavy chain constant (HCc) regions. Light chain variable regions (LCv) were cloned into both kappa and lambda human light chain constant (hLCc) regions. CMV promoters drive expression of heavy and light chains with BGH polyA tails.

Microbial Transglutaminase (MTG) Antibody Conjugations

10X MTGase enzyme buffer was prepared (500 mM sodium chloride, 500 mM sodium acetate, pH 5.8) and then diluted 10-fold in water for the resuspension of the MTG enzyme powder. For all antibody conjugations, MTG reactions were carried out with excess linker peptide, with ratios varying between 10:1 and 2.5:1 Lysine peptide:LLQGA site (1 mg/mL antibody or 6.5 μM antibody in the final reaction volume wherever possible). 10X MTGase reaction buffer consists of 1.5 M NaCl, 250 mM Tris-HCl pH 8). Reactions were carried out in 10-fold diluted MTGase reaction buffer (162.5 mM NaCl, 25 mM Tris-HCl, pH 8) at 37 ˚C for 1-2 hr. MTGase enzyme was included to achieve ~3.15 U/mL reaction volume. MilliQ water was used to fill the remaining volume to achieve the final desired reaction volume. Conjugates were purified by FPLC using an Enrich-SEC 650 10/300 column (Biorad, 780-1650) using PBS at a flow rate of 1.8 mL/min. Fractions were checked by reducing SDS-PAGE electrophoresis in cases where the peaks were close to overlapping and pooled before concentration and solvent exchange to 1X PBS using regenerated cellulose 30K amicon ultra spin filtration cartridges (Millipore, UFC503024) or Vivaspin6 30K MWCO (GE Healthcare, GE28-9322-96) spin filter tubes. Concentration was checked either by BCA assay or by extinction coefficient calculations on a Beckman spectrophotometer. Peptide conjugated antibodies were stored at -20 ˚C until further use.

Copper-Free Click Conjugations (Azide-Alkyne)

For all DBCO- or BCN-oligonucleotide conjugations, oligonucleotides bearing a 5'-terminal DBCO-TEG or BCN modifications (Glen Research, 10-1941-90) were duplexed. Duplexing occurred by mixing the passenger and guide strands together in a ~1:1 molar ratio, heating to 65 ˚C for 3-5 min, cooling at room temperature for another 3-5 min, and then cooling to 4 ˚C. Duplexed oligonucleotides were dried down either by vacuum evaporation or lyophilization to remove the 50% acetonitrile and then resuspended in 1X PBS 40 mM L-

Arginine with antibody-peptide-azide to achieve the desired final concentration in the reaction. Reactions were carried out at variable ratios (DBCO:azide) including 3:1 and 5:1 at 37 ˚C for 1 hr for DBCO or at RT overnight for BCN. For oligonucleotides modified with additional groups/peptides, HyNic conjugations and purification was carried out prior to oligonucleotide duplexing and copper-free click conjugation.

For copper-free click reactions between Azide-uEEDs and BCN-siRNAs, uEEDs were first dried down by vacuum evaporation followed by resuspension with the siRNA component to minimize the reaction volume. Conjugation reactions were incubated at room temperature overnight. Afterwards, conjugates were dried down by vacuum evaporation and resuspended in 20-50 µL of 50% ACN. Then conjugates were dried down again by vacuum evaporation. This process was repeated a total of three times to maximize the final conjugation efficiency. For test conjugation experiments, conjugates were next resuspended directly in 2X formamide loading buffer and run in a 15% urea gel (200V, 50-60 min) followed by methylene blue staining and imaging to assess conjugation efficiency. For larger scale ARC production, siRNA-uEED conjugates were stored at -20 ˚C until the TCO-tetrazine ligation reaction.

Oxime Ligation Reactions

The oxime ligation reactions were used primarily to conjugate a benzaldehyde-modified siRNA passenger strand with an amino-oxy-modified universal endosomal escape domain (uEED). Benzaldehyde- and amino-oxy-modified components were kept in 50% ACN. Samples were aliquoted according to the designated molar amounts needed for the reaction, but it was the amino-oxy-modified uEED that was always added in excess to the siRNA. A working stock of 5% aniline was prepared by diluting 100% aniline in 50% ACN. Designated amounts of oligonucleotide were mixed with uEED and aniline was added to achieve a final 1% concentration with ammonium acetate (pH 4.2) to a final 400 mM in the reaction volume. 50% ACN was used to fill the remaining volume based on volume calculations for each reaction.

Oxime ligation reaction tubes were incubated in the dark overnight. After incubation, a ~0.2 nmole sample of conjugate was aliquoted and lyophilized to remove acetic acid. Samples were resuspended with 8-10 µL formamide loading buffer and run on a 15% polyacrylamide Urea-PAGE gel. Urea gel was stained with methylene blue, destained with water, and imaged on a white transilluminator to assess conjugation efficiency.

EDC Cross-linking

1-ethyl-3-(3-dimethylaminopropyl)carbodiimide hydrochloride (EDC) (Thermo Scientific,, Catalog 22980) is a zero-length crosslinker used to couple carboxyl groups with primary amines to form an amide bond. In this case, it was used to conjugate the quillajasaponin (Saponin from Quillaja Saponaria Molina, Fisher Scientific CAS 74499-23-3) onto the surface amines of an anti-CD33 mAb that has been previously described. An EDC concentration of 18 mM was used for all test conjugation reactions from a 100 mM stock. Quillajasaponin was diluted in water to a 1.5 mg/mL concentration. mAb was added to the reaction mixture at a final reaction concentration of 6.25 µM (13.5 µg, ~0.09 nanomoles) followed by addition of saponin in excess (molar excess ranges from 10-fold to 400-fold). Water was added to achieve the calculated final test reaction volume. Test reactions were incubated at room temperature for 2.5 hr after which a 1 µg sample of conjugate was loaded and run on a 10% SDS PAGE gel. UV protein staining was done and a UV transilluminator was used for visualization and analysis of results.

WST-1 Cell Viability Assay

Cell proliferation and viability reagent WST-1 was obtained (Millipore Sigma, 5015944001) and used to assess the viability of cells after treatment with quillajasaponin (Saponin from Quillaja Saponaria Molina, Fisher Scientific CAS 74499-23-3). The WST-1 assay is a spectrophotometric quantification of cell proliferation and viability based on the cleavage of

WST-1, a tetrazolium salt, to a soluble formazan at the cell surface, an event dependent on glycolytic production of NADPH in viable cells. The amount of formazan dye produced correlates to metabolic activity and thus viability of the cells in culture. The WST-1 assay was performed according to manufacturer's protocol. Briefly, WST-1 reagent was added in a final 1:10 dilution to the well of a 48-well plate that had been treated with varying amounts of quillajasaponin for 24 hr (20 µL WST-1 reagent added per well, 200 µl final well volume) with H1299 dGFP cells. 48-well plate was incubated at 37 ˚C for about 3 hr. 48-well plate was analyzed on a plate reader, with an endpoint scan for the A440 nm wavelength to assess relative levels of formazan dye production based on the treatment conditions.

Streptavidin Magnetic Bead Pulldown

Streptavidin magnetic beads at a 4 mg/mL concentration were obtained (New England BioLabs, S1420S). A heat block was prepared at 65˚C. The following buffers were prepared: Elution buffer – 50% acetonitrile in water; Formamide loading buffer – 1 mM EDTA (pH 8.0), 2 mg Bromophenol Blue in formamide, NP40 wash buffer – 1X PBS, pH 7.0, 1% NP40 in water, ACN Wash buffer – 20% acetonitrile in water. NP40 and ACN wash buffers were kept on ice. 3 microcentrifuge tubes were labeled for each sample to be processed to hold the beads, depleted sample, and eluted sample. 500 µg of streptavidin magnetic beads were aliquoted into a clean tube per 0.2 nmoles of siRNA to be processed. A magnet was applied to the side of the tube for approximately 30-60 sec or until the beads successfully slid up the side of the tubes. Supernatant was removed and discarded. Added 100 µL of NP40 wash buffer and vortexed tubes to resuspend the beads. Magnet was applied to the side of the tube for 30-60 sec. Supernatant was removed and discarded. Biotinylated-siRNA solution was added to the magnetic beads and tubes were vortexed to mix contents. Samples were incubated at room temperature for 10 min. Tubes were occasionally vortexed to thoroughly mix beads and siRNA. After incubation, a magnet was applied to the side of the tubes and the remaining depleted

material was transferred to the previously labeled microcentrifuge tube. Beads were washed by adding 100 µL of NP40 wash buffer. Tubes were vortexed to resuspend beads. A magnet was then applied to the side of the tube and the supernatant was discarded. This step was repeated once more. 100 µL of ACN wash buffer was added and tubes were vortexed to resuspend the beads. A magnet was applied to the side of the tubes for about 30 seconds. Supernatant was removed. 25 µL of supernatant was added to the beads and tubes were vortexed to resuspend the beads. Samples were incubated at 65 ˚C for 2 min. Immediately afterwards, a magnet was applied to the samples and the supernatant was transferred into a clean microcentrifuge tube (eluted sample). Elution procedure was repeated once more, and elution fractions were pooled together. Eluted samples were analyzed by Urea-PAGE and/or MALDI-TOF analysis.

TCO-Tetrazine Ligation Reactions

TCO-tetrazine ligation reactions, also known as the inverse electron demand Diels-Alder click reaction, were performed between trans-cyclooctene (TCO)-containing siRNA-uEED conjugates and a methyltetrazine-PEG4-amine linker (BroadPharm, BP-22428). The TCO-siRNA components was added in excess to the mAb-tetrazine (Tz) component at variable ratios during the optimization experiments but at a 15-fold molar excess to the mAb-Tz component for the larger scale conjugation. First, the TCO-siRNA-uEED component was dried down by vacuum evaporation to remove all the 50% ACN. Dried material was resuspended directly with the mAb-Tz in 1X PBS to achieve the lowest possible reaction volume and maximize the concentration of the reaction. Conjugation reactions were mixed thoroughly and allowed to incubate at room temperature overnight. Conjugation efficiency was assessed by 10% SDS PAGE afterwards.

Purification of Conjugates

Antibody-RNA conjugates (ARCs) were purified by FPLC using an Enrich-SEC 650 10/300 column using with filtered 1X PBS in water at a flow rate of 1.8 mL/min. Absorbance spectra at 280 nm and 260 nm to assess the composition of eluted peaks and 500 µL fractions were collected for the peaks of interest. Fractions were checked by reducing SDS-PAGE electrophoresis and pooled. Fractions for desired peaks were pooled together and re-concentrated using Amicon spin filters, 30 kDa MWCO (Millipore) or Vivaspin6 30K MWCO (GE Healthcare) spin filters. Concentration was checked by either BCA assay or extinction coefficient calculations on a spectrophotometer.

siRNA-uEED conjugates were initially purified and analyzed by HPLC on a strong anion exchange (SAX) column (ZORBAX SAX 150 mm, Agilent) with an ammonium acetate (pH 4.2) gradient: 100 mM NH_4OAc for 10 min followed by a gradient up to 2 M NH_4OAc over the next 15 min, 2 M NH_4OAc for 10 min, and then step-wise reduction back to 100 mM NH_4OAc for the last 10 min of the HPLC run. siRNA-uEED conjugates and other uEED-containing conjugates were later run on a standard C18 HPLC column (Agilent 1200 Series Preparative HPLC Prep-C18 with a Prep-C18 30x250 mm column).

Cell Culture

THP-1 cells and Jurkat cells were cultured in RPMI medium (ThermoFisher) with 10% fetal bovine serum (FBS) (Sigma-Aldrich) and penicillin/streptomycin (basic THP-1 medium) for the earlier experiments and cell maintenance and later cultured in a richer medium comprising of RPMI 10% FBS, Pen/Strep, and additional supplementation with 1X Sodium Pyruvate, 1X nonessential amino acids (NEAAs), 1X GlutaMAX, and a 500 µM final B-mercaptoethanol (complete THP-1 medium). These suspension cells were kept in a 37 ˚C incubator with 5% CO_2. Cells were passaged when culture density reached near ~80-90% confluency in most cases.

ExpiCHO cells (ThermoFisher Scientific) were cultured according to manufacturer recommendations, using ExpiCHO Expression Medium at 37 ˚C incubation with 8% CO_2. For antibody production, ExpiCHO cultures were grown as 30-mL cultures in vented shaker flasks with constant shaking at 140 rpm. For regular maintenance, ExpiCHO cells were otherwise passaged when their density reached about 5 million/mL by diluting an aliquot of cells to a density between 100,000-300,000 cells/mL in fresh culture medium.

Adherent cells (293T cells and H1299 dGFP cells) were maintained in standard growth medium of Dulbecco's Modified Eagle Medium (DMEM) (Gibco/ThermoFisher) supplemented with 5-10% FBS and Penicillin/Streptamycin. Cells were allowed to grow to 80-90% confluency before passaging in a 1:10 dilution ratio to a new 10 cm cell culture dish. Trypsin-EDTA (0.25%) (Gibco/ThermoFisher) with phenol red was used for cell dissociation for each passage cycle.

Antibody and ARC Binding Studies

For antibody binding studies, Fluorescein-KAYA peptide or K-PEG6-TAMRA peptides were conjugated to an αCD33 antibody using MTG as described. Between 50,000 and 100,000 THP-1 or Jurkat cells were incubated with increasing concentrations of αCD33-Fluorescein or αCD33-TAMRA conjugates for 20 min at 4 ˚C in RPMI before being washed with 0.1% sodium azide in PBS and analyzed for TAMRA or fluorescein signal on by flow cytometry. Approximately 100,000 cells were pelleted with a centrifuge and resuspended in variable volumes of FACS buffer (PBS, 5 mM EDTA) or filtered 1X PBS with the addition of the desired antibody or antibody-conjugate. Cells were kept on ice during the binding studies and mixed by gentle tapping every 5-10 min for a total binding duration of 30 min. After the binding study duration, cells were washed three or four times with either 1X PBS or FACS buffer, followed by straining through a nylon mesh into FACS tubes. Cells were always kept on ice up until flow

cytometry analysis with an LSR II (BD Biosciences). FlowJo software was used to plot the resulting cell populations.

The ARC binding studies described in Chapter Three were performed with the additional step of treatment with a goat anti-human-FITC secondary antibody (ThermoFisher). THP-1 cells and Jurkat cells were pelleted and washed as previously described and treatment with conjugates or mAbs followed for the same duration. After several cycles of washes, binding was assessed via flow cytometry analysis.

Antibody-RNA Conjugate Treatments

Antibody-RNA conjugates (ARCs) were built by at least two conjugation reactions: MTG conjugation between mAb and linker peptide and either a HyNic reaction or copper-free click conjugation to the oligonucleotide (refer to previous sections for more details). ARCs were purified by an Enrich-SEC 650 10/300 column FPLC column. ARCs were concentrated with spin filter columns (30K MWCO). ARCs were then quantified by BCA protein assay.

THP-1 cells were plated at densities between 30,000 and 50,000 cells/well in a 48-well plate in a 100 µL volume. ARC treatments were prepared in 1.5 mL centrifuge tubes by mixing the calculated weight or moles of conjugate required to achieve the desired final concentration in the final 200 µL well volume for the experiment. Volume for treatment tubes was brought up to 100 µL in RPMI + 10% FBS media (standard culture media for THP-1s). Treatment tube contents were added to the designated wells to achieve a final volume of 200 µL per well with ARC treatment. Cells were analyzed by flow cytometry at 24 or 48 hr for a change in GFP expression (FITC channel signal).

For the treatment of ARCs with uEEDs, ARCs were first filtered through a 0.22 µm PVDF syringe filter to remove contaminants. A small amount was separated for SDS PAGE analysis. ARCs were kept in 1X PBS at 4 ˚C until treatment day. For treatment, ARCs were incorporated into a designated volume (usually 100 µL) of RPMI complete growth medium and then added to

a 100 µL volume of THP-1 dGFP cells. Cells were incubated at 37 ˚C (5% CO_2) for 72-120 hr followed by flow cytometry analysis to assess changes in GFP expression (FITC signal).

Oligonucleotide Transfections

Numerous oligonucleotide transfections were performed over the course of this dissertation project, though only a few are documented in this dissertation. Lipofectamine 2000 (ThermoFisher) and RNAiMax (ThermoFisher) transfection reagents were used to transfect siRNA and ASOs. Cells were plated on the day before the transfection for forward transfections. Specific cell densities that were plated varied widely based on experimental conditions and ranged anywhere from 20,000 cells/well to 75,000 cells/well in standard 48-well or 24-well cell culture plates. Transfections were performed firstly by preparing the transfection reagent master mix in OptiMEM medium (no antibiotics or other supplementation). 1 µL of transfection reagent was used per 100 µL of final volume per well of the cell culture plate. For example, transfection for cells in a 24-well plate are normally maintained with a 500 µL final transfection mixture and so would contain 5 µL of transfection reagent. The oligo portion was prepared separately, with a standard 1.5 mL microcentrifuge tube per treatment condition. Oligos were diluted where needed in OptiMEM medium without any supplementation. Oligos were added per treatment tube according to the calculations to achieve the desired final concentration per final well volume. Cells were placed in incubators at 37 ˚C with 5% CO_2 for 24 or 48 hr, depending on the desired time point for knockdown analysis by flow cytometry.

Flow Cytometry

An LSR II (BD Biosciences) flow cytometer was used to analyze fluorescent cell knockdown experiments, most often from ARC and oligonucleotides treatments and transfections. Cells were either centrifuged followed by media removal and resuspension in

FACS buffer (PBS, 1 mg/mL BSA, 5 mM EDTA) or were processed directly in their existing growth medium. Adherent cells were dissociated with Trypsin (0.25% EDTA) for about 10 minutes to ensure complete dissociation and a higher cell count for flow cytometry. Both adherent and suspension cells were then strained through a nylon mesh into FACS tubes. FACS tubes with cell samples were kept on ice to prevent cell clumping. Cells were assayed for GFP and/or TAMRA levels by plotting FITC and PE signals, respectively. Gates were set around the single cell populations of interest. Histograms were plotted using FlowJo™ (FlowJo LLC) software.

Fluorescence Microscopy

A Zeiss fluorescent microscope equipped with a camera was used to visualize the green and red fluorescent molecules or cells with the use of blue or green filters. Cell images were taken at 20X magnification on both bright field and fluorescence views. SPOT Advanced software was used for imaging and settings adjustments.

Universal Endosomal Escape Domains

Universal endosomal escape domains (uEEDs) were synthesized by our chemist, Satish Jadhav, with an azide group modification to allow for copper-free click conjugations of the uEEDs to the oligonucleotides. uEEDs were purified on a C18 HPLC column (Agilent 1200 Series Preparative HPLC Prep-C18 with a Prep-C18 30x250 mm column).

REFERENCES

Meade, B.R., Gogoi, K., Hamil, A.S., Palm-Apergi, C., Berg, A. van den, Hagopian, J.C., Springer, A.D., Eguchi, A., Kacsinta, A.D., Dowdy, C.F., Presente, A., Lönn, P., Kaulich, M., Yoshioka, N., Gros, E., Cui, X.-S., Dowdy, S.F., 2014. Efficient delivery of RNAi prodrugs containing reversible charge-neutralizing phosphotriester backbone modifications. Nat Biotechnol 32, 1256–1261. https://doi.org/10.1038/nbt.3078

CHAPTER THREE

BUILDING AN ARC

BUILDING AN ARC

ABSTRACT

There has been considerable clinical success with the use of antisense oligonucleotides (ASOs) and short interfering RNAs (siRNAs) to treat certain genetic diseases that affect the liver, central nervous system, and muscles. This success is a result of using tris-GalNAc targeting ligand or lipid nanoparticles (LNPs) as delivery vehicles for these oligonucleotides. Unfortunately, targeting extrahepatic diseases with oligonucleotides remains a challenging prospect due to the inherent biological characteristics that include targeted cell type, target receptor availability, and the location of the target. Beyond this, there is also the fundamental problem of very limited ability for oligonucleotides to access the cytoplasm.

Monoclonal antibodies (mAbs) have an unrivaled specificity and bioavailability that are well-suited to deliver oligonucleotides to many extrahepatic targets. However, many current conjugation strategies utilize nonspecific conjugation reactions that produce conjugates of highly variable Drug:Antibody ratios (DAR). This lack of specificity produces a heterogeneity in the final conjugate that may be suboptimal for its pharmacokinetics. Instead, the use of a homogeneous, chemically defined conjugates can allow for better control and analysis of the efficacy of a potential oligonucleotide therapeutic.

This chapter will detail the procedure that has been developed in our lab to produce homogeneous DAR-2 antibody-RNA conjugates (ARCs) with siRNAs. An ARC has several components and relies on the activity of a microbial transglutaminase (MTGase) enzyme to come together into its final form. ARCs produced in this way have good solubility and hold significant potential to target cell types beyond the liver.

INTRODUCTION

Short interfering RNAs (siRNAs) and antisense oligonucleotides (ASOs) have a great potential to target disease-associated genes with high specificity in a sequence-dependent manner. Where traditional small molecule inhibitors and monoclonal antibody therapies fail, oligonucleotide therapeutics can hit undruggable genetic targets. Most oligonucleotides, such as siRNAs, have a negatively charged backbone and sufficiently high molecular weight to prevent passive diffusion (Dowdy, 2017). Generally, naked oligonucleotides (siRNAs more than ASOs) cannot be taken up into cells nor escape the endosome if they are endocytosed into cells. Chemical modifications to the backbone and 2'-modifications to the ribose sugar of oligonucleotides, especially the more common 2'-OMe and 2'-F, have greatly increased their stability and potency (Khvorova and Watts, 2017), but these chemical modifications are not sufficient on their own to solve the delivery problem.

Targeting domains have improved the prospects of oligonucleotide therapeutics by allowing the direct targeting of specific cell types, depending on their surface receptors or location. One delivery strategy is to encapsulate siRNAs with lipid nanoparticle (LNP) formulations for extra protection, but LNPs predominately accumulate in the liver (Whitehead et al., 2009; Akinc et al., 2008). There are several drawbacks of LNPs, including their large 100 megaDa size, toxicity, and poor diffusion coefficient (Schroeder et al., 2010; Ishida et al., 2006). GalNAc is a targeting ligand that binds to the asialoglycoprotein receptor (ASGPR) on liver hepatocytes and is commonly used in several therapeutics (Springer and Dowdy, 2018; Setten et al., 2019). ASGPR is abundant on liver hepatocytes, making GalNAc an ideal targeting domain to deliver oligonucleotides to hepatocytes (Juliano, 2016; Nair et al., 2014). GalNAc-siRNA conjugates have shown significant clinical promise and efficacy (Balwani et al., 2020; Kosmas et al., 2018) as have GalNAc-ASOs (Prakash et al., 2014). But neither of these commonly used targeting domains can efficiently deliver oligonucleotides to extrahepatic targets.

Monoclonal antibodies (mAbs) have been extensively studied and are routinely used in antibody-drug conjugates (ADCs) to deliver cytotoxic cargo to cancer cells (de Paula Costa Monteiro et al., 2015; Younes et al., 2010; Krop et al., 2010). As discussed in Chapter One, ADCs have several key drawbacks. Firstly, off-target toxicity can lead to detrimental systemic side effects. Secondly, a higher DAR ADC can have reduced efficacy due to faster clearance rates (Hamblett et al., 2004). Also, the cytotoxic drug can passively diffuse back out of a cell and into neighboring healthy cells in what is termed the bystander effect (Malik et al., 2017). Replacing an ADC's cytotoxic payload with an oligonucleotide would instead provide greater specificity against the cancer cell without risking off-target toxicity from a toxin. After all, an oligonucleotide specific for an oncogenic mutation will not adversely affect the healthy version of the same gene if delivery to a normal cell occurs.

ADCs initially used nonspecific conjugation chemistries for their cytotoxic payloads. For example, gemtuzumab ozogamicin, the first clinically approved ADC, targets the CD33 receptor of abnormal myeloblasts of patients with acute myeloid leukemia (AML) and relies on nonspecific chemical crosslinking between primary amines on the antibody and an N-Hydroxysuccinimide ester (NHS)-ester reactive group on the calicheamicin drug to produce a stable amide bond (Hamann et al., 2002). Another example is trastuzumab-maytansinoid (DM1), an ADC that targets HER2 in breast cancer patients, that uses the same nonspecific NHS-ester conjugation chemistry (Lewis Phillips et al., 2008). Primary amines involved in this reaction are commonly found in the N-terminus of polypeptide chains and in the lysine amino acid side chains. Monoclonal antibodies are estimated to have at least 40 reactive lysine residues, producing hundreds of regioisomers, and highly variable DARs ranging between 0 and 6 or greater in the final antibody conjugate (Agarwal and Bertozzi, 2014). Consequently, variable DARs can lead to aberrant pharmacokinetics and stability of antibody conjugates. High DAR antibody conjugates are quickly cleared from circulation due in part to the excessive hydrophobicity of the conjugated drug and subsequent aggregation (Senter and Sievers, 2012).

Instead, the use of IgG cysteines as conjugation sites by reducing the cysteine disulfides and conjugating the drug onto the free sulfhydryl groups leads to lower heterogeneity, avoids or reduces aggregation issues, and limits the observed DAR range, while maintaining the same strong binding characteristics (Senter and Sievers, 2012; Doronina et al., 2003; Francisco et al., 2003).

Site-specific conjugation of the cytotoxic drug or other cargo demonstrates better pharmacokinetics and therapeutic efficacy. Engineering cysteine residues at specific locations within anti-MUC16 antibodies (MUC16 is a cell surface protein associated with ovarian cancer) allowed for well-defined-DAR ARCs that did not disrupt the antibody interchain disulfide bonds and led to great efficacy of the ADC in a mouse xenograft model of ovarian cancer (Junutula et al., 2008). An anti-CD123 ADC (SGN-CD123A) also used engineered cysteines to demonstrate effective killing of CD123-positive leukemic blasts while sparing CD123-negative cells in AML patient-derived xenograft models (Li et al., 2018). A cMet-targeting ADC (TR1801-ADC) that uses engineered cysteines in P3D12 anti-CMet antibodies demonstrated significant antitumor activity in rat preclinical models and is currently in Phase 1 clinical trials (Gymnopoulos et al., 2020; ClinicalTrials.gov).

The engineered cysteine approach relies on chemical crosslinking to conjugate a cytotoxic drug onto a monoclonal antibody. However, there are also enzymatic approaches for conjugations onto an antibody. In our lab, the microbial transglutaminase enzyme is routinely used for antibody conjugations and the sections that follow will describe our approach for site-specific conjugations of siRNAs onto antibodies to create ARCs.

MICROBIAL TRANSGLUTAMINASE ENZYME

The microbial transglutaminase enzyme is well known in the food industry and is used to catalyze the crosslinking reactions of food proteins including caseins, soybeanglobulins, gluten, actin, and myosins (Seguro et al., 1996). Microbial transglutaminase (MTG enzyme, or

MTGase) is an enzyme derived from *Streptoverticillium mobaraense* that catalyzes a transamidation reaction between the R groups of glutamine and lysine residues that results in the formation of an isopeptide bond between these two amino acids (**Figure 3.1**) (Seguro et al., 1996). Extensive experimentation with peptide libraries have demonstrated that there are specific amino acid motifs that optimally enable MTG enzyme activity, particularly the LQSP tetrapeptide (Caporale et al., 2015; Siegmund et al., 2015). The glutamine amino acid must be part of a larger amino acid sequence motif that allows for recognition by the MTG enzyme catalytic site. Microbial transglutaminases' efficiency is conformation-dependent and in the case of cetuximab, an anti-EGFR monoclonal antibody, none of the 64 surface glutamines were adequate substrates for the MTG enzyme (Siegmund et al., 2015; Jeger et al., 2010). The transamidation of glutamine residues to lysine residues is pH-dependent and unlike mammalian transglutaminase enzymes, the microbial enzymes have a different structure, are not regulated by calcium, and have a wider substrate versatility (Strop, 2014). The incorporation of an engineered MTG tag into proteins has allowed for site-specific conjugations in various contexts, including alkaline phosphate and single chain antibody fragments as reagents for immunoassays (Takazawa et al., 2004), between proteins and DNA (Strop, 2014; Takahara et al., 2017), and some anti-HER2 and anti-EGFR ADCs (Strop et al., 2013). There are other ADCs that use the LLQGA MTG tag (Farias et al., 2014). The success of site-selective protein conjugations with the MTG enzyme makes it an ideal tool to site-selectively conjugate oligonucleotides onto monoclonal antibodies.

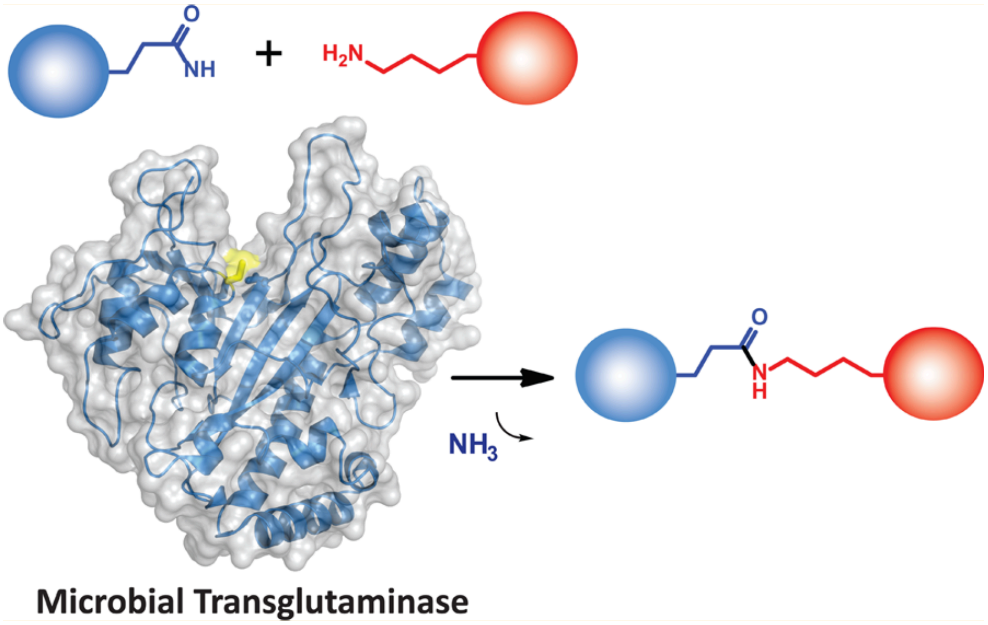

Figure 3.1. Mechanism of Microbial Transglutaminase
Microbial transglutaminase (MTG) enzyme catalyzes the conjugation reaction in which the glutamine residue (acyl donor) reacts with a primary amine (acyl acceptor), and a molecule of ammonia is released to generate an isopeptide bond. The primary amine is often provided by a reactive lysine residue on a peptide or other molecule, while the glutamine is incorporated into a larger MTG peptide tag that is designed to optimize MTG enzyme activity.

Taken from Strop, 2014.

RESULTS & DISCUSSION

The Antibodies

Designing a monoclonal antibody with a high binding affinity and therapeutic efficacy requires extensive time and resources. To allow for more efficient development of monoclonal antibodies (mAbs), amino acid sequences of heavy and light chains for mAbs used in the clinic were obtained from the patent literature. Furthermore, we chose to produce our own antibodies to allow for the addition of site-specific MTG conjugation handles. The ExpiCHO expression system uses a Chinese hamster ovary (CHO) cell line engineered for the purpose of large-scale protein expression, highly amenable to transfection and with high and reliable yields for a wide range of proteins (ThermoFisher). The ExpiCHO expression system has been used to reliably produce proteins like the human group-specific component (Gc) protein, a macrophage activating factor and promising candidate for immunotherapy (Nabeshima et al., 2020), and mAbs with yields on par with the yields obtained from human embryonic kidney (HEK) 293 cell expression systems (Zhong et al., 2019). We obtained the amino acid sequences for FDA approved mAbs targeting the CD33 and CD71 receptors.

Variable regions of these antibodies were cloned into Kappa or Lambda light chains and IgG1 or IgG4 heavy chains (Huggins et al., 2019). The MTGase conjugation handle, LLQGA (Farias et al., 2014), was cloned into the C-termini of the heavy chain cDNA and a translational termination codon was added immediately afterwards. The modified heavy and light chain plasmids were next transfected into suspension ExpiCHO cells. Heavy chains are about twice as large as light chains and therefore have an overall lower expression. To compensate for this, the heavy chain plasmid was transfected in 4:1 molar excess, relative to the light chain plasmid, for optimal mAb expression. Following plasmid transfection, Expi-CHO cells were incubated overnight at 37 ˚C on a shaker and then transferred to a 32 ˚C on a shaker for 10-14 days to allow for optimal mAb production.

Purification of mAbs proceeded first by pelleting the ExpiCHO cells and filtering the culture supernatant that contains the mAbs through 0.22 μm and 0.45 μm syringe filters to remove excess debris. The culture supernatant was then passed through a Protein A chromatography column. Protein A resin/beads bind strongly to the fragment crystallizable region (Fc) region of mAbs and efficiently sequester mAbs away from the remaining culture supernatant components. After Protein A resin binding, 3 washes were run through to remove other unwanted proteins that could remain. Protein A is denatured in low pH conditions, so elution with a ~pH 3.0 buffer yields highly pure mAbs. Following Protein A chromatography, the mAb solution was further purified by size-exclusion chromatography (SEC 650 column) on an FPLC to yield a cleaner product that was also buffer exchanged into 1X PBS. Total antibody yields with this procedure depend largely on the specific antibody, age of the culture reagents and cells, and tended to vary between batches. However, this approach usually produces between 5 to 20 mg of purified mAb per 30 mL ExpiCHO culture flask.

The Linkers

There are several linkers that have been produced in our lab that are compatible with our ARC-building approach. One common linker that we have used extensively is the KP1Z linker, a non-cleavable linker that consists of a lysine (K), a single PEG-6 spacer (P1), and an azide (Z) group (K-PEG_6-SG-N_3) that the oligonucleotide is conjugated to (**Figure 3.2**, top). Two other linkers that have been produced include an acid-cleavable hydrazone linker (**Figure 3.2**, middle) and a valine-citrulline (PABC) linker (**Figure 3.2**, bottom) that is cleavable by the lysosomal Cathepsin B (Dorywalska et al., 2016). Another linker is the KP1H (Lysine-PEG_6-Hynic) linker, most often used as part of our ASO-containing ARCs (see Chapter Four). Lastly, we also synthesized a KAYA-PEG_6-K-Fluorescein (KF) linker (**Figure 3.2**). The KF linker contains a lysine that provides the key primary amine for an MTG conjugation.

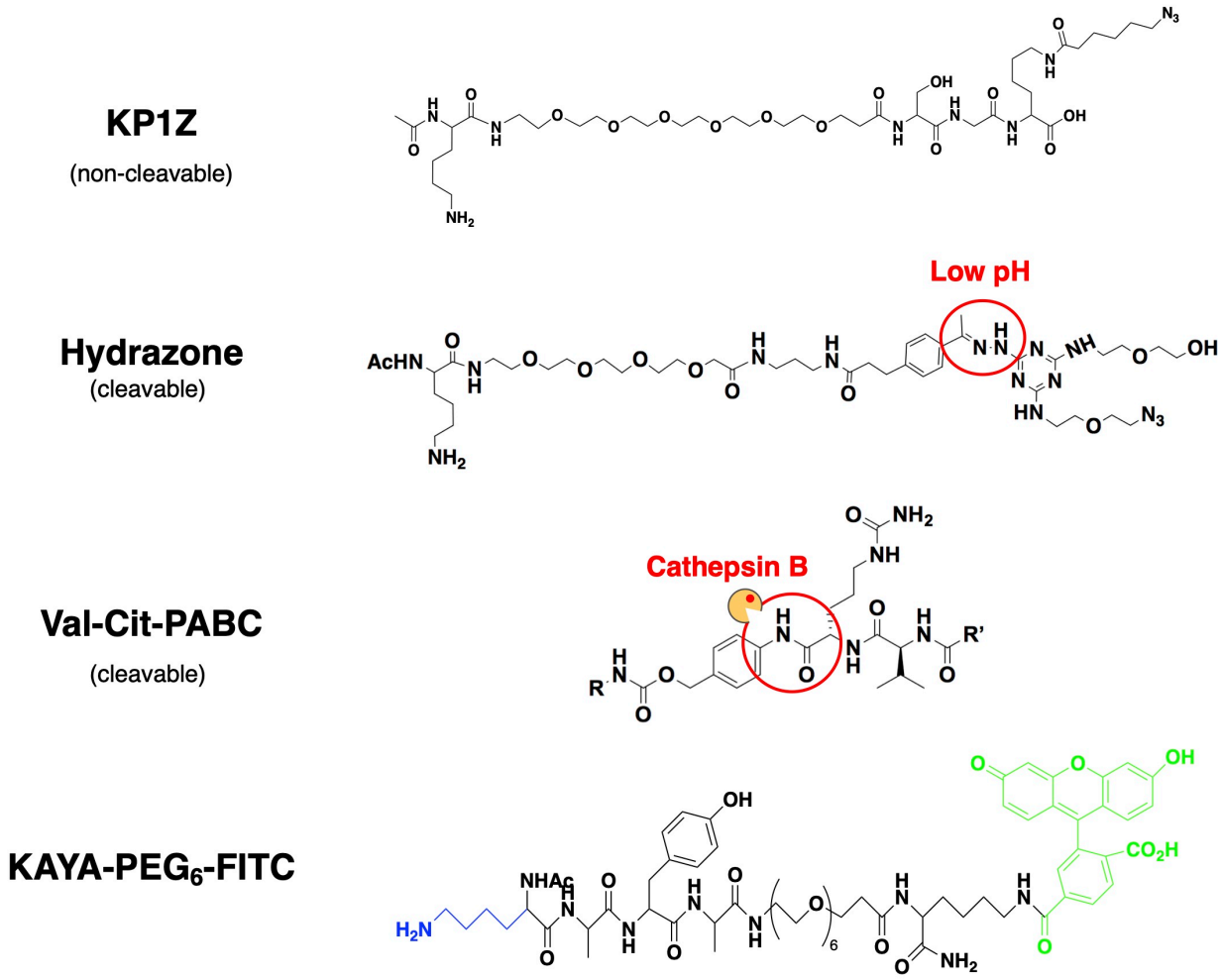

Figure 3.2. Some Linker Options with MTG Enzyme Compatibility
First, the Lysine-PEG_6-Azide (KP1Z) linker is non-cleavable and very efficiently conjugated onto MTG conjugation handles by the MTG enzyme. The azide-bearing terminus allows for the efficient Copper-free click conjugation reaction to a modified oligonucleotide. *Second*, the hydrazone linker becomes unstable at low pH and will be degraded in acidic conditions to release the oligonucleotide or cytotoxic drug cargo. *Third*, the valine-citrulline-PABC linker is susceptible to the lysosomal Cathepsin B enzyme. *Fourth,* the KAYA-PEG6-fluorescein (KF) linker used for imaging. These are all linkers that have been produced in our lab.

The activity of the MTG enzyme depends on several factors including the concentration of the reagents within the conjugation reaction, the antibody, and the linker itself. Previous experimentation in our lab determined that ~3.15 units of MTG enzyme per reaction, or 63 mg/mL concentration within the reaction volume, provided optimal MTG functionality, whereas concentrations that were too high led to off-target conjugation activity and concentrations that were too low led to an excessively lengthy reaction time. At this concentration, a 1 hr incubation resulted in the optimal conjugation with no off-target conjugation observed.

Between the antibody and the linker, the former is the more limited reagent. Therefore, to optimize MTG conjugation, it was necessary to vary the level of linker relative to mAb. Test conjugation reactions were set up where mAbs were reacted with excess linker at varying conjugation ratios (linker : mAb conjugation handle, there are two conjugation handles per mAb). Failure to include an excess amount of linker in the reaction led to random conjugations between surface lysine and glutamine residues of the antibodies resulting in self-conjugation and aggregation. In one example, MTG conjugation efficiency was tested for an anti-CD71 mAb and the KP1Z linker that we frequently used and a few other variants of the original KP1Z linker, termed KEP1Z and KFP1Z (**Figure 3.3**). The KP1Z:conjugation site ratios that were tested were 50:1, 25:1, 10:1, 5:1 with a follow-up repeat run to test 25:1, 5:1, 2.5:1, 1:1, and 0. The resulting SDS PAGE reducing gels revealed that KP1Z remained among the most efficient linker, whereas KEP1Z was considerably less compatible with the MTG enzyme at the same conjugation ratios. Not all linker peptides were equally efficient, even closely related linkers. The test conjugations were performed in a 15 µL total volume that contained the MTG reaction buffer, water, linker peptide, MTG enzyme, and mAb. These results highlight the efficiency of the MTG enzyme to modify a mAb at its MTG handle in a 1 hr incubation period at room temperature.

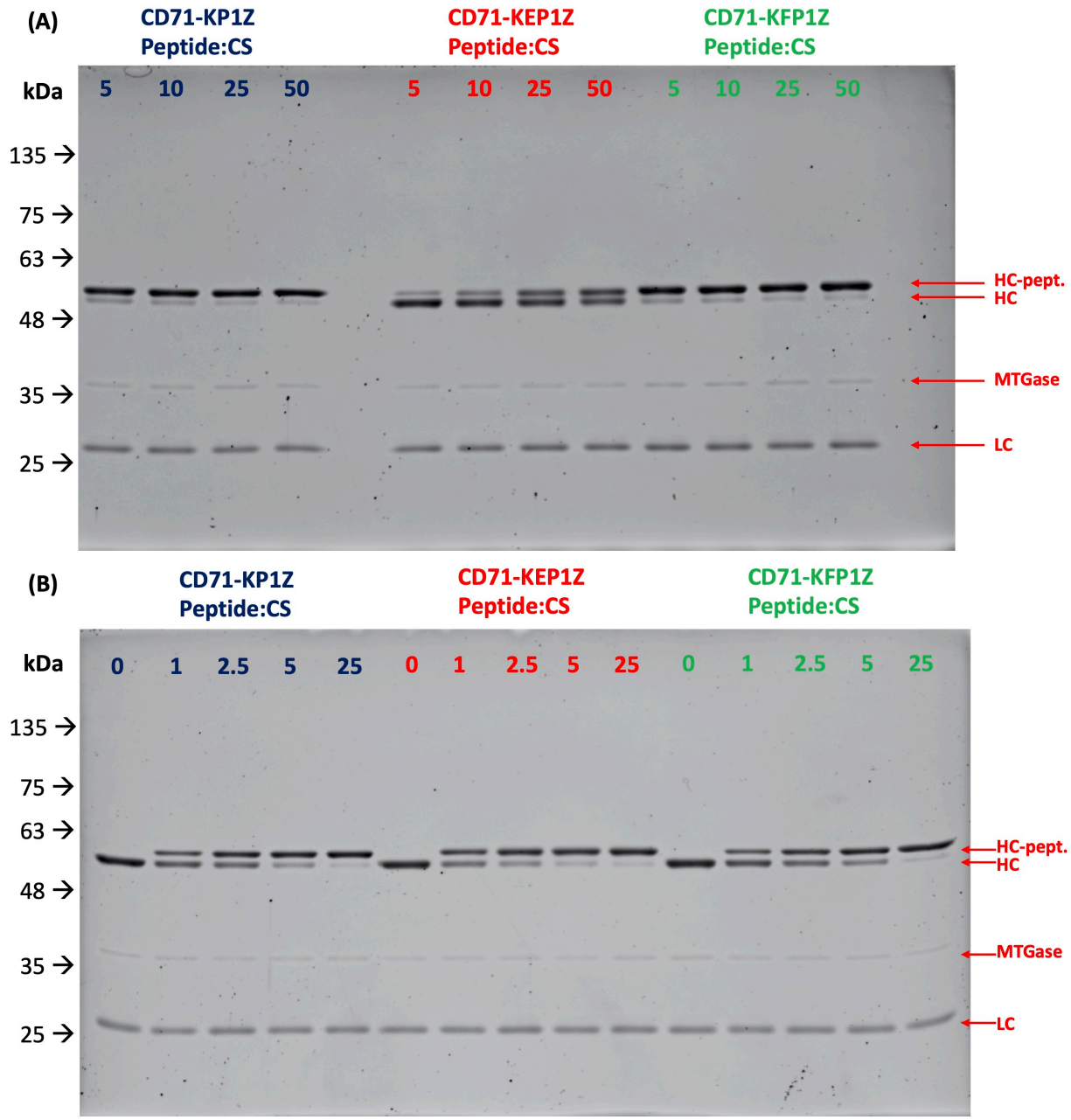

Figure 3.3. MTG Test Conjugations between Anti-CD71 & Linker Peptides
SDS PAGE reducing gel results for test MTG conjugations of anti-CD71 mAb and three linker peptides: KP1Z, KEP1Z, and KFP1Z. (a) The excess linker peptide conjugation ratios of 50, 25, 10, 5. MTG reaction standard 1 hour room temperature incubation, 63 mg/mL. (b) The follow-up experiment to gauge the more sensitive lower conjugation ratios for MTG efficiency: 25, 5, 2.5, 1, and 0. Molecular weight markers in kilodaltons (kDa). Abbreviations: CS, conjugation sites; HC, heavy chain; LC, light chain; MTGase, microbial transglutaminase enzyme.

The KAYA-PEG6-K-Fluorescein (KF) linker contains a fluorescene. To verify that MTG-mediated addition of a KF linker to a mAb does not lead to off-target conjugations, a KF peptide was MTG-conjugated to an anti-CD33 mAb by following the standard conditions of 1 hr room temperature incubation, 3.15 U/mL MTGase, and a 5-fold molar excess ratio of KF peptide to mAb (**Figure 3.4**) (Huggins et al., 2019). SDS PAGE gel electrophoresis analysis confirmed an increased molecular weight band of a successfully conjugated heavy chain species, as expected with one MTG handle per heavy chain, or two peptides per mAb (**Figure 3.4b**). SDS PAGE analysis indicated no aggregation between heavy or light chains, an event that would be observed by higher molecular weight bands above the unconjugated antibody control lane. Imaging on a gel dock confirmed an overlapping fluorescent signal where the heavy chain is found and an absence of nonspecific conjugation to the light chain (**Figure 3.4c**). The mAb-KF conjugate was cleaned up by a spin column to remove excess peptide.

To determine whether an MTG-conjugated linker adversely affected a mAb's binding specificity, CD33-positive acute myeloid leukemia THP-1 cells and CD33-negative Jurkat cells were treated with the mAb-KF conjugate followed by flow cytometry analysis (**Figure 3.4d**). Results from flow cytometry analysis confirmed that the mAb-KF conjugate bound THP-1 cells in a dose-dependent manner, but not Jurkat cells. MTG conjugation of linkers onto the MTG handles of mAbs therefore do not interfere with the antibody's ability to bind to its target receptor. Validation of mAb binding and conjugation efficacy next allowed for testing of antibody conjugates with RNA cargo to optimize the conjugation and purification procedures. The KP1Z ($K\text{-}PEG_6\text{-}SG\text{-}N_3$) linker was used to conjugate an siRNA to an anti-CD33 mAb. KP1Z is a dual function linker with a functional lysine for MTG conjugation to the mAb and an azide group for the copper-free click conjugation to siRNA molecules. Traditional copper click chemistry involves a reactive azide and cycloaddition with an alkyne group. However, the required organic copper catalyst denatures mAbs. Moreover, divalent copper (and other metal) ions can desulfurize or oxidize the phosphorothioate backbone groups that play a critical role in

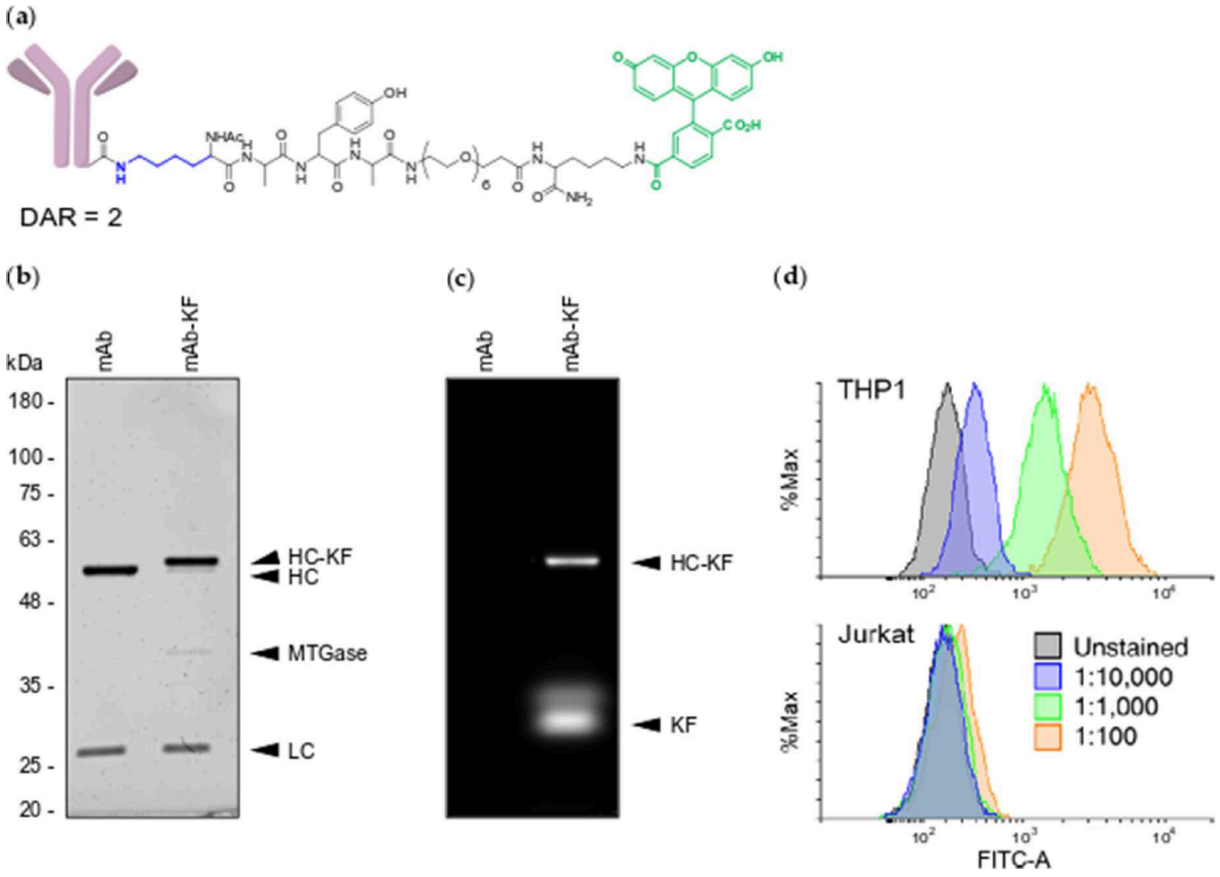

Figure 3.4. MTG conjugation of fluorescent peptide (KF) and anti-CD33 mAb. Conjugation of the KF fluorescent peptide and anti-CD33 proceeds by the activity of the MTG enzyme with great efficiency. (**a**) Structure of the anti-CD33 – KF conjugate. Fluorescein group appears in green while the reactive lysine of the KF peptide appears in blue. (**b**) SDS PAGE gel was run to assess the efficiency of the MTG conjugation, in comparison to an unconjugated anti-CD33 mAb. Heavy chain shift occurs as expected from the peptide conjugation. Molecular weight markers are shown in kilodaltons (kDa). Gel was UV protein stained followed by imaging. (**c**) FITC epifluorescence imaging of the same SDS PAGE gel to verify the successful conjugation of the fluorescent peptide. (**d**) Binding analysis of anti-CD33-KF conjugate on THP-1 (CD33-positive) and Jurkat (CD33-negative) cells by flow cytometry. Other abbreviations: HC, heavy chain; LC, light chain, HC-KF, heavy chain-KAYA-fluorescein peptide conjugate; KF, free KAYA fluorescein peptide; MTGase, microbial transglutaminase enzyme.

Taken from Huggins et al., 2019.

oligonucleotide stability (Ora et al., 1998). Instead, the inclusion of a cyclooctyne group allows for azide-mediated cycloaddition through ring strain interactions that proceed efficiently under physiological conditions (Agard et al., 2004). Copper-free click dibenzylcyclooctyl (DBCO) conjugation chemistry involves a commercially available 5'-DBCO modification to the passenger strand of an siRNA that does not interfere with conjugation efficiency and is stable throughout the conjugation and purification processes. Copper-free click conjugation chemistry is also compatible with solid-state oligonucleotide synthesis reagents that are used in our lab and is unreactive under the other conjugation reactions involved in the ARC building process. Importantly, the concentration of each reagent required in a copper-free click are low enough to maintain the solubility of all components.

An anti-CD33 mAb was reacted with the KP1Z linker added in a 5-fold molar excess to the mAb. Reaction conditions included 3.15 U/mL MTG enzyme and incubation was allowed to proceed at room temperature for 1 hr, resulting in an almost complete conjugation of KP1Z linker onto the mAb (**Figure 3.5**). Purifying an mAb-linker peptide conjugate is important to remove the excess linker and MTG enzyme to prevent interference in the conjugation reactions that followed and to avoid mAb heavy chain-heavy chain crosslinking, aggregation, and precipitation that will otherwise inevitably occur in long-term storage. After the MTG conjugation reaction, the mAb-KP1Z conjugate was purified by FPLC on a SEC column. All three components of the MTG reaction were separated well and allowed consolidation of the mAb-KP1Z from 4 fractions.

The Antibody-RNA (ARC) Conjugate

The passenger (sense) strand of an siRNA was synthesized with the addition of a 5'-DBCO-triethyleneglycol(TEG) linked phosphoramidite to allow for copper-free click conjugation between the KP1Z linker and the siRNA. To obtain double stranded (duplexed) siRNA, the

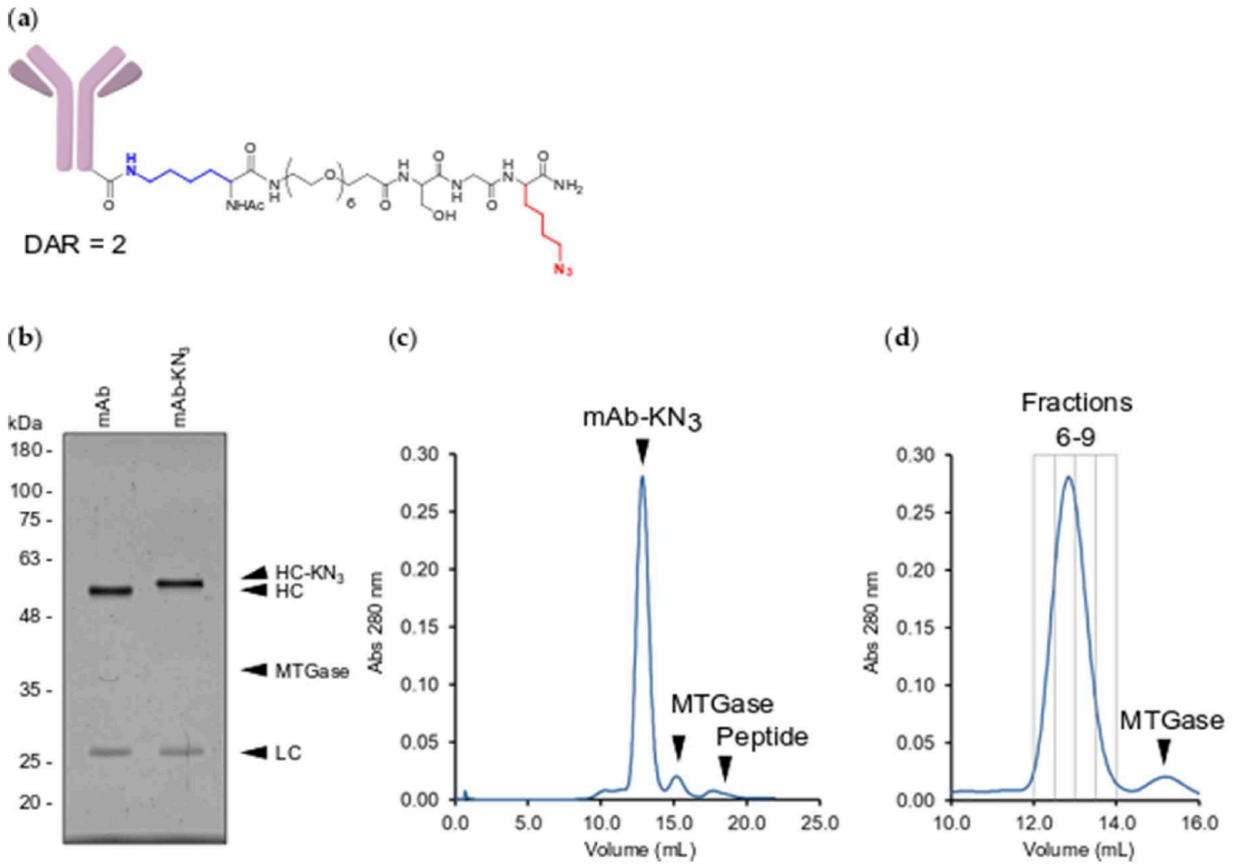

Figure 3.5. MTG Conjugation Reaction in the Larger ARC Building Process
This MTG conjugation reaction is the first of 2 or 3 reactions in the overall ARC building sequence. (**a**) Structure of the anti-CD33-KP1Z conjugate (note: KP1Z linker peptide is the same as KN_3 peptide). (**b**) SDS PAGE gel analysis of the MTG conjugation efficiency, UV protein stained. (**c**) Size exclusion chromatography (SEC) profile of the crude MTG conjugation reaction, which shows clearly defined peaks for each of the three components in the reaction. (**d**) Close-up of part c, in which the elution fractions for the anti-CD33-KP1Z conjugate are highlighted, free of MTGase or KP1Z peptide, and were subsequently pooled and concentrated. Abbreviations: KN_3, KP1Z linker peptide; mAb-KN_3, antibody-KP1Z conjugate; HC, heavy chain; LC, light chain; MTGase, microbial transglutaminase enzyme.

Taken from Huggins et al., 2019.

guide (antisense) strand was mixed with the DBCO-modified passenger strand at ~1:1 molar ratio, with a slight excess of guide strand to ensure complete siRNA duplexing. The siRNA mixture was heated to 65 ˚C for 3 min followed by cooling at room temperature for 3 min and then cooling to 4 ˚C for 4 min.

After the duplexed siRNA was obtained, the DBCO-containing siRNA was incubated overnight at 37 ˚C with the previously purified mAb-KP1Z conjugate. This incubation reaction was performed in 1X PBS supplemented with 40 mM L-Arginine. It was previously demonstrated that free arginine in the buffer can effectively suppress the tendency for proteins to aggregate, increases protein solubility, promotes protein structure, and is often used during protein purification procedures (Arakawa et al., 2007). Following the overnight copper-free click reaction, the ARC was purified through a SEC column on a FPLC, confirming that the soluble ARC can be separated from the unconjugated mAb-KP1Z (**Figure 3.6**). The ARC was eluted in three fractions and pooled together. The final, purified ARC was analyzed on an SDS PAGE gel compared to mAb-KP1Z and mAb only to confirm efficient copper-free click conjugation with no off-target conjugations onto the light chain. A duplexed siRNA molecule is approximately ~14 kDa, consistent with the SDS PAGE gel analysis that shows this expected corresponding shift from the mAb-KP1Z to the ARC sample lanes. Through the MTG conjugation, siRNA duplexing, and overnight copper-free conjugation reaction, a complete ARC was successfully built.

The final step after building the ARC is to assess its binding capabilities to ensure that the conjugation reactions and purification procedures did not adversely impact its ability to bind properly. The purified ARC was used to treat CD33-positive THP-1 cells. Cells were then analyzed by flow cytometry to determine the level of ARC binding (**Figure 3.7**). The anti-CD33 ARC or anti-CD33 mAbs only were added to THP-1 cells and washed several times with FACS buffer. To visualize the binding, a 1:200 dilution of goat anti-human FITC secondary antibody was applied to the treated cells and samples were run on a flow cytometer to observe the FITC

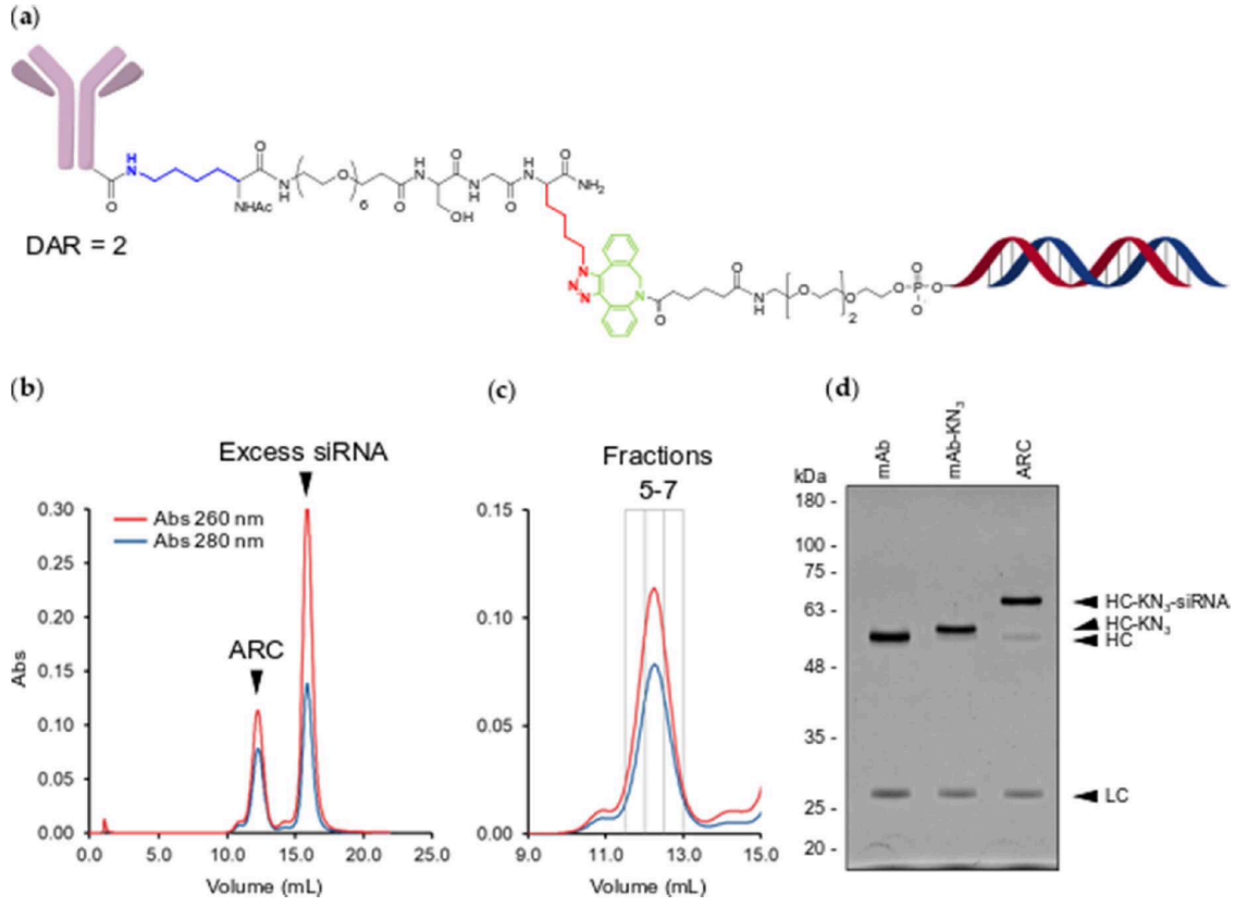

Figure 3.6. Final ARC Purification and Verification
Final ARC is shown here with purification details and gel electrophoresis confirmation. (**a**) Structure of the final ARC, with a KP1Z peptide linker, and a 5'-DBCO-containing duplexed siRNA. (**b**) SEC purification of final ARC conjugate after the overnight copper-free click reaction. (**c**) Close-up of the ARC peak in the SEC purification run to highlight the fractions of interest that were pooled and re-concentrated. (**d**) SDS PAGE gel analysis confirms the expected shift from adding a duplexed siRNA onto the existing anti-CD33-KP1Z conjugate. Gel was UV-protein stained and compared to the unconjugated controls. Abbreviations: KN_3, KP1Z linker peptide; mAb-KN_3, antibody-KP1Z conjugate; HC, heavy chain; LC, light chain.

Taken from Huggins et al., 2019.

signal for binding. The secondary antibody only control was also compared in the same flow cytometry experiment. The purified ARC and anti-CD33 only both avidly bound to CD33-popsitive THP-1 cells, whereas the control secondary FITC-labeled antibody did not show significant binding. Therefore, the conjugation reactions and overall purification procedures required to obtain the final ARC did not negatively affect the final ARC's ability to bind to its target receptor.

CONCLUSIONS

Oligonucleotide therapeutics, especially siRNAs and ASOs, have incredible potential to target currently undruggable disease prompting genes, especially in cancer. Delivery of oligonucleotides to the desired cell type or organ has been the biggest roadblock to progress. Lipid nanoparticles (LNPs) have proven to be a relatively successful vehicle for oligonucleotide delivery, yet they still possess a poor pharmacokinetic profile that limits their range of targets. They primarily accumulate in the liver and cannot be reliably used to target other organs through systemic administration. While GalNAc targeting domains avidly bind to the ASGPR receptor in liver hepatocytes and has proven to be the most effective liver targeting, like LNPS, GalNAc is limited to liver targets.

mAbs are excellent candidates for extrahepatic targeting because they have a high binding affinity for their target receptors, regardless of location in the human body and only limited by the accessibility of the mAb to the target tissue through systemic circulation. mAbs are routinely used in antibody-drug conjugates (ADCs) to deliver cytotoxic drugs to cancer cells. It therefore follows that the substitution of the cytotoxic drug with an oligonucleotide could provide an effective, alternate therapeutic – an antibody-RNA conjugate (ARC). Early development of ADCs employed many nonspecific approaches to conjugate cytotoxic drugs onto the mAb, but more recent work has demonstrated the promise and desirability of

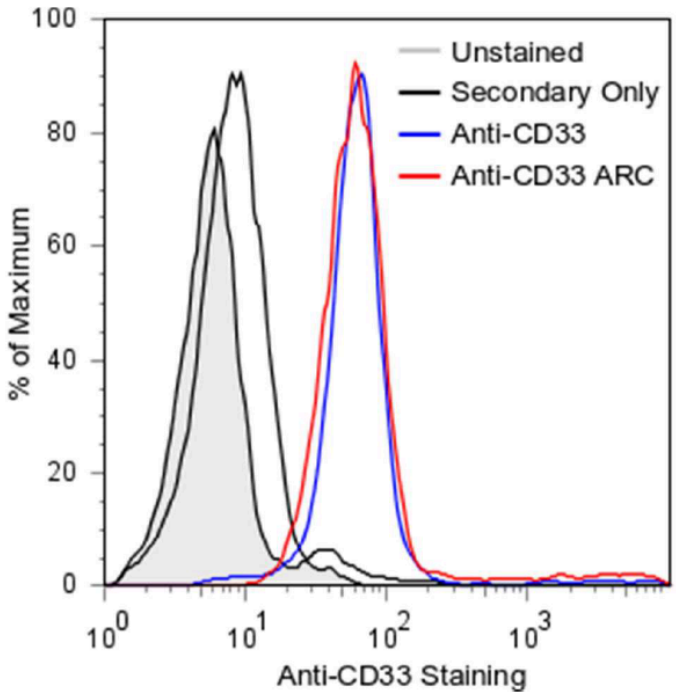

Figure 3.7. Final Purified ARC Retains Its Binding Affinity
The ARC described in this chapter can still bind to its target (CD33) receptor. THP-1 cells (CD33-positive) were treated with either secondary FITC-labeled antibody, anti-CD33 only, or the complete ARC, applied to THP-1 cells at a final 25 nM concentration. Both anti-CD33 and CD33-ARC produce the desire shift in FITC signal to confirm effective binding to THP-1 cells. Unstained cells appear in gray. Flow cytometry plot represents percent of maximum cell count.

Taken from Huggins et al., 2019.

generating highly defined therapeutic molecules through site-selective conjugation approaches.

This chapter has detailed the process of developing a well-defined ARC. MTG conjugation handles were engineered into C-termini of heavy chains of clinical mAbs and the ExpiCHO expression system was used to produce large quantities of these mAbs. MTGase is an enzyme routinely used in the food industry that mediates the formation of an isopeptide bond between a glutamine (within certain peptide tags) and a lysine residue. MTGase is relatively inexpensive and compatible with the reaction conditions needed to build an ARC. The linker can be customized to contain different groups, and in this case, the N-terminal lysine with C-terminal azide groups allowed for the efficient conjugation reactions first of the MTG reaction between mAb and linker and then of the copper-free click between the mAb-linker and a DBCO-modified siRNA. The reaction conditions have been optimized, as described in this chapter, to consistently produce ARCs with a DAR of 2. The reactions required for these ARCs do not generate any off-target conjugations. Moreover, none of these conjugation reactions or purification cycles adversely affect the final ARC's ability for binding to its target receptor.

ARCs are highly customizable based on the disease target. mAbs can easily be produced, there is a wide variety of linker peptides that can be used, and oligonucleotides can be synthesized against any genetic target. The conjugation of the different components is efficient in our current conditions and purification by size exclusion chromatography is straightforward. While the production of DAR 2 ARCs has been described here, it is easy to envision a different DAR ARC via the engineering of additional MTG conjugation handles and modification to the conjugation reaction ratios.

Though the approach to build a promising therapeutic ARC molecule has been developed, the problem of endosomal escape remains. The ARCs described in this chapter were unfortunately incapable of mediating an RNAi response. While an antibody can direct an oligonucleotide to the correct cell target and induce endocytosis, oligonucleotide access to the cytoplasm is extremely limited, especially for siRNAs. On the other hand, ASOs have been

observed to enter the cytoplasm and nucleus without assistance through gymnosis. The following chapter details the development of an ARC containing ASOs instead of siRNAs to determine whether the antibody-mediated delivery of ASOs fare any better than their siRNA counterparts.

ACKNOWLEDGEMENTS

Chapter Three has been published in part in *Molecules*, coauthored by this dissertation's author. The citation for the published work is: Huggins, I.J., Medina, C.A., Springer, A.D., van den Berg, A., Jadhav, S., Cui, X., Dowdy, S.F., 2019. Site Selective Antibody-Oligonucleotide Conjugation via Microbial Transglutaminase. Molecules 24, 3287. Arjen van den Berg performed some binding studies and produced some antibodies. Ian Huggins cloned and produced some antibodies and performed some cell treatments and flow cytometry analyses. Xianshu Cui synthesized the linker peptides. Oligonucleotides were previously synthesized by Aaron Springer. The work in this chapter was supported in part by the NCI training grant: T32 CA067754-22.

REFERENCES

Agard, N.J., Prescher, J.A., Bertozzi, C.R., 2004. A Strain-Promoted [3 + 2] Azide−Alkyne Cycloaddition for Covalent Modification of Biomolecules in Living Systems. J. Am. Chem. Soc. 126, 15046–15047. https://doi.org/10.1021/ja044996f

Agarwal, P., Bertozzi, C.R., 2015. Site-Specific Antibody–Drug Conjugates: The Nexus of Bioorthogonal Chemistry, Protein Engineering, and Drug Development. Bioconjugate Chem. 26, 176–192. https://doi.org/10.1021/bc5004982

Akinc, A., Zumbuehl, A., Goldberg, M., Leshchiner, E.S., Busini, V., Hossain, N., Bacallado, S.A., Nguyen, D.N., Fuller, J., Alvarez, R., Borodovsky, A., Borland, T., Constien, R., de Fougerolles, A., Dorkin, J.R., Narayanannair Jayaprakash, K., Jayaraman, M., John, M., Koteliansky, V., Manoharan, M., Nechev, L., Qin, J., Racie, T., Raitcheva, D., Rajeev, K.G., Sah, D.W.Y., Soutschek, J., Toudjarska, I., Vornlocher, H.-P., Zimmermann, T.S., Langer, R., Anderson, D.G., 2008. A combinatorial library of lipid-like materials for delivery of RNAi therapeutics. Nat Biotechnol 26, 561–569. https://doi.org/10.1038/nbt1402

Arakawa, T., Tsumoto, K., Nagase, K., Ejima, D., 2007. The effects of arginine on protein binding and elution in hydrophobic interaction and ion-exchange chromatography. Protein Expression and Purification 54, 110–116. https://doi.org/10.1016/j.pep.2007.02.010

Balwani, M., Sardh, E., Ventura, P., Peiró, P.A., Rees, D.C., Stölzel, U., Bissell, D.M., Bonkovsky, H.L., Windyga, J., Anderson, K.E., Parker, C., Silver, S.M., Keel, S.B., Wang, J.-D., Stein, P.E., Harper, P., Vassiliou, D., Wang, B., Phillips, J., Ivanova, A., Langendonk, J.G., Kauppinen, R., Minder, E., Horie, Y., Penz, C., Chen, J., Liu, S., Ko, J.J., Sweetser, M.T., Garg, P., Vaishnaw, A., Kim, J.B., Simon, A.R., Gouya, L., 2020. Phase 3 Trial of RNAi Therapeutic Givosiran for Acute Intermittent Porphyria. N Engl J Med 382, 2289–2301. https://doi.org/10.1056/NEJMoa1913147

Caporale, A., Selis, F., Sandomenico, A., Jotti, G.S., Tonon, G., Ruvo, M., 2015. The LQSP tetrapeptide is a new highly efficient substrate of microbial transglutaminase for the site-specific derivatization of peptides and proteins. Biotechnology Journal 10, 154–161. https://doi.org/10.1002/biot.201400466

ClinicalTrials.gov, 2019. TR1801-ADC in Patients with Tumors that Express c-Met (NCT03859752). https://clinicaltrials.gov/ct2/show/study/NCT03859752 (Accessed on 25 Oct. 2021)

de Paula Costa Monteiro, I., Madureira, P., de Vasconscelos, A., Humberto Pozza, D., Andrade de Mello, R., 2015. Targeting HER family in HER2-positive metastatic breast cancer: potential biomarkers and novel targeted therapies. Pharmacogenomics 16, 257–271. https://doi.org/10.2217/pgs.14.133

Doronina, S.O., Toki, B.E., Torgov, M.Y., Mendelsohn, B.A., Cerveny, C.G., Chace, D.F., DeBlanc, R.L., Gearing, R.P., Bovee, T.D., Siegall, C.B., Wahl, A.F., Meyer, D.L., Senter, P.D., 2003. Development of potent monoclonal antibody auristatin conjugates for cancer therapy. Nature Biotechnol 25, 778-784. https://doi.org/10.1038/nbt832

Dorywalska, M., Dushin, R., Moine, L., Farias, S.E., Zhou, D., Navaratnam, T., Lui, V., Hasa-Moreno, A., Casas, M.G., Tran, T.-T., Delaria, K., Liu, S.-H., Foletti, D., O'Donnell, C.J., Pons, J., Shelton, D.L., Rajpal, A., Strop, P., 2016. Molecular Basis of Valine-Citrulline-PABC Linker Instability in Site-Specific ADCs and Its Mitigation by Linker Design. Mol Cancer Ther 15, 958–970. https://doi.org/10.1158/1535-7163.MCT-15-1004

Dowdy, S.F., 2017. Overcoming cellular barriers for RNA therapeutics. Nat Biotechnol 35, 222–229. https://doi.org/10.1038/nbt.3802

Farias, S.E., Strop, P., Delaria, K., Galindo Casas, M., Dorywalska, M., Shelton, D.L., Pons, J., Rajpal, A., 2014. Mass Spectrometric Characterization of Transglutaminase Based Site-Specific Antibody–Drug Conjugates. Bioconjugate Chem. 25, 240–250. https://doi.org/10.1021/bc4003794

Francisco, J.A., Cerveny, C.G., Meyer, D.L., Mixan, B.J., Klussman, K., Chace, D.F., Rejniak, S.X., Gordon, K.A., DeBlanc, R., Toki, B.E., Law, C.-L., Doronina, S.O., Siegall, C.B., Senter, P.D., Wahl, A.F., 2003. cAC10-vcMMAE, an anti-CD30–monomethyl auristatin E conjugate with potent and selective antitumor activity. Blood 102, 1458–1465. https://doi.org/10.1182/blood-2003-01-0039

Gymnopoulos, M., Betancourt, O., Blot, V., Fujita, R., Galvan, D., Lieuw, V., Nguyen, S., Snedden, J., Stewart, C., Villicana, J., Wojciak, J., Wong, E., Pardo, R., Patel, N., D'Hooge, F., Vijayakrishnan, B., Barry, C., Hartley, J.A., Howard, P.W., Newman, R., Coronella, J., 2020. TR1801-ADC: a highly potent cMet antibody–drug conjugate with high activity in patient-derived xenograft models of solid tumors. Mol Oncol 14, 54–68. https://doi.org/10.1002/1878-0261.12600

Hamann, P.R., Hinman, L.M., Hollander, I., Beyer, C.F., Lindh, D., Holcomb, R., Hallett, W., Tsou, H.-R., Upeslacis, J., Shochat, D., Mountain, A., Flowers, D.A., Bernstein, I., 2002. Gemtuzumab Ozogamicin, A Potent and Selective Anti-CD33 Antibody−Calicheamicin Conjugate for Treatment of Acute Myeloid Leukemia. Bioconjugate Chem. 13, 47–58. https://doi.org/10.1021/bc010021y

Hamblett, K.J., Senter, P.D., Chace, D.F., Sun, M.M.C., Lenox, J., Cerveny, C.G., Kissler, K.M., Bernhardt, S.X., Kopcha, A.K., Zabinski, R.F., Meyer, D.L., Francisco, J.A., 2004. Effects of Drug Loading on the Antitumor Activity of a Monoclonal Antibody Drug Conjugate. Clin Cancer Res 10, 7063–7070. https://doi.org/10.1158/1078-0432.CCR-04-0789

Huggins, I.J., Medina, C.A., Springer, A.D., van den Berg, A., Jadhav, S., Cui, X., Dowdy, S.F., 2019. Site Selective Antibody-Oligonucleotide Conjugation via Microbial Transglutaminase. Molecules 24, 3287. https://doi.org/10.3390/molecules24183287

Ishida, T., Ichihara, M., Wang, X., Yamamoto, K., Kimura, J., Majima, E., Kiwada, H., 2006. Injection of PEGylated liposomes in rats elicits PEG-specific IgM, which is responsible for rapid elimination of a second dose of PEGylated liposomes. Journal of Controlled Release 112, 15–25. https://doi.org/10.1016/j.jconrel.2006.01.005

Jeger, S., Zimmermann, K., Blanc, A., Grünberg, J., Honer, M., Hunziker, P., Struthers, H., Schibli, R., 2010. Site-Specific and Stoichiometric Modification of Antibodies by Bacterial Transglutaminase. Angewandte Chemie International Edition 49, 9995–9997. https://doi.org/10.1002/anie.201004243

Juliano, R.L., 2016. The delivery of therapeutic oligonucleotides. Nucleic Acids Res 44, 6518–6548. https://doi.org/10.1093/nar/gkw236

Junutula, J.R., Raab, H., Clark, S., Bhakta, S., Leipold, D.D., Weir, S., Chen, Y., Simpson, M., Tsai, S.P., Dennis, M.S., Lu, Y., Meng, Y.G., Yang, J., Lee, C.C., Duenas, E., Gorrell, J., Katta, V., Kim, A., Flagella, K., Venook, R., Ross, S., Spencer, S.D., Wong, W.L., Lowman, B., Vandlen, R., Sliwkowski, M.X., Scheller, R.H., Polakis, P., Mallet, W., 2008. Site-specific conjugation of a cytotoxic drug to an antibody improves the therapeutic index. Nature Biotechnology 33, 925-932. https://doi.org/10.1038/nbt.1480

Khvorova, A., Watts, J.K., 2017. The chemical evolution of oligonucleotide therapies of clinical utility. Nat Biotechnol 35, 238–248. https://doi.org/10.1038/nbt.3765

Kosmas, C., Muñoz Estrella, A., Sourlas, A., Silverio, D., Hilario, E., Montan, P., Guzman, E., 2018. Inclisiran: A New Promising Agent in the Management of Hypercholesterolemia. Diseases 6, 63. https://doi.org/10.3390/diseases6030063

Krop, I.E., Beeram, M., Modi, S., Jones, S.F., Holden, S.N., Yu, W., Girish, S., Tibbitts, J., Yi, J.-H., Sliwkowski, M.X., Jacobson, F., Lutzker, S.G., Burris, H.A., 2010. Phase I Study of

Trastuzumab-DM1, an HER2 Antibody-Drug Conjugate, Given Every 3 Weeks to Patients With HER2-Positive Metastatic Breast Cancer. JCO 28, 2698–2704. https://doi.org/10.1200/JCO.2009.26.2071

Lewis Phillips, G.D., Li, G., Dugger, D.L., Crocker, L.M., Parsons, K.L., Mai, E., Blättler, W.A., Lambert, J.M., Chari, R.V.J., Lutz, R.J., Wong, W.L.T., Jacobson, F.S., Koeppen, H., Schwall, R.H., Kenkare-Mitra, S.R., Spencer, S.D., Sliwkowski, M.X., 2008. Targeting HER2-Positive Breast Cancer with Trastuzumab-DM1, an Antibody–Cytotoxic Drug Conjugate. Cancer Res 68, 9280–9290.

Li, F., Sutherland, M.K., Yu, C., Walter, R.B., Westendorf, L., Valliere-Douglass, J., Pan, L., Cronkite, A., Sussman, D., Klussman, K., Ulrich, M., Anderson, M.E., Stone, I.J., Zeng, W., Jonas, M., Lewis, T.S., Goswami, M., Wang, S.A., Senter, P.D., Law, C.-L., Feldman, E.J., Benjamin, D.R., 2018. Characterization of SGN-CD123A, A Potent CD123-Directed Antibody–Drug Conjugate for Acute Myeloid Leukemia. Mol Cancer Ther 17, 554–564. https://doi.org/10.1158/1535-7163.MCT-17-0742

Malik, P., Phipps, C., Edginton, A., Blay, J., 2017. Pharmacokinetic Considerations for Antibody-Drug Conjugates against Cancer. Pharm Res 34, 2579–2595. https://doi.org/10.1007/s11095-017-2259-3

Nabeshima, Yoko, Abe, C., Kawauchi, T., Hiroi, T., Uto, Y., Nabeshima, Yo-ichi, 2020. Simple method for large-scale production of macrophage activating factor GcMAF. Sci Rep 10, 19122. https://doi.org/10.1038/s41598-020-75571-y

Nair, J.K., Willoughby, J.L.S., Chan, A., Charisse, K., Alam, Md.R., Wang, Q., Hoekstra, M., Kandasamy, P., Kel'in, A.V., Milstein, S., Taneja, N., O'Shea, J., Shaikh, S., Zhang, L., van der Sluis, R.J., Jung, M.E., Akinc, A., Hutabarat, R., Kuchimanchi, S., Fitzgerald, K., Zimmermann, T., van Berkel, T.J.C., Maier, M.A., Rajeev, K.G., Manoharan, M., 2014. Multivalent *N* -Acetylgalactosamine-Conjugated siRNA Localizes in Hepatocytes and Elicits Robust RNAi-Mediated Gene Silencing. J. Am. Chem. Soc. 136, 16958–16961. https://doi.org/10.1021/ja505986a

Ora, M., Peltomäki, M., Oivanen, M., Lönnberg, H., 1998. Metal-Ion-Promoted Cleavage, Isomerization, and Desulfurization of the Diastereomeric Phosphoromonothioate Analogues of Uridylyl(3',5')uridine. J. Org. Chem. 63, 2939–2947. https://doi.org/10.1021/jo972112n

Prakash, T.P., Graham, M.J., Yu, J., Carty, R., Low, A., Chappell, A., Schmidt, K., Zhao, C., Aghajan, M., Murray, H.F., Riney, S., Booten, S.L., Murray, S.F., Gaus, H., Crosby, J., Lima, W.F., Guo, S., Monia, B.P., Swayze, E.E., Seth, P.P., 2014. Targeted delivery of antisense oligonucleotides to hepatocytes using triantennary *N* -acetyl galactosamine improves potency 10-fold in mice. Nucleic Acids Research 42, 8796–8807. https://doi.org/10.1093/nar/gku531

Schroeder, A., Levins, C.G., Cortez, C., Langer, R., Anderson, D.G., 2010. Lipid-based nanotherapeutics for siRNA delivery: Symposium: Lipid-based siRNA nanotherapeutics. Journal of Internal Medicine 267, 9–21. https://doi.org/10.1111/j.1365-2796.2009.02189.x

Seguro, K., Nio, N., Motoki, M., Pearce, J., 1996. Some Characteristics of a Microbial Protein Cross-Linking Enzyme: Transglutaminase. Macromolecular Interactions in Food Technology, Chapter 21, ACS Symposium Series. American Chemical Society, Washington, DC. https://doi.org/10.1021/bk-1996-0650

Senter, P.D., Sievers, E.L., 2012. The discovery and development of brentuximab vedotin for use in relapsed Hodgkin lymphoma and systemic anaplastic large cell lymphoma. Nat Biotechnol 30, 631–637. https://doi.org/10.1038/nbt.2289

Setten, R.L., Rossi, J.J., Han, S., 2019. The current state and future directions of RNAi-based therapeutics. Nat Rev Drug Discov 18, 421–446. https://doi.org/10.1038/s41573-019-0017-4

Siegmund, V., Schmelz, S., Dickgiesser, S., Beck, J., Ebenig, A., Fittler, H., Frauendorf, H., Piater, B., Betz, U.A.K., Avrutina, O., Scrima, A., Fuchsbauer, H., Kolmar, H., 2015. Locked by Design: A Conformationally Constrained Transglutaminase Tag Enables Efficient Site-Specific Conjugation. Angew. Chem. Int. Ed. 54, 13420–13424. https://doi.org/10.1002/anie.201504851

Springer, A.D., Dowdy, S.F., 2018. GalNAc-siRNA Conjugates: Leading the Way for Delivery of RNAi Therapeutics. Nucleic Acid Therapeutics 28, 109–118. https://doi.org/10.1089/nat.2018.0736

Strop, P., Liu, S.-H., Dorywalska, M., Delaria, K., Dushin, R.G., Tran, T.-T., Ho, W.-H., Farias, S., Casas, M.G., Abdiche, Y., Zhou, D., Chandrasekaran, R., Samain, C., Loo, C., Rossi, A., Rickert, M., Krimm, S., Wong, T., Chin, S.M., Yu, J., Dilley, J., Chaparro-Riggers, J., Filzen, G.F., O'Donnell, C.J., Wang, F., Myers, J.S., Pons, J., Shelton, D.L., Rajpal, A., 2013. Location Matters: Site of Conjugation Modulates Stability and Pharmacokinetics of Antibody Drug Conjugates. Chemistry & Biology 20, 161–167. https://doi.org/10.1016/j.chembiol.2013.01.010

Strop, P., 2014. Versatility of Microbial Transglutaminase. Bioconjugate Chem. 25, 855–862. https://doi.org/10.1021/bc500099v

Takahashi, M., Contu, V.R., Kabuta, C., Hase, K., Fujiwara, Y., Wada, K., Kabuta, T., 2017. SIDT2 mediates gymnosis, the uptake of naked single-stranded oligonucleotides into living cells. RNA Biology 14, 1534–1543. https://doi.org/10.1080/15476286.2017.1302641

Takazawa, T., Kamiya, N., Ueda, H., Nagamune, T., 2004. Enzymatic labeling of a single chain variable fragment of an antibody with alkaline phosphatase by microbial transglutaminase. Biotechnol. Bioeng. 86, 399–404. https://doi.org/10.1002/bit.20019

ThermoFisher Scientific. ExpiCHO Expression System. https://www.thermofisher.com/us/en/home/life-science/protein-biology/protein-expression/mammalian-protein-expression/transient-mammalian-protein-expression/expicho-expression-system.html (Accessed 25 October 2021)

Whitehead, K.A., Langer, R., Anderson, D.G., 2009. Knocking down barriers: advances in siRNA delivery. Nat Rev Drug Discov 8, 129–138. https://doi.org/10.1038/nrd2742

Younes, A., Bartlett, N.L., Leonard, J.P., Kennedy, D.A., Lynch, C.M., Sievers, E.L., Forero-Torres, A., 2010. Brentuximab Vedotin (SGN-35) for Relapsed CD30-Positive Lymphomas. N Engl J Med 363, 1812–1821. https://doi.org/10.1056/NEJMoa1002965

Zhong, X., Ma, W., Meade, C., Tam, A., Llewellyn, E., Cornell, R., Cote, K., Scarcelli, J., Marshall, J., Tzvetkova, B., Figueroa, B., DiNino, D., Sievers, A., Lee, C., Guo, J., Mahan, E., Francis, C., Lam, K., D'Antona, A., Zollner, R., Zhu, H., Kriz, R., Somers, W., Lin, L., 2019. Transient CHO expression platform for robust antibody production and its enhanced N-glycan sialylation on therapeutic glycoproteins. Biotechnol Prog 35. https://doi.org/10.1002/btpr.2724

CHAPTER FOUR

ASO ARCs & ACUTE MYELOID LEUKEMIA

ASO ARCs & ACUTE MYELOID LEUKEMIA

ABSTRACT

Monoclonal antibodies (mAbs) are attractive vehicles for the delivery of oligonucleotides to extrahepatic targets. With high binding affinities for their target receptors, antibodies have very good bioavailability and are used in numerous antibody-drug conjugate therapies to deliver cytotoxic drugs. Substitution of the cytotoxic drugs with oligonucleotides to obtain an antibody-RNA conjugate has great potential to transform the capacity to combat many diseases with greater efficacy based on specific genetic characteristics of the disease. Cancer is only one of many diseases that oligonucleotide therapeutics could effectively treat.

Unfortunately, monoclonal antibodies cannot induce endosomal escape for its cargo. While mAbs have been shown to have good binding capabilities that lead to endocytosis, the antibody conjugates remain trapped within the cell. Under these conditions, oligonucleotides are unable to reach the cytoplasm. Short interfering RNAs (siRNAs) are far too large and unable to access the cytoplasm on their own. Antisense oligonucleotides (ASOs) have circumstances demonstrated the ability to passively enter cells, albeit to a limited degree, through poorly understood mechanism termed gymnosis.

The previous chapter described our procedure for building ARCs with siRNAs, but ARCs in this form have been ineffective in many circumstances, likely due to the inability to escape the endosome. This chapter instead outlines an ARC with ASOs instead, to determine whether having ASOs instead of siRNAs makes a difference. The ASO ARCs described here were made in the context of acute myeloid leukemia (AML), a prevalent hematological malignancy. These ARCs were tested against a simple GFP reporter system in an AML cell line to analyze the potential gene knockdown with the ASOs. The observed absence of solid GFP knockdown further underscores the need for an endosomal escape strategy.

INTRODUCTION

Antisense Oligonucleotides

Antisense oligonucleotides (ASOs) are short, single stranded oligonucleotides that can mediate gene knockdown in the cell nucleus by recruiting the ubiquitously expressed RNase H1 enzyme to cleave the RNA side of an RNA-DNA duplex when an ASO binds its target mRNA (Roberts et al., 2020). This type of ASO is called a gapmer, characterized by 3 or 5 RNA bases on either side of a 10-base DNA gap (termed a 3-10-3 or 5-10-5 gapmer). Other types of ASOs include splice switching ASOs and steric blocking ASOs (see Chapter One), but gapmer ASOs have been of particular interest in our lab for their potential to knock down target gene expression. The pathway for a gapmer ASO can be divided into three general stages. First, in the prehybridization stage, ASOs must navigate through the cell and achieve a sufficiently high concentration at the locations where their target mRNAs are found (Crooke, 2017). During this stage, there are at least several dozen intracellular proteins that can bind to the phosphorothioate (PS) backbone of an ASO, including some with nucleic-acid binding domains or other chaperone proteins that depending on their concentration, can attenuate or enhance ASO potency (Wang et al., 2016; Vickers and Crooke, 2014). The second stage, hybridization, occurs when an ASO finds and binds to its target RNA sequence, ASO potency and specificity depends largely on RNA structure, but the proteins involved in facilitating this event remain largely unknown (Crooke, 2017; Lima et al., 2014). RNase H enzymes 1 and 2 cleave only the RNA part of an DNA-RNA duplex. Even though RNase H2 is found most abundantly in cells, only RNase H1 participates in gapmer ASO-mediated gene silencing most likely because RNase H1 resides in both the nucleus and cytoplasm while RNase H2 is usually found strongly bound to chromatin (Wu et al., 2004; Lima et al., 2004; Lima et al., 2007). RNase H1 is the only nuclease that carries out the antisense-mediated RNA cleavage (Lima et al., 2016).

There are eight ASOs that have been FDA approved to treat numerous conditions such as spinal muscular atrophy (nusinersen, a splice switching ASO), hypercholesteremia or cardiovascular disease (mipomersen, a gapmer ASO), transthyretin amyloidosis (inotersen, another gapmer ASO), and others (Smith and Zain, 2018; Benson et al., 2018). Refer to Chapter One for more details. The pharmacological benefits of ASOs, especially RNase H dependent gapmers, are a result of decades of extensive research. The PS modification on its own has greatly enhanced the clinical efficacy of ASOs by enhancing their stability and ability to enter cells and 2'-OMe and 2'-MOE modifications have further enhanced their pharmacokinetic profiles (Agrawal et al, 1991; Liang et al., 2016; Crooke et al., 2017a). But ASOs are sometimes locally administered, such as with nusinersen that is intrathecally administered after which the ASO will spread into the cerebrospinal fluid and brain parenchyma. Systemic administration may otherwise be more inefficient in the delivery of ASOs to extrahepatic targets and may not generate a sufficiently beneficial therapeutic response. That said, the clinically approved splice switching ASOs targeting Duchenne muscular dystrophy abnormalities are intravenously administered and can still accomplish their function.

All macromolecular therapeutics enter cells via endocytosis, where they mostly remain trapped until their degradation or transport back into the extracellular space. Unlike siRNAs however, PS ASOs can gradually cross the cell membrane and escape the endosome by a poorly understood mechanism called gymnosis without the aid of transfection reagents or electroporation (Dowdy, 2017). While gymnosis largely remains a black box, there are several important observations about this process. Firstly, rapidly expanding cells including cancer cells take up ASOs more rapidly and efficiently (Iversen et al., 1992). The uptake process begins when a PS ASO adsorbs to the cell surface, an event that can be reduced with competition of other PS ASOs, thus reducing the desired antisense activity. After adsorption, uptake can occur by various pathways, but the pathways that lead to effective antisense activity include surface protein interactions that lead to uptake (including integrins and scavenger receptors) or receptor

mediated endocytosis (caveolin- and/or clathrin-dependent) (Crooke et al., 2017b). PS ASOs that are taken up by gymnosis are active in only a limited number of cells, suggesting that gymnosis in many other cell lines occurs via non-productive pathways and likely depends on the surface protein composition of a cell (Juliano et al., 2013; Juliano et al., 2012; Crooke et al., 2017b). But much more remains a mystery at this time, from the identity of the specific factors that promote productive pathway uptake versus non-productive, the mechanism by which ASOs escape the endosome, and other proteins involved in helping the ASOs reach their RNA targets. In the absence of endosomal escape enhancers, ASOs on their own or as part of a larger conjugate may be more promising than siRNAs for gene silencing.

Monoclonal Antibody Conjugates

Significant development of monoclonal antibody (mAb) therapeutics has brought exciting successes in delivering cytotoxic drugs to target cells (Agarwal and Bertozzi, 2014; de Paula Costa Monteiro et al., 2015; Younes et al., 2010) that mAbs are now highly attractive delivery vehicles. Development of conjugation chemistries have allowed for specific placement of conjugation handles, linkers, and therapeutic cargo. The linkers have been extensively developed and carefully crafted to be the right length, have good stability, contain the proper chemical groups for the correct conjugation chemistries, and even inherent cleavable properties under desired conditions (Lu et al., 2016). A variety of linkers have been used in our lab when building antibody-RNA conjugates (ARCs) and reaction conditions to incorporate them into ARCs have been optimized extensively.

There are numerous considerations and obstacles that apply to mAbs and mAb-conjugate therapeutic approaches. Antibody internalization rates can be highly variable, significantly affecting a mAb conjugate's efficacy, and not all receptors internalize upon an mAb binding. For example, even with high CD21 receptor expression, anti-CD21 mAbs fail to internalize when they bind due to the formation of a complex with CD19 on the B cell surface

that inhibits uptake, while anti-CD19 mAbs can only internalize in the absence of CD21 (Ingle et al., 2008). Rate of internalization also impacts an mAb or mAb-conjugate's tumor penetration and in a tumor spheroid experiment it was observed that the antibodies with faster internalization rate reached deeper inside the spheroid (Ackerman et al., 2008). Binding affinity can also affect mAb efficacy. Trastuzumab and C6.5-IgG are two mAbs that bind the HER2 receptor at different locations and thus do not compete for binding (Reddy et al., 2011). It was observed that trastuzumab with a higher binding affinity (KD = 0.1 x 10^{-10} M) penetrate SK-OV-3 tumor xenografts 20% less deeply than C6.5-IgG mAbs (KD 2.7 x 10^{-8} M), suggesting that having a faster off-rate grants mAbs better access to the interior of a tumor (Rudnick et al., 2011). Receptor-mediated endocytosis occurs by a clathrin-dependent mechanism and is the predominant uptake route for mAb conjugates. After entering the cell, antibodies will go through the endosomal pathway and will either be recycled back to the cell membrane or be degraded in the lysosome (Ritchie et al., 2013). mAbs do not reach the cytoplasm. Endosomal escape arguably remains the biggest problem to overcome for mAb conjugates.

The significance of the inability of mAbs or mAb conjugates to escape the endosome is made evident by the lackluster results of other ARCs or the very narrow conditions under which other ARCs have shown some level of efficacy. Genentech's THIOMAB ARCs relied on engineered cysteines, maleimide-modified siRNA, and either a reducible N-succinimidyl-4-(2-pyridyldithio)butyrate (SPDB) linker or a non-reducible succinimidyl-4-[N-maleimidomethyl]cyclohexane-1-carboxylate (SMCC) linker to produce DAR 1 and DAR 2 (50-50 split) conjugates (Cuellar et al., 2014). Various antibodies were incorporated into the THIOMAB ARC platform to target receptors such as TENB2, HER2, and Mesothelin, but in all cases exhibited poor knockdown at unacceptably high doses. ARCs were found to accumulate in the lysosomes within 25 hr of cell treatment and only a very small fraction of siRNAs ever reached the cytoplasm through an unknown mechanism, leading the authors of this study to

conclude that their ARCs were delivered to and mostly remained trapped in the endosomal compartments (Cuellar et al., 2014).

Another example is the Anti-CD33-MXD3-ASO conjugate that aimed to target the MYC-associated factor X dimerization protein 3, prevalent in acute lymphoblastic leukemia (ALL) (Satake et al., 2016). This ASO ARC used 2'-MOE modified PS ASOs with nonspecific NHS-conjugation chemistry onto the surface amines of the anti-CD22 mAb. Unfortunately, the authors failed to properly characterize the ARCs that they built, so even though they report reasonable knockdown of their target gene in ALL cells (Satake et al., 2016), albeit at very high treatment concentrations, they leave unconfirmed whether the mechanism of knockdown occurred through actual antisense activity instead of hydrophobic aggregation of protein conjugates and subsequent cytotoxicity that can occur with protein conjugates that rely on nonspecific conjugation chemistries (Senter and Sievers, 2012).

A different example of an antibody-ASO conjugate is against the CD44 and EphA2 receptors on glioblastoma stem cells with the aim of knocking down DRR/FAM107A, an oncogenic driver that promotes an aggressive form of glioblastoma multiforme (Arnold et al., 2018). This ARC also relied on NHS-activated ester conjugation for nonspecific crosslinking of the ASO onto the mAbs' surface lysine residues; binding and internalization was confirmed by flow cytometry. These ARCs localized to the lysosome primarily and even though there was only limited DRR knockdown reported with the anti-CD44 but not the anti-EphA2 conjugate, this study (Arnold et al., 2018) still shows the advantage that gapmer ASOs could have over siRNAs in the absence of an endosomal escape-capable conjugate.

A successful ARC should meet several criteria in order to have a reasonable chance at therapeutic efficacy. First, the target surface receptor must be abundantly expressed on the cell type of interest. Receptors with low expression will not provide many avenues for an ARC to bind and internalize, whereas a higher receptor density will allow more shots on goal for the ARC. Second, the target receptor must be exclusive to or overexpressed in the target cell type

relative to the surrounding and distant cell types in order to reduce off-target effects and/or the sequestration of the ARC non-productively, away from its intended target. Third, the target receptor should at most undergo minimal secretion only, as secreted receptors will competitively bind the ARC in circulation and minimize the latter's therapeutic potential. An ARC must have high endocytosis rates by targeting a cell surface receptor with an mAb that has shown efficient internalization rate to allow sufficient ARC to enter the target cells. Lastly, and perhaps the hardest aspect to verify or control, successful gene knockdown will ultimately depend on the ARC being processed through the appropriate intracellular trafficking route for the oligonucleotide cargo to be able to access the cytoplasm and nucleus.

Cancer is generally a disease ripe with potential genetic candidates for an ARC to target. Solid tumors are generally harder for antibody therapeutics to target because of the tumor microenvironment and the physical tumor itself impedes proper mAb penetration, depending on the surrounding neovascularization. Moreover, solid tumors can induce the hypercoagulation of blood, leading to cancer stroma formation and an inhibition of the enhanced permeability retention (EPR) effect (Matsumura, 2021). Tissue factor (TF) induces coagulation and is expressed on many human cancer cells. As cancer grows it invades surrounding tissues, it destroys adjacent healthy and malignant vessels and leads to micro-hemorrhaging, fibrin clot formation, and collagen formation, all barriers to mAbs (Stein et al., 2006; Saito et al., 2011). Targeting hematological malignancies are theoretically easier because the target tumor cells are already out in the blood vessels and therefore more accessible to mAb therapeutics. For this reason, my work turned to the building of an ASO ARC against acute myeloid leukemia.

Acute Myeloid Leukemia

Acute myeloid leukemia (AML) is a blood cancer that originates in the bone marrow, specifically arising from cells either at the myeloid progenitor or myeloblast stage of differentiation (**Figure 4.1**). When cells at these stages become malignant, they become

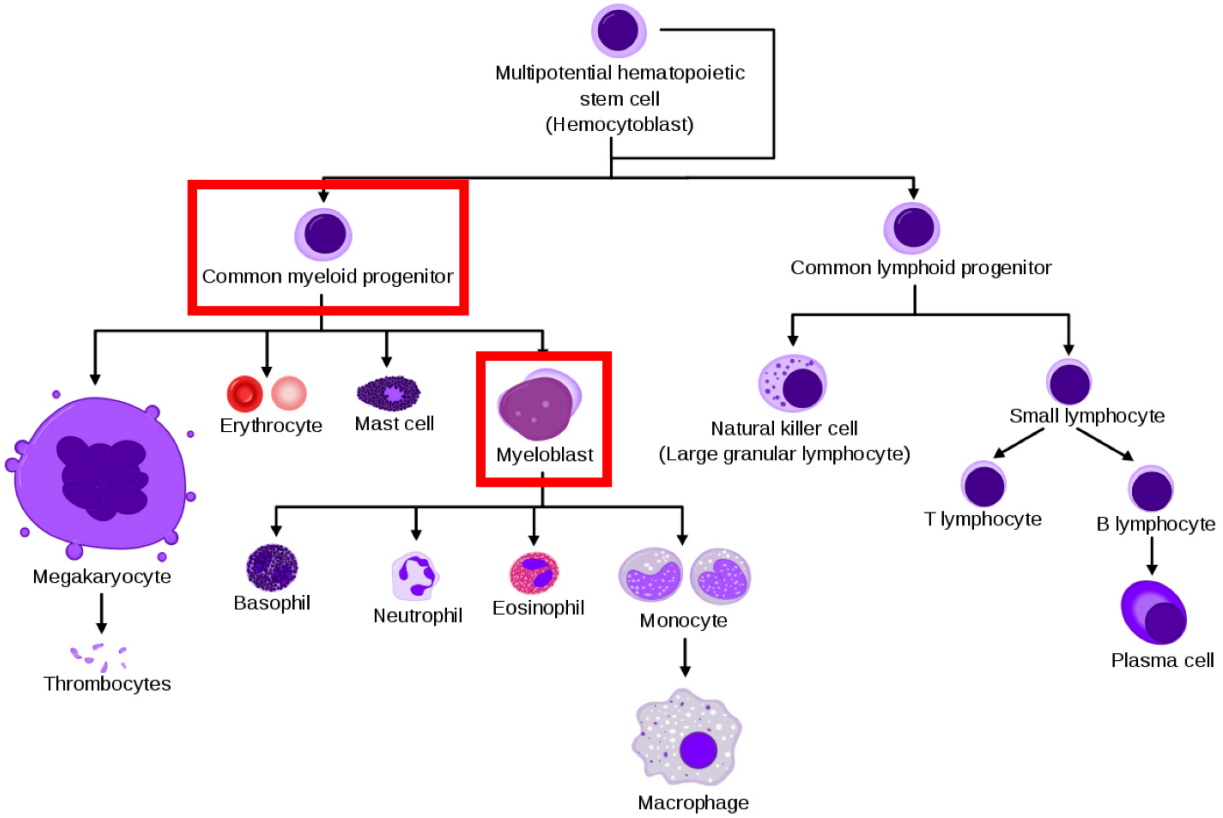

Figure 4.1. Origin of Acute Myeloid Leukemia
Acute myeloid leukemia (AML) arises when any of numerous key mutations or any of the commonly observed chromosomal translocations occurs at the myeloid progenitor or myeloblast stage of hematopoietic stem cell differentiation (marked by red boxes) to initiate the malignancy that is characterized by abnormal leukocyte increase and decreased red blood cell counts.

Adapted from Juzenas et al., 2017.

arrested in an immature state and continue to divide ceaselessly. Though these blasts begin in the bone marrow, they quickly move into the blood and may also later spread into the lymph nodes, liver, and other organs (American Cancer Society, 2018). AML is characterized by an increased leukocyte count from the excessively proliferating immature white blood cells and a decreased red blood cell count that occurs because the AML blasts crowd out other blood cell types in the bone marrow (Longo, 2017).

AML is one of the most prevalent hematological malignancies, accounting for about a third of all new leukemia diagnoses, according to the American Cancer Association. AML can arise in children, young adults, and older patients, with an average age of diagnosis of about 67 years of age and an overall poor 5-year survival rate of about 25% (Kell, 2016). The current standard of care for AML is chemotherapy, which can achieve initial remission rates of ~80%, but in older patients, there is a higher relapse frequency of >80% of treated patients (De Kouchkovsky and Abdul-Hay, 2016; Burnett et al., 2011; Hourigan et al., 2017). The most common treatment is chemotherapy wherein patients are treated by a “3+7” schedule as an induction therapy with cytarabine for seven days in conjunction with an anthracycline (often daunorubicin) for three days (Ohtake et al., 2011; Graubert and Stone, 2014). Due to high relapse rates, disease-free survival (DFS) remains at 40% in young adults and <10% in adults over 60 (Kell, 2016; Graubert and Stone, 2014).

Next-generation targeted small molecule drugs are incapable of adapting to cancer cells’ resistance-conferring mutations and can drive drug resistance and aggressive relapse (Wilson et al., 2012). While immunotherapy-based approaches to treat AML, such as chimeric antigen T-cell (CAR-T) therapy as well as ADCs have shown promise in treating AML, these approaches come with significant cytotoxic side effects that result in nonspecific killing of normal cells (Laszlo et al., 2014; Kenderian et al., 2015). There remains a great need to develop a precision therapeutic that can specifically target and kill AML cells, based on their genetic translocations and mutations, while sparing normal cells.

Chromosomal translocations are frequent in AML and often result in the formation of fusion oncogenes that drive leukemia cell growth and survival (Krivtsov and Armstrong, 2007; Ohtake et al., 2011). The mixed lineage leukemia (*MLL*) gene on chromosome 11q23 is frequently altered by chromosomal translocations found in AML (Krivtsov and Armstrong, 2007; Meyer et al., 2006; Huret et al., 2001). The MLL gene encodes a H3 lysine 4 (H3K4) histone methyltransferase that positively regulates gene expression, including Hox genes (Meyer et al., 2006). AML patients with an MLL-AF9 fusion t(9;11) translocation have a particularly aggressive disease and poor clinical outcome (Ohtake et al., 2011; Stavropoulou et al., 2016). In AML, the MLL gene has been shown to form translocations with over 60 different genes resulting in MLL-fusion oncogenes that are thought to drive clonal growth and survival (Meyer et al., 2006; Welch et al., 2012). Beyond chromosomal translocations, there are numerous common oncogenic mutations in genes such as NPM1, a phosphoprotein in the p53 pathway; FLT3, a tyrosine kinase receptor involved in hematopoiesis; CEBPA, a transcription factor involved in blood cell differentiation; DNMT3A, a DNA methyltransferase; and IDH1, an isocitrate dehydrogenase enzyme (Graubert et al., 2014; De Kouchkovsky and Abdul-Hay, 2016; Burnett et al., 2011; Klco et al., 2014). It remains unclear if primary and recurrent AMLs are solely dependent on expression of the MLL-fusion driver oncogene or if additional de novo oncogenic mutations are acquired after therapeutic intervention that confers further growth and survival. It has been suggested that loss of MLL-AF9 results in AML tumor cell differentiation and cell death (Fleischmann et al., 2014; Kawagoe et al., 2001), so there is merit to targeting MLL-AF9.

AML cancer cells express relatively high levels of CD33 on their cell surface (Meyer et al., 2006; Fleischman et al., 2014), making CD33 a promising target for ARC targeting against AML cells. Gemtuzumab ozogamicin (GO) is an ADC that was FDA approved in 2000, consisting of an anti-CD33 mAb conjugated with a hydrazone linker to calicheamicin nonspecifically through the use of NHS-ester chemical crosslinking (van der Velden et al., 2001; Hamann et al., 2002). GO binds the CD33 receptor on AML blasts which triggers its uptake into

the cell, followed by hydrolytic release of calicheamicin within the endosomal pathway. Its greatest efficacy is against higher CD33-expressing AML blasts (Jager et al., 2011). CD33 internalization is controlled by cytoplasmic immunoreceptor tyrosine-based inhibitory motifs (ITIMs). Point mutations to these ITIMs significantly reduces the therapeutic efficacy of GO, as does low CD33 expression (defined as <80% of AML blast cells with positive CD33 staining) (Walter et al., 2005). Toxicity issues and an absence of concrete overall survival improvements led to GO being pulled from the market, but adjustments to administer as fractionated doses to prevent excessive toxicity allowed its reintroduction into the clinic more recently. GO was FDA approved for the second time in September 2017 as a therapy in conjunction with daunorubicin and cytarabine as well as on its own for adult patients with a newly diagnosed AML that is confirmed to be CD33-positive. When combined with chemotherapy, GO was shown to result in event-free survival of 13.6 months (compared to 8.8 months for the chemotherapy on its own) while GO alone resulted in median overall survival of almost 5 months, compared to 3.6 months without (Jen et al., 2018).

An ARC that targets an ASO to CD33 positive cells will not only have the specificity of the against the target receptor, but also against the target sequence. PS ASOs have the potential to escape the endosome without assistance. This chapter describes an ASO ARC designed to target the GFP sequence for use in a THP-1 cell line that was modified to endogenously express the destabilized GFP gene. The goal of this simplified model is to have an easy reporter system to quickly gauge ARC efficacy before moving on to the targets of greater interest, namely the MLL-AF9 fusion oncogene.

RESULTS & DISCUSSION

Monoclonal Antibodies

As described in the previous chapter, the amino acid sequence for FDA-approved gemtuzumab, an anti-CD33 mAb, was obtained from patent literature. The amino acid sequences for the heavy chain (HC) and light chain (LC) were cloned into kappa or lambda LCs and IgG1 HCs. Due to the increased size of the HCs, an increased ratio (4-fold excess) of the HC plasmid was co-transfected with the LCs. MTG conjugation handles were also cloned into the C-terminus of HCs to allow for MTG-mediated site-specific conjugation of the ASOs. The ExpiCHO expression system was used to produce full-length anti-CD33 mAbs, following manufacturer's recommendations of 30 mL culture sizes in polycarbonate vent cap flasks and other transfection and culture maintenance guidelines. After two weeks, the cell supernatant was collected and filtered through 0.45 µm and 0.22 µm syringe filters followed by Protein A purification to isolate the mAbs (**Figure 4.2**). The mAbs of interest came out in elution fractions #2 and #3 and those were pooled together. Next, mAbs were buffer exchanged and cleaned up further via size exclusion chromatography column (SEC 650) on an FPLC into 1X PBS. The fractions for the mAb peak were collected, pooled, and re-concentrated by spin filtration with either Amicon spin filters (30K MWCO) or GE Healthcare Vivaspin 6 spin filters (30K MWCO). Final concentration of mAb preps were determined by either BCA protein assay (ThermoFisher) or by spectrophotometer quantification based on the extinction coefficient estimates.

Lys-PEG6-Hynic Linker

The linker used for this ASO ARC was synthesized in our lab and consists of a lysine residue, a PEG_6 spacer, and HyNic (hydrazinonicotinic acid) for a HyNic conjugation. This linker will be referred to as the KP1H linker from here on out. The conjugation reaction between a benzaldehyde group and hydrazinonicotinic acid will form a stable hydrazone linkage. The

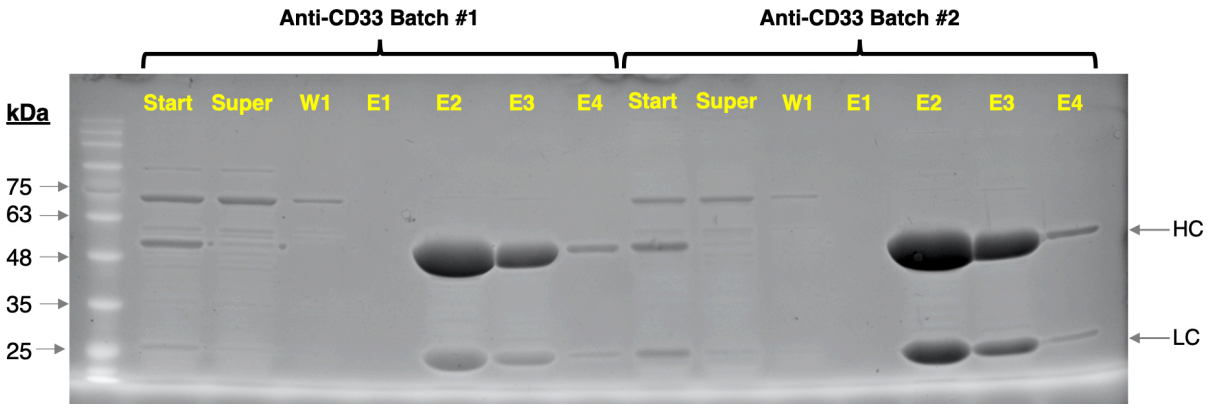

Figure 4.2. Protein A Purification of anti-CD33 mAbs
Protein A resin binds to the Fc region of mAbs and is used to isolate mAbs. The 10% SDS PAGE gel shown outlines two anti-CD33 mAb preps and the typical fractions that are collected and tested as quality control. Start refers to the starting material before filtration; Super refers to the filtered cell supernatant; W1 refers to the first wash of the Protein A after mAbs have been bound. A second wash and sometimes third wash is often done but not shown in this gel. E1-E4 refers to 4 elution fractions for each mAb prep; of note, most of the mAb yield is eluted in the 2nd and 3rd fractions. These two fractions are pooled together and further purified via size exclusion chromatography to buffer exchange into 1X PBS. Molecular weight bands shown are in kilodaltons (kDa). HC, heavy chain; LC, light chain.

lysine residue contains the primary amine needed for the MTG conjugation while the HyNic group is the conjugation point to the ASOs. To determine the optimal conjugation ratio between the anti-CD33 mAb and the KP1H linker peptide, test conjugations were run with the standard MTG conjugation reaction conditions: 3 U/mL of MTGase enzyme, room temperature incubation for 1 hour, 1X final MTGase reaction buffer (150 mM NaCl, 25 mM Tris-HCl, pH 8), mAb concentration within reaction of ~6 μM, and excess KP1H linker peptide, with molar ratios relative to mAb of 50:1, 25:1, 10:1, 5:1 (**Figure 4.3**). The MTG reaction mixture was mixed well by pipetting. After the 1-hour incubation, the test conjugations were run on a 10% SDS-PAGE gel (120V 24 minutes followed by 180V 36 minutes) followed by UV protein staining and imaging on a UV transilluminator.

The MTG conjugation between KP1H and anti-CD33 conjugation handles was surprisingly efficient, showing >90% efficiency at the lowest ratio of 5:1 (KP1H:mAb conjugation sites). The MTG conjugation resulted in DAR 2 mAb-peptide conjugates. This ratio was used for future MTG conjugations between this mAb and linker peptide to streamline the ARC building procedure with ASOs.

ARC Building Process

The anti-CD33 mAb that was engineered in the Dowdy lab contains a C-terminal heavy chain MTG conjugation handle to allow for site specific conjugation. There are two conjugation reactions required to build a basic ASO ARC (**Figure 4.4**). The general workflow for preparing an ASO ARC is as follows. The first reaction is the HyNic conjugation reaction between the KP1H peptide and the ASO. The excess linker peptide is purified away by a size exclusion chromatography column called the Zeba 7k MWCO column (ThermoFisher) which is a miniature version of the larger SEC 650 FPLC column. The Zeba 7k SEC column efficiently removed the excess KP1H peptide from the first reaction. This step can and has alternatively been performed by the FPLC size exclusion (SEC 650) column too.

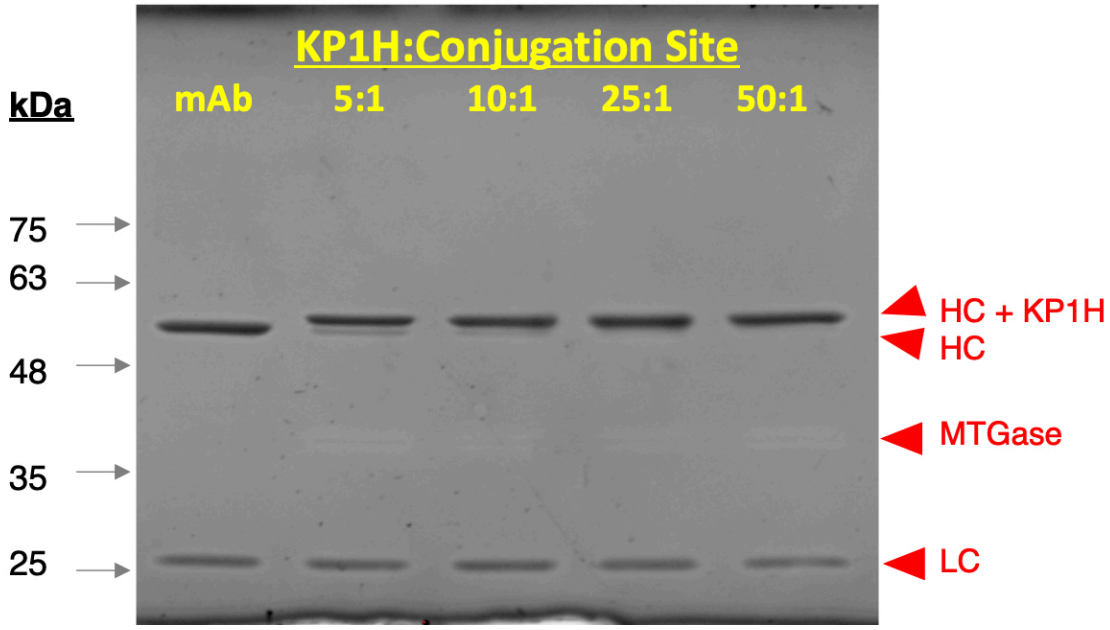

Figure 4.3. Test MTG Conjugations for KP1H Linker Peptide
MTG test conjugations between KP1H linker peptide and anti-CD33 mAb proceeded with great efficiency (>90%) at the lowest ratio tested. Molecular weight markers are in kilodaltons (kDa). Abbreviations: KP1H, Lys-PEG_6-HyNic linker peptide; MTGase, microbial transglutaminase enzyme; HC, heavy chain; LC, light chain.

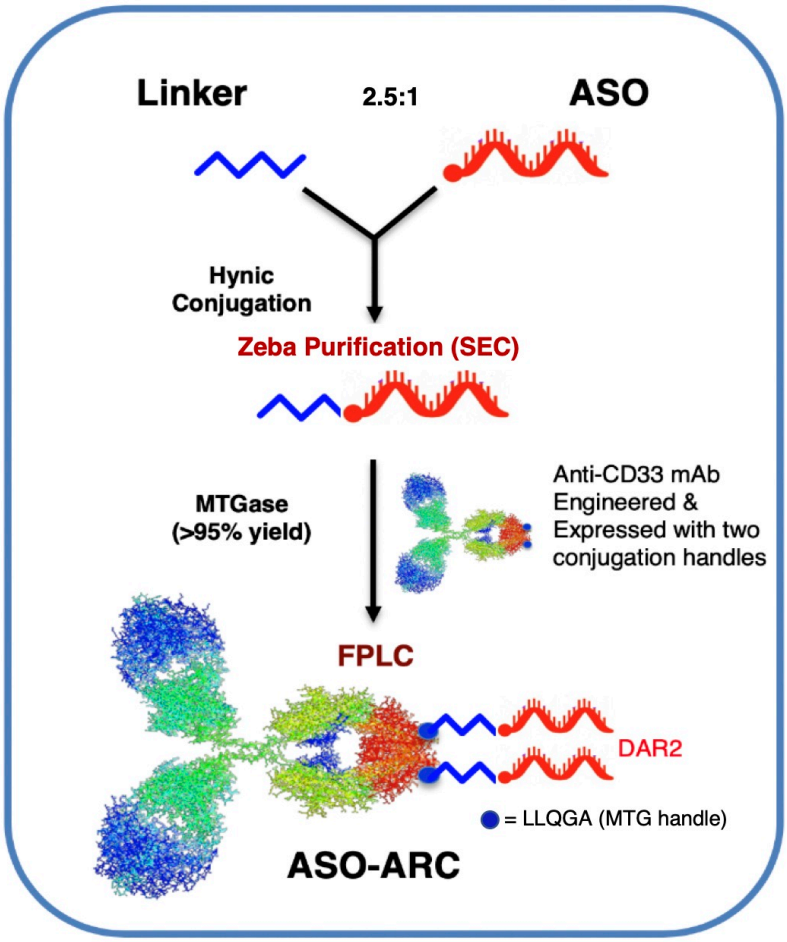

Figure 4.4. ASO-ARC Conjugations
The starting point is a linker, custom synthesized in our lab, to have a terminal hydrazide/HyNic group. The ASOs used for these anti-CD33 ARCs are 5-10-5 gapmers. HyNic conjugation occurs at room temperature. Excess peptide is then removed with a size exclusion column. The linker-ASO is then conjugated with the MTGase enzyme onto the MTG handles engineered into the C-terminal heavy chains of the anti-CD33 mAbs following reaction conditions previously described. The final ARC must be FPLC-purified to eliminate excess unconjugated material and the MTGase enzyme. The pure ARC is collected over several FPLC fractions.

The second conjugation reaction is the MTG conjugation with the MTGase enzyme to attach the KP1H-ASO onto the MTG tags of the anti-CD33 mAb. Following the MTG reaction, the final ARC must be purified by FPLC to remove excess MTGase enzyme and other unconjugated material. The final ARC can be quantified by BCA protein assay or with the use of the extinction coefficient estimate for the full ARC based on its individual components.

Custom ASOs & the First Conjugation Reaction

Two previously obtained sequences for GFP were the basis for the design of ASO gapmers (termed GFP-6 and GFP-I). ASO synthesis utilized a phosphotriester with a terminal benzaldehyde conjugation handle (Ax) to conjugate onto a hydrazide-containing peptide (KP1H). The ASOs that were synthesized have a full phosphorothioate (PS) backbone. They are 5-10-5 gapmer ASOs with 5 2'-OMe modified RNA bases flanking each side of a 10-base DNA central gap (**Figure 4.5a**). Three phosphodiester linkages (PO) were built into the ASO to provide a point of instability with the intention of self-dissociation at that point when encountering the reducing endosomal environment of the target cells. Additionally, some of these ASOs contained a reducible disulfide (SS) linkage as an added point of instability. These ASOs were synthesized with a terminal benzaldehyde (Ax) group to provide a conjugation handle for the HyNic reaction with the linker peptide KP1H. These modifications are permissible for the oligonucleotide to maintain its solubility. Prior to the first conjugation reaction, the ASOs were first dried down by vacuum evaporation to remove the 50% acetonitrile in which oligonucleotides are ordinarily prepared and purified.

The HyNic conjugation reaction occurs between an aromatic aldehyde and a hydrazinonicotinamide group (**Figure 4.5b**), catalyzed by aniline in the reaction mixture. To make the GFP ASO ARCs, one of four ASOs (GFP-6 or GFP-I with/without the disulfide SS modification) was reacted with KP1H linker peptide. KP1H was added in 2.5-fold molar excess

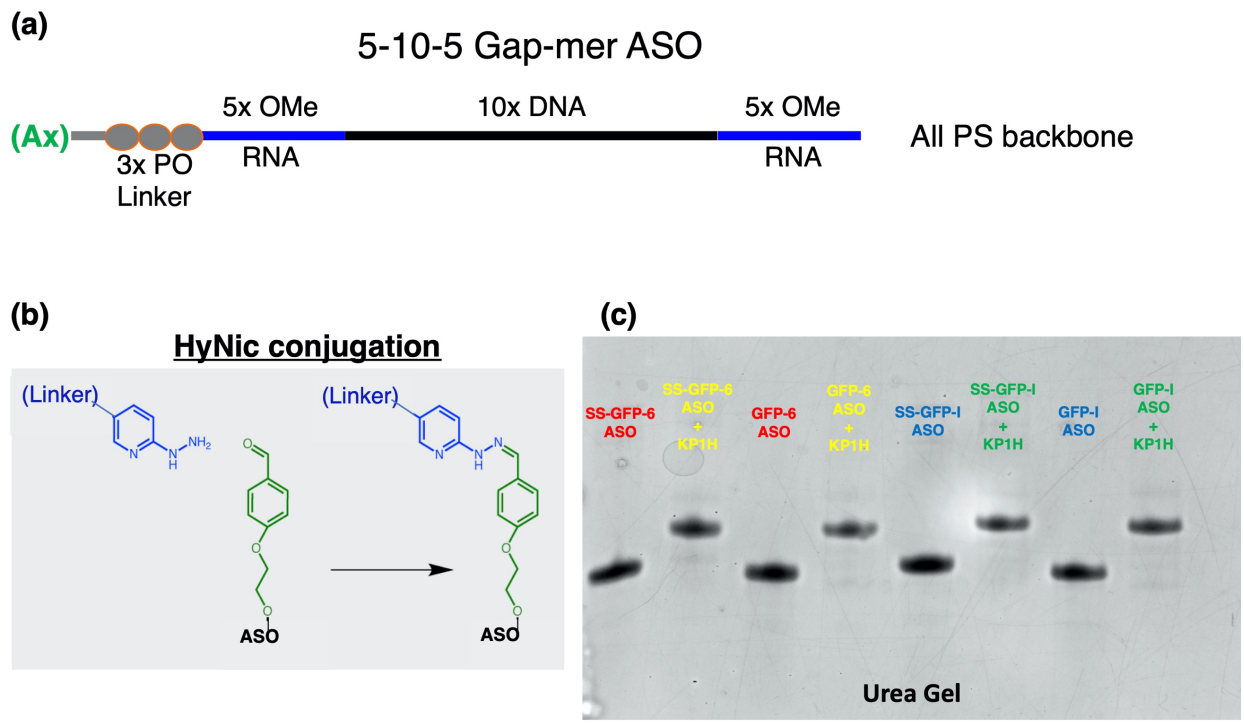

Figure 4.5. ASOs and ASO-Linker Conjugations.
The first conjugation reaction in the ASO ARC building process is the HyNic conjugation. **(a)** The ASOs that were synthesized are 5-10-5 gapmers with 2'-OMe modified RNA bases flanking the central 10-base DNA gap. The entire backbone contains the phosphorothioate modification. ASOs were synthesized with a terminal benzaldehyde group to enable compatibility with HyNic conjugation conditions. A triple phosphodiester linker was added to enable a source of instability when the ASOs have been internalized. Additionally, some ASOs included a disulfide group for easier dissociation from the mAb within the reducing environment of the endosome. **(b)** Schematic of the HyNic conjugation chemistry that occurs between an aromatic aldehyde and a hydrazinonicotinamide group. **(c)** Urea denaturing gel shows successful and efficient conjugation between linker peptide Lys-PEG_6-HyNic (KP1H) and ASO after a 90-minute room temperature incubation in the dark. Abbreviations: PO, phosphodiester group; PS, phosphorothioate group; Ax, terminal benzaldehyde modification for ASO; SS, reversible disulfide linkage.

to the ASOs followed by the addition of 10% aniline to achieve a final 1% within the total reaction volume. HyNic conjugation reactions were incubated at room temperature for 90 minutes in the dark. Following completion of the reaction, 0.5 nmoles of ASO and ASO-linker were loaded into a urea gel and run at 200V for 1 hr to analyze the conjugation efficiency. Urea gel was stained with methylene blue and imaged on a gel dock transilluminator with Coomassie Blue settings (**Figure 4.5c**). HyNic conjugations were nearly 100% efficient.

MTG Conjugation & Final ASO ARC

The second step is the MTG conjugation between the KP1H-ASO conjugate and the anti-CD33 mAb. KP1H-ASO conjugates were quantified by using A260 measurements and extinction coefficient estimates. MTG enzyme was reconstituted in MTG enzyme buffer to a final concentration of 63 mg/mL. An excess molar ratio (7.5-fold) of KP1H-ASO was reacted with MTG-tagged anti-CD33 mAb. 10X MTG reaction buffer was added to achieve a final $1/10^{th}$ final reaction volume. MilliQ water was added to adjust the final volume as needed. MTG enzyme was added to achieve a final concentration of 3 U/mL within the reaction. Final anti-CD33 mAb concentration within the reaction volume was 6 μM. The reaction was mixed well by pipetting and incubated at room temperature for 1 hr.

Following MTG reaction completion, ARCs were purified by size exclusion chromatography (Bio-Rad, SEC 650 10 x 300 gel filtration column) to remove excess unconjugated KP1H-ASO and the MTG enzyme. Absorbance was measured at 280 nm and 260 nm to identify peaks of interest containing the mAbs and ASOs. The highest purity fractions were pooled and concentrated with an Amicon 3K MWCO spin filter by loading the pooled fractions into the top chamber of the spin filter and then spinning at 4000 *g* for 25 to 35 min until a volume lower than 250 μL was achieved. Purified, concentrated ARCs were next quantified with a BCA protein assay. Unfortunately, the resultant yields were poor due to the several rounds of purification and concentration procedures, at 15-27.5% final yield per ARC. To assess

the efficiency of the MTG conjugation and status of the final ARC, a 10% SDS PAGE gel was run to compare to a standard, unconjugated anti-CD33 mAb (**Figure 4.6**). SDS PAGE gel was run at 160V for 1 hr followed by UV protein staining for about 20 min and visualization on a UV transilluminator. The final ARCs appeared to be conjugated with great efficiency following the MTG conjugation. As expected, the SS-ASO-containing ARCs showed poor conjugation efficiency due to the reducing loading buffer used for the SDS PAGE gel.

ARC Treatment

AML cells almost universally express the CD33 on their cell surface and is the target of the FDA-approved gemtuzumab ozogamicin. THP-1 cells are a monocytic cell line derived from the peripheral blood of a male pediatric AML patient (ATCC). THP-1 cells are suspension cells that express the CD33 receptor on their surface. For this reason, THP-1 cells were selected for *in vitro* testing of the ASO ARCs described in this chapter. THP-1 cells were modified to endogenously express the destabilized GFP gene into what here will be referred to as the THP-1 dGFP cell line. THP-1 cells also contain the MLL-AF9 fusion oncogene (Fleischmann et al., 2014), making this the ideal cell line for future experimentation on this particularly aggressive translocation.

To determine whether treating THP-1 dGFP cells results in GFP knockdown, an ARC treatment experiment was performed using the purified ARCs obtained and described in the previous section. ARCs were prepared within a volume of 100 µL with RPMI medium supplemented with 10% FBS and Penicillin/Streptomycin. THP-1 dGFP cells were aliquoted so that each well contained 30,000 cells/well in a volume of 100 µL. After adding the 100 µL ARC treatment mixture, the final volume per well with THP-1 dGFP cells was 200 µL. The ARC final concentrations per well that were tested were: 25 nM, 50 nM, and 100 nM for each of the four

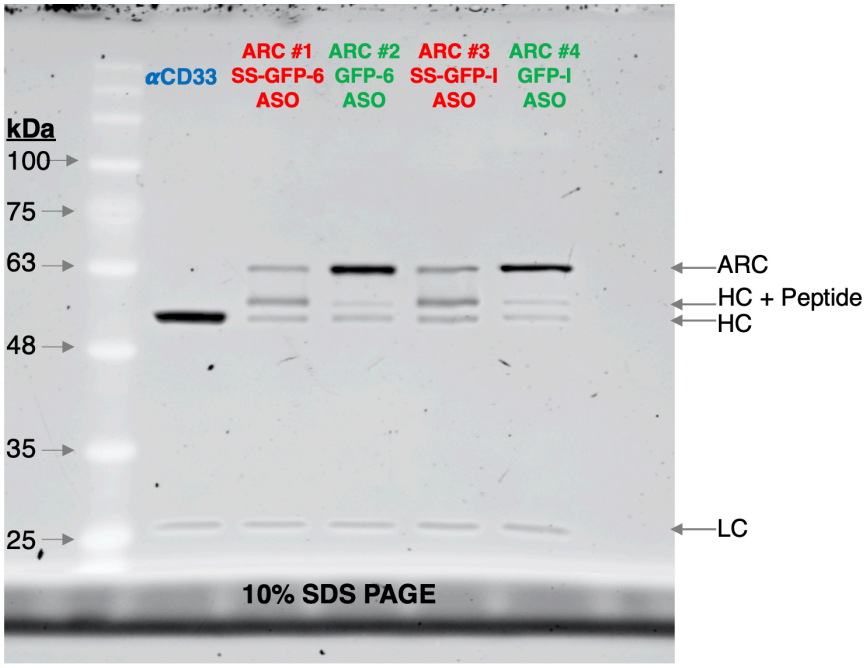

Figure 4.6. ASO-ARCs After MTG Conjugation and Purification
SDS PAGE gel (10%) showing the final ARCs after MTG conjugation reaction and purification by size exclusion chromatography on an FPLC. The MTG conjugation had a high efficiency and successfully conjugated >90% of the anti-CD33 mAb used in reaction. Note that ARCs that contain an SS-ASO show poor conjugation because they were run in reducing loading buffer, dissociating the ASO-KP1H from the mAb as expected. ARCs with the non-SS-ASOs showed minimal unconjugated species. Molecular weight markers shown are in kilodaltons (kDa). Abbreviations: ARC, Antibody-RNA conjugate; SS, reversible disulfide linker; HC, heavy chain; LC, light chain.

ARCs that were made. The contents of every well were mixed by pipetting up and down after the addition of the ARC treatment. Cells were incubated at 37 ˚C for 48 hr.

At 48 hr, cells were assayed for GFP expression by flow cytometry at the VA Flow Cytometry Core (**Figure 4.7**). Unfortunately, no knockdown was observed, results were inconsistent, and if anything, GFP expression was slightly increased. The conclusion of this experiment is simply that the ASOs were unable to escape the endosome in sufficient levels to mediate knockdown, or they were otherwise unable to knock down GFP expression by any noticeable degree.

There are several potential reasons that could explain the poor results observed with these ARCs. The anti-CD33 mAb was cloned using the clinically approved gemtuzumab sequences and is already well known to bind and internalize into CD33-positive AML cells, so it's unlikely that the problem is one of mAb binding and internalizing into THP-1 cells. A quick binding experiment was done to confirm that this batch of anti-CD33 mAb can bind to THP-1 cells. An anti-CD33-TAMRA conjugate was prepared to examine binding. Generation of this conjugate was straightforward with the use of a Lys-PEG_6-TAMRA (KP1-TAMRA) peptide that was synthesized in our lab. TAMRA, or 5-Carboxytetramethylrhodamine, is a fluorescent dye that is commonly used for protein or oligonucleotide labeling. It is reddish in appearance with an excitation at 546 nm and emission at 579 nm that is easily measurable by flow cytometry.

KP1-TAMRA peptide was conjugated in 5-fold molar excess to the anti-CD33 mAb conjugation sites by the standard MTG conjugation conditions that have previously been described. Briefly, standard conjugation conditions are: 3 U/mL MTG enzyme per reaction, final 1X MTG reaction buffer, and anti-CD33 mAb and peptide both in 1X PBS. Conjugation reaction proceeded with a room temperature incubation of about 1 hour. Conjugate was purified by size exclusion chromatography on an FPLC to remove excess KP1-TAMRA peptide. Fractions of interest were pooled together and re-concentrated with an Amicon 30K MWCO spin filter. Purified conjugate was quantified by BCA protein assay.

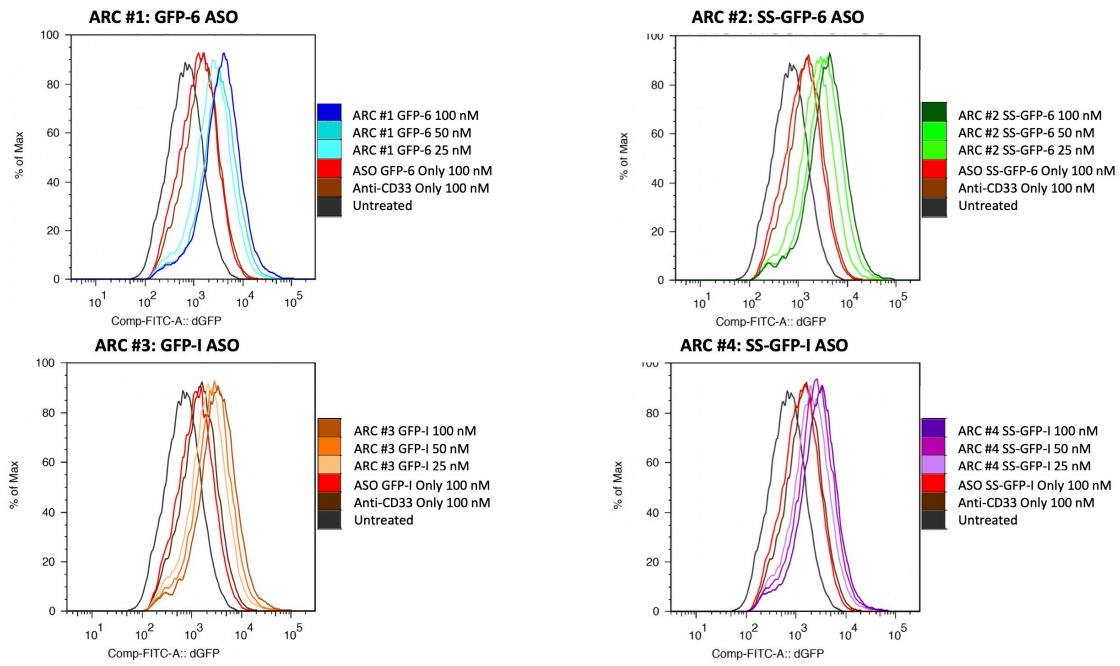

Figure 4.7. ARC Treatment of THP-1 dGFP Cells
The four ARCs with GFP ASOs were tested on our THP-1 dGFP cell line to assess GFP knockdown. 30,000 THP-1 dGFP cells were tested for each treatment condition and three doses of ARC were tested: 25 nM, 50 nM, and 100 nM. Treated cells were incubated at 37˚C for 48 hours followed by flow cytometry analysis, assaying FITC signal for GFP expression. Note that all plots are represented as percent maximum cell count. Abbreviations: ARC, Antibody-RNA conjugate; SS, disulfide linker.

The binding analysis was performed firstly by preparing FACS stain buffer (HBSS without calcium and magnesium, 5 mM EDTA, 20 mM HEPES, 2% FBS, pH 7.4). One million cells of regular THP-1 cells and of our THP-1 dGFP cell line was aliquoted. Centrifuge was cooled to 4 ˚C and cell samples were centrifuged for 5 minutes at 400 *g*. Supernatant was removed and cell pellets were resuspended in FACS stain buffer to wash the cells. Cells were centrifuged once more and resuspended in FACS stain buffer. 100,000 cells were aliquoted into tubes in a 100 µL volume and then treated in a 150 µL volume (final volume = 250 µl for binding experiment) of anti-CD33-TAMRA conjugate to achieve final concentrations of 0.1 nM, 1 nM, 10 nM, and 100 nM. Samples were kept cold in an ice bucket to avoid conjugate internalization. Binding was allowed to proceed for 25 min, and tubes were flicked to continue mixing every ~5 min. After binding completion, cell samples were washed by repeated cycles of centrifuging, supernatant aspiration, and resuspension in fresh FACS stain buffer. After the last wash, cells were passed through a cell strainer and loaded onto a flow cytometer at the VA Flow Cytometry Core to assay for an increase in PE signal which would confirm successful TAMRA-conjugate binding (**Figure 4.8a**). Both THP-1 cell lines that were tested showed a dose-dependent increase in CD33 binding when stained with anti-CD33-TAMRA conjugate. As predicted, the mAbs are not the problem in the ARCs that were tested.

Next, the GFP ASOs were tested on their own to assess GFP knockdown in THP-1 dGFP cells after lipid transfection. RNAiMax (ThermoFisher) was the transfection reagent of choice for these ASO transfections. THP-1 dGFP cells were seeded at a concentration of 20,000 cells/well on the day before the transfections. The following day, ASO stocks were diluted accordingly into treatment tubes for subsequent addition into the respective wells using OptiMEM media to arrive at the final volume. The RNAiMax master mix was prepared in OptiMEM media separately and then mixed with the ASO treatment aliquots to allow for complex formation for 30 min at room temperature. Finally, the treatments were added to the respective wells. The four GFP ASOs used in the ARCs (**Figure 4.7**) were transfected, to

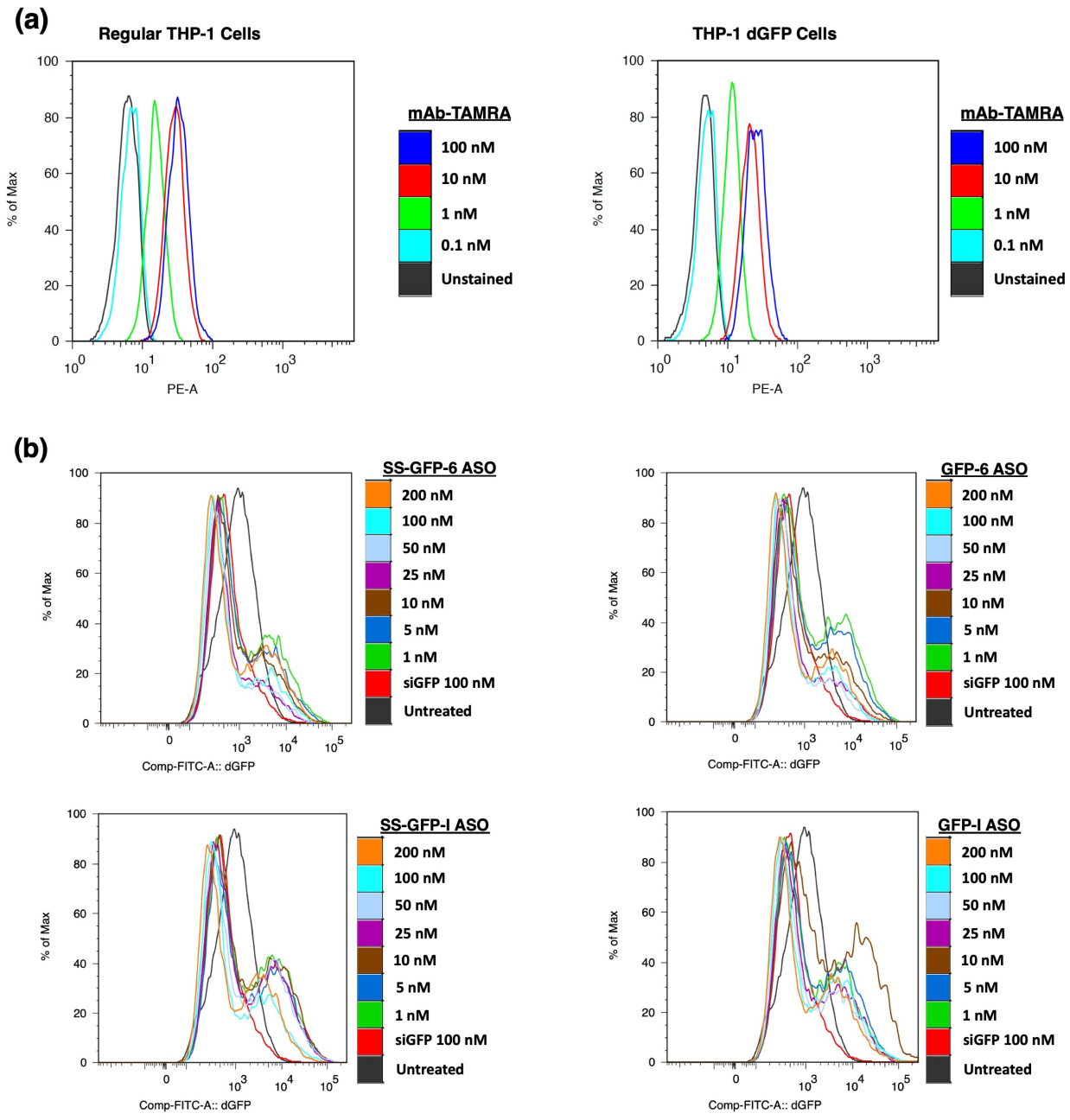

Figure 4.8. Anti-CD33 Binding Analysis & ASO Transfections
(**a**) The batch of anti-CD33 mAb that was used for the ARCs was re-tested for binding capacity to CD33-positive THP-1 cells and THP-1 dGFP cells. KP1-TAMRA peptide was conjugated to the mAbs and PE signal was assayed by flow cytometry. (**b**) ASOs were lipid transfected into THP-1 dGFP cells with RNAiMax transfection reagent and assayed for GFP knockdown at 24 hours. All plots are presented as percent maximum cell count.

achieve the final concentrations of: 1 nM, 5 nM, 10 nM, 25 nM, 50 nM, 100 nM, and 200 nM. Several untreated cell controls and an siGFP positive control were also included. Cells were incubated at 37 ˚C for 24 hr followed by flow cytometry analysis of FITC signal by the VA Flow Cytometry Core (**Figure 4.8b**). Unfortunately, suspension cells like THP-1 cells are not amenable to lipid transfections, leading to inconclusive results that suggest that perhaps there could have been some level of knockdown but it's difficult to tell definitively. Results suggest that there was likely at least a low level of GFP knockdown in THP-1 dGFP cells.

Cell delivery by electroporation was tried numerous times for these same GFP ASOs with variable voltage-capacitance-resistance settings and pulse sequences, ASO doses, and cell densities, but in all cases, resulting GFP knockdown analyses was equally lackluster as with the lipid transfections. While electroporation is a better method of introducing an oligonucleotide into suspension cells, it led extensive cell death (which is consistent with the approach) and highly inconsistent results and no appreciable knockdown. Unfortunately, attempts to further optimize electroporation protocols was ended when it became evident that no combination of settings led to a reliable readout or even hinted at successful ASO internalization.

To confirm that transfection reagents were viable and could induce ASO internalization, transfection tests were performed on 293T cells and H1299 cells (a non-small cell lung carcinoma cell line). The first part with 293Ts involved the generation of ASO-FITC conjugates by using an SS-GFP-I ASO and maleimide-FITC molecule. The SS-ASO was reduced by the mixing of 17 nmoles of SS-ASO with 170 nmoles of TCEP reducing agent and room temperature incubation for 30 minutes. Maleimide-FITC was added to the reaction in a 10-fold molar excess to the ASO and incubated at 37 ˚C for 2 hr. A Zeba 7K MWCO size exclusion column was used to remove excess dye. ASO and ASO-FITC conjugates were assessed with a urea gel by running 0.25 nmoles of each sample for 53 min at 200V. An Alexa 488 filter was used to image the FITC conjugate on a gel dock followed by methylene blue staining and imaging with Coomassie Blue settings (**Figure 4.9a**). Conjugation was relatively inefficient and a

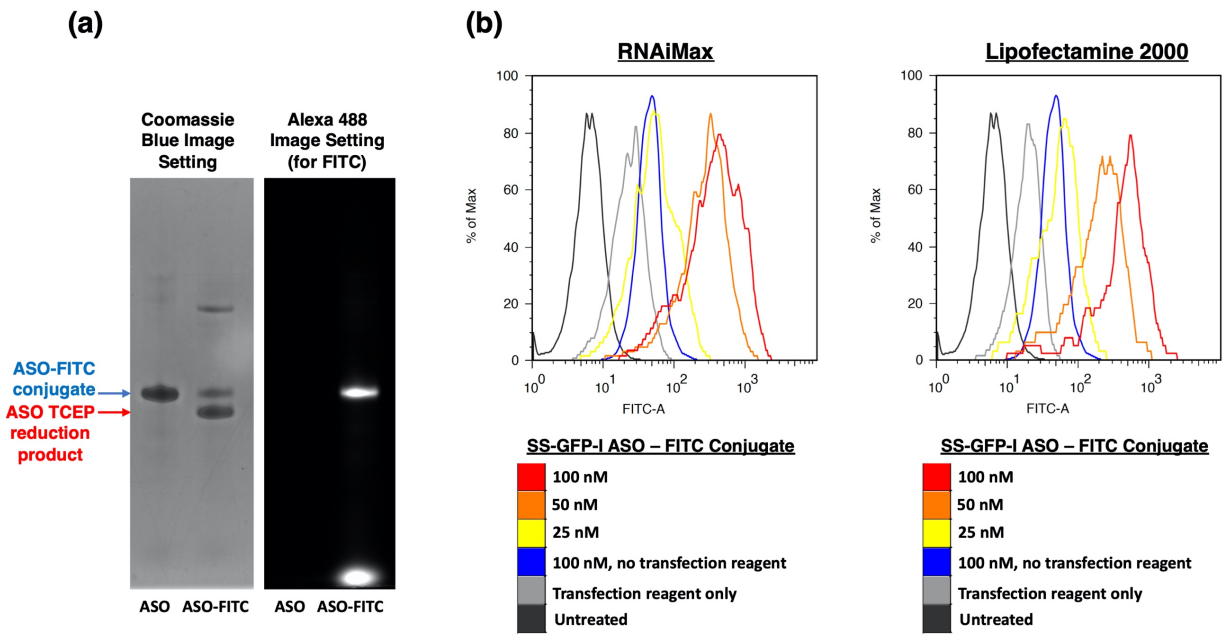

Figure 4.9. ASO-FITC Conjugate for Lipid Transfection Reagent Test
ASO-FITC conjugates were prepared to test the functionality of the transfection reagents. (**a**) SDS PAGE 10% gel analysis of SS-GFP-I ASO only versus SS-GFP-I ASO-FITC conjugate. Conjugation was not very efficient. Of note, the maleimide-FITC reagent is only ~500 Daltons in size, so the shift is expected to be undetectable on a gel. Alexa 488 imaging confirms ASO-FITC conjugate. (**b**) Flow cytometry analysis for the transfection of 293T cells with ASO-FITC conjugates. Plots are shown as percent maximum cell count.

gel shift from the addition of FITC was indiscernible due to the small size of FITC (~500 Daltons). Fluorescence imaging of the gel did confirm some level of ASO-FITC conjugate. 293T cells were reverse transfected with SS-ASO-FITC conjugates by adding 75,000 cells in a 400 µL volume into a 100 µL volume of ASO conjugate with OptiMEM (ASO conjugate doses tested were 10 nM, 50 nM, and 100 nM. Transfection reagents Lipofectamine 2000 (ThermoFisher) and RNAiMax (ThermoFisher) were both tested in this experiment. Controls included were untreated cells, cells with transfection reagent only and cells with ASO conjugate only without transfection reagent. Flow cytometry was used to analyze FITC signal for a shift in response to ASO-FITC uptake after 48 hr in 293T cells (**Figure 4.9b**). Although there was much cell death and relatively inefficient conjugations, it was difficult to make definitive conclusions. There was some level of FITC signal increase or stimulation of auto-fluorescence in response to adding ASO or transfection reagent on its own. Flow cytometry analysis suggest some level of dose-dependent increase in FITC signal with both transfection reagents and it is likely that the transfection successfully allowed the ASO conjugate internalization.

To follow-up on the previous experiment, an ASO-TAMRA conjugate was prepared between an SS-GFP ASO and a maleimide-TAMRA molecule. Conjugation procedure was similar to the procedure described above: ASO disulfides were reduced with TCEP reducing agent with a room temperature incubation of 45 min followed by addition of maleimide-TAMRA in a 20-fold molar excess to the ASO and an incubation at 37 ˚C for 2 hr. Excess dye was removed with a Zeba 7K column. ASO-TAMRA conjugate was verified by urea gel analysis. 293T cells and H1299 dGFP cells were transfected with the ASO-TAMRA conjugates at the doses of 10 nM, 50 nM, 100 nM, 500 nM, and 1 µM with RNAiMax (ThermoFisher). Cells were analyzed by flow cytometry after 48 hr to assay for PE signal (**Figure 4.10a**). Flow cytometry analysis confirmed a dose dependent increase in PE signal in both 293T and H1299 dGFP cell lines. Moreover, fluorescence microscopy imaging was completed to complement flow cytometry data for which H1299 dGFP representative images are shown (**Figure 4.10b**).

Figure 4.10. SS-GFP ASO-TAMRA Conjugates for Lipid Transfection Verification
SS-GFP ASOs were conjugated to maleimide-TAMRA molecules after a reducing reaction of the ASO followed by 20-fold molar excess addition of maleimide-TAMRA and a 2-hr incubation at 37 ˚C incubation. ASO-TAMRA conjugates were transfected with RNAiMax into 293T cells and H1299 dGFP cell lines at doses that range from 10 nM to 1 μM. (**a**) Cells were assayed by flow cytometry 48 hours after transfection to analyze changes in PE signal (for the presence of TAMRA internalization). (**b**) Fluorescence microscopy representative images for H1299 dGFP transfections are shown for the 24 and 48 hr time points. Bright-field and fluorescent images are shown side by side followed by the overlay. Flow cytometry plots are shown as percent maximum cell count.

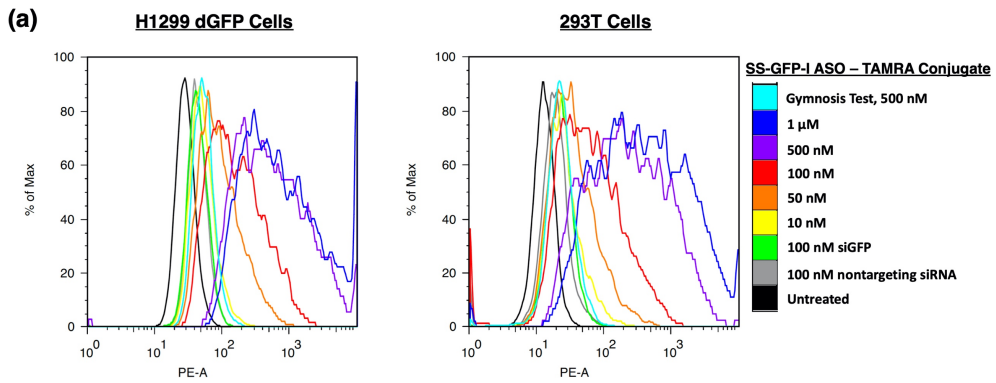
(a)
H1299 dGFP Cells
293T Cells
% of Max
PE-A
SS-GFP-I ASO – TAMRA Conjugate
Gymnosis Test, 500 nM
1 µM
500 nM
100 nM
50 nM
10 nM
100 nM siGFP
100 nM nontargeting siRNA
Untreated

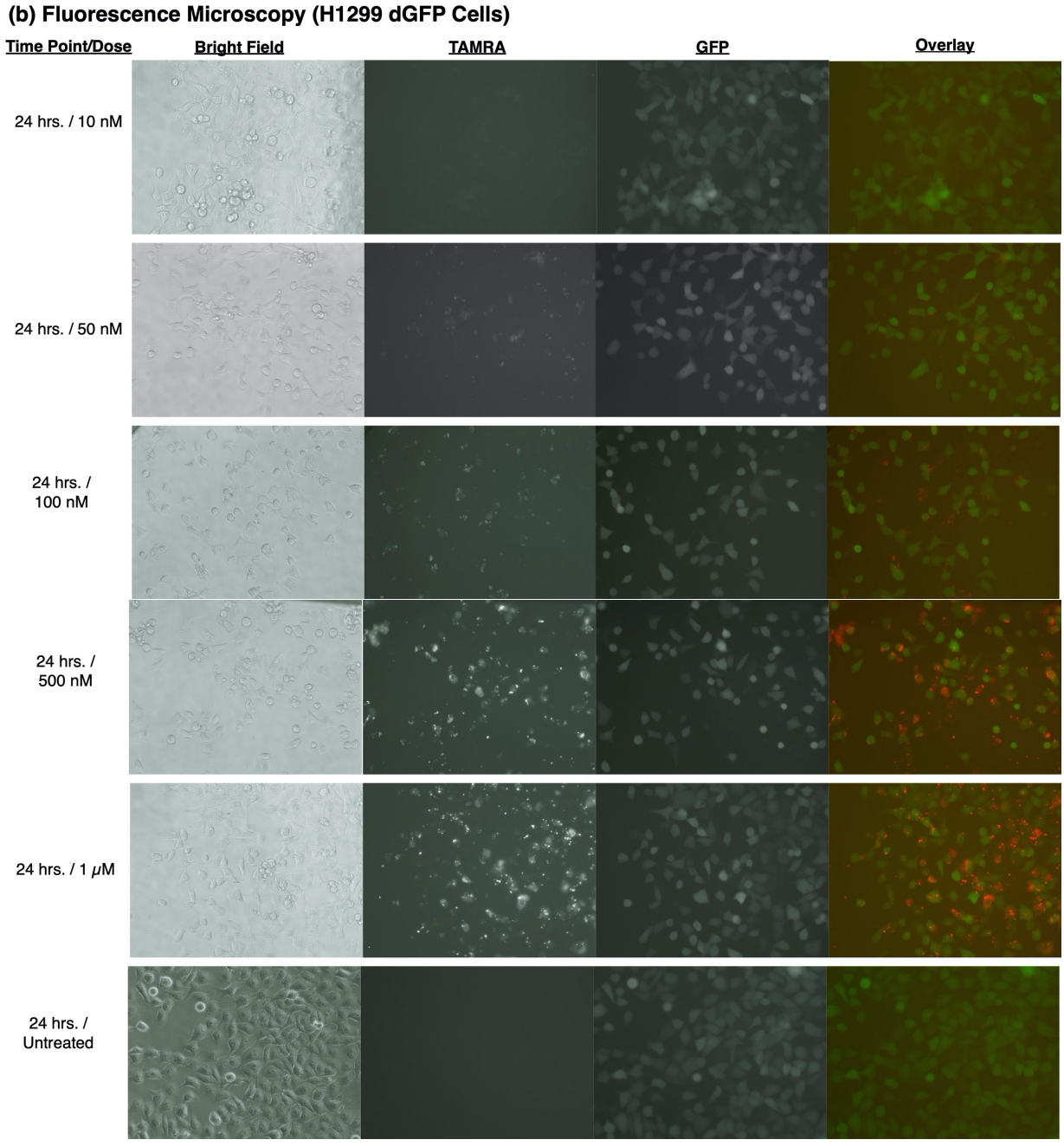
(b) Fluorescence Microscopy (H1299 dGFP Cells)
Time Point/Dose
Bright Field
TAMRA
GFP
Overlay
24 hrs. / 10 nM
24 hrs. / 50 nM
24 hrs. / 100 nM
24 hrs. / 500 nM
24 hrs. / 1 µM
24 hrs. / Untreated

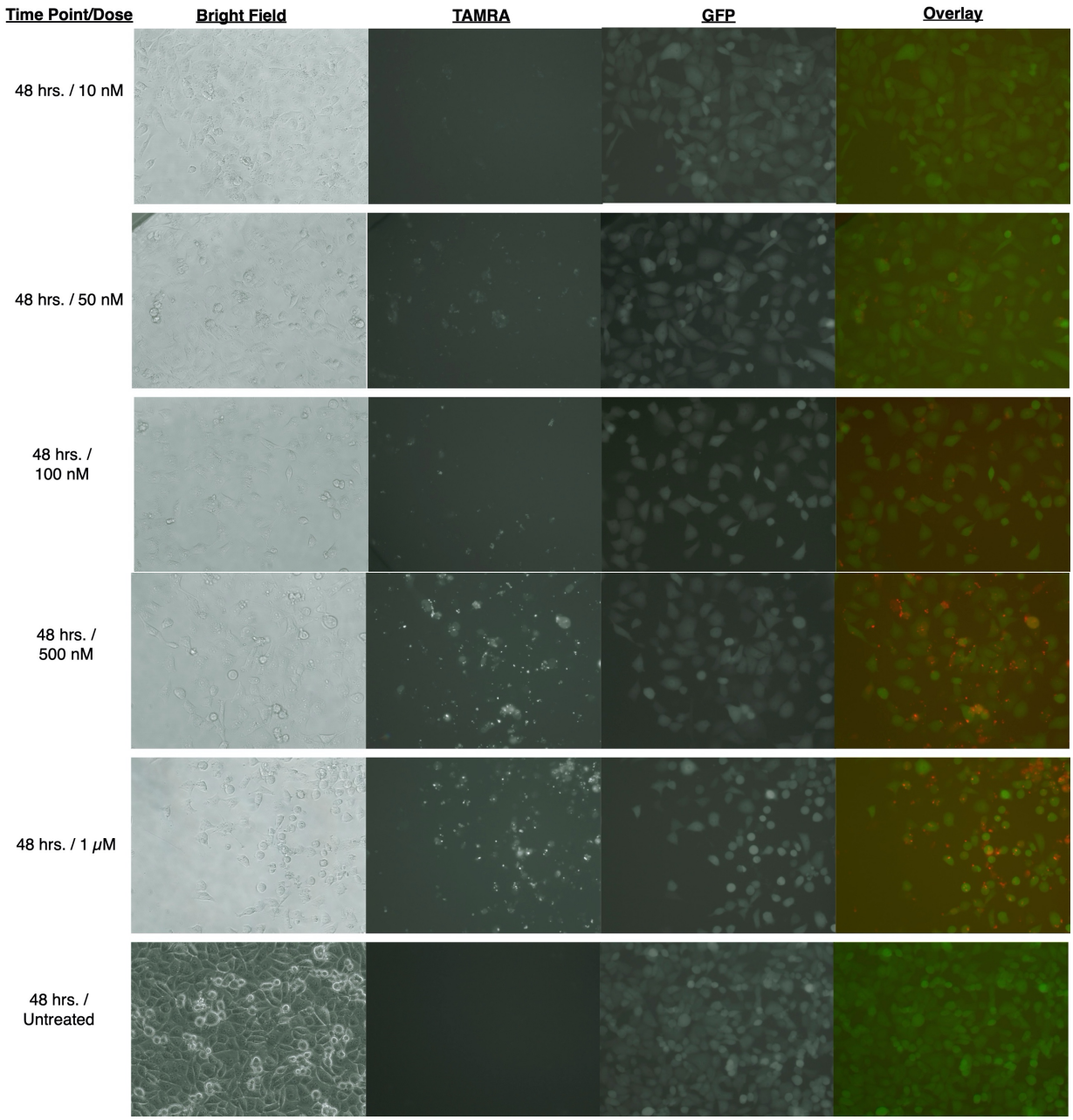

Figure 4.10. SS-GFP ASO-TAMRA Conjugates for Lipid Transfection Verification, continued.

Fluorescence imaging confirms that the transfection reagents were successful in inducing ASO conjugate internalization into the cells. These results confirm that the problem is not related to any transfection reagent used in the procedure.

The problematic component in the ARC is the GFP ASO. There are several reasons why these ASOs may not be able to successfully knockdown GFP. One possibility is that the ASOs are being sequestered or trafficked by the incorrect proteins that prevent them from accessing the nucleus. Passive diffusion of ASOs into the cytoplasm and nucleus is not possible for all ASOs nor all cell types and it's entirely possible that these specific ASOs cannot undergo gymnosis or the cells used in these experiments are not conducive to gymnosis. Only a fraction of PS ASOs can enter cells by gymnosis (Crooke et al., 2017b) and these specific GFP ASOs may be incapable of gymnotic uptake into AML cell cytoplasm due to the specific cell surface or endosomal protein repertoire of AML cells and/or ASO processing in AML cells may simply occur by non-productive pathways. It may also be the case that ASOs are binding to endosomal TLR9 and triggering an innate immune response to a certain extent, thereby stimulating general nonspecific expression of a collection of genes that includes GFP.

Another potential issue is the CD33 receptor count on THP-1 cells, which are estimated to number between 8,000 and 20,000 per THP-1 cell surface (Laszlo et al., 2014). By contrast, the success of GalNAc conjugates is attributed to the high ASGPR density on liver hepatocytes, which number in the millions per hepatocyte with fast recycling times (Dowdy, 2017). CD33 receptors likely undergo considerably slower cycling time between the endosome and back to the surface, relative to ASGPR in hepatocytes. Another possibility is that the endogenously expressed dGFP gene is not spliced or only minimally spliced, thereby being exported to the cytoplasm far too quickly for the nuclear-localized ASOs to have time to find and bind to the mRNA and initiate an RNase H-mediated antisense response. Lastly, another potential problem with the GFP ASOs is that the specific sequences are not optimal for GFP targeting. Sequences that work for an siRNA may not be effective for ASOs and targeting random sections of a given

gene often do not lead to an efficient knockdown response. Unfortunately, screening large numbers of oligonucleotides to attempt to identify an optimal sequence for incorporation into ASO syntheses requires extensive time and resources and is beyond the scope of this project. The final issue is the absence of endosomal escape enhancers that, whether gymnosis works for these PS ASOs and/or these AML cells or not, would still be expected to improve delivery of any oligonucleotide conjugate.

CONCLUSIONS

Oligonucleotides, siRNAs and ASOs especially, have shown strong potencies against their genetic targets. Monoclonal antibodies (mAbs) have repeatedly been used to deliver cytotoxic drug cargos (ADCs) to target cells with a high degree of specificity, based on their target cell surface receptor. The remaining challenge is that oligonucleotides and other mAb-conjugated molecules are unable to access the cytoplasm of cells beyond the liver. siRNA remains trapped in endosomes due to their size and charge and can only escape into the cytoplasm in extremely limited numbers, if that. On the other hand, ASOs have been observed under certain circumstances to passively diffuse into the endosome and into the cytoplasm by a poorly understood phenomenon termed gymnosis. It follows that perhaps an ASO-mAb conjugate would fare better than its siRNA counterpart in effecting gene silencing.

AML was chosen as the disease against to test an ASO ARC. THP-1 cells were derived from an AML patient, express the CD33 receptor as well as the MLL-AF9 fusion oncogene that is found in many AML cases, and suspension cell targets like AML cells are more accessible to antibody therapeutics than solid tumors. An ARC with an anti-CD33 mAb and GFP ASOs was made successfully with a different conjugation chemistry than was used for the siRNA ARCs described in Chapter Three. GFP was chosen due to the availability of an established THP-1 dGFP cell line in our lab, enabling a very efficient reporter system to quickly analyze ARC efficacy. Pure, structurally defined ARCs were made and verified, and conjugation reactions

were highly efficient. Unfortunately, these ARCs failed to knock down GFP expression in THP-1 dGFP cells.

Troubleshooting several aspects of the ARCs suggested that the ASOs were the problematic component of the ARCs that were made. Numerous potential problems with the ASOs were proposed, ranging nonproductive cell uptake and endosomal trafficking to the actual ASO sequences used and more. It is possible that a combination of these issues could be true at once and to varying degrees, explaining the absence of a solid GFP knockdown. The difficulty of using an ASO in these ARCs underscores the criticality of finding ways to enhance an oligonucleotide's access to the cytoplasm where it can efficiently silent its target gene.

Without an improved endosomal escape, ARCs and similar oligonucleotide conjugates will remain unable to reach their maximum therapeutic potential for systemic extrahepatic targeting. The following chapter describes part of the ongoing work in our lab towards the development and testing of what we call universal endosomal escape domains (uEEDs). uEEDs are still very much in development and their ultimate success or failure will be revealed in time.

ACKNOWLEDGEMENTS

Chapter Four contains unpublished material that was coauthored in part by Alex Hamil and Xianshu Cui. This dissertation's author was the primary researcher and author of this material. Oligonucleotides were synthesized by Alex Hamil and the linker peptides were synthesized by Xianshu Cui. The work in this chapter was supported by the NCI training grant: T32 CA067754-22. Steven Dowdy provided guidance throughout the work presented in this chapter.

REFERENCES

Ackerman, M.E., Pawlowski, D., Wittrup, K.D., 2008. Effect of antigen turnover rate and expression level on antibody penetration into tumor spheroids. Mol Cancer Ther 7, 2233–2240. https://doi.org/10.1158/1535-7163.MCT-08-0067

Agarwal, P., Bertozzi, C.R., 2015. Site-Specific Antibody–Drug Conjugates: The Nexus of Bioorthogonal Chemistry, Protein Engineering, and Drug Development. Bioconjugate Chem. 26, 176–192. https://doi.org/10.1021/bc5004982

Agrawal, S., Temsamani, J., Tang, J.Y., 1991. Pharmacokinetics, biodistribution, and stability of oligodeoxynucleotide phosphorothioates in mice. Proceedings of the National Academy of Sciences 88, 7595–7599. https://doi.org/10.1073/pnas.88.17.7595

American Cancer Society, 2018. What Is Acute Myeloid Leukemia (AML)? ACA. https://www.cancer.org/cancer/acute-myeloid-leukemia/about/what-is-aml.html

Arnold, A.E., Malek-Adamian, E., Le, P.U., Meng, A., Martínez-Montero, S., Petrecca, K., Damha, M.J., Shoichet, M.S., 2018. Antibody-Antisense Oligonucleotide Conjugate Downregulates a Key Gene in Glioblastoma Stem Cells. Molecular Therapy - Nucleic Acids 11, 518–527. https://doi.org/10.1016/j.omtn.2018.04.004

ATCC, 2021. THP-1, TIB-202. ATCC Human Cells. https://www.atcc.org/products/tib-202

Benson, M.D., Waddington-Cruz, M., Berk, J.L., Polydefkis, M., Dyck, P.J., Wang, A.K., Planté-Bordeneuve, V., Barroso, F.A., Merlini, G., Obici, L., Scheinberg, M., Brannagan, T.H., Litchy, W.J., Whelan, C., Drachman, B.M., Adams, D., Heitner, S.B., Conceição, I., Schmidt, H.H., Vita, G., Campistol, J.M., Gamez, J., Gorevic, P.D., Gane, E., Shah, A.M., Solomon, S.D., Monia, B.P., Hughes, S.G., Kwoh, T.J., McEvoy, B.W., Jung, S.W., Baker, B.F., Ackermann, E.J., Gertz, M.A., Coelho, T., 2018. Inotersen Treatment for Patients with Hereditary Transthyretin Amyloidosis. N Engl J Med 379, 22–31. https://doi.org/10.1056/NEJMoa1716793

Burnett, A., Wetzler, M., Löwenberg, B., 2011. Therapeutic Advances in Acute Myeloid Leukemia. JCO 29, 487–494. https://doi.org/10.1200/JCO.2010.30.1820

Crooke, S.T., 2017. Molecular Mechanisms of Antisense Oligonucleotides. Nucleic Acid Therapeutics 27, 70–77. https://doi.org/10.1089/nat.2016.0656

Crooke, S.T., Baker, B.F., Witztum, J.L., Kwoh, T.J., Pham, N.C., Salgado, N., McEvoy, B.W., Cheng, W., Hughes, S.G., Bhanot, S., Geary, R.S., 2017a. The Effects of 2′- *O* -Methoxyethyl Containing Antisense Oligonucleotides on Platelets in Human Clinical Trials. Nucleic Acid Therapeutics 27, 121–129. https://doi.org/10.1089/nat.2016.0650

Crooke, S.T., Wang, S., Vickers, T.A., Shen, W., Liang, X., 2017b. Cellular uptake and trafficking of antisense oligonucleotides. Nat Biotechnol 35, 230–237. https://doi.org/10.1038/nbt.3779

Cuellar, T.L., Barnes, D., Nelson, C., Tanguay, J., Yu, S.-F., Wen, X., Scales, S.J., Gesch, J., Davis, D., van Brabant Smith, A., Leake, D., Vandlen, R., Siebel, C.W., 2015. Systematic evaluation of antibody-mediated siRNA delivery using an industrial platform

of THIOMAB–siRNA conjugates. Nucleic Acids Research 43, 1189–1203. https://doi.org/10.1093/nar/gku1362

De Kouchkovsky, I., Abdul-Hay, M., 2016. 'Acute myeloid leukemia: a comprehensive review and 2016 update.' Blood Cancer Journal 6, e441–e441. https://doi.org/10.1038/bcj.2016.50

Dowdy, S.F., 2017. Overcoming cellular barriers for RNA therapeutics. Nat Biotechnol 35, 222–229. https://doi.org/10.1038/nbt.3802

Fleischmann, K.K., Pagel, P., Schmid, I., Roscher, A.A., 2014. RNAi-mediated silencing of MLL-AF9 reveals leukemia-associated downstream targets and processes. Mol Cancer 13, 27. https://doi.org/10.1186/1476-4598-13-27

Graubert, T., Stone, R., 2014. AML Genomics for the Clinician. Seminars in Hematology 51, 322–329. https://doi.org/10.1053/j.seminhematol.2014.08.006

Hamann, P.R., Hinman, L.M., Beyer, C.F., Lindh, D., Upeslacis, J., Flowers, D.A., Bernstein, I., 2002. An Anti-CD33 Antibody−Calicheamicin Conjugate for Treatment of Acute Myeloid Leukemia. Choice of Linker. Bioconjugate Chem. 13, 40–46. https://doi.org/10.1021/bc0100206

Hourigan, C.S., Gale, R.P., Gormley, N.J., Ossenkoppele, G.J., Walter, R.B., 2017. Measurable residual disease testing in acute myeloid leukaemia. Leukemia 31, 1482-1490. https://doi.org/10.1038/leu.2017.113

Huret, J., Dessen, P., Bernheim, A., and the Groupe Français de Cytogénétique Oncologique, 2001. An Atlas on Chromosomes in Hematological Malignancies. Example: 11q23 and MLL partners. Leukemia 15, 987–989. https://doi.org/10.1038/sj.leu.2402135

Ingle, G.S., Chan, P., Elliott, J.M., Chang, W.S., Koeppen, H., Stephan, J.-P., Scales, S.J., 2007. High CD21 expression inhibits internalization of anti-CD19 antibodies and cytotoxicity of an anti-CD19-drug conjugate. Br J Haematol 0, 071107180602002-??? https://doi.org/10.1111/j.1365-2141.2007.06883.x

Iversen, P.L., Zhu, S., Meyer, A., Zon, G., 1992. Cellular Uptake and Subcellular Distribution of Phosphorothioate Oligonucleotides into Cultured Cells. Antisense Research and Development 2, 211–222. https://doi.org/10.1089/ard.1992.2.211

Jager, E., van der Velden, V.H.J., te Marvelde, J.G., Walter, R.B., Agur, Z., Vainstein, V., 2011. Targeted Drug Delivery by Gemtuzumab Ozogamicin: Mechanism-Based Mathematical Model for Treatment Strategy Improvement and Therapy Individualization. PLoS ONE 6, e24265. https://doi.org/10.1371/journal.pone.0024265

Jen, E.Y., Ko, C.-W., Lee, J.E., Del Valle, P.L., Aydanian, A., Jewell, C., Norsworthy, K.J., Przepiorka, D., Nie, L., Liu, J., Sheth, C.M., Shapiro, M., Farrell, A.T., Pazdur, R., 2018. FDA Approval: Gemtuzumab Ozogamicin for the Treatment of Adults with Newly Diagnosed CD33-Positive Acute Myeloid Leukemia. Clin Cancer Res 24, 3242–3246. https://doi.org/10.1158/1078-0432.CCR-17-3179

Juliano, R.L., Ming, X., Nakagawa, O., 2012. Cellular Uptake and Intracellular Trafficking of Antisense and siRNA Oligonucleotides. Bioconjugate Chem. 23, 147–157. https://doi.org/10.1021/bc200377d

Juliano, R.L., Carver, K., Cao, C., Ming, X., 2013. Receptors, endocytosis, and trafficking: the biological basis of targeted delivery of antisense and siRNA oligonucleotides. Journal of Drug Targeting 21, 27–43. https://doi.org/10.3109/1061186X.2012.740674

Juzenas, S., Venkatesh, G., Hübenthal, M., Hoeppner, M.P., Du, Z.G., Paulsen, M., Rosenstiel, P., Senger, P., Hofmann-Apitius, M., Keller, A., Kupcinskas, L., Franke, A., Hemmrich-Stanisak, G., 2017. A comprehensive, cell specific microRNA catalogue of human peripheral blood. Nucleic Acids Research 45, 9290–9301. https://doi.org/10.1093/nar/gkx706

Kawagoe, H., Kawagoe, R., Sano, K., 2001. Targeted down-regulation of MLL-AF9 with antisense oligodeoxyribonucleotide reduces the expression of the HOXA7and -A10 genes and induces apoptosis in a human leukemia cell line, THP-1. Leukemia 15, 1743–1749. https://doi.org/10.1038/sj.leu.2402262

Kell, J., 2016. Considerations and challenges for patients with refractory and relapsed acute myeloid leukaemia. Leukemia Research 47, 149–160. https://doi.org/10.1016/j.leukres.2016.05.025

Kenderian, S.S., Ruella, M., Shestova, O., Klichinsky, M., Aikawa, V., Morrissette, J.J.D., Scholler, J., Song, D., Porter, D.L., Carroll, M., June, C.H., Gill, S., 2015. CD33-specific chimeric antigen receptor T cells exhibit potent preclinical activity against human acute myeloid leukemia. Leukemia 29, 1637–1647. https://doi.org/10.1038/leu.2015.52

Klco, J.M., Spencer, D.H., Miller, C.A., Griffith, M., Lamprecht, T.L., O'Laughlin, M., Fronick, C., Magrini, V., Demeter, R.T., Fulton, R.S., Eades, W.C., Link, D.C., Graubert, T.A., Walter, M.J., Mardis, E.R., Dipersio, J.F., Wilson, R.K., Ley, T.J., 2014. Functional Heterogeneity of Genetically Defined Subclones in Acute Myeloid Leukemia. Cancer Cell 25, 379–392. https://doi.org/10.1016/j.ccr.2014.01.031

Krivtsov, A.V., Armstrong, S.A., 2007. *MLL* translocations, histone modifications and leukaemia stem-cell development. Nature Reviews 7, 823-833. https://doi.org/10.1038/nrc2253

Laszlo, G.S., Estey, E.H., Walter, R.B., 2014. The past and future of CD33 as therapeutic target in acute myeloid leukemia. Blood Reviews 28, 143–153. https://doi.org/10.1016/j.blre.2014.04.001

Liang, X.-H., Shen, W., Sun, H., Kinberger, G.A., Prakash, T.P., Nichols, J.G., Crooke, S.T., 2016. Hsp90 protein interacts with phosphorothioate oligonucleotides containing hydrophobic 2′-modifications and enhances antisense activity. Nucleic Acids Res 44, 3892–3907. https://doi.org/10.1093/nar/gkw144

Lima, W.F., Nichols, J.G., Wu, H., Prakash, T.P., Migawa, M.T., Wyrzykiewicz, T.K., Bhat, B., Crooke, S.T., 2004. Structural Requirements at the Catalytic Site of the Heteroduplex Substrate for Human RNase H1 Catalysis. Journal of Biological Chemistry 279, 36317–36326. https://doi.org/10.1074/jbc.M405035200

Lima, W.F., Rose, J.B., Nichols, J.G., Wu, H., Migawa, M.T., Wyrzykiewicz, T.K., Siwkowski, A.M., Crooke, S.T., 2007. Human RNase H1 Discriminates between Subtle Variations in the Structure of the Heteroduplex Substrate. Mol Pharmacol 71, 83–91. https://doi.org/10.1124/mol.106.025015

Lima, W.F., Vickers, T.A., Nichols, J., Li, C., Crooke, S.T., 2014. Defining the Factors That Contribute to On-Target Specificity of Antisense Oligonucleotides. PLoS ONE 9, e101752. https://doi.org/10.1371/journal.pone.0101752

Lima, W.F., Murray, H.M., Damle, S.S., Hart, C.E., Hung, G., De Hoyos, C.L., Liang, X.-H., Crooke, S.T., 2016. Viable *RNaseH1* knockout mice show RNaseH1 is essential for R loop processing, mitochondrial and liver function. Nucleic Acids Res 44, 5299–5312. https://doi.org/10.1093/nar/gkw350

Longo, Dan L., 2017. Hematology and Oncology. 2nd ed., McGraw-Hill Education Medical.

Lu, J., Jiang, F., Lu, A., Zhang, G., 2016. Linkers Having a Crucial Role in Antibody–Drug Conjugates. IJMS 17, 561. https://doi.org/10.3390/ijms17040561

Matsumura, Y., 2021. Barriers to antibody therapy in solid tumors, and their solutions. Cancer Sci 112, 2939–2947. https://doi.org/10.1111/cas.14983

Meyer, C., Schneider, B., Jakob, S., Strehl, S., Attarbaschi, A., Schnittger, S., Schoch, C., Jansen, M.W.J.C., van Dongen, J.J.M., den Boer, M.L., Pieters, R., Ennas, M.-G., Angelucci, E., Koehl, U., Greil, J., Griesinger, F., zur Stadt, U., Eckert, C., Szczepański, T., Niggli, F.K., Schäfer, B.W., Kempski, H., Brady, H.J.M., Zuna, J., Trka, J., Nigro, L.L., Biondi, A., Delabesse, E., Macintyre, E., Stanulla, M., Schrappe, M., Haas, O.A., Burmeister, T., Dingermann, T., Klingebiel, T., Marschalek, R., 2006. The MLL recombinome of acute leukemias. Leukemia 20, 777–784. https://doi.org/10.1038/sj.leu.2404150

Ohtake, S., Miyawaki, S., Fujita, H., Kiyoi, H., Shinagawa, K., Usui, N., Okumura, H., Miyamura, K., Nakaseko, C., Miyazaki, Y., Fujieda, A., Nagai, T., Yamane, T., Taniwaki, M., Takahashi, M., Yagasaki, F., Kimura, Y., Asou, N., Sakamaki, H., Handa, H., Honda, S., Ohnishi, K., Naoe, T., Ohno, R., 2011. Randomized study of induction therapy comparing standard-dose idarubicin with high-dose daunorubicin in adult patients with previously untreated acute myeloid leukemia: the JALSG AML201 Study. Blood 117, 2358–2365. https://doi.org/10.1182/blood-2010-03-273243

Reddy, S., Shaller, C.C., Doss, M., Shchaveleva, I., Marks, J.D., Yu, J.Q., Robinson, M.K., 2011. Evaluation of the Anti-HER2 C6.5 Diabody as a PET Radiotracer to Monitor HER2 status and Predict Response to Trastuzumab Treatment. Clin Cancer Res 17, 1509–1520. https://doi.org/10.1158/1078-0432.CCR-10-1654

Ritchie, M., Tchistiakova, L., Scott, N., 2013. Implications of receptor-mediated endocytosis and intracellular trafficking dynamics in the development of antibody drug conjugates. mAbs 5, 13–21. https://doi.org/10.4161/mabs.22854

Roberts, T.C., Langer, R., Wood, M.J.A., 2020. Advances in oligonucleotide drug delivery. Nat Rev Drug Discov 19, 673–694. https://doi.org/10.1038/s41573-020-0075-7

Rudnick, S.I., Lou, J., Shaller, C.C., Tang, Y., Klein-Szanto, A.J.P., Weiner, L.M., Marks, J.D., Adams, G.P., 2011. Influence of Affinity and Antigen Internalization on the Uptake and Penetration of Anti-HER2 Antibodies in Solid Tumors. Cancer Res 71, 2250–2259. https://doi.org/10.1158/0008-5472.CAN-10-2277

Saito, Y., Hashimoto, Y., Kuroda, J., Yasunaga, M., Koga, Y., Takahashi, A., Matsumura, Y., 2011. The inhibition of pancreatic cancer invasion-metastasis cascade in both cellular signal and blood coagulation cascade of tissue factor by its neutralisation antibody. European Journal of Cancer 47, 2230–2239. https://doi.org/10.1016/j.ejca.2011.04.028

Satake, N., Duong, C., Yoshida, S., Oestergaard, M., Chen, C., Peralta, R., Guo, S., Seth, P.P., Li, Y., Beckett, L., Chung, J., Nolta, J., Nitin, N., Tuscano, J.M., 2016. Novel Targeted Therapy for Precursor B-Cell Acute Lymphoblastic Leukemia: Anti-CD22 Antibody-MXD3 Antisense Oligonucleotide Conjugate. Mol Med 22, 632–642. https://doi.org/10.2119/molmed.2015.00210

Senter, P.D., Sievers, E.L., 2012. The discovery and development of brentuximab vedotin for use in relapsed Hodgkin lymphoma and systemic anaplastic large cell lymphoma. Nat Biotechnol 30, 631–637. https://doi.org/10.1038/nbt.2289

Smith, C.I.E., Zain, R., 2019. Therapeutic Oligonucleotides: State of the Art. Annu. Rev. Pharmacol. Toxicol. 59, 605–630. https://doi.org/10.1146/annurev-pharmtox-010818-021050

Stavropoulou, V., Kaspar, S., Brault, L., Sanders, M.A., Juge, S., Morettini, S., Tzankov, A., Iacovino, M., Lau, I.-J., Milne, T.A., Royo, H., Kyba, M., Valk, P.J.M., Peters, A.H.F.M., Schwaller, J., 2016. MLL-AF9 Expression in Hematopoietic Stem Cells Drives a Highly Invasive AML Expressing EMT-Related Genes Linked to Poor Outcome. Cancer Cell 30, 43–58. https://doi.org/10.1016/j.ccell.2016.05.011

Stein, P.D., Beemath, A., Meyers, F.A., Skaf, E., Sanchez, J., Olson, R.E., 2006. Incidence of Venous Thromboembolism in Patients Hospitalized with Cancer. The American Journal of Medicine 119, 60–68. https://doi.org/10.1016/j.amjmed.2005.06.058

van der Velden, V.H.J., te Marvelde, J.G., Hoogeveen, P.G., Bernstein, I.D., Houtsmuller, A.B., Berger, M.S., van Dongen, J.J.M., 2001. Targeting of the CD33-calicheamicin immunoconjugate Mylotarg (CMA-676) in acute myeloid leukemia: in vivo and in vitro saturation and internalization by leukemic and normal myeloid cells. Blood 97, 3197–3204. https://doi.org/10.1182/blood.V97.10.3197

Vickers, T.A., Crooke, S.T., 2014. Antisense Oligonucleotides Capable of Promoting Specific Target mRNA Reduction via Competing RNase H1-Dependent and Independent Mechanisms. PLoS ONE 9, e108625. https://doi.org/10.1371/journal.pone.0108625

Walter, R.B., Raden, B.W., Kamikura, D.M., Cooper, J.A., Bernstein, I.D., 2005. Influence of CD33 expression levels and ITIM-dependent internalization on gemtuzumab ozogamicin–induced cytotoxicity Blood 105, 1295-1302.

Wang, S., Sun, H., Tanowitz, M., Liang, X., Crooke, S.T., 2016. Annexin A2 facilitates endocytic trafficking of antisense oligonucleotides. Nucleic Acids Res gkw595. https://doi.org/10.1093/nar/gkw595

Welch, J.S., Ley, T.J., Link, D.C., Miller, C.A., Larson, D.E., Koboldt, D.C., Wartman, L.D., Lamprecht, T.L., Liu, F., Xia, J., Kandoth, C., Fulton, R.S., McLellan, M.D., Dooling, D.J., Wallis, J.W., Chen, K., Harris, C.C., Schmidt, H.K., Kalicki-Veizer, J.M., Lu, C., Zhang, Q., Lin, L., O'Laughlin, M.D., McMichael, J.F., Delehaunty, K.D., Fulton, L.A., Magrini, V.J., McGrath, S.D., Demeter, R.T., Vickery, T.L., Hundal, J., Cook, L.L., Swift, G.W., Reed, J.P., Alldredge, P.A., Wylie, T.N., Walker, J.R., Watson, M.A., Heath, S.E., Shannon, W.D., Varghese, N., Nagarajan, R., Payton, J.E., Baty, J.D., Kulkarni, S., Klco, J.M., Tomasson, M.H., Westervelt, P., Walter, M.J., Graubert, T.A., DiPersio, J.F., Ding, L., Mardis, E.R., Wilson, R.K., 2012. The Origin and Evolution of Mutations in Acute Myeloid Leukemia. Cell 150, 264–278. https://doi.org/10.1016/j.cell.2012.06.023

Wilson, T.R., Fridlyand, J., Yan, Y., Penuel, E., Burton, L., Chan, E., Peng, J., Lin, E., Wang, Y., Sosman, J., Ribas, A., Li, J., Moffat, J., Sutherlin, D.P., Koeppen, H., Merchant, M., Neve, R., Settleman, J., 2012. Widespread potential for growth-factor-driven resistance to anticancer kinase inhibitors. Nature 487, 505–509. https://doi.org/10.1038/nature11249

Wu, H., Lima, W.F., Zhang, H., Fan, A., Sun, H., Crooke, S.T., 2004. Determination of the Role of the Human RNase H1 in the Pharmacology of DNA-like Antisense Drugs. Journal of Biological Chemistry 279, 17181–17189. https://doi.org/10.1074/jbc.M311683200

Younes, A., Bartlett, N.L., Leonard, J.P., Kennedy, D.A., Lynch, C.M., Sievers, E.L., Forero-Torres, A., 2010. Brentuximab Vedotin (SGN-35) for Relapsed CD30-Positive Lymphomas. N Engl J Med 363, 1812–1821. https://doi.org/10.1056/NEJMoa1002965

CHAPTER FIVE

UNIVERSAL ENDOSOMAL ESCAPE DOMAINS

UNIVERSAL ENDOSOMAL ESCAPE DOMAINS

ABSTRACT

Advances in oligonucleotide chemistry have led to significant improvements in the stability, potency, and versatility of RNA therapeutics. Oligonucleotides stand at the forefront of precision medicine. A high degree of target specificity has led to success in the clinic for oligonucleotide therapeutics with targets in the liver, central nervous system, and muscles. However, current oligonucleotide therapies are limited by their delivery systems: lipid nanoparticles and GalNAc primarily deliver oligos to the liver only, while local administration of oligonucleotides is required for targets in central nervous system. Systemic extrahepatic targeting remains a challenge in large part due to the difficulty for therapeutics to reach the cytoplasm of target cells. Monoclonal antibodies can adeptly target cell receptors beyond the liver with excellent binding affinity, but cannot deliver their cargo into the cytoplasm. Moreover, only a limited number of antisense oligonucleotides can traverse the endosome unassisted to reach the cytoplasm or nucleus where they effect their gene silencing function. Failure to escape the endosome results in attenuated therapeutic efficacy at best.

Existing peptide transduction domains or cell penetrating peptides attempt to circumvent this obstacle, but fall short for numerous reasons and can be technically difficult to incorporate into larger macromolecular conjugates. Nature has provided some successful models for endosomal escape. However, these approaches can be difficult to synthetically reproduce or incorporate into macromolecular therapeutics while maintaining an acceptable safety and toxicity profile for clinical use. Our lab has been developing a wide array of molecules, termed universal endosomal escape domains, to try to overcome current limitations. This chapter will provide a general overview of these endosomal escape domains, their purification, conjugations, and some related results observed up until now.

INTRODUCTION

Decades of research has led to the use of various 2'-modifications in the ribose sugar (most commonly 2'-OMe and 2'-F) and phosphorothioate modifications to the backbone (Smith and Zain, 2019). The wide variety of modifications have significantly increased oligonucleotides' metabolic stability and potency (Setten et al., 2019). Superb binding affinities and customizability have allowed oligonucleotides to epitomize precision medicine. An oligonucleotide's pharmacokinetic properties, such as the stability conferred by sugar and backbone modifications, can be optimized independently of its pharmacophore properties, namely nucleotide sequence (Khvorova and Watts, 2017). And yet, for all their potential, oligonucleotides have limited therapeutic efficacy on their own.

Oligonucleotide therapies currently in clinical use have succeeded for a variety of reasons. Patisiran (Alnylam Pharmacueticals) consists of 19 + 2-mer with partially 2'-OMe modified siRNA within a lipid nanoparticle (LNP) formulation that targets the TTR gene in patients with hereditary transthyretin amyloidosis (Roberts et al., 2020; Hu et al., 2020). Givosiran (Alnylam Pharmaceuticals) is the first GalNAc-siRNA conjugate that targets the ALAS1 gene in patients with acute hepatic porphyria that significantly reduced porphyria attacks in patients (Balwani et al., 2020). Inclisiran (Alnylam/Novartis) is another GalNAc-siRNA conjugate that targets proprotein convertase subtilisin-kexin type 9 (PCSK9) in patients with hypercholesteremia and atherosclerotic cardiovascular disease to inhibit binding to the low-density lipoprotein (LDL) receptors (Kosmas et al., 2018). Both LNPs and GalNAc targeting vehicles accumulate in or localize almost exclusively in the liver. These delivery vehicles are highly adept at liver targeting but cannot reliably target other tissues. Even in these cases, only a small fraction of siRNAs escapes into the cytoplasm, ~0.3% siRNAs from GalNAc-siRNA conjugates manage to escape into the hepatocyte cytoplasm (Brown et al., 2020).

Local administration has also led to effective clinical responses with some ASOs. Intrathecal administration of nusinersen (Ionis Pharmaceuticals) leads to effective distribution of

this ASO throughout the cerebrospinal fluid and brain parenchyma in patients with spinal muscular atrophy (SMA) (Wurster and Ludolph, 2018). Fomivirsen was a first generation ASO that was administered via intravitreal injection. Other ASOs for Duchenne's muscular dystrophy are administered intravenously for systemic distribution, such as eteplirsen (Sarepta Therapeutics), golodirsen (Sarepta), and viltolarsen (Nippon Shinyaku) (Gagliardi and Ashizawa, 2021), though it can reasonably be expected that targeted delivery of these ASOs would significantly improve their potency while reducing their toxicity profiles.

Monoclonal antibodies (mAbs) are highly attractive delivery vehicles for oligonucleotides and other drugs. Unfortunately, mAbs are not able to escape from the endosome into the cytoplasm after endocytosis. As described in the previous chapter, attempts at antibody-RNA conjugates have resulted in minimal activity, but lots of therapeutic potential. mAbs are either recycled back to the plasma membrane or degraded in the lysosome (Ritchie et al., 2013). Ultimately, the problem of ARCs is not necessarily about mAbs, because mAbs excel at targeting specific cell surface receptors, but rather, the problem that ARCs have is an absence of endosomal escape motifs to aid the conjugate after endocytosis. The following discussion builds on the corresponding section in Chapter One and details possible mechanisms employed by cell penetrating peptides (CPPs), also known as peptide transduction domains (PTDs).

Revisiting Cell Penetrating Peptides (CPPs)/Peptide Transduction Domains (PTDs)

There are multiple factors that influence the ability of a CPP/PTD to access a cell's cytoplasm, including peptide sequence, physical-chemical properties of a peptide, local peptide concentration, local lipid composition, and cellular interactions with the peptide (Kauffman et al., 2015). Cytosolic access can occur by a variety of internalization mechanisms. CPP activity can involve direct lysis of the plasma membrane (undesirable for therapeutics), spontaneous membrane translocation by passive diffusion across the membrane, energy-dependent membrane translocation that usually involves endocytosis followed by changes in endosomal

conditions (i.e., pH) that can activate peptide function, localized or temporary disruption of the plasma membrane upon reaching certain conditions (i.e., reaches a threshold localized peptide concentration), or energy-dependent plasma membrane disruption where certain triggering conditions lead to endosomal membrane disruption (i.e., local peptide concentration, pH changes, etc.) (Kauffman et al., 2015).

Endocytic pathways are commonly used by pathogens. For example, the anthrax toxin and the vesicular stomatitis virus (VSV) are both readily endocytosed into cells. Anthrax is composed of three polypeptide chains, one of which (protective antigen) forms a complex with the other two (lethal factor, oedema factor) and effectively binds cell surface receptors to trigger endocytosis (Gruenberg and van der Goot, 2006). Once inside, endosomal acidification leads to the protective antigen insertion into the membrane of intralumenal vesicles and formation of a channel that allows the lethal factor and oedema factor to translocate through the channel and reach the cytoplasm (Gruenberg and van der Goot, 2006). VSV is an enveloped virus that is internalized into cells via clathrin-mediated endocytosis, sent through multivesicular bodies (MVBs) and, with endosomal acidification, uses its envelope to fuse to the membrane of intralumenal vesicles where eventual release of the nucleocapsid into the cytoplasm occurs (Lichty et al., 2004; Le Blanc et al., 2005). Both anthrax and VSV ultimately rely on interactions between the intralumenal vesicles and endosomal membrane for the productive release of toxin/viral material into the cell cytoplasm.

The naturally occurring *tat* sequence comes from the *tat* transcription factor of the human immunodeficiency virus (HIV) that contains an arginine-rich motif and is internalized by endocytosis (Kaplan et al., 2005). Experimentation with shorter versions of the TAT protein led to the identification of a critical nine amino acid sequence, rich in arginine residues (RKKRRQRRR), as the main driver of cell transduction (Lönn and Dowdy, 2015). The shorter peptide sequence allowed for easier incorporation into macromolecular conjugates. TAT-mediated cellular uptake relies on macropinocytosis (Wadia et al., 2004). TAT and many other

CPP/PTDs involve electrostatic interactions between the cationic delivery peptides and the anionic cell surface molecules, especially glycosaminoglycans (Vives, 2003; Chen et al., 2015). Most CPPs are short cationic peptides that rely on electrostatic interactions with cell surface molecules for efficient internalization.

Mutation experiments of the trans-activating protein led to the discovery of penetratin, a 16-residue helix from antennapedia homeoprotein (from *Drosophila*) that mediates internalization through endocytosis (Derossi et al., 1994; Dupont et al., 2011). Penetratin is also a positively charged peptide that binds to negatively charged glycosaminoglycans and to anionic lipids on the cell surface. It can internalize by direct translocation into cells or by endocytosis, depending on cell membrane composition and peptide concentration, but interestingly has a similar binding affinity to phospholipid membrane models that lack glycosaminoglycans (Alves et al., 2011). However, penetratin is highly dependent on the presence of glycosaminoglycans for internalization (Bechara et al., 2015). When penetratin is present at high density on the plasma membrane, it aggregates into B-sheet structures that leads to the disruption of synthetic membranes (Lee et al., 2010).

As discussed in Chapter One, melittin is a 26-amino acid alpha helical peptide that forms pores in the membranes it encounters. Derived from the European honeybee, it can lyse membranes after it reaches a critical concentration and reconfiguration in position (Lee et al., 2008; Hou et al., 2015). Because of its high toxicity, melittin is a highly impractical peptide for reliable use *in vivo*. One group coupled melittin to liposomes by the introduction of functionalized polyethylene glycol (PEG)-lipids to physically sequester melittin until it reached the endosomal compartment where the increased acidification would cleave the hydrazone linker and release melittin inside of endosomes (Oude Blenke et al., 2017). In this case, the chemistries used for the simple conjugates are incompatible with proteins and antibodies, rendering this approach impractical for *in vivo* applications. Arrowhead Pharmaceuticals utilized melittin in GalNAc conjugate with cholesterol and pH-sensitive masking of the melittin group to

show an increased endosomal escape rate in the liver (Wong et al., 2012). Arrowhead's compounds in clinical trials, ARC-520 and ARC-521 contained siRNAs targeting the X gene in Hepatitis B cases, but their clinical trials were stopped by the FDA due to extensive toxicity and the death of a non-human primate in preclinical studies (Springer and Dowdy, 2018). Melittin, though effective at pore formation through membranes, remains too toxic for reliable use in therapeutics.

One more notable example of successful endosomal escape is found with the influenza virus. The influenza virus' hemagglutinin (HA) N-terminal domain is a pH-sensitive amphipathic fusion domain with alpha-helical conformation that inserts itself into the endosomal membrane and at an endosomal pH of 5 changes in conformation to create a sharp bend and thereafter a hydrophobic pocket (Han et al., 2011). This conformational change into a V-shaped structure triggers a viral-host cell membrane fusion that can stress and disrupt the lipid membrane stability, facilitating the formation and enlargement of fusion pores (Han et al., 2011). The addition of the HA2 domain, consisting of the N-terminal 20 amino acids of the hemagglutinin protein, to a TAT-peptide enhanced endosomal escape *in vitro* as observed by increased GFP expression in a TAT-Cre reporter system (Wadia et al., 2004).

There are some limitations to a large number of reported CPPs in the literature. A compiled database of 747 unique CPPs revealed that 63% of CPPs deliver only dyes and 33% deliver other small molecules strictly as proof of principle analyses, while delivery of larger, clinically useful molecules like proteins or oligonucleotides are much rarer in CPP literature (Kauffman et al., 2015). This is significant because larger macromolecules or conjugates may affect how a CPP interacts with the plasma and endosomal membranes and may not be effectively predicted by simple, smaller CPP-dye conjugates. The use of CPPs to help endosomal escape for clinically useful molecules remains a challenge.

Efficiency and mechanism of internalization of CPPs varies significantly and can overlap between the different types of internalization mechanisms previously mentioned (Gautam et al.,

2012). Predicting a CPP's mode of action is difficult to do and cannot reliably be achieved simply with the peptide sequence and structure information (Gautam et al., 2012). Many factors contribute to the efficacy and mechanism of CPPs, including peptide concentration, local concentration at the membrane, lipid composition, and specific cell surface protein interactions with the CPP and different mechanisms can potentially be employed by the same CPP under different conditions (Kauffman et al., 2015). Moreover, synthetic lipid membrane models fall short of accurately representing the complexity and heterogeneity of cell membranes, further weakening the predictive power of synthetic modeling (Wimley and Hristova, 2011; Kauffman et al., 2015). Another key limitation of CPPs is the exceptionally high peptide concentration required for successful internalization into the cell cytoplasm, usually in the low micromolar range and often requiring a 10 μM concentration for efficacy (Melikov et al., 2015; Tünnemann et al., 2006; Hällbrink et al., 2004; Lönn et al., 2016). However, exorbitantly high peptide concentrations will saturate the cell surface and may interfere with proper cellular functions and viability.

There is a great need for a structurally defined molecule that can enhance endosomal escape without toxicity or a high concentration requirement. Our lab is currently developing a new type of molecule, termed a universal endosomal escape domain (uEED), that is chemically customizable with modifications for site-specific conjugations, modular in structure to allow length adjustment, and intended to be compatible with current purification procedures for incorporation into larger macromolecular conjugates. uEEDs remain a work in progress, as the next section will describe.

RESULTS & DISCUSSION

Our lab recently developed a platform to synthesize a wide array of molecules termed universal endosomal escape domains (uEEDs). uEEDs are hydrophilic-masked molecules with a hydrophobic core that is designed to embed itself into the endosomal membrane after the

hydrophilic mask is removed inside of the endosome (**Figure 5.1**). The synthesis platform for uEEDs allows for highly customizable multimeric units of uEED to be produced to achieve variable lengths. The hydrophilic mask improves the stability and solubility of the uEED and the larger molecule that it is conjugated to. The objective is for the hydrophobic core units within the uEED multimers to embed themselves into the endosomal membrane with sufficiently high local concentration to destabilize it and allow the oligonucleotides to escape into the cytoplasm. The uEED molecules can be modified with different chemical groups to enable conjugations with oligonucleotides. Oligonucleotides can be conjugated to a monoclonal antibody (mAb) via various linkers that were described in previous chapters. Incorporating uEEDs into antibody-RNA conjugates (ARCs) is a straightforward process that builds on the procedures described in Chapter Three and Chapter Four. One such example will be described later. A uEED is designed to facilitate endosomal escape of the oligonucleotide into the cytoplasm (**Figure 5.2**). There are variable chemical or structural modifications that can be implemented to try to enable its intended endosomal escape function. While initial versions of uEEDs have not produced the desired endosomal escape, there is at least one new version of uEED currently under development that remains to be examined and tested. The platform used to produce uEEDs enables a wide latitude of customizability for the development and testing of future generations of uEEDs.

Initial work centered around the optimization of the conjugation reactions between uEEDs and siRNA and purification conditions for these conjugates. A variety of uEED lengths were produced, termed Qb6, Qb12, and Qb18, wherein Qb6 refers to a uEED composed of 6 monomeric units of the uEED (Figure 5.1). The initial conjugation chemistry used was an oxime ligation, wherein an aldehyde or benzaldehyde group is conjugated to an aminooxy group with the addition of an aniline or other catalyst to form a stable oxime linkage (**Figure 5.3a**) (Ulrich et al., 2013; Rashidian et al., 2013). Test conjugation reactions were set up by aliquoting 0.3 nanomoles (nmoles) of a biotinylated GFP passenger strand with a benzaldehyde modification

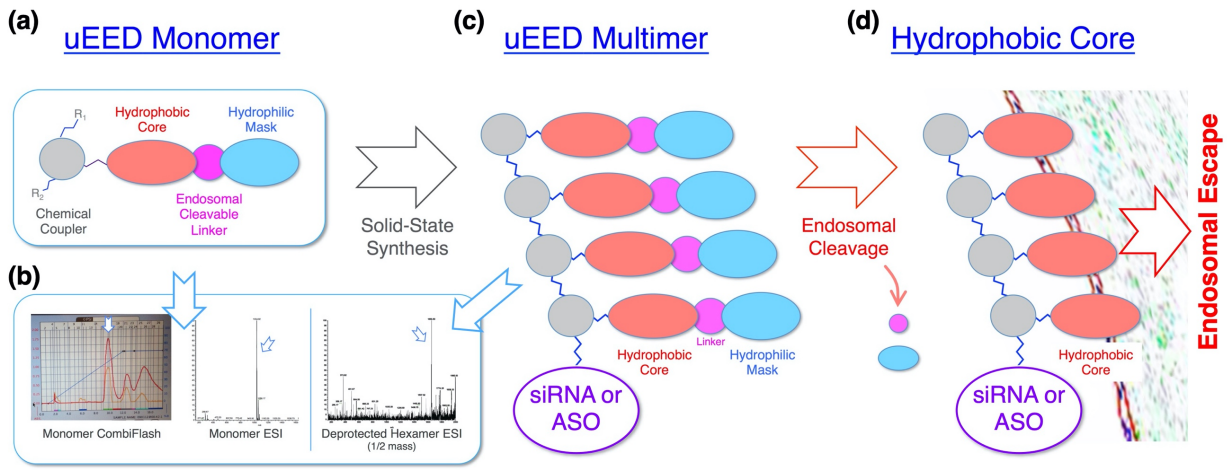

Figure 5.1. Universal Endosomal Escape Domain Overview
(**a**) The basic monomeric unit of a universal endosomal escape domain (uEED) consists of a chemical coupler, a hydrophobic core, cleavable linker designed to dissociate in the endosome, and a hydrophilic mask for greater stability and solubility. (**b**) Purification of uEEDs produce the desired peak whose mass is confirmed by electrospray mass spectrometry. (**c**) uEED monomers can be assembled as multimers to include 6, 12, 18, or any other length of individual monomers. It contains an azide modification for conjugation onto siRNAs or ASOs via copper-free click chemistry. (**d**) Upon internalization into the endosome, endosomal conditions will lead to the cleavage of the uEED linker and removal of the hydrophilic masks. When the hydrophobic cores are exposed, they are expected to insert themselves into the endosomal membrane and lead to localized destabilization.

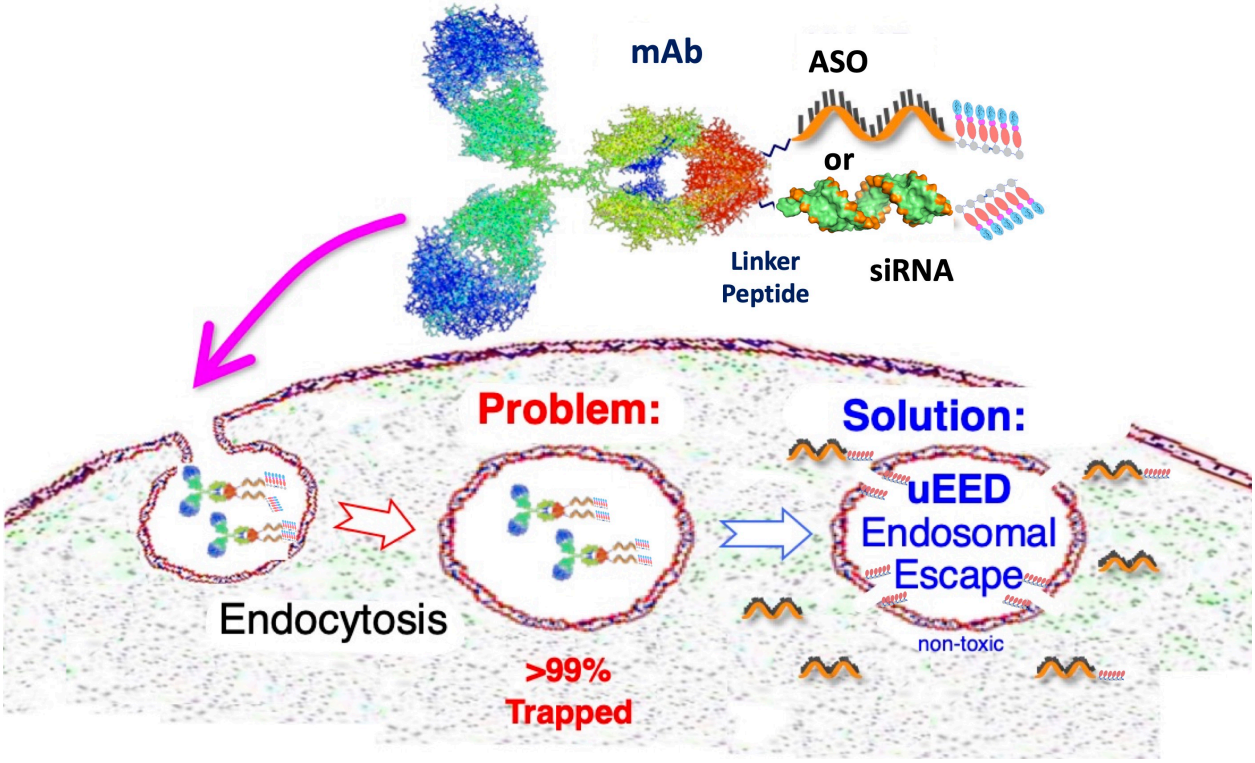

Figure 5.2. Schematic for ARC-uEED Mechanism.
Universal endosomal escape domains can be conjugated onto either siRNAs or ASOs. The oligo-uEED conjugate will then be conjugated onto a peptide linker as previously described, which in turn will be conjugated via the MTGase enzyme onto the MTG handles of a monoclonal antibody. The objective is for uEEDs to facilitate endosomal escape by exposing their hydrophobic cores inside the acidic endosome and allowing them to embed into the endosomal membrane to destabilize it sufficiently for the oligonucleotides to reach the cytoplasm. Abbreviations: mAb, monoclonal antibody; ASO, antisense oligonucleotide; siRNA, short interfering RNA; uEED, universal endosomal escape domain.

into separate tubes. A 5% aniline solution was prepared by diluting 100% aniline in 50% acetonitrile (ACN). Test reactions were prepared in ammonium acetate buffer (400 mM final) and individual components were added to 0.3 nmoles of the siRNA passenger strand. Qb6 uEEDs were added to the reaction mixture to achieve final excess molar ratios of uEED:oligo of 1:1, 5:1, 10:1, and 25:1. 5% aniline was added to achieve a final 1% content within the reaction volume. Test reactions were incubated at room temperature overnight in the dark, or for about 20 hours. The following day, 0.2 nmoles (two-thirds of the reaction) was separated from each reaction and brought up with 20 µL of 50% ACN. Samples were dried down by vacuum evaporation. Next, samples were resuspended in 10 µL of 2X formamide loading buffer and loaded into a 15% urea gel. The urea gel was run at 200V for 50 min followed by methylene blue staining and imaging on a gel dock (**Figure 5.3b**). A control HyNic conjugation was performed on an available M-lycotoxin (dMLG) peptide in 5-fold molar excess, using the same catalyst and same reaction conditions as the oxime ligation to verify the conjugation ability of the siRNA passenger strand and the reagents' viabilities. Conjugation efficiencies were poor until the highest ratio tested at 25:1 (uEED:oligo), which was moderately efficient. It is important to note that the composition of the uEEDs does not run as well on a urea gel leading to the observed smears for these samples. The dMLG test HyNic conjugation proceeded with greater efficiency though even a 5-fold molar excess is likely not enough for this specific peptide either. These results indicate that a high molar excess ratio of uEED will be required for adequate ARC preparation with Qb6 uEEDs. The oxime ligation chemistry may not be the most efficient for use in large-scale conjugate production due to the high molar requirement of uEEDs.

The remaining 0.1 nmoles of test reaction samples were analyzed by matrix-assisted laser desorption/ionization time-of-flight (MALDI-TOF) mass spectrometry. MALDI-TOF mass spectrometry uses a pulsed laser to hit the loaded samples over individual shots in their loading matrices to ionize and cause desorption (release from the surface) of the sample to generate ions from more complex molecules. MALDI-TOF then reflects the ions with an electric field that

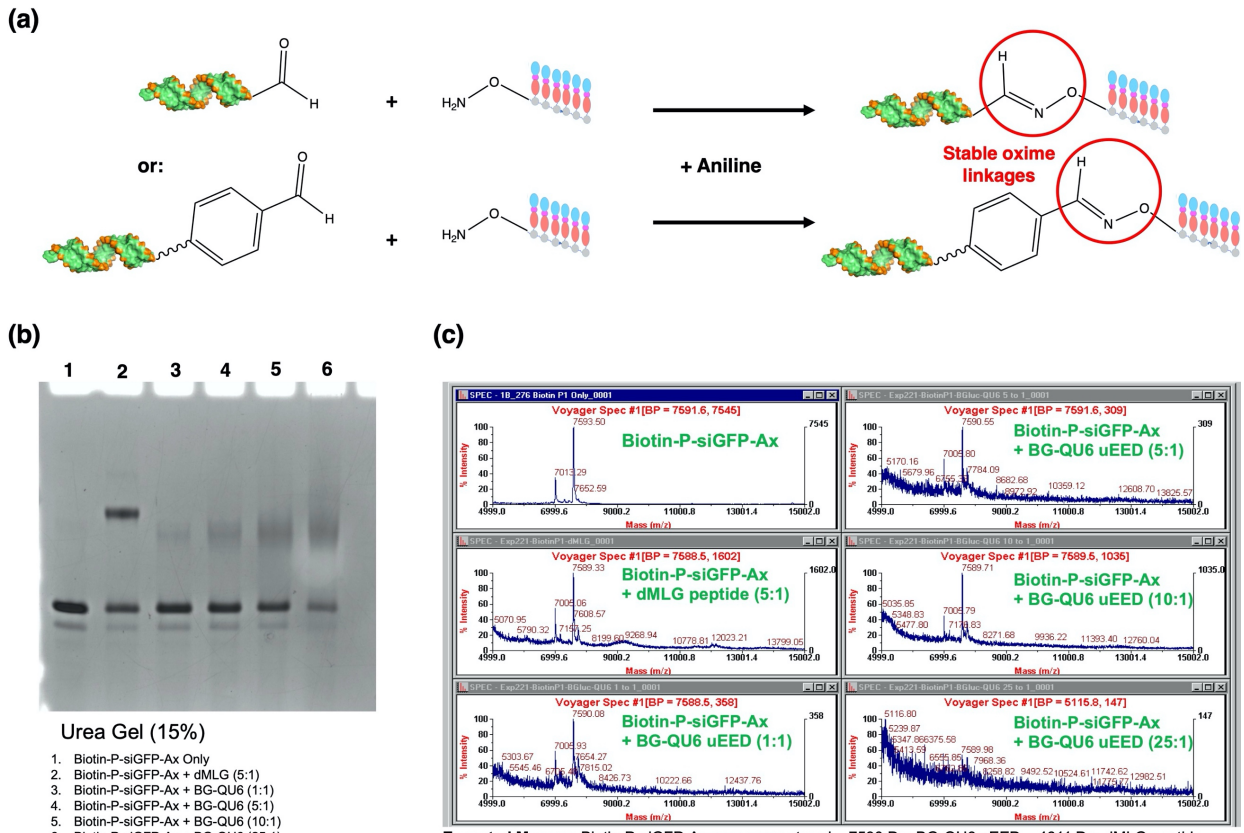

Expected Masses: Biotin-P-siGFP-Ax passenger strand – 7590 Da; BG-QU6 uEED – 4611 Da; dMLG peptide – 4449 Da; siGFP-uEED – 12039 Da; siGFP-dMLG – 12201.

Figure 5.3. Oxime Ligation Test Conjugations.
The initial approach to incorporating uEEDs into oligonucleotide conjugates. (**a**) Oxime ligation conjugation reaction uses an aniline catalyst to create stable oxime linkages between aldehyde or benzaldehyde groups and amino-oxy groups. (**b**) Urea gel (15%) to assess conjugation efficiency between an siGFP passenger strand and the BG-QU6 uEEDs after an overnight oxime ligation conjugation reaction. Methylene blue staining followed by gel dock imaging with the Coomassie blue filter settings. Note that the urea gel ratios displayed represent either dMLG peptide-to-siGFP passenger strand molar ratio or uEED-to-siGFP passenger strand molar ratio. (**c**) MALDI-TOF spectra of the conjugation reactions shown in the urea gel in (b). Expected masses are as indicated. THAP matrix was used to prepare and load samples onto plate. MALDI settings: negative mode; laser intensity = 3220; shots/spectrum = 400; delay (nsec) = 100; mass range (Da) 5,000-15,000; low mass gate (Da) = 500. Abbreviations: uEED, universal endosomal escape domain; Biotin-P-siGFP-Ax, or siGFP, both refer to biotinylated siGFP passenger strand with benzaldehyde modification.

shoots the ions through a tall column that analyzes the flight speed of ions, measuring mass over charge (m/z) of the original molecule. MALDI-TOF is used routinely for protein and oligonucleotide analyses, to verify purity and accurate mass measurements (Leushner, 2001). The oxime ligation test conjugation samples were loaded onto MALDI plates with (THAP) matrix and flown on a MALDI-TOF mass spectrometer to assess whether the shift in mass from uEED conjugation supports the urea gel results. While the urea gel showed at least small shifts from partial conjugations, mass spectrometry analyses failed to find any new peaks entirely, corresponding to the larger conjugate (**Figure 5.3c**). Expected mass shifts were absent from the mass spectra of these test conjugations. This may simply be attributed to the difficulty in successfully flying more complex molecules, especially these oligonucleotide-uEED conjugates.

At first, purification of uEED conjugates was done on a strong anion exchange (SAX) HPLC column (ZORBAX Ion Exchange - Strong Anion Exchange column, Agilent). The reason for opting for gradient purification by anion exchange was twofold. First, excess uEEDs needed to be separated from the oligo conjugate. Second, anion exchange would possibly allow for separation of different conjugate species (based on uEED multimer count as well as molecular changes in response to serum treatments) and thereby allow for analysis of relative mass shifts from different treatments.

A large-scale conjugation oxime ligation reaction was set up between a new batch of uEED (termed BG-UQb6 in this experiment) and an siGFP passenger strand with the benzaldehyde modification. To maintain a low reaction volume and thereby increase conjugation efficiency, uEED (157 nmoles) and siGFP (10 nmoles) components were aliquoted in separate tubes and allowed to dry overnight by vacuum evaporation. Reaction components were resuspended in 50% ACN and combined (15.7-fold excess of uEED relative to siGFP passenger strand). The final reaction volume was supplemented with ammonium acetate buffer and a final 1% aniline content. Oxime ligation reaction was incubated for 2 days at 37 ˚C on a PCR block. After the incubation period, 0.2 nmoles of the crude conjugate was run on a 15%

urea gel to assess the conjugation efficiency (**Figure 5.4a**). The extended incubation time and more concentrated oxime ligation proved to be more efficient than previously observed in this case, albeit uEED-containing conjugates still run as a smear, likely due to impurities from the uEED preparation in this crude conjugate.

Next, 50% ACN was added to bring up the final volume to 150 µL in preparation for loading into the HPLC. Conjugate was loaded onto the HPLC and run on an ammonium acetate gradient using the anion exchange SAX column. The conjugate came off in a clean peak (**Figure 5.4b**). Fractions for the siGFP-Qb6 conjugate were pooled and lyophilized overnight. siGFP-Qb6 was resuspended in 50% ACN on the following day and flown on the MALDI to check for a mass shift. Unfortunately, MALDI showed no spectra for any sample, likely due to the residual purification buffer that led to inadequate sample drying and some level of incompatibility with the THAP matrix that is normally used. Instead, the conjugate was lyophilized again, resuspended in 50% ACN and then re-purified on an HPLC C18 column for further cleaning and complete buffer exchange into 50% ACN. C18 purification resulted in a large, somewhat irregularly shaped peak from which 6 fractions were collected, pooled, and lyophilized overnight (**Figure 5.4c**). Conjugate was lyophilized overnight and resuspended in 50% ACN for a total of 3 times. Unfortunately, the double purification cycles resulted in a low final conjugate yield of about 25%, but it was more than sufficient to analyze the final conjugation efficiency.

A 15% urea gel was run to compare siGFP passenger strand only versus siGFP-Qb6 uEED conjugate (**Figure 5.4d**). The urea gel was stained with methylene blue prior to imaging. Results revealed an efficient conjugation reaction with a clean siGFP-Qb6 conjugate. siGFP-Qb6 and siGFP passenger strand only were spotted onto THAP matrix and analyzed by MALDI-TOF. MALDI spectra revealed a slightly raised peak close to the expected mass of the siGFP-Qb6 conjugate, albeit in relatively low resolution due to the difficulty of flying more complex molecules (**Figure 5.4e**). The MALDI-TOF cannot easily analyze uEED-containing conjugates

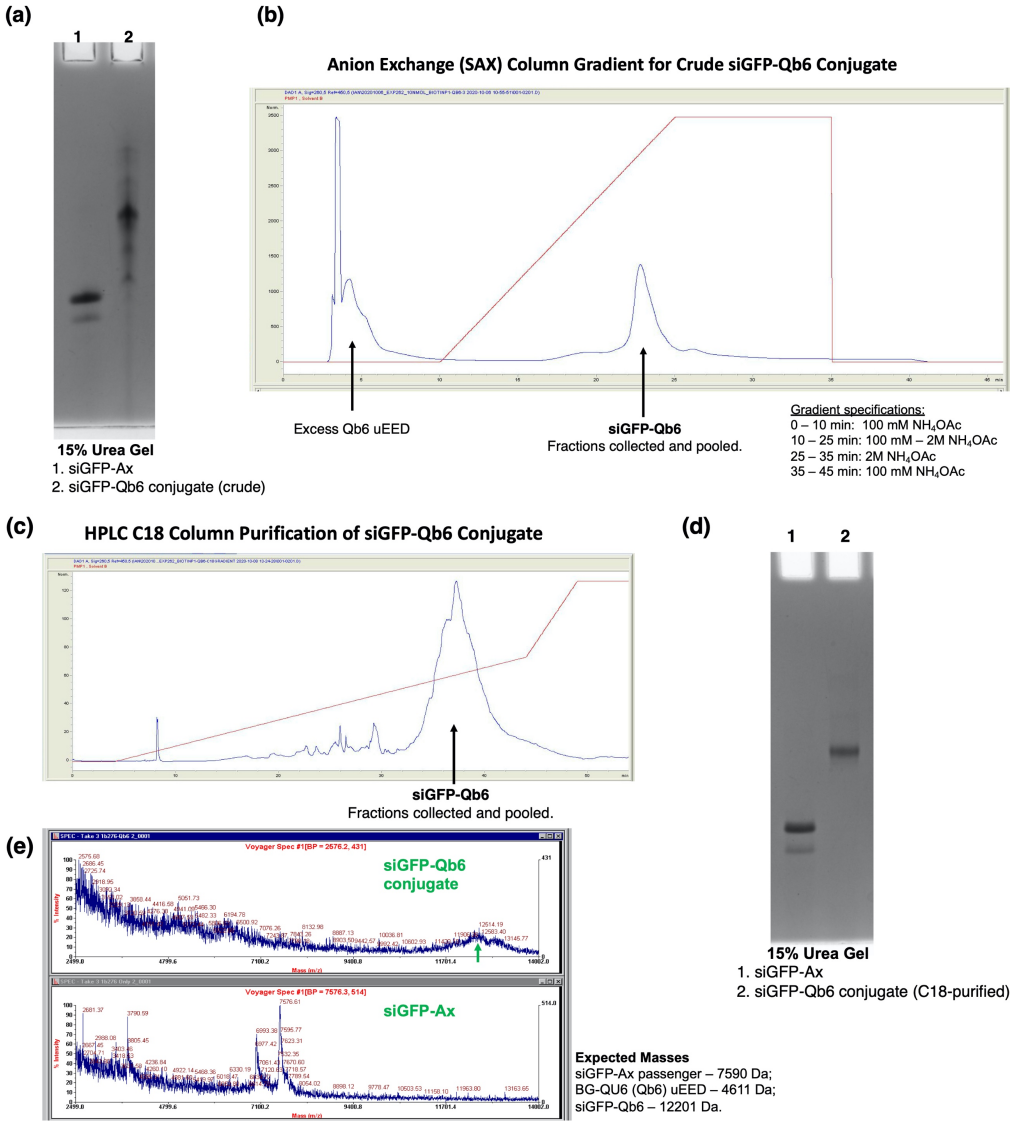

Figure 5.4. Large-Scale siGFP-Qb6 uEED Conjugate Workflow.
(a) Urea gel (15%) showing the crude siGFP-Qb6 conjugate after a 2-day incubation for oxime ligation reaction, compared to the siGFP passenger strand only. **(b)** Anion exchange purification with a SAX column on HPLC produces a clean peak for the siGFP-Qb6 conjugate and effectively removes excess unconjugated material. **(c)** C18 purification of siGFP-Qb6 conjugate performed to further clean the conjugate, results in a prominent peak whose fractions were collected and lyophilized 3 times. **(d)** Urea gel (15%) after C18 purification for comparison to starting passenger strand. **(e)** MALDI-TOF analysis to compare siGFP passenger strand and siGFP-Qb6 conjugate. Low, broad peak appears near expected conjugate mass (green arrow). THAP matrix was used for loading samples onto MALDI plate. MALDI settings: laser intensity = 963; shots/spectrum = 200; mass range (Da) = 3,000-14,000; Delay time = 150 nsec for conjugate and 125 nsec for oligo; negative mode. Abbreviations: Qb6, refers to the BG-QU6 uEED, a 6X uEED multimer; Ax, benzaldehyde modification for oxime ligation compatibility.

and in many previous cases was either inconsistent or not at all successful in detecting conjugate peaks or uEED-only peaks. One possible reason for the improved success in this case may be the extensive purification and lyophilization cycles that were performed prior to final analysis.

uEEDs are designed to perform their function when exposed to serum and then to the endosomal environment. Part of the synthesis process involves the inclusion of a methyl ester group on the hydrophilic mask of the uEED monomeric units. While this methyl ester would ordinarily interfere with the required lysosomal enzymatic function, uEED exposure to serum esterases can remove this methyl ester that remains from the synthesis stage and allow for proper enzymatic processing in the lysosome. After internalization, a lysosomal enzyme is expected to cleave off the hydrophilic mask of the uEED and expose the hydrophobic core.

To verify this activity for the Qb6 uEED, a biotin-siGFP passenger strand with a benzaldehyde modification was conjugated to a Qb6 uEED by the oxime ligation approach previously described using an 8-fold molar excess of Qb6 uEED. The siGFP-Qb6 conjugate was then incubated with either heat-inactivated human serum or N,N-Diisopropylethylamine (DIPEA), an amine and organic compound used as a base to mimic the function of the lysosomal enzyme. siGFP-Qb6 was incubated in DIPEA for 1 hr at room temperature or in human serum for 4 hr at 37 ˚C. Following incubation, serum-treated conjugate was cleaned up by isolating with streptavidin magnetic beads to remove unwanted serum components from the incubation mixture. siRNA pulldown with streptavidin magnetic beads was done on 0.5 nmoles of the conjugate and involved an NP40 wash buffer and 50% ACN in water as an elution buffer (refer to Chapter 2 for full details). siGFP-Qb6 conjugates were then duplexed with an siGFP guide strand modified with Cy3 dye for better visualization. Hybridization of the guide strand occurred by briefly heating both components at 65 ˚C and mixing in an equimolar ratio, followed by a 20-min room temperature incubation.

Samples were run on a 10% urea gel to compare to an untreated siGFP-Qb6 duplexed conjugate. Cells were imaged with a fluorescent filter for Cy3 dye on a gel dock to assess treatment effects on the conjugate (**Figure 5.5a**). Urea gel analysis revealed a lower molecular-weight species for the DIPEA-treated siGFP-Qb6 and established a baseline for the chemical mimic of lysosomal enzyme-mediated cleavage of the hydrophilic mask of the uEED. The serum-treated siGFP-Qb6 sample revealed a downward shift relative to the untreated conjugate but still above the serum-treated conjugate. This band was strongly indicative of the predicted intermediate species of the uEED after the methyl ester group has been removed but before being exposed to the lysosomal environment.

To confirm this assessment, individual monomeric units of the Qb6 uEED were exposed to either DIPEA or mouse serum. The hydrophobic core portion of a uEED monomer was run on a C18 HPLC column to establish a reference peak (**Figure 5.5b**). Monomeric Qb6 uEED units were prepared in a final 50 µL volume of 50% DMF in water followed by the addition of 100 µL mouse serum and a room temperature incubation for 4 hr. Serum proteins were precipitated out by the addition of 300 µL of 100% acetonitrile and supernatant was collected and dried by vacuum evaporation. Sample was resuspended in 50% ACN and a small fraction was run on an HPLC C18 column to assess condition of monomeric units after mouse serum treatment, monomeric unit at 0 hr (**Figure 5.5c**) and after 4 hr (**Figure 5.5d**). The most prominent peak near the center represents the methyl ester-containing uEED monomer (**Figure 5.5c**) and disappears after 4 hr in mouse serum (**Figure 5.5d**), demonstrating a rapid removal of the methyl ester group in mouse serum after just a few hours. The remainder of the serum-treated sample was mixed with the lysosomal enzyme (500 U/mL in 0.2% NaCl) and incubated at 37 ˚C for 18 hr. After incubation completion, the sample volume was brought up in 300 µL acetonitrile to precipitate out the enzyme, sample supernatant was vortexed and run through a C18 HPLC column (**Figure 5.5e**). The resulting HPLC trace reveals a new peak on the right that runs

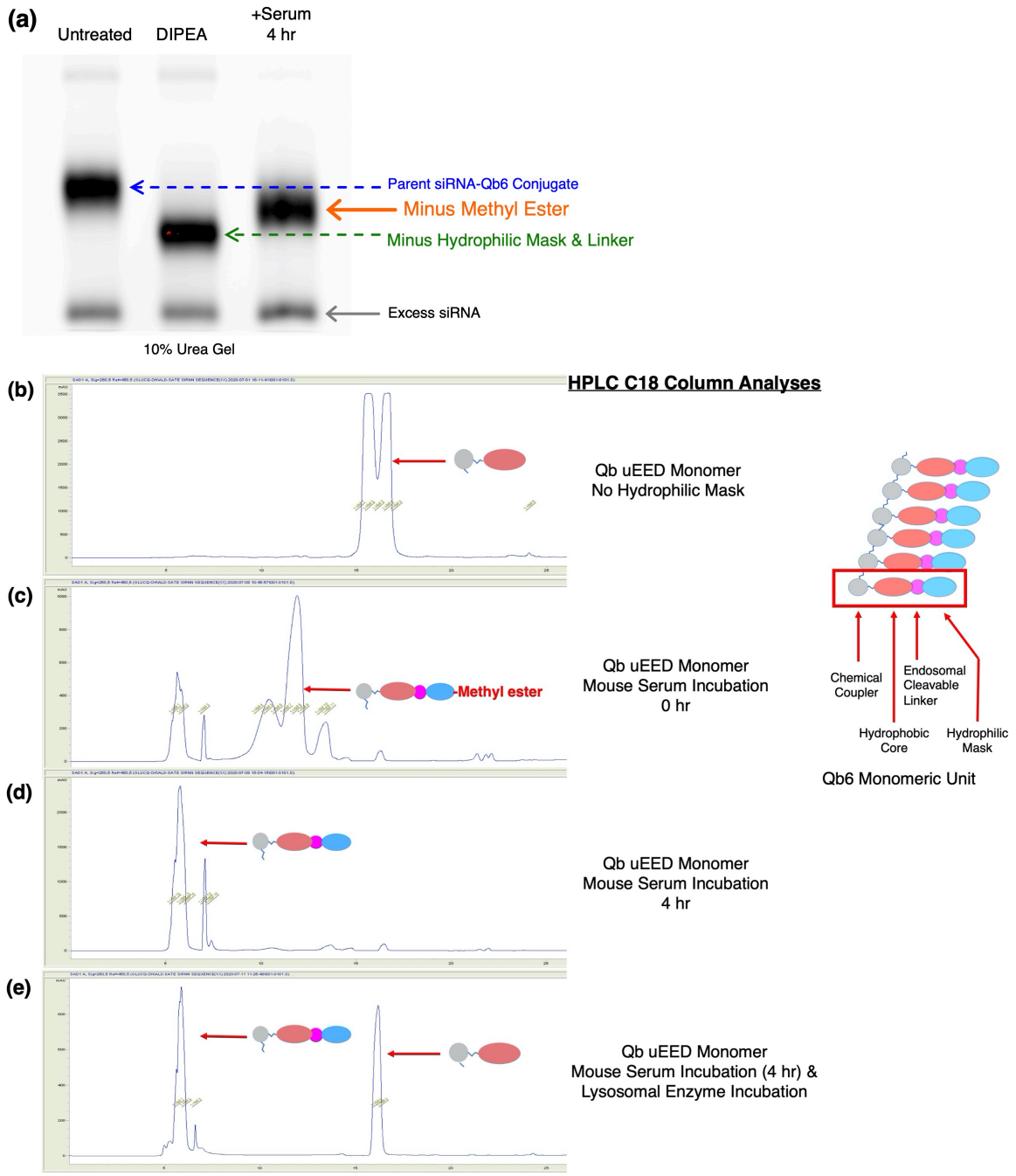

Figure 5.5. Qb uEED Monomer Serum Tests.
uEED serum testing to assess its functionality. (**a**) Urea gel (10%) analysis of siGFP-Qb6 conjugate: untreated, DIPEA treatment to mimic lysosomal enzyme, and serum treatment. Duplexed siGFP biotin passenger strand with Cy3-siGFP guide strand. (**b**) HPLC C18 column analysis of monomeric unit from Qb6 uEED without a hydrophilic mask or cleavable linker. (**c**) HPLC C18 column analysis of the full monomeric unit at the 0 hr time point in mouse serum. (**d**) HPLC C18 column analysis of the full monomeric unit after 4 hr incubation in mouse serum. (**e**) HPLC C18 column analysis of monomeric unit from Qb6 uEED after both mouse serum and lysosomal enzyme incubations. Abbreviations: Qb, a single uEED monomer; DIPEA, N,N-Diisopropylethylamine base and chemical mimic for lysosomal enzyme; uEED, universal endosomal escape domain.

in the same position where the control hydrophobic core portion of the uEED monomer appeared (**Figure 5.5b**). These results confirm the expected mechanism action of the Qb6 uEED. Serum exposure can remove the remaining methyl-ester group and subsequent exposure to the lysosomal enzyme will completely remove the hydrophilic mask to expose the uEED's hydrophobic core.

The reason for the earlier use of a SAX column for HPLC purification and assays was to use anion exchange to separate uEEDs and uEED conjugates in their different states (i.e., serum treatment, DIPEA treatment) and determine whether uEEDs functioned as predicted. The SAX column was never successful at separating uEEDs in their different states into clean peaks. Moreover, the use of ammonium acetate buffer made it difficult to work with these conjugates, fly on the MALDI, and led to the increased lyophilization and purification requirements. The use of urea gel analysis and HPLC analysis on a C18 column (Figure 5.5) obviated the need for a SAX column. The HPLC C18 column was thereafter used for any oligonucleotide, uEED, and uEED-conjugate purifications and analyses.

The inefficiency of the oxime ligation reaction previously observed and therefore the high molar requirement for uEED with this conjugation chemistry led to the identification of alternate chemistries and chemical modifications to the siRNA and uEEDs to facilitate the development of uEED-containing ARCs. Copper-free click chemistry relies on cyclooctyne addition between alkyne and azide groups, promoted by ring strain, very similarly to the copper-free click between azide and DBCO groups that was previously described. Therefore, the next generation of Qb6 uEEDs were synthesized with an azide group. An alternate conjugation approach for conjugating an oligonucleotide to a monoclonal antibody (mAb) is the inverse electron demand Diels-Alder click reaction between a tetrazine group and a trans-cyclooctene (TCO) groups and promoted by ring strain interactions (Oliveira et al., 2017; Sarrett et al., 2021) (**Figure 5.6a**). siRNA passenger strands were synthesized with terminal cyclooctyne (BCN) functionalized

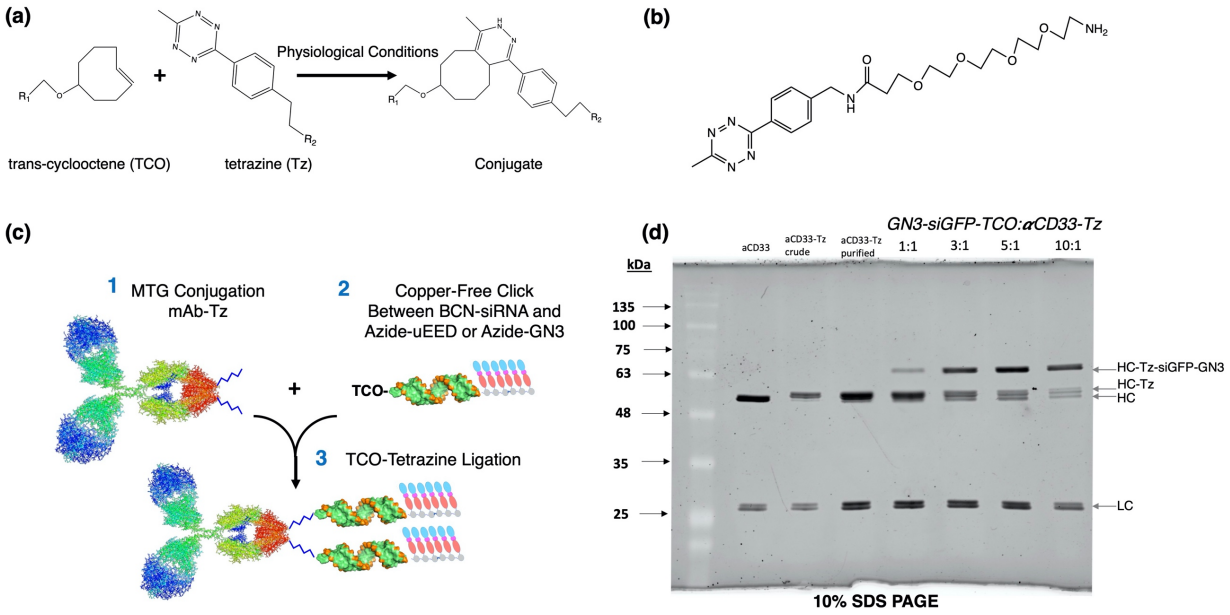

Figure 5.6. Overview of TCO-Tetrazine Ligation.
(**a**) Schematic of TCO-Tetrazine ligation between a TCO-containing molecule and a tetrazine-containing molecule. (**b**) Linker utilized was a commercially available methyltetrazine-PEG4-amine linker to enable a TCO-tetrazine ligation on one end and an MTG conjugation on the opposite end. (**c**) Schematic of conjugation reactions involved in building a more complex ARC with uEEDs or GN3. The first reaction is the MTG conjugation between the Tz linker and the anti-CD33 or other mAb. The second conjugation is the copper free click between the BCN group on the siRNA and the azide group on the uEED or the GN3 molecule. The third conjugation is the TCO-tetrazine ligation to obtain the final ARC product. (**d**) SDS PAGE (10%) gel of the TCO-Tz ligation test conjugations, testing different excess molar ratios of the siGFP-TCO conjugate. Note that siGFP-TCO had to be blocked with GN3-Azide to prevent cross reactivity with the TCO-Tz ligation. Molecular weight markers are shown in kilodaltons (kDa). Abbreviations: TCO, trans-cyclooctene group; Tz, tetrazine group; mAb, monoclonal antibody; BCN, terminal siRNA cyclooctene modification for copper-free click; GN3, tris-GalNAc-Azide; HC, heavy chain; LC, light chain.

group as well as a trans-cyclooctene (TCO) group for dual-conjugation capacity. A commercially available methyltetrazine-PEG4-amine linker was purchased (BroadPharm) (**Figure 5.6b**). The methyltetrazine-PEG4-amine linker allows for the conjugation between an mAb and the amine end of the linker via MTG conjugation and for an inverse electron demand Diels-Alder click reaction (TCO-tetrazine ligation) between the tetrazine end of the linker and the siRNA passenger strand's TCO modification (**Figure 5.6c**).

To determine the optimal conjugation ratio for the TCO-tetrazine ligation between the siRNA passenger strand and mAb, a large scale MTG conjugation was completed with 45-fold molar excess of methyltetrazine-PEG4-amine (Tz) linker to anti-CD33 mAb. Following this MTG conjugation, mAb-Tz was purified by size exclusion chromatography (SEC 650 column) on an FPLC to remove excess linker. The BCN group of an siGFP with BCN and TCO modfications was blocked with a tris-GalNAc-Azide (GN3-Az) group via copper free click chemistry (3-fold molar excess of GalNAc molecule) to prevent cross reactivity between the BCN group and the TCO-tetrazine ligation, resulting in a GN3-siGFP-TCO molecule ready for conjugation tests with mAb-Tz. Test conjugations were set up between the GN3-siGFP-TCO and mAb-Tz conjugates, with GN3-siGFP-TCO molar excess ratios of 1:1, 3:1, 5:1, and 10:1. After mixing the two components together, reactions were allowed to proceed for 4 hours at room temperature. Samples were loaded and run on a 10% SDS PAGE gel alongside mAb only, mAb-Tz (crude), and mAb-Tz (purified) (120V, 24 min → 180V, 36 min). SDS PAGE gel was then UV protein stained for about 20 min followed by imaging on a UV transilluminator gel dock (**Figure 5.6d**). The best conjugation ratio was determined to be 10:1 of siRNA-TCO excess or higher. The SDS PAGE gel shows the roughly 7.5 kDa expected shift after conjugation of siGFP passenger strand by this new conjugation approach. The shift from the conjugation of the methyltetrazine linker (MW 363.4) to the anti-CD33 mAb was very slight as expected.

Next, Qb6 uEEDs were incorporated into an anti-CD33 ARC. A GN3-control ARC was also made to be able to compare to the uEED-containing ARC. Test conjugation reactions were

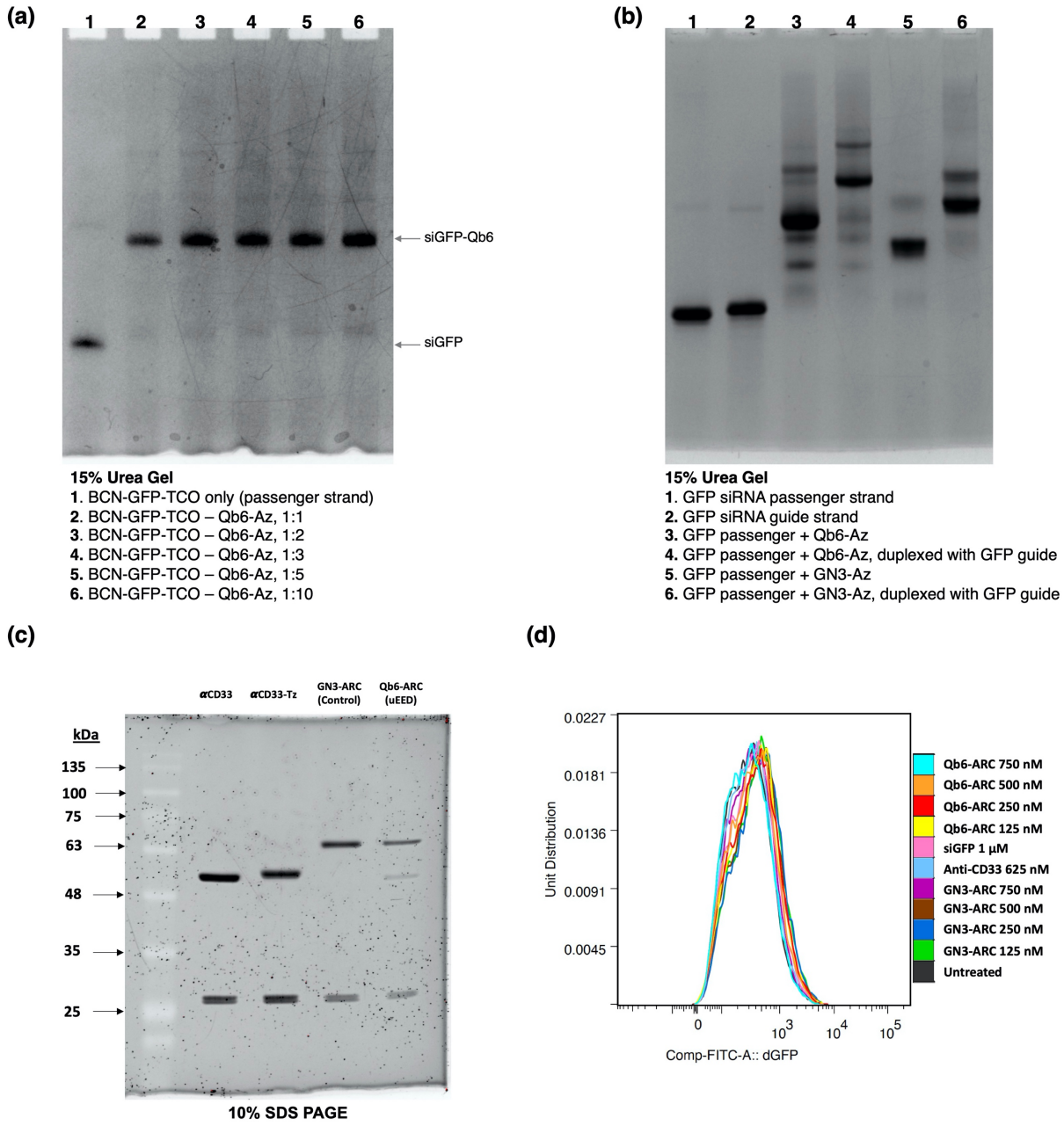

Figure 5.7. uEED- and Control-ARC Conjugations and Treatment
Optimization and conjugations for ARCs with uEEDs. (**a**) Copper-free click test conjugations between siGFP passenger strand and Qb6 uEEDs, 15% urea gel and methylene blue staining. (**b**) Analysis of siGFP-uEED conjugates after first conjugation and then after duplexing with guide strand, compared to individual siGFP strands, 15% urea gel and methylene blue staining. (**c**) Final ARCs: control (GN3-ARC) and uEED (Qb6-ARC) and the mAb-tetrazine conjugate intermediate step, compared to mAb only. 10% SDS PAGE gel with UV protein staining. Molecular weight markers shown are in kilodaltons (kDa). (**d**) Flow cytometry analysis of FITC signal to assess changes in GFP expression in THP-1 dGFP cell line. Abbreviations: BCN, cyclooctene modification; TCO, trans-cyclooctene modification; Qb6, uEED with 6 monomeric units; Az, azide for copper free click conjugation; GN3, tris-GalNAc.

set up to assess the efficiency of the copper free click reaction between the Qb6-Azide uEED and the BCN-siGFP-TCO passenger strand. Test conjugations were set up in PCR tubes to achieve Qb6-Az:siGFP ratios of 1:1, 2:1, 3:1, 5:1, and 10:1. Samples were incubated overnight at 37 ˚C. After the overnight incubation, samples were dried down by vacuum evaporation, resuspended in 50% ACN, and then dried down again by vacuum evaporation. This step was repeated twice more. Samples were resuspended in 2X formamide loading buffer and run on a 15% urea gel. The gel was stained with methylene blue followed by imaging (**Figure 5.7a**). The click reaction with BCN proceeded with great efficiency.

Larger-scale BCN conjugation reactions were set up between the BCN-siGFP-TCO passenger strand and either Qb6-Azide uEED or GN3-Azide for the control ARC with the azide-containing molecules in 3-fold molar excess to the siGFP passenger strands. Conjugations were incubated at 37 ˚C overnight. siGFP-Qb6 and siGFP-GN3 conjugates were duplexed with a siGFP guide strand by mixing the conjugates with the guide strand in a 1:1 molar ratio, heating at 65 ˚C for 5 min, and incubating at room temperature for 30 minutes. Aliquots were separated at every step of the conjugation process and then analyzed on a 15% urea gel to assess conjugation efficiencies (**Figure 5.7b**). The most prominent bands for each conjugate stage demonstrated a relatively high efficiency for both GN3- and Qb6- containing conjugates, despite additional bands that appeared from either impurities or aggregation between components.

A large scale MTG conjugation was set up between an anti-CD33 mAb and the methyltetrazine-PEG4-amine linker. The tetrazine linker was added in a 45-fold excess molar ratio relative to the mAb content and the mAb was included to achieve a final concentration of 16.67 μM within the reaction volume. MTG enzyme was prepared as previously described in MTG enzyme buffer and added to the reaction to achieve 3 U/mL of enzyme. 10X MTGase reaction buffer (NaCl 1.5 M, Tris-HCl pH 8.0 250 mM) was added to a final 1X content in the reaction and MilliQ water was used to complete the final calculated reaction volume. MTG conjugation was incubated at 37˚C for 2.5 hr. After incubation, a small amount of crude

conjugate was separated for SDS PAGE gel analysis. Anti-CD33-Tz conjugate was purified by size exclusion chromatography (SEC 650 column) on an FPLC to remove excess tetrazine linker. Anti-CD33-Tz fractions were pooled and concentrated with Vivaspin 6 (GE Healthcare) spin filters.

Anti-CD33-Tz conjugates were reacted with a 15-fold molar excess of Qb6-siGFP-TCO or GN3-siGFP-TCO for the final TCO-Tz ligation reaction. The Qb6-siGFP-TCO and GN3-siGFP-TCO conjugates were dried down by vacuum evaporation followed by their resuspension directly with anti-CD33-Tz in 1X PBS. TCO-Tz ligation reaction was allowed to incubate at room temperature overnight to ensure the best possible conjugation efficiency. Final conjugates and previous intermediates were run on a 10% SDS PAGE gel, followed by UV protein staining and imaging (**Figure 5.7c**). SDS PAGE analysis confirmed highly efficient conjugations at every step of the ARC building process.

Lastly, these ARCs were tested on our THP-1 dGFP cell line. THP-1 dGFP cells were seeded within a 100 µL volume in a 48-well plate. Qb6- and GN3- ARCs were filtered through a 0.22 µm syringe filter to eliminate any contaminants and then prepared within a 100 µL volume of RPMI complete growth medium to account for final treatment concentrations of 125 nM, 250 nM, 500 nM, and 750 nM. siGFP duplex only and anti-CD33 mAb only control treatment conditions were prepared in 100 µL RPMI complete growth medium to account for final concentrations of 1 µM and 625 nM, respectively. ARC and control treatment samples were added to the THP-1 dGFP cells to achieve final well volumes of 200 µL. Cells were incubated at 37 ˚C for 4 days. Afterwards, cells were filtered through a nylon mesh membrane, followed by flow cytometry analysis of FITC signal for GFP at the VA Flow Cytometry Core (**Figure 5.7d**).

Unfortunately, the incorporation of the Qb6 uEED into ARCs does not appear to improve its ability to knockdown the GFP expression of target THP-1 dGFP cells when compared to the GN3-containing control ARC. This suggests that the Qb6 uEED is unable to cause sufficient or

any endosomal membrane destabilization to allow siRNAs to escape into the cytoplasm. In its current form, the Qb6 uEED appears to be ineffective.

CONCLUSIONS

Endosomal escape remains the limiting barrier for oligonucleotide therapeutics. siRNAs cannot be internalized into cells on their own while ASOs under limited but not well-understood circumstances can internalize into cells by gymnosis. For this reason, successful siRNA therapeutics to date involve the use of a GalNAc targeting ligand or LNPs for liver targets but cannot reliably be used against extrahepatic targets. Successful ASO therapeutics are primarily used against either liver targets or other CNS targets by intrathecal injection into the cerebrospinal fluid, though limited therapeutic responses have been observed from intravenous administration against muscle cells in the context of Duchenne muscular dystrophy.

There are many limitations to the function of studied CPPs/PTDs to date and attempts to incorporate them into larger macromolecular conjugates have not yielded significant successes. Because of this, our lab developed certain versions and is currently developing new versions of uEEDs. A uEED monomer is comprised of a chemical coupler, hydrophobic core, endosomal-cleavable linker, and a hydrophilic mask. When exposed to serum, the uEED monomer lost its methyl ester group, a vestige from the synthesis procedure. After incubation with a lysosomal enzyme, the hydrophilic mask was successfully cleaved off as expected. Monomers can be synthesized in chains to form uEED multimers of variable lengths. Conjugation onto an antibody required a shift from previous conjugation chemistries to accommodate the various components needed for an ARC. Copper free click chemistry with a BCN group was used to conjugate an siRNA to the uEED. An MTG conjugation was used between the mAb and tetrazine linker. Lastly, a TCO-tetrazine ligation reaction was required to conjugate the mAb-Tz and oligo-uEED halves and obtain the complete ARC product. These conjugation reactions were optimized to achieve high efficiencies of the ARCs. Unfortunately, inclusion of Qb6 uEEDs in ARCs resulted

in no measurable knockdown of GFP expression in THP-1 dGFP cells when compared to the control (non-uEED) ARCs.

The Qb6 uEED was not able to promote endosomal escape for these ARCs. It is likely that the Qb structure is inadequate for the purpose of membrane destabilization. Earlier versions of the uEED were not successful either. A new version of the uEED is currently under development and has not been tested yet. Whether this or any future generation of uEED will ultimately result in the successful enhancement of endosomal escape remains to be seen. Only time will tell whether uEEDs are the correct approach to solving the endosomal escape enigma that currently limits the real therapeutic potential of oligonucleotide therapeutics.

ACKNOWLEDGEMENTS

Chapter Five contains unpublished material that was coauthored in part by Ian Huggins, Satish Jadhav, and Yu Yan Kwan. This dissertation's author was the primary researcher and author of this material. Ian Huggins established the conjugation reaction conditions for the earlier generations of uEEDs and conjugation chemistries. Synthesis of uEEDs and oligonucleotides and the HPLC analysis of the uEED monomeric unit was performed by Satish Jadhav. Later batches of anti-CD33 monoclonal antibodies were produced by Yu Yan Kwan. Steven Dowdy provided guidance throughout the work presented in this chapter.

REFERENCES

Alves, I.D., Bechara, C., Walrant, A., Zaltsman, Y., Jiao, C.-Y., Sagan, S., 2011. Relationships between Membrane Binding, Affinity and Cell Internalization Efficacy of a Cell-Penetrating Peptide: Penetratin as a Case Study. PLoS ONE 6, e24096. https://doi.org/10.1371/journal.pone.0024096

Balwani, M., Sardh, E., Ventura, P., Peiró, P.A., Rees, D.C., Stölzel, U., Bissell, D.M., Bonkovsky, H.L., Windyga, J., Anderson, K.E., Parker, C., Silver, S.M., Keel, S.B., Wang, J.-D., Stein, P.E., Harper, P., Vassiliou, D., Wang, B., Phillips, J., Ivanova, A., Langendonk, J.G., Kauppinen, R., Minder, E., Horie, Y., Penz, C., Chen, J., Liu, S., Ko, J.J., Sweetser, M.T., Garg, P., Vaishnaw, A., Kim, J.B., Simon, A.R., Gouya, L., 2020.

Phase 3 Trial of RNAi Therapeutic Givosiran for Acute Intermittent Porphyria. N Engl J Med 382, 2289–2301. https://doi.org/10.1056/NEJMoa1913147

Bechara, C., Pallerla, M., Burlina, F., Illien, F., Cribier, S., Sagan, S., 2015. Massive glycosaminoglycan-dependent entry of Trp-containing cell-penetrating peptides induced by exogenous sphingomyelinase or cholesterol depletion. Cell. Mol. Life Sci. 72, 809–820. https://doi.org/10.1007/s00018-014-1696-y

Brown, C.R., Gupta, S., Qin, J., Racie, T., He, G., Lentini, S., Malone, R., Yu, M., Matsuda, S., Shulga-Morskaya, S., Nair, A.V., Theile, C.S., Schmidt, K., Shahraz, A., Goel, V., Parmar, R.G., Zlatev, I., Schlegel, M.K., Nair, J.K., Jayaraman, M., Manoharan, M., Brown, D., Maier, M.A., Jadhav, V., 2020. Investigating the pharmacodynamic durability of GalNAc–siRNA conjugates. Nucleic Acids Research 48, 11827–11844. https://doi.org/10.1093/nar/gkaa670

Chen, C.-J., Tsai, K.-C., Kuo, P.-H., Chang, P.-L., Wang, W.-C., Chuang, Y.-J., Chang, M.D.-T., 2015. A Heparan Sulfate-Binding Cell Penetrating Peptide for Tumor Targeting and Migration Inhibition. BioMed Research International 2015, 1–15. https://doi.org/10.1155/2015/237969

Dowdy, S.F., 2017. Overcoming cellular barriers for RNA therapeutics. Nat Biotechnol 35, 222–229. https://doi.org/10.1038/nbt.3802

Dupont, E., Prochiantz, A., Joliot, A., 2011. Penetratin story: an overview. Methods Mol. Biol. 683, 21-29. https://doi.org/10.1007/978-1-4939-2806-4_2

Gagliardi, M., Ashizawa, A.T., 2021. The Challenges and Strategies of Antisense Oligonucleotide Drug Delivery. Biomedicines 9, 433. https://doi.org/10.3390/biomedicines9040433

Gautam, A., Singh, H., Tyagi, A., Chaudhary, K., Kumar, R., Kapoor, P., Raghava, G.P.S., 2012. CPPsite: a curated database of cell penetrating peptides. Database 2012, bas015–bas015. https://doi.org/10.1093/database/bas015

Gruenberg, J., van der Goot, F.G., 2006. Mechanisms of pathogen entry through the endosomal compartments. Nature Reviews Molecular Cell Biology 7, 495-504. https://doi.org/10.1038/nrm1959

Hällbrink, M., Oehlke, J., Papsdorf, G., Bienert, M., 2004. Uptake of cell-penetrating peptides is dependent on peptide-to-cell ratio rather than on peptide concentration. Biochimica et Biophysica Acta (BBA) - Biomembranes 1667, 222–228. https://doi.org/10.1016/j.bbamem.2004.10.009

Han, X., Bushweller, J.H., Cafiso, D.S., Tamm, L.K., 2001. Membrane structure and fusion-triggering conformational change of the fusion domain from influenza hemagglutinin. Nature Struct. Biology 8, 715-720. https://doi.org/10.1038/90434

Hou, K.K., Pan, H., Schlesinger, P.H., Wickline, S.A., 2015. A role for peptides in overcoming endosomal entrapment in siRNA delivery — A focus on melittin. Biotechnology Advances 33, 931–940. https://doi.org/10.1016/j.biotechadv.2015.05.005

Hu, B., Zhong, L., Weng, Y., Peng, L., Huang, Y., Zhao, Y., Liang, X.-J., 2020. Therapeutic siRNA: state of the art. Sig Transduct Target Ther 5, 101. https://doi.org/10.1038/s41392-020-0207-x

Kaplan, I.M., Wadia, J.S., Dowdy, S.F., 2005. Cationic TAT peptide transduction domain enters cells by macropinocytosis. Journal of Controlled Release 102, 247–253. https://doi.org/10.1016/j.jconrel.2004.10.018

Kauffman, W.B., Fuselier, T., He, J., Wimley, W.C., 2015. Mechanism Matters: A Taxonomy of Cell Penetrating Peptides. Trends in Biochemical Sciences 40, 749–764. https://doi.org/10.1016/j.tibs.2015.10.004

Khvorova, A., Watts, J.K., 2017. The chemical evolution of oligonucleotide therapies of clinical utility. Nat Biotechnol 35, 238–248. https://doi.org/10.1038/nbt.3765

Kosmas, C., Muñoz Estrella, A., Sourlas, A., Silverio, D., Hilario, E., Montan, P., Guzman, E., 2018. Inclisiran: A New Promising Agent in the Management of Hypercholesterolemia. Diseases 6, 63. https://doi.org/10.3390/diseases6030063

Le Blanc, I., Luyet, P.-P., Pons, V., Ferguson, C., Emans, N., Petiot, A., Mayran, N., Demaurex, N., Fauré, J., Sadoul, R., Parton, R.G., Gruenberg, J., 2005. Endosome-to-cytosol transport of viral nucleocapsids. Nat Cell Biol 7, 653–664. https://doi.org/10.1038/ncb1269

Lee, M.-T., Hung, W.-C., Chen, F.-Y., Huang, H.W., 2008. Mechanism and kinetics of pore formation in membranes by water-soluble amphipathic peptides. PNAS 105, 5087-5092.

Lee, C.-C., Sun, Y., Huang, H.W., 2010. Membrane-Mediated Peptide Conformation Change from α-Monomers to β-Aggregates. Biophysical Journal 98, 2236–2245. https://doi.org/10.1016/j.bpj.2010.02.001

Leushner, J., 2001. MALDI TOF mass spectrometry: an emerging platform for genomics and diagnostics. Exp. Rev. Molecular Diagnostics 1, 11-18. https://doi.org/10.1586/14737159.1.1.11

Lichty, B.D., Power, A.T., Stojdl, D.F., Bell, J.C., 2004. Vesicular stomatitis virus: re-inventing the bullet. Trends in Mol Medicine 10, 210-216. https://doi.org/10.1016/j.molmed.2004.03.003

Lönn, P., Dowdy, S.F., 2015. Cationic PTD/CPP-mediated macromolecular delivery: charging into the cell. Expert Opinion on Drug Delivery 12, 1627–1636. https://doi.org/10.1517/17425247.2015.1046431

Lönn, P., Kacsinta, A.D., Cui, X.-S., Hamil, A.S., Kaulich, M., Gogoi, K., Dowdy, S.F., 2016. Enhancing Endosomal Escape for Intracellular Delivery of Macromolecular Biologic Therapeutics. Sci Rep 6, 32301. https://doi.org/10.1038/srep32301

Melikov, K., Hara, A., Yamoah, K., Zaitseva, E., Zaitsev, E., Chernomordik, L.V., 2015. Efficient entry of cell-penetrating peptide nona-arginine into adherent cells involves a transient increase in intracellular calcium. Biochemical Journal 471, 221–230. https://doi.org/10.1042/BJ20150272

Oliveira, B.L., Guo, Z., Bernardes, G.J.L., 2017. Inverse electron demand Diels–Alder reactions in chemical biology. Chem. Soc. Rev. 46, 4895–4950. https://doi.org/10.1039/C7CS00184C

Oude Blenke, E., Sleszynska, M., Evers, M.J.W., Storm, G., Martin, N.I., Mastrobattista, E., 2017. Strategies for the Activation and Release of the Membranolytic Peptide Melittin from Liposomes Using Endosomal pH as a Trigger. Bioconjugate Chem. 28, 574–582. https://doi.org/10.1021/acs.bioconjchem.6b00677

Rashidian, M., Mahmoodi, M.M., Shah, R., Dozier, J.K., Wagner, C.R., Distefano, M.D., 2013. A Highly Efficient Catalyst for Oxime Ligation and Hydrazone–Oxime Exchange Suitable for Bioconjugation. Bioconjugate Chem. 24, 333–342. https://doi.org/10.1021/bc3004167

Ritchie, M., Tchistiakova, L., Scott, N., 2013. Implications of receptor-mediated endocytosis and intracellular trafficking dynamics in the development of antibody drug conjugates. mAbs 5, 13–21. https://doi.org/10.4161/mabs.22854

Roberts, T.C., Langer, R., Wood, M.J.A., 2020. Advances in oligonucleotide drug delivery. Nat Rev Drug Discov 19, 673–694. https://doi.org/10.1038/s41573-020-0075-7

Sarrett, S.M., Keinänen, O., Dayts, E.J., Roi, G.D., Rodriguez, C., Carnazza, K.E., Zeglis, B.M., Inverse electron demand Diels-Alder click chemistry for pretargeted PET imaging and radioimmunotherapy. Nature Protocols 16, 3348-3381. https://doi.org/10.1038/s41596-021-00540-2

Setten, R.L., Rossi, J.J., Han, S., 2019. The current state and future directions of RNAi-based therapeutics. Nat Rev Drug Discov 18, 421–446. https://doi.org/10.1038/s41573-019-0017-4

Smith, C.I.E., Zain, R., 2019. Therapeutic Oligonucleotides: State of the Art. Annu. Rev. Pharmacol. Toxicol. 59, 605–630. https://doi.org/10.1146/annurev-pharmtox-010818-021050

Springer, A.D., Dowdy, S.F., 2018. GalNAc-siRNA Conjugates: Leading the Way for Delivery of RNAi Therapeutics. Nucleic Acid Therapeutics 28, 109–118. https://doi.org/10.1089/nat.2018.0736

Tünnemann, G., Martin, R.M., Haupt, S., Patsch, C., Edenhofer, F., Cardoso, M.C., 2006. Cargo-dependent mode of uptake and bioavailability of TAT-containing proteins and peptides in living cells. FASEB j. 20, 1775–1784. https://doi.org/10.1096/fj.05-5523com

Ulrich, S., Boturyn, D., Marra, A., Renaudet, O., Dumy, P., 2013. Oxime Ligation: A Chemoselective Click-Type Reaction for Accessing Multifunctional Biomolecular Constructs. Chemistry EU 20, 34-41. https://doi.org/10.1002/chem.201302426

Vives, E., 2003. Cellular uptake of the Tat peptide: an endocytosis mechanism following ionic interactions. J. Mol. Recognit. 16, 265-271. https://doi.org/10.1002/jmr.636

Wimley, W.C., Hristova, K., 2011. Antimicrobial Peptides: Successes, Challenges and Unanswered Questions. J Membrane Biol 239, 27–34. https://doi.org/10.1007/s00232-011-9343-0

Wong, S.C., Klein, J.J., Hamilton, H.L., Chu, Q., Frey, C.L., Trubetskoy, V.S., Hegge, J., Wakefield, D., Rozema, D.B., Lewis, D.L., 2012. Co-Injection of a Targeted, Reversibly Masked Endosomolytic Polymer Dramatically Improves the Efficacy of Cholesterol-Conjugated Small Interfering RNAs *In Vivo*. Nucleic Acid Therapeutics 22, 380–390. https://doi.org/10.1089/nat.2012.0389

Wadia, J.S., Stan, R.V., Dowdy, S.F., 2004. Transducible TAT-HA fusogenic peptide enhances escape of TAT-fusion proteins after lipid raft micropinocytosis. Nature Medicine 24, 310-315. https://doi.org/10.1038/nm996

Wurster, C.D., Ludolph, A.C., 2018. Nusinersen for spinal muscular atrophy. Ther Adv Neurol Disord 11, 1-3. https://doi.org/10.1177/1756285618754459

CHAPTER SIX

CONCLUSIONS AND FUTURE DIRECTIONS

CONCLUSIONS AND FUTURE DIRECTIONS

ABSTRACT

The development of chemical modifications of the ribose sugars and backbones of oligonucleotides has revolutionized the field of medicine. With increased metabolic stability and potency, oligonucleotides have become a highly attractive therapeutic platform. For the first time, oligonucleotides have gained a fighting chance to survive in physiological conditions long enough to effect their gene silencing function. However, despite the potential and promise of oligonucleotides, it soon became clear that oligonucleotides held unfavorable pharmacokinetic properties. The discovery that full phosphorothioate (PS)-modified ASOs were, in certain limited cases, able to passively enter a cell through gymnosis without help from a delivery vehicle led to an explosion of PS ASOs in clinical trials, especially those with targets in the central nervous system (CNS). Meanwhile, the incorporation of siRNAs into either lipid nanoparticle (LNP) formulations or *tris*-N-acetylgalactosamine (GalNAc) conjugates provided apt delivery strategies for siRNAs against liver targets. Yet, for all the successes against targets in the liver and CNS, the success of oligonucleotide therapeutics against extrahepatic and non-CNS targets remains frustratingly elusive. Regardless of target, endosomal escape remains an additional problem that continues to prevent oligonucleotide therapeutics from reaching their full potential.

To attempt to address these challenges, I worked on the development of our Antibody-RNA Conjugate (ARC) platform to test monoclonal antibodies (mAbs), various conjugation strategies, ASOs and siRNAs within ARCs, and optimized many of the intermediary procedures involved in the processes to build ARCs. mAbs have a very high binding affinity for their target cell surface receptors and are promising delivery vehicles for targets outside of the liver. Moreover, I worked on the testing and optimization of conjugation and purification procedures of the universal endosomal escape domains (uEEDs) that are currently in development in our lab. uEEDs consist of several customizable components that were designed with the goal of

endosomal membrane destabilization. Building ASO- or siRNA-containing ARCs was successful, with good site-selective conjugation efficiencies. Conjugation of different linkers and oligonucleotides did not interfere with an ARC's binding avidity or specificity. Unfortunately, ARCs were unable to mediate gene silencing in their target cells and the addition of uEEDs to ARCs saw no improvement in this regard. My work establishes a baseline methodology for building standard ARC-uEED conjugates that can readily be modified to test future generations of the uEED molecules.

INTRODUCTION

The introduction of PS modifications to the backbones of ASOs resulted in an unprecedented improvement in metabolic stability and deliverability. Consequently, PS backbones quickly became (and remain) a standard ASO modification (Agrawal et al., 1988; Stec et al., 1998; Eckstein, 2014). The replacement of one oxygen atom with a sulfur atom in the phosphodiester linkage boosts the ASO pharmacokinetics by allowing ASOs to bind serum albumin and other blood proteins, and granting resistance from RNase degradation (Dowdy, 2017). Increased stability allows for extended circulation times and the PS modifications also reduce immune stimulation due to the elimination of the unmethylated CpG dinucleotides ordinarily found in PO-backbone ASOs (Eckstein, 2014). Modifications at the 2'-position of the ribose sugar also confer essential improvements to ASOs. The most common 2'-modifications are the 2'-Fluoro, 2'-O-methyl, and 2'-methoxyethyl modifications. In all cases, 2' modifications lead to increased protection against RNases, a reduction in innate immune recognition and response, and an increased binding affinity (Khvorova and Watts, 2017; Dowdy, 2017). Perhaps most significant for the prospect of ASOs is the observation that a full PS-modified backbone allows a small percentage of ASOs (1-2%) to gradually cross the lipid bilayer and escape endosomes into the cytoplasm without the aid of a transfection reagent, a phenomenon termed gymnosis, first observed in LNA PS ASOs (Stein et al., 2010). Only a small fraction of PS ASOs is active after uptake by gymnosis and gymnosis only occurs in a limited number of cell types, suggesting that non-productive uptake occurs in many other cell lines or not at all (Crooke et al., 2017). Not much is known about the gymnotic mechanism of action or the specific proteins involved in "productive" ASO uptake (Crooke et al., 2017; Dowdy, 2017).

Key types of ASOs include splice switching ASOs and Gapmer ASOs, with the former altering the splicing patterns of the target gene, such as *SMN2* to include exon 7 and produce a full length SMN protein in patients with spinal muscular atrophy (Nusinersen, Ionis Pharmaceuticals), and the latter consisting of 3-5 RNA bases flanking a central 10 base DNA

gap that recruits the ubiquitous RNase H enzyme to cleave the RNA of a DNA-RNA hybrid, such as with Inotersen (Ionis/Akcea) that targets an abnormal mutation in the *TTR* gene that produces abnormal transthyretin plasma protein in transthyretin amyloidosis (Scoles et al., 2019; Sikora et al., 2015; Benson et al., 2018). As of this writing, eight ASO drugs have received FDA approval to treat conditions including Duchenne muscular dystrophy, spinal muscular atrophy, and transthyretin amyloidosis (Gagliardi and Ashizawa, 2021).

siRNAs have benefited from many of the same modifications of ASOs. However, constraints of the RNAi machinery means that Argonaute 2 (Ago2) tolerates only one or two phosphorothioates at the ends of both siRNA strands, modifications that nevertheless still improve the stability, potency, and duration of the RNAi response (Dowdy, 2017). As with ASOs, 2'-modifications also confer improved binding affinity, protection from RNases and a reduced immune response (Dowdy, 2017). 2'-modifications like 2'-O-methyl and 2'-Fluoro are generally well tolerated by the RNAi machinery, especially 2'-Fluoro that shares a very similar electronegativity to the native 2'-OH group (Blidner et al., 2007), and both 2'-F and 2'-OMe modifications support the C3'-endo "pucker" conformation and strengthen the A-form helical structure for improved positioning into the cleavage center of the RISC complex (Ipsaro and Joshua-Tor, 2015; Khvorova and Watts, 2017).

Oligonucleotides have the potential to pharmaco-evolve against frequently genetically changing diseases, like cancer, to keep pace with the oncogenic mutations that arise, a characteristic that no other therapeutic modality is capable of (Dowdy, 2017). But unlike ASOs, siRNAs are too large and negatively charged to be able to cross cell or endosomal membranes in most cases, except for a very small amounts in the liver, making naked siRNAs pharmacokinetically ineffective on their own (Juliano, 2016), leading to their prompt removal by renal filtration minutes after injection into a mouse (Merkel et al., 2009). To overcome this limitation, siRNAs can be encapsulated within an LNP formulation or conjugated to GalNAc for delivery to hepatocytes. GalNAc conjugates distribute mainly to the liver and kidney, but even

though GalNAc conjugates that fail to bind ASGPR on their first pass will get cleared by the kidney, the GalNAc targeting ligand still significantly improves deliverability of oligonucleotides (Cui et al., 2021). LNPs mask an siRNA's negative charge, provides it with additional protection against RNase degradation, and improves its circulation time (Schoreder et al., 2010; Rappaport et al., 1995; van de Water et al., 2006). LNPs accumulate primarily in the liver, making them ideal delivery vehicles for siRNAs against liver targets (Akinc et al., 2008; Zimmermann et al., 2006). A high abundance of the asialoglycoprotein receptor (ASGPR) on hepatocytes makes GalNAc an ideal targeting ligand for delivery of siRNAs to the liver because ASGPR is efficiently internalized when bound to GalNAc and recycled back to the surface within 15 minutes (Juliano, 2016; Khvorova and Watts, 2017). GalNAc-siRNA conjugates are dramatically smaller and simpler than LNP-based siRNA delivery systems and can effectively be taken up after binding to the ASGPR receptors into the endosome from where ~0.3% of siRNA is able to escape across the endosomal membrane through an unknown mechanism (Brown et al., NAR 2020).

Despite success against liver and CNS targets, successful delivery of oligonucleotides to other targets remains a significant challenge. mAbs are ideal vehicles for delivery to extrahepatic targets because they have a high binding affinity for their target receptors and can often trigger receptor-mediated endocytosis upon binding (Tarcic and Yarden, 2013). Unfortunately, neither mAbs nor their oligonucleotide cargo can escape the endosome. Genentech's THIOMAB ARCs were developed against a variety of receptors, but in all cases, they accumulated in lysosomes within 25 hours with very poor siRNA escape and generally exhibited poor knockdown at unacceptably high doses (Cuellar et al., 2014). However, a different ARC using 2'-MOE-modified PS ASOs showed reasonable knockdown against ALL targets, but high doses were required, and the antisense-mediated knockdown was not clear either (Satake et al., 2016). Another ARC targeted the DRR oncogenic driver in glioblastoma multiform also using ASOs but showed limited target gene knockdown when using an anti-CD44

mAb (Arnold et al., 2018). In all of these cases, gene knockdown from ARC treatment was relatively limited and required very high doses.

Endosomal entrapment remains a significant problem for all RNA therapeutics, including mAb-oligonucleotide conjugates. Results till now suggest that incorporation of endosomal escape mechanisms are critical to the success of oligonucleotide therapeutics, and without them, oligonucleotides, especially siRNAs, will likely remain highly inefficient outside of the liver. Even for liver targets, successful endosomal escape mechanisms could greatly reduce dose requirements for existing GalNAc-siRNA conjugates. The question, therefore, is not whether endosomal escape mechanisms are needed, but rather, what the best approach to achieving endosomal escape is and how to successfully implement it into existing therapeutic modalities.

CONCLUSIONS

Antibody-RNA Conjugates (ARCs)

Building the standard ARC first required the optimization of the conjugation conditions. The microbial transglutaminase (MTGase) enzyme was selected due to its high efficiency in mediating the transamidation between the R groups of glutamine and lysine residues to create an isopeptide bond (Seguro et al., 1996) (Figure 3.1). Random protein or antibody surface glutamines are often unreactive with MTGase and none of the 64 surface glutamines of cetuximab, an anti-EGFR mAb, were shown to be promising substrates for MTGase (Siegmund et al., 2015). Instead, there are specific amino acid motifs that have shown particularly high MTGase activity for this transamidation reaction, such as the LQSP tetrapeptide (Caporale et al., 2015) or the LLQGA tag (Farias et al., 2014). The LLQGA MTG tag was selected for our mAbs and was cloned into the C-termini of the heavy chain cDNA with a termination codon afterwards. The mAbs we used were cloned based on the amino acid sequences found in the patent literature (Huggins et al., 2019). The ExpiCHO expression system was used to produce

our MTG-tagged mAbs after transfection of the heavy chain and light chain plasmids. A stable linker, K-PEG_6-SG-N_3 (KP1Z) was selected for these conjugation reactions and was optimized for the best MTG conjugation ratio and compared to other similar linker peptides (Figure 3.3).

I confirmed by SDS PAGE gel electrophoresis that the MTG conjugation of a linker peptide to a mAb did not lead to off-target conjugations nor heavy chain or light chain aggregation. Binding studies were performed on CD33-positive THP-1 cells after conjugation of a fluorescent peptide onto anti-CD33 mAbs to confirm that the MTG conjugation did not negatively alter a mAb's binding affinity. The KP1Z linker peptide contains two key functional groups: a lysine for MTG conjugation and an azide group for copper-free click conjugation to the siRNA. Inclusion of a cyclooctene group in the oligonucleotide allows for efficient azide-mediated cycloaddition through ring strain interactions (Agard et al., 2004). As expected, the MTG conjugation between an anti-CD33 mAb and KP1Z linker, with the latter in 5-fold molar excess, led to an efficient conjugation reaction. siRNA was duplexed and then conjugated onto mAb-KP1Z via copper free click chemistry overnight. The copper free click reaction was >90% efficient and SDS PAGE analysis confirmed a DAR 2 ARC. Subsequent purification of the ARCs by size exclusion chromatography on an FPLC resulted in clear separation between the different components that allowed for the isolation of the final, pure ARC. Flow cytometry analyses confirmed that ARCs maintained their binding capabilities after the conjugation reactions and purifications. Production of a structurally defined, DAR 2 ARC via site-specific conjugations was achieved and purification and conjugation conditions were optimized. Unfortunately, these ARCs were unable to generate successful gene silencing results. Failure to elicit an RNAi knockdown is likely due to the absence of endosomal escape mechanisms to allow the siRNAs to reach the cytoplasm.

The failure of siRNA-ARCs raised the question of whether ASO-ARCs would fare any better. While siRNAs are too large and charged to cross the endosomal membrane, ASOs have in certain circumstances been observed to cross into the cytoplasm through gymnosis (Juliano

et al., 2013; Crooke et al., 2017). An anti-CD33 GFP ARC was created for proof of principle testing against our CD33-positive THP-1 dGFP cell line. A LLQGA-tagged anti-CD33 mAb was used for this ARC. The anti-CD33 CDR sequences were taken from the patent literature of gemtuzumab and expressed through the ExpiCHO cell line as before. Due to the differences in chemistries between oligonucleotides, a K-PEG_6-HyNic (KP1H) was used for the conjugation reactions. Using the standard MTG conjugations as before, the mAb-KP1H MTG test conjugation reactions revealed significant efficiencies (>90%) (Figure 4.3). The HyNic conjugation reaction between the KP1H linker peptide and the benzaldehyde groups of GFP ASOs led to equally efficient conjugations (Figure 4.5). The final MTG conjugation between the anti-CD33 mAb and KP1H-ASO conjugate was successfully completed with an expected high efficiency (Figure 4.6) and purified by size exclusion chromatography on an FPLC. While conjugation and purification procedures were completed without a problem, ASO ARCs with four different GFP ASOs were equally unsuccessful at knocking down target GFP expression in THP-1 dGFP cells. The most likely reasons for this failure are the inability of these specific ASOs to productively reach the nuclei of this specific cell type. It is likely that ASOs in these cells are directed through non-productive pathways and never had the opportunity to reach the nuclei in sufficiently high numbers. Despite these possibilities, the problem can still be traced back to the absence of a highly efficient viable endosomal escape mechanism. Though these GFP ASOs were not sufficient to make the difference in this case, it stands to reason that having had endosomal escape improvements could have still allowed far greater numbers of ASOs into the cytoplasm and thereafter the nucleus to knockdown GFP expression.

Universal Endosomal Escape Domains

Endosomal entrapment of oligonucleotides is the most prominent limiting factor of mAb-oligonucleotide therapeutics. The Dowdy lab has developed and continues to develop universal endosomal escape domains (uEEDs) to try to overcome the endosomal entrapment problem.

uEEDs are comprised of a chemical coupler, a hydrophobic core, a linker that can be cleaved by a lysosomal enzyme, and a hydrophilic mask (Figure 5.1). The intended function of uEEDs is to be internalized with an ARC and promote endosomal escape. In response to the increasing acidification within the endosomal pathway and into the lysosome, a ubiquitous lysosomal enzyme will cleave the linker to remove the hydrophilic masks and expose the hydrophobic cores that will thereafter embed themselves into the endosomal membrane in a sufficiently high local concentration to destabilize the membrane. uEEDs are highly modular in nature and can be synthesized at variable lengths of individual monomers. HPLC analyses revealed that exposure of a uEED monomer to serum removed a vestigial methyl ester group from the synthesis stage that would otherwise interfere with interactions with the lysosomal enzyme and that subsequent incubation with the lysosomal enzyme removed the entire hydrophilic mask as predicted (Figure 5.5).

My work focused primarily on the Qb6 uEED. The latest version of this uEED was synthesized with an azide modification to allow for a copper-free click reaction to the BCN-modified siRNA. Purification and conjugation procedures were optimized to account for new conjugation chemistries that allowed for the inclusion of uEEDs onto ARCs. A methyltetrazine-PEG4-amine linker was used to conjugate an anti-CD33 mAb to the siRNA-uEED conjugate with high conjugation efficiencies (>90%) for the final ARC-uEED product (Figure 5.7). Unfortunately, treatment of an anti-CD33 siGFP ARC-uEED failed to knock down GFP expression in our THP-1 dGFP cell line, indicating that these Qb6 uEEDs are unable to promote endosomal escape.

FUTURE DIRECTIONS

The ARC-uEED platform is highly modular and conducive to modifications at any section of the uEED monomer. This allows for rapid modifications to the mAb, linkers, oligonucleotides, and even uEEDs. The uEEDs themselves are also modular and can be updated with

modifications to the hydrophobic core, the uEED backbone, and the length of a given uEED molecule to experiment with possible improvements that may promote endosomal escape. The uEEDs will undoubtedly need advances for the prospects of endosomal escape to improve. Endosomal entrapment remains the key problem of oligonucleotide therapeutics against extrahepatic targets and uEEDs stand as a highly innovative approach to try to resolve this problem. While initial generations of uEEDs have encountered no successful improvements in endosomal escape, the next version of the uEED is currently under development. Whether this upcoming generation or any forthcoming generation of uEED will succeed in promoting endosomal escape remains to be seen. Only time will tell whether uEEDs are the correct approach to overcoming the problem of endosomal entrapment.

There are two other approaches with the potential to improve endosomal escape and may bear fruit in the future.

Triterpenoid Saponins

Triterpenoid saponins refer to a wide variety of plant glycosides that consist of an aglycone structure and variable sugar side chains and are known for their membrane permeabilizing and hemolytic properties (Baumann et al., 2000; Böttger et al, 2012; Bachran et al., 2006). The composition of the sugar side chain content has a significant impact on the saponin's activity (Bachran et al., 2006). For example, it was reported that saponins with two side chains induce a reduction in activity in comparison to those with only one sugar side chain (Woldemichael and Wink, 2001) whereas it was conversely reported that increasing number of side chains increased membrane permeability (Yamasaki et al., 1987). Triterpenoid saponins have a pentacyclic C30 terpene skeleton as a backbone and at least one covalently bound sugar chain that are composed of numerous different sugars (**Figure 6.1**) (Fuchs et al., 2017).

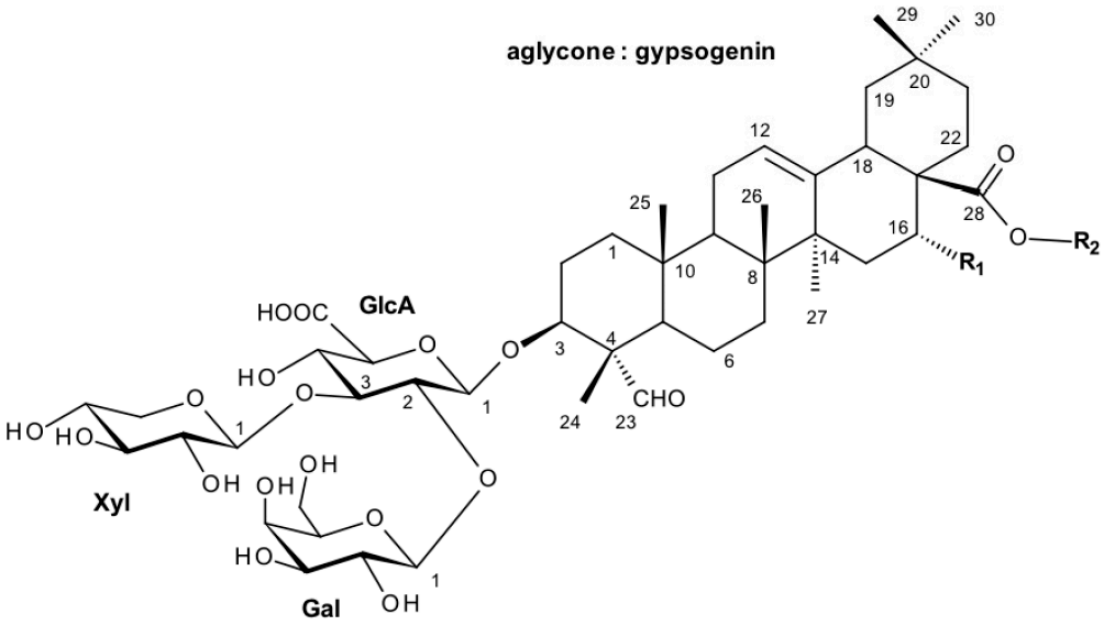

Figure 6.1. General Structure of a Triterpenoid Saponin
The structure of triterpenoid saponin includes a C30 terpene skeleton. There are many combinations of sugar side chains at the R_2 location, while R_1 consists of either an H or OH. The displayed residues at carbon #3 and carbon #4 and a sugar chain of at least 4 sugar units at carbon #28 are required for enhancement of the cytotoxicity of protein toxins (Böttger et al., 2013; Fuchs et al., 2017).

Taken from Fuchs et al., 2017.

Saponins have different abilities for membrane perturbation and permeabilization. The nonpolar triterpene backbone and polar sugar chains makes all triterpenoid saponins amphiphilic and thus able to interact with both hydrophilic and lipophilic compounds (Fuchs et al., 2017). The mechanism by which saponin-mediated membrane perturbation occurs is not well understood, but it has been postulated that the process begins with the incorporation of saponins into the cell membrane via interactions between the lipophilic aglycone and hydrophobic membrane, followed by complexation with membrane sterols like cholesterol, leading to accumulation into matrices and eventually membrane curvature and disruption (Augustin et al., 2011, Fuchs et al., 2017). It has also been observed that saponins from the *Saponaria* species induce clathrin-mediated endocytosis of a saporin toxin (Weng et al., 2008). A few better-studied saponins for endosomal escape enhancement of protein toxins come from the *Gypsophila* species (SA1641 and SA 1657) and from the *Saponaria officinalis* species (SO1861) (Thakur et al., 2013). SA1641 was observed through live cell imaging to enhance the endosomal escape of toxin-based therapeutics at a non-toxic concentration with an Alexa Fluor 488 reporter assay (Gilabert-Oriol et al., 2014). Addition of the S01861 saponin to the treatment cocktail of trastuzumab-saporin or cetuximab-saporin conjugates enhanced the antibody-dependent cell-mediated cytotoxicity in human breast cancer cell lines (Gilabert-Oriol et al., 2013). The SO1861 saponin also improved the activity of saporin-based immunotoxins in human leukemia and lymphoma cells, an observation attributed to increased endosomal escape (Holmes et al., 2015). Limitations to the use of saponins in these examples are that the saponins were added *in trans* to the toxin or toxin-conjugate being analyzed, but site-specific conjugations were glaringly absent. Saponins can vary in toxicity and systemic administration would be clinically untenable. Saponins also lack practical conjugation-capable groups for site-specific conjugations, further compounding the problem.

I performed some work with the commercially available saponin from *Quillaja Saponaria* Molina (Fisher Scientific) (**Figure 6.2a**). The quillajasaponin from the *Quillaja Saponaria* Molina

is a well-known representative of the triterpenoid saponin class (Fuchs et al., 2017). There was no conjugation compatibility between our existing linkers and the quillajasaponin so instead I tried direct conjugation onto an anti-CD33 mAb using the 1-ethyl-3-(3-dimethylaminopropyl)carbodiimide hydrochloride (EDC) reagent (ThermoFisher), a zero-length crosslinker that reacts with a carboxyl and amine group to form an amide bond (ThermoFisher). After numerous experiments to try to optimize the EDC-mediated conjugation, limited conjugation was observed by SDS PAGE (10%) gel electrophoresis and subsequent UV protein staining (**Figure 6.2b**). Perhaps 1 or 2 quillajasaponin (MW 2284.4) compounds were conjugated per heavy chain and light chain of the anti-CD33 mAb. A WST-1 cell viability assay tested doses from 0-100 µg/mL revealed a low IC50 of ~15-20 µg/mL for quillajasaponin in H1299 dGFP cells (non-small cell lung cancer cell line that expresses GFP) (**Figure 6.2c**), and was highly cytotoxic at the doses tested. It has been identified in literature that 1.5 µg/mL (~3.28 µM) of quillajasaponin is the optimal concentration to preserve cell viability but still produce the observed toxin/endosomal escape activity, and quillajasaponin's IC50 is estimated to be about ~10 µg/mL in a HER14 cell line with toxicity varying based on the cell line (Bachran et al., 2006). Quillajasaponin-mediated endosomal escape or toxin enhancement unfortunately required a concentration too high to be compatible with ARC doses *in vitro* and therefore was an impractical saponin for experimentation.

Sapreme Technologies based in the Netherlands is at the forefront of incorporating saponins into macromolecular conjugates for the purpose of endosomal escape enhancement. A recent patent (Fuchs, 2021) details different conjugation strategies for covalent conjugations either non-specifically via maleimide conjugations or more site-specific conjugations onto proteins and mAbs via the saponin's glucuronic acid or aldehyde groups and the inclusion of oligonucleotides or other toxins into the conjugate. This patent further shows knockdown with the SO1861 saponin as well as and other saponins *in vitro* and *in vivo*. Sapreme Technologies reported favorable preclinical data at the Oligonucleotide Therapeutics Society Annual

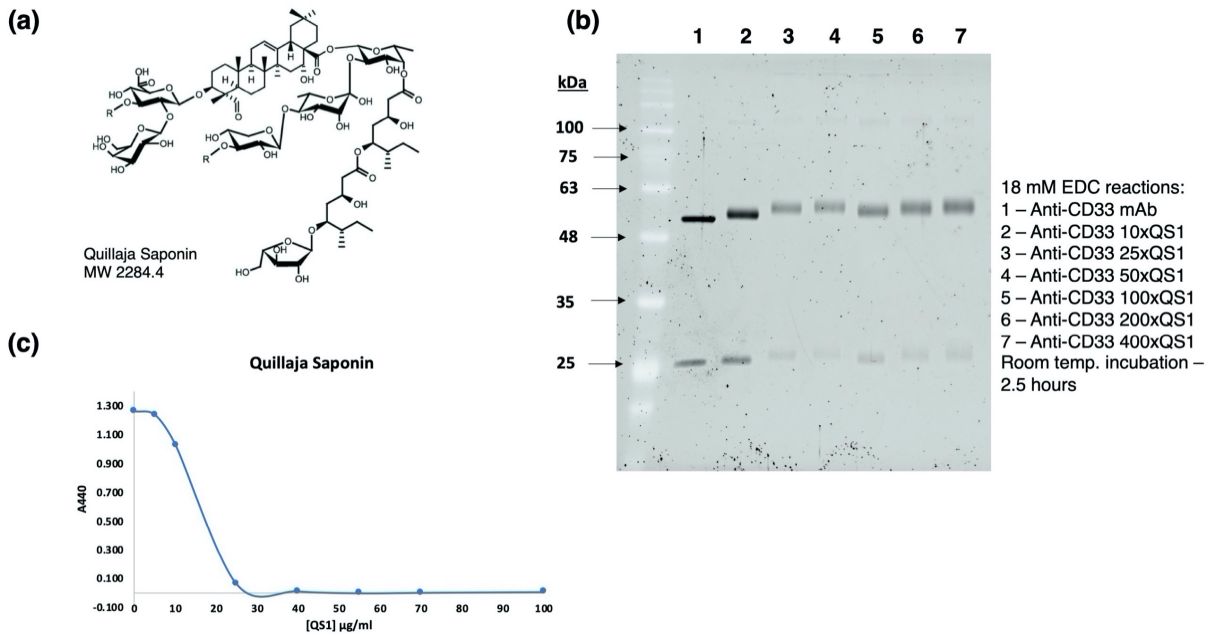

Figure 6.2. Quillajasaponin Conjugations and Cell Viability
(**a**) Structure of saponin from Quillaja Saponaria Molina, a representative of the triterpenoid saponins. (**b**) SDS PAGE (10%) gel electrophoresis of Anti-CD33-quillajasaponin conjugates, with variable excess molar ratios of the saponin. 18 mM EDC reagent used for crosslinking in all cases and the reaction was incubated at room temperature for 2.5 hours. (**c**) WST-1 cell viability assay of quillajasaponin on H1299 dGFP cells shows high toxicity above 10 µg/mL. Reduction of A440 signal means a reduction in cell viability. Abbreviations: MW, molecular weight; kDa, kilodaltons; QS1, quillajasaponin.

Part (a), structure, taken from Fisher Scientific.

Conference in 2021 for enhancement of endosomal escape *in vitro* and *in vivo* and at the 2020 Annual Conference demonstrated the successful use of a saponin (SPT001) to improve the release of ASOs and other payloads *in vitro* in EGFR-positive A431 cells and with GalNAc conjugates in hepatocytes in both *cis* and *trans* configurations (Sapreme Technologies). However, no outside groups have reported yet on use of their SO1861 saponin.

Retrograde Transport

Some plant toxins, including ricin, abrin, viscumin, and Shiga toxins are known to bind to cell surface receptors to trigger endocytosis and are subsequently transported to and through the trans-Golgi network, the Golgi apparatus and the endoplasmic reticulum (ER) to ultimately gain access into the cell cytoplasm (Juliano et al., 2012). For Shiga toxin, cholesterol appears to be a membrane requirement for transport from the endosome to the Golgi apparatus (Falguieres et al., 2001), while for other toxins like ricin, transport to the Golgi occurs independent of membrane cholesterol content (Spilsberg, 2003). The Golgi is essential to mediate the retrograde transport of toxins and is in most cases a requirement for intoxication (Sandvig et al., 2013). Numerous other proteins also undergo retrograde transport, such as EGFR signaling receptor, soluble antigens, the furin protease, and many others involved in receptor or enzyme recycling, as well as trafficking factors, including clathrin have been implicated in retrograde transport (Johannes and Popoff, 2008; Lauvrak et al., 2004).

A literature search fails to reveal any concrete examples of attempted therapeutic delivery by tapping into the retrograde transport system to direct the cargo in the same way as toxins. It is not unreasonable to consider retrograde trafficking-competent factors and even pathogenic toxins as potential models for cytoplasmic delivery. Exploiting toxins, or certain active structural components, may promote successful delivery of a therapeutic through the trans-Golgi network and into the cytoplasm. For example, the Shiga toxin contains the nontoxic B-subunit (STxB) that is responsible for binding to the host cell toxin receptor (glycosphingolipid

Gb3), leading to endocytosis and into recycling endosomes from where they are transported to the ER, the trans-Golgi network, the Golgi membranes, and later into the cytoplasm (Johannes and Popoff, 2008). Incorporating the STxB subunit into macromolecular conjugates may lead to its rerouting through the retrograde transport pathway, as was done in one example to target exogenous peptides and deliver antigens to dendritic cells to induce primary T cell immunity (Adotevi et al., 2007). Alternatively, it may be possible to produce and conjugate ER localization peptides and/or Golgi localization peptides onto oligonucleotide conjugates to attempt to trigger its passage through the retrograde pathway. For example, the two HEAT repeat (HT18 and HT19) sequences and two intervening interunit spacers (IUS17 and IUS18) from the mammalian target of rapamycin (mTOR, amino acids 931-1039) was sufficient to target an enhanced green fluorescent protein (EGFP) to the Golgi after transient expression in HeLa cells (Liu and Zheng, 2007). While insufficient research has been done to support or reject the retrograde strategy for oligonucleotide conjugate delivery, the idea of harnessing the retrograde transport pathway for potential cytoplasmic delivery of oligonucleotide conjugates at least merits further exploration.

Cancer

Many current therapies for cancer are severely limited and often fail to fully eradicate cancer from patients. Current therapies are generally limited to the druggable genome and are unable to pharmaco-evolve to the changing mutational landscape of a cancer tumor. However, oligonucleotides have the potential to excel where many other approaches might fail. siRNAs and ASOs can target the undruggable targets and mediate successful gene knockdowns, and by targeting specific mutations they are able to spare healthy cells. Oligonucleotides can also be used to target multiple targets simultaneously to achieve synthetic lethality (Michiue et al, 2009; Kacsinta and Dowdy, 2016). Oligonucleotides are the epitome of personalized medicine, and they hold huge potential for the treatment of cancer and many other diseases.

Unfortunately, oligonucleotides are hindered by endosomal entrapment that prevent their cytosolic access and this significantly reduces their efficacy. mAbs excel at targeting oligonucleotides to extrahepatic tissues, but they cannot promote endosomal escape for its oligonucleotide cargo. Endosomal entrapment remains a key problem for oligonucleotide therapeutics. Different approaches are under development and in the early stages and their final success or failure is still yet unknown. But whether it is uEEDs, or saponins, or the retrograde transport of oligonucleotides, or some entirely different approach that can overcome the endosomal entrapment of oligos, the one certain result from overcoming this problem is the opening of the therapeutic door to begin testing the ability of oligonucleotide therapeutics to treat cancer.

REFERENCES

Adotevi, O., Vingert, B., Freyburger, L., Shrikant, P., Lone, Y.-C., Quintin-Colonna, F., Haicheur, N., Amessou, M., Herbelin, A., Langlade-Demoyen, P., Fridman, W.H., Lemonnier, F., Johannes, L., Tartour, E., 2007. B Subunit of Shiga Toxin-Based Vaccines Synergize with α-Galactosylceramide to Break Tolerance against Self Antigen and Elicit Antiviral Immunity. J Immunol 179, 3371–3379. https://doi.org/10.4049/jimmunol.179.5.3371

Agard, N.J., Prescher, J.A., Bertozzi, C.R., 2004. A Strain-Promoted [3 + 2] Azide−Alkyne Cycloaddition for Covalent Modification of Biomolecules in Living Systems. J. Am. Chem. Soc. 126, 15046–15047. https://doi.org/10.1021/ja044996f

Agrawal, S., Goodchild, J., Civeira, M.P., Thornton, A.H., Sarin, P.S., Zamecnik, P.C., 1988. Oligodeoxynucleoside phosphoramidates and phosphorothioates as inhibitors of human immunodeficiency virus. Proceedings of the National Academy of Sciences 85, 7079–7083. https://doi.org/10.1073/pnas.85.19.7079

Akinc, A., Zumbuehl, A., Goldberg, M., Leshchiner, E.S., Busini, V., Hossain, N., Bacallado, S.A., Nguyen, D.N., Fuller, J., Alvarez, R., Borodovsky, A., Borland, T., Constien, R., de Fougerolles, A., Dorkin, J.R., Narayanannair Jayaprakash, K., Jayaraman, M., John, M., Koteliansky, V., Manoharan, M., Nechev, L., Qin, J., Racie, T., Raitcheva, D., Rajeev, K.G., Sah, D.W.Y., Soutschek, J., Toudjarska, I., Vornlocher, H.-P., Zimmermann, T.S., Langer, R., Anderson, D.G., 2008. A combinatorial library of lipid-like materials for delivery of RNAi therapeutics. Nat Biotechnol 26, 561–569. https://doi.org/10.1038/nbt1402

Augustin, J.M., Kuzina, V., Andersen, S.B., Bak, S., 2011. Molecular activities, biosynthesis and evolution of triterpenoid saponins. Phytochemistry 72, 435–457. https://doi.org/10.1016/j.phytochem.2011.01.015

Bachran, C., Sutherland, M., Heisler, I., Hebestreit, P., Melzig, M.F., Fuchs, H., 2006. The Saponin-Mediated Enhanced Uptake of Targeted Saporin-Based Drugs is Strongly Dependent on the Saponin Structure. Exp Biol Med (Maywood) 231, 412–420. https://doi.org/10.1177/153537020623100407

Baumann, E., Stoya, G., Völkner, A., Richter, W., Lemke, C., Linss, W., 2000. Hemolysis of human erythrocytes with saponin affects the membrane structure. Acta Histochemica 102, 21–35. https://doi.org/10.1078/0065-1281-00534

Benson, M.D., Waddington-Cruz, M., Berk, J.L., Polydefkis, M., Dyck, P.J., Wang, A.K., Planté-Bordeneuve, V., Barroso, F.A., Merlini, G., Obici, L., Scheinberg, M., Brannagan, T.H., Litchy, W.J., Whelan, C., Drachman, B.M., Adams, D., Heitner, S.B., Conceição, I., Schmidt, H.H., Vita, G., Campistol, J.M., Gamez, J., Gorevic, P.D., Gane, E., Shah, A.M., Solomon, S.D., Monia, B.P., Hughes, S.G., Kwoh, T.J., McEvoy, B.W., Jung, S.W., Baker, B.F., Ackermann, E.J., Gertz, M.A., Coelho, T., 2018. Inotersen Treatment for Patients with Hereditary Transthyretin Amyloidosis. N Engl J Med 379, 22–31. https://doi.org/10.1056/NEJMoa1716793

Blidner, R.A., Hammer, R.P., Lopez, M.J., Robinson, S.O., Monroe, W.T., 2007. Fully 2'-Deoxy-2'-Fluoro Substituted Nucleic Acids Induce RNA Interference in Mammalian Cell Culture. Chem Biol Drug Design 70, 113–122. https://doi.org/10.1111/j.1747-0285.2007.00542.x

Böttger, S., Hofmann, K., Melzig, M.F., 2012. Saponins can perturb biologic membranes and reduce the surface tension of aqueous solutions: A correlation? Bioorganic & Medicinal Chemistry 20, 2822–2828. https://doi.org/10.1016/j.bmc.2012.03.032

Böttger, S., Westhof, E., Siems, K., Melzig, M.F., 2013. Structure–activity relationships of saponins enhancing the cytotoxicity of ribosome-inactivating proteins type I (RIP-I). Toxicon 73, 144–150. https://doi.org/10.1016/j.toxicon.2013.07.011

Brown, C.R., Gupta, S., Qin, J., Racie, T., He, G., Lentini, S., Malone, R., Yu, M., Matsuda, S., Shulga-Morskaya, S., Nair, A.V., Theile, C.S., Schmidt, K., Shahraz, A., Goel, V., Parmar, R.G., Zlatev, I., Schlegel, M.K., Nair, J.K., Jayaraman, M., Manoharan, M., Brown, D., Maier, M.A., Jadhav, V., 2020. Investigating the pharmacodynamic durability of GalNAc–siRNA conjugates. Nucleic Acids Research 48, 11827–11844. https://doi.org/10.1093/nar/gkaa670

Caporale, A., Selis, F., Sandomenico, A., Jotti, G.S., Tonon, G., Ruvo, M., 2015. The LQSP tetrapeptide is a new highly efficient substrate of microbial transglutaminase for the site-specific derivatization of peptides and proteins. Biotechnology Journal 10, 154–161. https://doi.org/10.1002/biot.201400466

Crooke, S.T., Wang, S., Vickers, T.A., Shen, W., Liang, X., 2017b. Cellular uptake and trafficking of antisense oligonucleotides. Nat Biotechnol 35, 230–237. https://doi.org/10.1038/nbt.3779

Cuellar, T.L., Barnes, D., Nelson, C., Tanguay, J., Yu, S.-F., Wen, X., Scales, S.J., Gesch, J., Davis, D., van Brabant Smith, A., Leake, D., Vandlen, R., Siebel, C.W., 2015. Systematic evaluation of antibody-mediated siRNA delivery using an industrial platform

of THIOMAB–siRNA conjugates. Nucleic Acids Research 43, 1189–1203. https://doi.org/10.1093/nar/gku1362

Cui, H., Zhu, X., Li, S., Wang, P., Fang, J., 2021. Liver-Targeted Delivery of Oligonucleotides with N-Acetylgalactosamine Conjugation. ACS Omega 6, 16259–16265. https://doi.org/10.1021/acsomega.1c01755

Dowdy, S.F., 2017. Overcoming cellular barriers for RNA therapeutics. Nat Biotechnol 35, 222–229. https://doi.org/10.1038/nbt.3802

Eckstein, F., 2014. Phosphorothioates, Essential Components of Therapeutic Oligonucleotides. Nucleic Acid Therapeutics 24, 374–387. https://doi.org/10.1089/nat.2014.0506

Falguières, T., Mallard, F., Baron, C., Hanau, D., Lingwood, C., Goud, B., Salamero, J., Johannes, L., 2001. Targeting of Shiga Toxin B-Subunit to Retrograde Transport Route in Association with Detergent-resistant Membranes. MBoC 12, 2453–2468. https://doi.org/10.1091/mbc.12.8.2453

Farias, S.E., Strop, P., Delaria, K., Galindo Casas, M., Dorywalska, M., Shelton, D.L., Pons, J., Rajpal, A., 2014. Mass Spectrometric Characterization of Transglutaminase Based Site-Specific Antibody–Drug Conjugates. Bioconjugate Chem. 25, 240–250. https://doi.org/10.1021/bc4003794

Fisher Scientific. Thermo ScientificTM Saponin, pract., from Quillaja Saponaria Molina. CAS 74499-23-3/Thermo Scientific 419231000. https://www.fishersci.com/shop/products/saponin-pract-quillaja-saponaria-molina/AC419231000

Fuchs, H., Niesler, N., Trautner, A., Sama, S., Jerz, G., Panjideh, H., Weng, A., 2017. Glycosylated Triterpenoids as Endosomal Escape Enhancers in Targeted Tumor Therapies. Biomedicines 5, 14. https://doi.org/10.3390/biomedicines5020014

Fuchs, H., 2021. Saponin conjugated to epitope binding proteins. WIPO Patent W02020126064A1. https://patents.google.com/patent/WO2020126064A1/

Gagliardi, M., Ashizawa, A.T., 2021. The Challenges and Strategies of Antisense Oligonucleotide Drug Delivery. Biomedicines 9, 433. https://doi.org/10.3390/biomedicines9040433

Gilabert-Oriol, R., Thakur, M., von Mallinckrodt, B., Hug, T., Wiesner, B., Eichhorst, J., Melzig, M.F., Fuchs, H., Weng, A., 2013. Modified Trastuzumab and Cetuximab Mediate Efficient Toxin Delivery While Retaining Antibody-Dependent Cell-Mediated Cytotoxicity in Target Cells. Mol. Pharmaceutics 10, 4347–4357. https://doi.org/10.1021/mp400444q

Gilabert-Oriol, R., Thakur, M., von Mallinckrodt, B., Bhargava, C., Wiesner, B., Eichhorst, J., Melzig, M., Fuchs, H., Weng, A., 2014. Reporter Assay for Endo/Lysosomal Escape of Toxin-Based Therapeutics. Toxins 6, 1644–1666. https://doi.org/10.3390/toxins6051644

Holmes, S.E., Bachran, C., Fuchs, H., Weng, A., Melzig, M., Flavell, S.U., Flavell, D.J., 2014. Triterpenoid saponin augmentation of saporin-based immunotoxin cytotoxicity for human leukaemia and lymphoma cells is partially immunospecific and target molecule

dependent. Immunpharm Immunotox 37, 42-55. https://doi.org/10.3109/08923973.2014.971964

Huggins, I.J., Medina, C.A., Springer, A.D., van den Berg, A., Jadhav, S., Cui, X., Dowdy, S.F., 2019. Site Selective Antibody-Oligonucleotide Conjugation via Microbial Transglutaminase. Molecules 24, 3287. https://doi.org/10.3390/molecules24183287

Ipsaro, J.J., Joshua-Tor, L., 2015. From guide to target: molecular insights into eukaryotic RNA-interference machinery. Nat Struct Mol Biol 22, 20–28. https://doi.org/10.1038/nsmb.2931

Juliano, R.L., Ming, X., Nakagawa, O., 2012. Cellular Uptake and Intracellular Trafficking of Antisense and siRNA Oligonucleotides. Bioconjugate Chem. 23, 147–157. https://doi.org/10.1021/bc200377d

Juliano, R.L., Carver, K., Cao, C., Ming, X., 2013. Receptors, endocytosis, and trafficking: the biological basis of targeted delivery of antisense and siRNA oligonucleotides. Journal of Drug Targeting 21, 27–43. https://doi.org/10.3109/1061186X.2012.740674

Juliano, R.L., 2016. The delivery of therapeutic oligonucleotides. Nucleic Acids Res 44, 6518–6548. https://doi.org/10.1093/nar/gkw236

Kacsinta, A.D., Dowdy, S.F., 2016. Current views on inducing synthetic lethal RNAi responses in the treatment of cancer. Exp Op Biol Therapy 16, 161-172. https://doi.org/10.1517/14712598.2016.1110141

Khvorova, A., Watts, J.K., 2017. The chemical evolution of oligonucleotide therapies of clinical utility. Nat Biotechnol 35, 238–248. https://doi.org/10.1038/nbt.3765

Lauvrak, S.U., Torgersen, M.L., Sandvig, K., 2004. Efficient endosome-to-Golgi transport of Shiga toxin is dependent on dynamin and clathrin. Journal of Cell Science 117, 2321–2331. https://doi.org/10.1242/jcs.01081

Liu, X., Zheng, X.F.S., 2007. Endoplasmic Reticulum and Golgi Localization Sequences for Mammalian Target of Rapamycin. MBoC 18, 1073–1082. https://doi.org/10.1091/mbc.e06-05-0406

Matranga, C., Tomari, Y., Shin, C., Bartel, D.P., Zamore, P.D., 2005. Passenger-Strand Cleavage Facilitates Assembly of siRNA into Ago2-Containing RNAi Enzyme Complexes. Cell 123, 607–620. https://doi.org/10.1016/j.cell.2005.08.044

Merkel, O.M., Librizzi, D., Pfestroff, A., Schurrat, T., Béhé, M., Kissel, T., 2009. In Vivo SPECT and Real-Time Gamma Camera Imaging of Biodistribution and Pharmacokinetics of siRNA Delivery Using an Optimized Radiolabeling and Purification Procedure. Bioconjugate Chem. 20, 174–182. https://doi.org/10.1021/bc800408g

Michiue , H., Eguchi, A., Scadeng, M., Dowdy, S.F., 2009. Induction of in vivo synthetic lethal RNAi responses to treat glioblastoma. Cancer Biol Ther. 8, 2306-2313. https://doi.org/10.4161/cbt.8.23.10271

Rappaport, J., Hanss, B., Kopp, J.B., Copeland, T.D., Bruggeman, L.A., Coffman, T.M., Klotman, P.E., 1995. Transport of phosphorothioate oligonucleotides in kidney: Implications for molecular therapy. Kidney International 47, 1462–1469. https://doi.org/10.1038/ki.1995.205

Sandvig, K., Skotland, T., van Deurs, B., Klokk, T.I., 2013. Retrograde transport of protein toxins through the Golgi apparatus. Histochem Cell Biol 140, 317–326. https://doi.org/10.1007/s00418-013-1111-z

Sapreme Technologies, 2021. Sapreme Presents Promising New Preclinical Data at 17th Annual Meeting of Oligonucleotide Therapeutics Society. https://sapreme-technologies.com/news/#20210927

Schroeder, A., Levins, C.G., Cortez, C., Langer, R., Anderson, D.G., 2010. Lipid-based nanotherapeutics for siRNA delivery: Symposium: Lipid-based siRNA nanotherapeutics. Journal of Internal Medicine 267, 9–21. https://doi.org/10.1111/j.1365-2796.2009.02189.x

Scoles, D.R., Minikel, E.V., Pulst, S.M., 2019. Antisense oligonucleotides: A primer. Neurol Genet 5, 1-8. https://doi.org/10.1212/NXG.0000000000000323

Seguro, K., Nio, N., Motoki, M., Pearce, J., 1996. Some Characteristics of a Microbial Protein Cross-Linking Enzyme: Transglutaminase. Macromolecular Interactions in Food Technology, Chapter 21, ACS Symposium Series. American Chemical Society, Washington, DC. https://doi.org/10.1021/bk-1996-0650

Siegmund, V., Schmelz, S., Dickgiesser, S., Beck, J., Ebenig, A., Fittler, H., Frauendorf, H., Piater, B., Betz, U.A.K., Avrutina, O., Scrima, A., Fuchsbauer, H., Kolmar, H., 2015. Locked by Design: A Conformationally Constrained Transglutaminase Tag Enables Efficient Site-Specific Conjugation. Angew. Chem. Int. Ed. 54, 13420–13424. https://doi.org/10.1002/anie.201504851

Sikora, J.L., Logue, M.W., Chan, G.G., Spencer, B.H., Prokaeva, T.B., Baldwin, C.T., Seldin, D.C., Connors, L.H., 2015. Genetic variation of the transthyretin gene in wild-type transthyretin amyloidosis (ATTRwt). Hum Genet 134, 111–121. https://doi.org/10.1007/s00439-014-1499-0

Spilsberg, B., van Meer, G., Sandvig, K., 2003. Role of Lipids in the Retrograde Pathway of Ricin Intoxication: Role of Lipids in Ricin Intoxication. Traffic 4, 544–552. https://doi.org/10.1034/j.1600-0854.2003.00111.x

Stec, W.J., Karwowski, B., Boczkowska, M., Guga, P., Koziołkiewicz, M., Sochacki, M., Wieczorek, M.W., Błaszczyk, J., 1998. Deoxyribonucleoside 3‘- *O* -(2-Thio- and 2-Oxo-“spiro”-4,4-pentamethylene-1,3,2-oxathiaphospholane)s: Monomers for Stereocontrolled Synthesis of Oligo(deoxyribonucleoside phosphorothioate)s and Chimeric PS/PO Oligonucleotides. J. Am. Chem. Soc. 120, 7156–7167. https://doi.org/10.1021/ja973801j

Stein, C.A., Hansen, J.B., Lai, J., Wu, S., Voskresenskiy, A., H∅g, A., Worm, J., Hedtjärn, M., Souleimanian, N., Miller, P., Soifer, H.S., Castanotto, D., Benimetskaya, L., Ørum, H., Koch, T., 2010. Efficient gene silencing by delivery of locked nucleic acid antisense

oligonucleotides, unassisted by transfection reagents. Nucleic Acids Research 38, e3–e3. https://doi.org/10.1093/nar/gkp841

Thakur, M., Weng, A., Pieper, A., Mergel, K., von Mallinckrodt, B., Gilabert-Oriol, R., Görick, C., Wiesner, B., Eichhorst, J., Melzig, M.F., Fuchs, H., 2013. Macromolecular interactions of triterpenoids and targeted toxins: Role of saponins charge. International Journal of Biological Macromolecules 61, 285–294. https://doi.org/10.1016/j.ijbiomac.2013.07.008

ThermoFisher Scientific. EDC (1-ethyl-3-(3-dimethylaminopropyl)carbodiimide hydrochloride. https://www.thermofisher.com/order/catalog/product/22980

van de Water, F.M., Boerman, O.C., Wouterse, A.C., Peters, J.G.P., Russel, F.G.M., Masereeuw, R., 2006. Intravenously Administered Short Interfering RNA Accumulates in the Kidney and Selectively Suppresses Gene Function in Renal Proximal Tubules. Drug Metab Dispos 34, 1393–1397. https://doi.org/10.1124/dmd.106.009555

Wang, Y., Juranek, S., Li, H., Sheng, G., Wardle, G.S., Tuschl, T., Patel, D.J., 2009. Nucleation, propagation and cleavage of target RNAs in Ago silencing complexes. Nature 461, 754–761. https://doi.org/10.1038/nature08434

Weng, A., Bachran, C., Fuchs, H., Melzig, M.F., 2008. Soapwort saponins trigger clathrin-mediated endocytosis of saporin, a type I ribosome-inactivating protein. Chemico-Biological Interactions 176, 204–211. https://doi.org/10.1016/j.cbi.2008.08.004

Woldemichael, G.M., Wink, M., 2001. Identification and Biological Activities of Triterpenoid Saponins from *Chenopodium quinoa*. J. Agric. Food Chem. 49, 2327–2332. https://doi.org/10.1021/jf0013499

Yamasaki, Y., Ito, K., Enomoto, Y., Sutko, J.L., 1987. Alterations by saponins of passive Ca2+ permeability and Na+-Ca2+ exchange activity of canine cardiac sarcolemmal vesicles. Biochimica et Biophysica Acta (BBA) - Biomembranes 897, 481–487. https://doi.org/10.1016/0005-2736(87)90445-7

Zimmermann, T.S., Lee, A.C.H., Akinc, A., Bramlage, B., Bumcrot, D., Fedoruk, M.N., Harborth, J., Heyes, J.A., Jeffs, L.B., John, M., Judge, A.D., Lam, K., McClintock, K., Nechev, L.V., Palmer, L.R., Racie, T., Röhl, I., Seiffert, S., Shanmugam, S., Sood, V., Soutschek, J., Toudjarska, I., Wheat, A.J., Yaworski, E., Zedalis, W., Koteliansky, V., Manoharan, M., Vornlocher, H.-P., MacLachlan, I., 2006. RNAi-mediated gene silencing in non-human primates. Nature 441, 111–114. https://doi.org/10.1038/nature04688